Interactome of Ixr1, HMGB1 and HMGB2 proteins in relation to their cellular functions

Aida Inés Barreiro Alonso

PhD Thesis

2017

Directors: Dra. Mª Esperanza Cerdán Villanueva and Dra. Mónica Lamas Maceiras

Programa Oficial de Doutoramento en Bioloxía Celular e Molecular

UNIVERSIDADE DA CORUÑA

El presente trabajo, **Interactome of Ixr1, HMGB1 and HMGB2 proteins in relation to their cellular functions**, presentado por Doña Aida Inés Barreiro Alonso para aspirar al grado de doctor en Bioquímica, ha sido realizado bajo nuestra dirección en el Departamento de Biología, de la Universidad de A Coruña.

Revisado el texto. Estamos conformes con su presentación para ser juzgado.

A Coruña, 9 de noviembre de 2017

VºBº

Dra. Mº Esperanza Cerdán Villanueva

Catedrática de Bioquímica y Biología Molecular

VºBº

Dra. Mónica Lamas Maceiras

Profesora de Bioquímica y Biología Molecular

La autora de este trabajo ha disfrutado durante la realización de esta tesis de un contrato a cargo de proyecto por la Universidade da Coruña (julio de 2013-noviembre de 2013), un contrato predoctoral asociado al plan I2C de la Xunta de Galicia para el año 2013 (1 diciembre 2013-30 noviembre 2016). Parte del trabajo se realizó en el "Wellcome Trust Sanger Institute" (Hinxton, United Kingdom) entre septiembre de 2016 y Marzo de 2017 en el grupo "Proteomic Mass Spectrometry". Esta estancia fue financiada por el programa de ayudas predoctorales para estancias Inditex-UDC y por las ayudas para estancias pre y posdoctorales de investigación para personal de grupos de la agrupación estratégica CICA-INIBIC.

La realización de este trabajo ha sido posible gracias a la financiación obtenida de los proyectos del Instituto de Salud Carlos III con referencia PI14/01031 y de la Xunta de Galicia (Consolidación Grupos referencia Competitiva Contractos no. CN2012-118 y ED431C 2016-012), ambos cofinanciados por FEDER. El trabajo realizado durante la estancia de investigación en el Wellcome Trust Sanger Institute fue financiado por el Wellcome Trust (grant number WT098051).

A mis padres

"I'm not a genius but I'm a terrific package of experience"

(Chinese Fortune cookie, Sanger Institute, Cambridge 2017)

En primer lugar me gustaría dar las gracias a Mª Esperanza Cerdán Villanueva y Mónica Lamas Maceiras, mis dos directoras de Tesis sin las cuales hoy no estaría aquí. Gracias por darme la oportunidad de aprender lo que de verdad significa "investigar" y de haberme dado la oportunidad no sólo de llevar a cabo mi Tesis doctoral si no de conocer a gente increíble que ya forman parte de mi vida.

Como no, agradecer también a todos los profesores del laboratorio de Bioquímica de la UDC, Mª Isabel González Siso, Esther Rodríguez Belmonte, Manuel Becerra Fernández, Marian Freire Picos y Ana Rodríguez Torres la ayuda que me han prestado estos años.

Y ahora viene lo difícil, a mí siempre me ha gustado leer las dedicatorias de las tesis y en el laboratorio de bioquímica ya me habéis hecho caer la lagrimilla más de una vez, pero ya os adelanté que a mí esto no se me da tan bien…En primer lugar quiero daros un GRACIAS enorme a todos los que habéis formado parte del laboratorio de Bioquímica durante los años en los que he hecho la tesis, porque gracias a vosotros he disfrutado de esta etapa. Cuando un experimento no sale y no tienes ni idea de por qué no ha salido, lo mejor que te puede pasar es tener a amigos que además de apoyarte en todo momento te dan soluciones y fuerzas para seguir. Porque me acuerdo cuando seguía a Ángel nada más entrar en el laboratorio y curioseaba lo que hacía. Gracias Ángel por ser un super-predecesor, por contestar mails, whattsapps y skypes, y ayudarme desde donde estés, porque eres un crack y aunque no te guste que te lo diga…"Eres mi Rafa". Mi Mariu, mi Mari, y mi Olalla, las tres chicas del laboratorio de bioquímica del 2013, tendría mil cosas que deciros, he pasado muchísimos momentos con vosotras en el laboratorio pero los más importantes son los que he pasado fuera, porque hemos pasado bodas, un bebé (y otro que llegará pronto), clases descoordinadas de aerolatinos y spinning, paseos con helados,

momentos de risas y momentos no tan alegres pero que te unen un montón. Agustín, te admiro, admiro como has sido capaz de mantener la calma durante tu tesis y como consigues tranquilizarme y razonar conmigo, gracias por ayudarme todo este tiempo. Marta, nuestra "adoptada" del INIBIC, nos tienes que visitar más porque nos tienes muy abandonados con lo que nos gusta que vengas… Desde hace un tiempo se nos unió nuestra última adquisición, Maria "peque", el labo ya no sería el mismo sin tus aventuras-desventuras y mil anécdotas. No me olvido de Ana, mi primera TFG, y mucho más que eso, me has demostrado que siempre hay que mirar adelante y seguir con fuerza. Y aunque ya te he mencionado antes Mónica, te vuelvo a incluir aquí, entre los del "Labo", porque sin ti el labo no sería lo que es. Y por supuesto Juanjo, mi vecino incondicional de escritorio y de poyata y sobre todo un gran amigo, un enorme gracias por aguantarme y tener una santa paciencia conmigo todos estos años.

Hay muchas personas que habéis formado parte de este etapa en el laboratorio de Bioquímica a los que también me gustaría daros las gracias como a Rosa, Kamila, Blanca, Martín, Maya, Kike, Isabel…y muchos más que seguramente me estoy dejando en el tintero.

Me gustaría también agradecerle a la Dra. Ángela Figueroa la oportunidad de aprender nuevas técnicas durante los meses que me acogieron en su grupo del INIBIC. Y por supuesto este aprendizaje no habría sido posible sin la ayuda de Raquel, Olalla, Isa, Andrea y mucha más gente del INIBIC que me ayudaron durante el tiempo que estuve allí, ¡gracias por acogerme en el grupo!

Durante la realización de la tesis llevé a cabo una estancia de 6 meses en el Mass Spectrometry group (Team 17) en el Wellcome Trust Sanger Institute, tengo que dar un enorme gracias a la Dra. Mercedes Pardo, porque sin ella esta estancia no habría sido posible, por hacer

que me sintiese totalmente integrada en el grupo y por toda la ayuda que me dio, gracias por ayudarme esos meses y seguir ayudándonos ahora. Como la mayor parte de las personas del grupo no hablan español voy a cambiar de idioma… I would like to thank Dr. Jyoti Choudhary, Team 17 leader, for accepting me in her group and giving me support as if I was one of her team´s member, thank you for believing in my work and for all the help. I learn a lot during my stay in the Team 17, but It was not just lab work, my months in Cambrdige were an amazing experience during which I met amazing people: Junting, Charly, George, Sharna…It wouldn´t have been the same without you! I would also want to thank the other Team 17 members Chris, Lu, Theo, Hendrik and Olallo.

Hay una persona que aunque no es de ninguno de los laboratorios en los que he estado ha tenido un papel importante durante todo este tiempo, Santi (mi Ferro). Durante la tesis no todos son momentos buenos, también hay enfados, frustración y desánimos, que son los más difíciles, gracias por estar conmigo en todos esos momentos y apoyarme todo este tiempo.

Probablemente el gracias más grande que tengo que dar es a mis padres, porque si es cierto que Esperanza y Mónica me dieron la oportunidad de llevar a cabo mi tesis en este laboratorio, no habría llegado a este punto sin ellos, sin su apoyo. Gracias por permitirme estudiar lo que he querido y por el apoyo, no sólo durante la carrera si no en todo lo que he hecho después porque sin vosotros no estaría donde estoy hoy. ¡Muchas gracias!

Como no puedo mencionar a todo el mundo que me gustaría en estos agradecimientos, voy a dar un GRACIAS general a todos aquellos que formáis parte de mi vida y que me habéis apoyado durante este tiempo.

Contents

Short Abstracts

ABSTRACT

The *Saccharomyces cerevisiae* protein, Ixr1, and human HMGB1 and HMGB2 proteins belong to the HMGB protein family. The main objective of this work was to identify new proteins binding Ixr1, HMGB1 and HMGB2 in order to increase the knowledge about their cellular functions.

In yeast Ixr1 has activator or repressor activity on transcription in different promoters and controls the hypoxic response. The transcriptional activator domain of Ixr1 has been identified in its NH_2 term in this study. Interactome studies show that Ixr1 binds to Ssn8 and this interaction might mediate the repressor function of Ixr1 on several promoters. Other proteins identified share functions associated to glucose metabolism, stress, and ribosome biogenesis among others. Differential phosphorylation of Ixr1 was observed depending on oxygen availability.

The HMGB1 and HMGB2 interactomes were studied using different techniques as yeast two-hybrid assays and purification methods coupled with mass spectrometry. This study was carried out in cancerous and non-cancerous ovarian and prostate epithelial cells. Results showed the wide range of functions linked to their interacting partners. The interaction of HMGB1 with KRT7 and RBBP7 was validated by complementary techniques. HMGB1 specific interactions associated to cisplatin treatment of these cells were also identified in this study**.**

RESUMEN

La proteína de *Saccharomyces cerevisiae* Ixr1, y las proteínas humanas HMGB1 y HMGB2 se engloban dentro de la familia de proteínas HMGB. El principal objetivo de este trabajo ha sido la identificación de proteínas no previamente descritas que se unen a Ixr1, HMGB1 y HMGB2, para así poder ampliar el conocimiento sobre las funciones celulares de las proteínas HMGB.

En levaduras, Ixr1 tiene un papel activador o represor de la transcripción sobre distintos promotores y controla la respuesta a hipoxia. El dominio de activación transcripcional de Ixr1 ha sido localizado en su extremo amino en este estudio. Ixr1 se une con Ssn8 y esta interacción puede mediar su papel represor sobre los promotores de algunos genes. Ixr1 además interacciona con proteínas relacionadas con el metabolismo de glucosa, estrés y biogénesis de ribosomas entre otras. Se ha detectado que Ixr1 presenta una fosforilación diferencial en función de la disponibilidad de oxígeno.

Se ha llevado a cabo un estudio del interactoma de HMGB1 y HMGB2 mediante técnicas como el sistema de doble híbrido o purificaciones acopladas a espectrometría de masas en células epiteliales de ovario y próstata tumorales y no tumorales. Los resultados obtenidos ponen de manifiesto la amplia variedad de funciones asociadas a las proteínas que interactúan con HMGB1 o HMGB2. Se ha validado la interacción de HMGB1 con KRT7 y RBBP7 mediante otras técnicas complementarias. Así como también se han identificado interacciones específicas de HMGB1 en células tratadas con cisplatino.

RESUMO

A proteína de *Saccharomyces cerevisiae* Ixr1, e as proteínas humanas HMGB1 e HMGB2 englóbanse dentro da familia de proteínas HMGB. O principal obxectivo deste traballo foi a identificación de proteínas non previamente descritas que se unen a Ixr1, HMGB1 e HMGB2, para así poder ampliar o coñecemento sobre as funcións celulares das proteínas HMGB.

En lévedos, Ixr1 ten un papel activador ou represor da transcrición sobre distintos promotores e controla a resposta a hipoxia. O dominio de activación transcripcional de Ixr1 foi localizado no seu extremo amino neste estudo. Ixr1 únese con Ssn8 e esta interacción pode mediar o seu papel represor sobre os promotores dalgúns xenes. Ixr1 ademais, interacciona con proteínas relacionadas co metabolismo de glicosa, stress e ribosomais entre outras. Detectouse que Ixr1 presenta unha fosforilación diferencial en función da dispoñibilidade de osíxeno.

Levouse a cabo un estudo do interactoma de HMGB1 e HMGB2 mediante técnicas como o sistema de dobre híbrido ou purificacións e espectrometría de masas en células epiteliais de ovario e próstata tumorais e non tumorais. Os resultados obtidos poñen de manifesto a ampla variedade de funcións asociadas ás proteínas que interactúan con HMGB1 ou HMGB2. Hase validado a interacción de HMGB1 con KRT7 e RBBP7 mediante outras técnicas complementarias. Así como tamén se identificaron interaccións específicas de HMGB1 en células tratadas con cisplatino.

Introduction

Eukaryotic HMG proteins are classified in three families named HMGA, HMGB, and HMGN. The specific functional domain defining each family is the “AT hook” in HMGA, the “HMG-box” in HMGB, and the “nucleosomal binding domain” in HMGN proteins (Bustin, 2001).

In this thesis we study functional interactions of three HMGB proteins, Ixr1 from *Saccharomyces cerevisiae* and human HMGB1 and HMGB2, with other proteins trying to find new clues about their functions. HMGB proteins are nowadays a focus of interest due to their participation in cellular processes like epigenetic control of gene expression, aging, disease, or regenerative cellular therapies. Remarkably, HMGB1 and HMGB2 are over-expressed in many types of cancer, including those of etiology based on oxidative damage as recently reviewed (Barreiro-Alonso *et al.*, 2016).

The seven HMGB proteins from *S. cerevisiae*, might be considered as chromatin architectural proteins, but with wide influence on gene expression (Misteli, 2001). Two of them, Rox1 and Ixr1, also function as specific transcriptional factors on regulated promoters. Rox1 is a specific transcriptional regulator of the hypoxic yeast regulon (Kastaniotis and Zitomer, 2000) and it is homologous to the SOX family of transcriptional factors from metazoan, which play important roles in tissue homeostasis, organogenesis, and cell fate decision during developmental processes (She and Yang, 2015). Ixr1 has a dual function as specific transcription factor during hypoxic and oxidative stress responses, and it is also a protein involved in DNA repair (Vizoso-Vázquez, Lamas-Maceiras, *et al.*, 2017). Human HMGB1 and HMGB2 are structurally related to Ixr1 and, like Ixr1, have two in tandem HMG-box domains folded in the characteristic L-shaped architecture. Each domain is formed by three alpha-helix-folds. In HMGB1,

the first domain includes amino acids 1–79, and the second is formed by amino acids 89–163. The carboxyl terminus, including amino acids 186–215, is acidic, negatively charged, and interacts with residues within and between the two HMG-boxes (Knapp *et al.*, 2004). Similarly to Ixr1, HMGB1 and HMGB2 also participate in transcriptional regulation and DNA repair and are able to bind DNA-cisplatin adducts (Zamble *et al.*, 1996; Reeves, 2015). The role of HMGB proteins from yeast and multicellular eukaryotes, with special emphasis in human, and in reference to gene regulation and DNA repair, has been compared in a recent a review (Vizoso-Vázquez, Barreiro-Alonso, *et al.*, 2017).

The biological functions of HMGB1 change in normal and cancer cells and depend on its redox state and cellular location. In the nucleus HMGB1 contributes to nucleosome dynamics, chromosomal stability and telomere maintenance (Polanská *et al.*, 2012). It also modulates gene transcription and recombination (Bustin, 1999), nucleotide excision repair (NER), mismatch repair (MMR), base excision repair (BER), and double strand break repair (DSBR) among others (Polanská *et al.*, 2012). In the cytoplasm HMGB1 stimulates autophagy, inhibits apoptosis, and regulates mitochondrial morphology and function (Lange and Vasquez, 2009). HMGB1 is actively secreted by macrophages, monocytes, natural killer cells, and dendritic cells after stimulation. It is finally released from necrotic or injured cells, mainly during oxidative stress (Tang *et al.*, 2006; Tsung *et al.*, 2007). After cellular externalization, it binds to several cell surface receptors in other cells, principally to the receptor for advanced glycation end products (RAGE) and toll-like receptors (TLRs) and activates nuclear factor kappa B (NF-κB) signaling (Park *et al.*, 2004) and other signaling pathways (Lange

and Vasquez, 2009). As a result, HMGB1 behaves as an alarmin and modulates immune and inflammatory responses, promotes cell proliferation, angiogenesis, and cell adhesion and migration.

In the first chapter we analyze which region of Ixr1 is involved in transcriptional activation. We also use the yeast-two-hybrid technology to test Ixr1 interactions with three factors that have been previously identified as important players in the yeast hypoxic response, Cyc8, Tup1 and Ssn8. Finally we extend the interactome analysis to the whole repertory of yeast proteins by co-purification and mass spectrometry identification.

In the second chapter we present a proteomic study of HMGB1 partners based on immunoprecipitation of HMGB1 from a non-cancerous immortalized prostate epithelial cell line (PNT2). In addition, HMGB1 and HMGB2 were used as baits in yeast two-hybrid screening of libraries from prostate (HPEpiC) and ovary (HOSEpiC) primary epithelial cell lines and from healthy ovary tissue as well.

In the third chapter we extend the use of yeast-two-hybrid methods to find proteins that interact with HMGB1 and HMGB2 in cancer cell lines of prostate (PC-3) and ovary (SKOV-3) derived from epithelial cells. Validation of the data set by analysis of co-immunoprecipitation, sub-cellular co-localization and co-regulated expression is also presented.

In the fourth chapter large scale HMGB1 immunoprecipitation assays coupled to Mass Spectrometry (MS) analysis are used to identify novel HMGB1 interactions in ovarian and prostate cells in nuclear and cytoplasmic cellular fractions. The most promising interactions have been studied in more detail.

Cisplatin is a drug used in chemotherapy of prostate, ovary and other cancer types, and its cytotoxic effect has been attributed to its binding to DNA, causing structural and regulatory changes, which induce cellular death (Wang and Lippard, 2005). Unfortunately the efficiency of cisplatin treatment is frequently hampered by acquired resistance, because cells activate mechanisms to evade chemotherapy-induced apoptosis or other cell death pathways (Marquez and Xu, 2012). Considering the implication of HMGB1 in these processes, in the last chapter we have used methods of co-immunoprecipitation with HMGB1-antibodies and later MS identification of proteins that interact specifically with HMGB1 in prostate and ovary cancer cells treated with cisplatin.

The identification of HMGB1 or HMGB2-binding proteins, which are associated with specific cancerous processes or with mechanisms of cisplatin resistance, is a field of interest for ongoing translational cancer research. In addition, basic scientific research will also benefit from the discovery of new proteins that will allow to explain cellular processes through the interaction with HMGB proteins in the nucleus or cytoplasm.

REFERENCES

Barreiro-Alonso A, Lamas-Maceiras M, Rodríguez-Belmonte E, Vizoso-Vázquez Á, Quindós M, Cerdán ME. 2016. High Mobility Group B Proteins, Their Partners, and Other Redox Sensors in Ovarian and Prostate Cancer. *Oxid. Med. Cell. Longev.*, **2016**.

Bustin M. 1999. Regulation of DNA-Dependent Activities by the Functional Motifs of the High-Mobility-Group Chromosomal Proteins. *Mol. Cell. Biol.*, **19**: 5237–5246.

Bustin M. 2001. Revised nomenclature for high mobility group (HMG) chromosomal proteins. *Trends Biochem. Sci.*, **26**: 152–153.

Kastaniotis A, Zitomer R. 2000. Rox1 mediated repression. Oxygen dependent repression in yeast. *Adv. Exp. Med. Biol.*, **475**: 185–195.

Knapp S, Müller S, Digilio G, Bonaldi T, Bianchi ME, Musco G. 2004. The long acidic tail of high mobility group box 1 (HMGB1) protein forms an extended and flexible structure that interacts with specific residues within and between the HMG boxes. *Biochemistry*, **43**: 11992–11997.

Lange SS, Vasquez KM. 2009. HMGB1: The Jack-of-all-Trades Protein is a Master DNA Repair Mechanic. *Mol Carcinog.*, **48**: 571–580.

Marquez RT, Xu L. 2012. Bcl-2:Beclin 1 complex: multiple, mechanisms regulating autophagy/apoptosis toggle switch. *Am. J. Cancer Res.*, **2**: 214–221.

Misteli T. 2001. Protein Dynamics: Implications for Nuclear Architecture and Gene Expression. *Science*, **291**: 843–847.

Park JS, Svetkauskaite D, He Q, Kim J-Y, Strassheim D, Ishizaka A, Abraham E. 2004. Involvement of Toll-like Receptors 2 and 4 in Cellular Activation by High Mobility Group Box 1 Protein. *J. Biol. Chem.*, **279**: 7370–7377.

Polanská E, Dobšáková Z, Dvořáčková M, Fajkus J, Štros M. 2012. HMGB1 gene knockout in mouse embryonic fibroblasts results in reduced telomerase activity and telomere dysfunction. *Chromosoma*, **121**: 419–431.

Reeves R. 2015. High mobility group (HMG) proteins: Modulators of chromatin structure and DNA repair in mammalian cells. *DNA Repair (Amst).*, **36**: 122–136.

She ZY, Yang WX. 2015. SOX family transcription factors involved in diverse cellular events during development. *Eur. J. Cell Biol.*, **94**: 547–563.

Tang D, Shi Y, Kang R, Li T, Xiao W, Wang H, Xiao X. 2006. Hydrogen peroxide stimulates macrophages and monocytes to actively release HMGB1. *J. Leukoc. Biol.*, **81**: 741–747.

Tsung A, Klune JR, Zhang X, Jeyabalan G, Cao Z, Peng X, Stolz DB, Geller DA, Rosengart MR, Billiar TR. 2007. HMGB1 release induced by liver ischemia involves Toll-like receptor 4–dependent reactive oxygen species production and calcium-mediated signaling. *J. Exp. Med.*, **204**: 2913–2923.

Vizoso-Vázquez A, Barreiro-Alonso A, Rico-Díaz A, Lamas-Maceiras M, Rodríguez-Belmonte E, Becerra M, González-Siso M., Cerdán M. 2017. HMGB proteins from yeast to human. Gene regulation, DNA repair and beyond. In *Old Yeasts - New Questions*.

Vizoso-Vázquez A, Lamas-Maceiras M, Fernandez-Leiro R, Rico-Diaz A, Becerra M, Cerdan ME. 2017. Dual function of Ixr1 in transcriptional regulation and recognition of cisplatin-DNA adducts is caused by differential binding through its two HMG-boxes. *Biochim. Biophys. Acta*, **1860**: 256–269.

Wang D, Lippard SJ. 2005. Cellular processing of platinum anticancer drugs. *Nat. Rev. Discov.*, **4**: 307–320.

Zamble DB, Mu D, Reardon JT, Sancar A, Lippard SJ. 1996. Repair of cisplatin-DNA adducts by the mammalian excision nuclease. *Biochemistry*, **35**: 10004–10013.

Objectives

The objective of the research work planned in this doctoral thesis is to analyze the interactions of Ixr1p, HMGB1 and HMGB2 with other cellular proteins using different methodologies. The characterization of these interactions is very helpful in order to understand the role of HMGB proteins in the cellular mechanisms of response to hypoxia and DNA damage. This knowledge can be used in future development of diagnosis and treatment strategies as well as in the control of mechanisms of resistance to platinum-derived drugs in cancer chemotherapy.

The specific objectives in this work are

1. To find Ixr1 binding proteins that are involved in transcriptional regulation in *Saccharomyces cerevisiae.*

2. To discover new HMGB1 and HMGB2 binding proteins in epithelial cells from human ovary and prostate.

3. To analyze the interactome of HMGB1 and HMGB2 in cancerous cells of epithelial origin from human ovary and prostate using a Yeast-Two-Hybrid (Y2H) approach.

4. To analyze the nuclear and cytoplasmic interactome of HMGB1 in cancerous cells of epithelial origin from ovary and prostate using a Co-immunoprecipitation/Mass Spectromerty approaches.

5. To discover specific proteins that bind HMGB1 after cisplatin treatment of cancerous cells of epithelial origin from ovary and prostate.

Chapter 1

The HMGB protein Ixr1 interacts with other proteins involved in transcriptional regulation

INTRODUCTION

Ixr1 is a *Saccharomyces cerevisiae* transcriptional factor that extensively regulates the response to hypoxia (Vizoso-Vazquez *et al.*, 2012) and has been also related to DNA repair (McA'Nulty and Lippard, 1996). We have previously characterized the interactions of Ixr1 with specific DNA sequences from the promoters of *ROX1* (Castro-Prego *et al.*, 2009) and *HEM13* (Castro-Prego *et al.*, 2010), two hypoxic genes regulated by this factor. Ixr1 binds to DNA through its 2 in-tandem high mobility group box (HMG-box) domains and we have shown that differential DNA-binding through these domains explains the recognition of cis-regulatory sequences or damaged DNA (Vizoso-Vazquez *et al.*, 2017). Besides, in-tandem arrangement of the 2 HMG-boxes in Ixr1 is required to form a stable complex with specific regulatory sequences that allows transcriptional activation of regulated genes *in vivo* (Vizoso-Vazquez *et al.*, 2017).

Although Ixr1 interaction with DNA targets in regulated promoters has been studied, the knowledge about the mechanisms by which this interaction affects transcriptional or post-transcriptional events modulating gene expression is poorly known. Transcriptional regulation implies a complex interplay among gene-specific transcriptional factors, co-regulators, general transcription factors (GTFs), and RNA polymerases acting on the chromatin template. In *S. cerevisiae,* during aerobic growth, the transcriptional repressor Rox1, other protein containing a single HMG-box domain (Deckert *et al.*, 1999), by interaction with the co-repressor complex Cyc8 (alias Ssn6)-Tup1 represses hypoxic genes (Zitomer, Limbach, *et al.*, 1997; Zitomer, Carrico, *et al.*, 1997). During hypoxia, rapid degradation of Rox1 (Deckert *et*

al., 1995) and interaction of Cyc8 with Sut1 relieves this repression (Regnacq *et al.*, 2001). *IXR1* is among the genes repressed by Rox1 in normoxia, and whose expression increases during hypoxia (Castro-Prego *et al.*, 2009). When oxygen availability is limiting, the mechanisms allowing high expression of hypoxic genes are not only based on de-repression; in addition, activation mechanisms usually have an important role in this scenario (Lowry *et al.*, 1990; Abramova *et al.*, 2001; Cohen *et al.*, 2001; Castro-Prego *et al.*, 2009). Indeed, positive mechanisms for *IXR1* activation during hypoxia have been described (Castro-Prego *et al.*, 2009).

In eukaryota, the mediator complex functions relaying signals from transcriptional activator or repressor factors to the RNA polymerase II (Poss *et al.*, 2013). The mediator complex in *S. cerevisiae* contains 21 core subunits and it is reversibly associated to the four-subunit Cdk8 kinase module composed by the kinase-cyclin pair Ssn3-Ssn8 (alias Srb10-Srb11), Med12 and Med13. However, mediator composition varies depending on the purification methods (Liu *et al.*, 2001) and/or growth conditions (Petrenko *et al.*, 2016). The kinase-cyclin pair Ssn3-Ssn8 is involved in transcriptional regulation (activation or repression) of diverse yeast genes, including those modulated by aerobic-hypoxic conditions (Becerra *et al.*, 2002; Nuñez *et al.*, 2007). However, the interconnection between the Ssn3-Ssn8 pair and Ixr1 has not been previously explored, in spite of that, all these factors are related to the hypoxic response in yeast.

Here, we present the first analysis about Ixr1 interactions with three factors that have been previously identified as important players in the yeast hypoxic response, Cyc8, Tup1 and Ssn8. We have also co-purified Ixr1 and interacting proteins, which have been identified by mass spectrometry

looking for putative co-regulators of transcription. Post-translational modification of Ixr1 associated to aerobic or hypoxic conditions have also been studied.

MATERIALS AND METHODS

Yeats strains and culture conditions

Growth transformation and handling of yeasts were carried out according to standard procedures. Cells were grown at 30 °C in YPD (2% glucose, 2% bacto-peptone, 1% yeast extract) or complete synthetic media, CM, prepared as previously described (Zitomer and Hall, 1976) with omissions of amino acids (CM-Aa), adenine (CM-Ade) or uracil (CM-Ura) when required for identification or selection of transformed cells. For hypoxic growth, cells were cultured in anaerobic jars with the GasPack EZAnaerobe system from Becton, Dickinson and Company (Franklin Lakes, NJ, USA), and under these conditions (oxygen concentration <1%), the medium was supplemented with 20 mg/l ergosterol and 0.5% Tween 80.

Construction of IXR1 derivatives and detection of transcriptional activation

IXR1 and derivatives with deletions in the NH_2 and COOH ends were cloned in frame to the Gal4 DNA binding domain (DNA-BD) in the plasmid pGBKT7 (Clontech, CA, USA). This vector allows high level expression of fusion proteins due to the constitutive *ADH1* promoter, and carries the *TRP1* gene that is used for auxotrophic selection in yeast. The constructs were verified by sequencing. Yeast Y2HGold cells (MATa, *trp1-901, leu2-3, 112, ura3-52, his3-200, gal4Δ, gal80Δ, LYS2::GAL1UAS-Gal1TATA-His3, GAL2UAS-*

Gal2TATA-Ade2 URA3:: MEL1UAS-Mel1TATA, AUR1-C MEL1) (Clontech, CA, USA) were transformed with constructions carrying Ixr1 and derivatives (described in Figure 1A) and plated in CM-Trp for selection. Activation of reporter genes (*HIS3*, *ADE2* and alfa-*GAL*) in the transformed cells was checked by testing growth in CM-Trp-His, CM-Trp-Ade and X-alfa-Gal activity. The enzymatic activity of α-galactosidase was measured using 4-nitrophenyl-α-D-galactopyranoside (α-PNPG). Transformed cells were grown to an OD_{600} of 3-4. Yeast pellets were collected by centrifugation at 3000 x g and vortexed with glass beads in 20 mM Tris pH 7.4 to obtain protein extracts; cell debris were eliminated by centrifugation. 150 µl of the supernatant was incubated for 5 min at 30 ºC. Reaction was started by addition of 150 µl 10 mM α-PNPG in reaction buffer (61 mM citric acid and 77 mM Na_2HPO4, pH 4). Aliquots of the reaction were stopped at three different times (5, 10 and 20 minutes) by mixing 100 µL of the reaction volume with 100 µl of 1 M Na_2CO_3. The release of p-nitrophenol (PNP) was measured by UV absorbance at 400 nm. α-galactosidase activity is given as specific activity in nmol/min mg. Protein concentration was determined by the Bradford assay (Bradford, 1976).

Yeast two hybrid (Y2H)

IXR1 was cloned in the plasmids pGAD-C2 (Amp^r ori 2µ *GAL4*-AD *LEU2*) and pGBD-C2 (Amp^r ori 2µ *GAL4*-BD *TRP1*) previously described (James *et al.*, 1996) and their selected partners (*TUP1, CYC8, SSN8*) were cloned in pGBD-C2 by PCR amplification and homologous recombination with the linear plasmid and PCR products in the yeast strain PJ69-4A (MATa *trp1-901 leu2-3 112 ura3-52 his3-200 gal4Δ gal80Δ LYS2::GAL1-HIS3 GAL2-ADE2 met2::GAL7-lacZ*) (James *et al.*, 1996). The primers used for the

constructions are related in Supplementary table 1. Y2H assays were carried out by the method previously described (James *et al.*, 1996) based on the reconstruction of the transcriptional activator Gal4 and with three reporter genes (*ADE2, HIS3* and *lacZ*) under its control. The constructions pGAD-C2-ScSrb11p (Ssn8) and pGBD-C2-ScSrb10p (Ssn3) previously described (Nuñez *et al.*, 2007) were used to obtain a positive control of interaction with Ssn8. The constructions pGAD-C2-Ixr1 and pGBD-C2-Ixr1 were used to test dimmer formation as previously suggested (Vizoso-Vazquez *et al.*, 2017). The yeast strain PJ69-4A (James *et al.*, 1996) was co-transformed with the corresponding pGAD-C2 and pGBD-C2 derivatives and transformed cells were selected in CM-Leu-Trp. Candidates were tested in CM-Ade, CM-His, and for beta-galactosidase activity in filters. Positive interactions were quantified by beta-galactosidase assays carried out in triplicate with independent colonies of transformed cells. Galactosidase activity measurements were performed according to the method of Guarente (Guarente, 1983) modified for implementation in Eppendorf tubes and following the release of the colored product o-nitrophenol (ONP) from the synthetic substrate o-nitrophenyl-β-D-galactopyranoside (ONPG) (Sigma-Aldrich). The activity was measured in cell-free extracts from 10 ml of culture, after resuspending the cells in buffer Z (100 mM Na_2HPO_4, 40 mM NaH_2PO_4, 10 mM KCl, 1.6 mM $MgSO_4$ and 2.7 ml of β-mercaptoethanol per liter of solution, pH 7). Mechanic lysis was performed with glass beads (Sigma-Aldrich) and 100 µl of sample were diluted into 400 µl of buffer Z pre-incubated at 30 °C for 5 minutes. Then, 250 µl of substrate solution (ONPG 4 mg/ml dissolved in distilled water) were added. The reaction was stopped by adding 250 µl Na_2CO_3 1 M and the mixture was centrifuged at 17000 x g for 5 minutes. ONP released was determined

spectrophotometrically at A_{420}. β-galactosidase activity is expressed in nmoles ONPG hydrolyzed min^{-1} mg^{-1} of total protein in the extract. A molar extinction coefficient of 4500 M^{-1} cm^{-1} was used in the calculation.

Affinity-co-purification of Ixr1 and its partner binding proteins from the YEpFLAG-1 vector

IXR1 was amplified using the primers AVV023 + AVV024 (Supplementary table 1) and cloned by homologous recombination in the high-copy plasmid YEpFLAG-1 (Amp^r ori 2µ FLAG *TRP1*) (Eastman Kodak Company). BJ3505 cells (MATa *pep4::HIS3 prb1-Δ1.6R lys2-208 trp1-Δ101 ura3-52 gal2 can*) were transformed with the construction and after plating in CM-Trp, transformed cells were grown in rich media YPHSM (Eastman Kodak Company). The final construct was expressed from the cells grown in 2 l YPHSM medium [1.5%(w/v) glucose, 3%(v/v) glycerol, 1%(w/v) yeast extract and 8%(w/v) peptone] in aerobic conditions at 30 ºC and 150 rpm for 72 h in a 2 l Erlenmeyer flask (2:1 ratio). Cells were collected by centrifugation (11800 x g for 10 min at 4 ºC) and the cell pellets were resuspended in buffer A (Tris-HCl pH 7.5, 150 mM NaCl, EDTA 2 mM, DTT 2 mM, 10% glycerol) supplemented with protease inhibitors (complete Mini Protease Inhibitor Cocktail, Roche). Cells were lysed by glass-bead vortexing, followed by centrifuge clarification at 30000 x g for 30 min at 4 ºC. The collected supernatants were loaded onto a gravity column containing anti-FLAG M2 affinity gel (Sigma Chemical, USA) previously equilibrated with buffer A. Protein complexes with Ixr1 were then eluted with FLAG peptide (DYKDDDDK) dissolved in buffer A and at 100 µg/ml. The protein solution was concentrated by ultrafiltration with Amicon Ultra-4 (Millipore).

Identification of Ixr1 and partners was carried out by MS analysis in the Proteomic unit of Instituto Investigaciones Biomédicas A Coruña (INIBIC). MALDI-TOF-TOF (Matrix-Assisted Laser Desorption/Ionization) was used to identify Ixr1 interacting proteins. Purified Ixr1 and bound proteins were concentrated, digested with trypsin and peptide composition was analyzed in the Proteomic unit of INIBIC. The samples were analyzed using the MALDI-TOF/TOF mass spectrometer 4800 Proteomics Analyzer (ABSCIEX, Framingham, MA) and 4000 Series ExplorerTM software (ABSCIEX). Data Explorer version 4.2 (ABSCIEX) was used for spectra analyses and generation of peak lists. Mass spectra were internally calibrated using auto-proteolytic trypsin fragments and externally calibrated using a standard peptide mixture (Sigma-Aldrich). Protein identification was carried out using ProteinPilot™ software v.4.0 (ABSciex). Each spectrum was searched in the Uniprot/Swissprot database for *S. cerevisiae*. Search parameters within ProteinPilot were set with trypsin cleavage specificity; methyl methanethiosulfate (MMTS) modified cysteine as fixed modifications; biological modification "ID focus" settings; and a protein minimum confidence score of 95%. Only proteins identified with at least 95% confidence, or a Prot Score (protein confidence measure) of at least 1.3 were reported. The results obtained from ProteinPilot were exported to Microsoft Excel for further analyses. Proteins identified by less than two unique peptides were discarded before functional mining. Functional networks among the identified Ixr1 preys were studied with STRING (Szklarczyk *et al.*, 2017).

Affinity-Co-purification of Ixr1 and its partner proteins from the YCplac33 vector

IXR1 tagged with FLAG in its N-terminus was cloned in the centromeric plasmid Ycplac33 (Amp^r, URA3, lacZ, ori 2µ) (Gietz and Sugino, 1988) by PCR amplification using the primers ECV775AV and ECV776AV containing *BamH*I and *Hind*III restriction sites for convenient digestion and subsequent ligation into the plasmid MCS (Supplementary table 1). This allows low *IXR1* expression under the regulation of its own promoter in aerobic conditions. To allow the purification of Ixr1 protein and its counterparts, a FLAG-tag was added to the N-terminus by inverted PCR using the primers AVV241 and AVV242 (Supplementary table 1), as previously described (Qi and Scholthof, 2008). The *S. cerevisiae* strain, W303*Δixr1* (Rodríguez-Lombardero *et al.*, 2012) was transformed with the construction. Ten liters of CM-Ura were used to grow transformed yeast overnight, until reaching exponential growth phase. Cells were lysed in a Beadbeater disruptor using glass beads. Subsequent steps to purify Ixr1 and binding proteins were performed as described above. Identification of proteins after trypsin digestion was done in the Proteomic unit of INIBIC using the MALDI-TOF/TOF mass spectrometer 4800 as explained in the previous section.

Identification of Ixr1 post-translational modifications

To determine specific phosphorylations, Ixr1 was expressed under the *ADH2* promoter in aerobic conditions from the YEpFLAG-1 construction above explained. Besides, Ixr1 with a HBH-tag in the COOH-terminal end was integrated in the *S. cerevisiae* W303 strain by PCR amplification of the HBH-TRP1 cassette with the primers AVV247 + AVV248 (Supplementary table 1),

homologous recombination and positive selection in CM-Trp plates. The HBH-tag is a derivative of the HB-tag series containing a bacterially derived biotinylation signal flanked by hexa-histidine motifs (Tagwerker *et al.*, 2006). The Ixr1-HBH was purified in denaturing conditions after hypoxic growth following the protocols and conditions previously described (Tagwerker *et al.*, 2006). In contrast to other tandem affinity purification methods, this strategy allows a two-step purification under high stringent (fully denaturing) conditions, avoiding undesirable loss of posttranslational modifications during cell lysis and guaranteeing the preservation of protein modifications in the *in vivo* state derived from particular culture conditions. The samples from both purifications were analyzed by LC-MS/MS (LTQ_Velos) in the "Centro de Biología Molecular Severo Ochoa" (CBMSO) protein chemistry facility.

RESULTS

Ixr1 activates transcription during normoxia when recruited to a heterologous promoter

It has been previously reported that Ixr1 is a repressor of hypoxic genes during normoxia (Lambert *et al.*, 1994; Bourdineaud *et al.*, 2000), although also acts as activator of other groups of genes (Vizoso-Vazquez *et al.*, 2012). We have confirmed that Ixr1 is able to activate transcription by directed recruitment to a heterologous promoter using the native Ixr1 protein and three mutants obtained by deletion of the amino, carboxyl or both terminal sequences (Figure 1A) using the plasmid pGBKT7 and yeast cells from Clontech (Clontech, CA, USA) as explained in materials and methods.

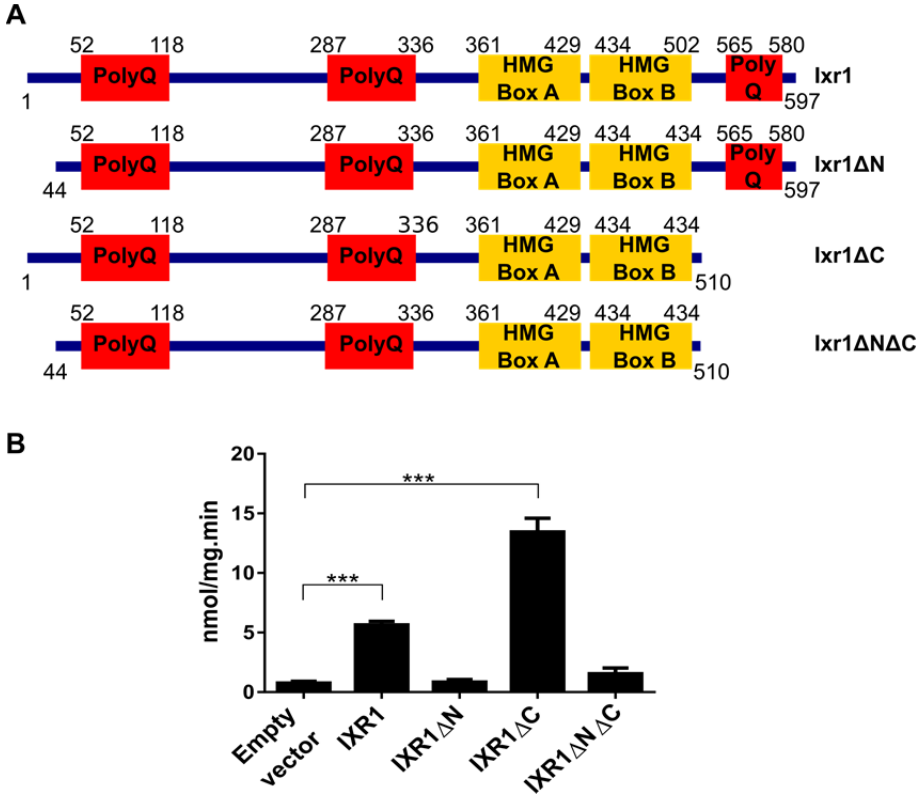

Figure 1. Functional domains in Ixr1. **(A)** Schematic representation of Ixr1 domains and deletions used in this study. **(B)** Transcriptional activator assay for the Ixr1 variants recruited to the *MEL1* promoter. Three biological replicas and two technical duplicates of each were carried out. Statistical significance was evaluated by a t-student test. *** p<0,001.

The fusion of the Gal4-DNA binding domain to Ixr1 allows expression of heterologous reporter genes under the control of Gal4, in absence of the Gal4 activator domain. Cells were able to grow in CM-Ade-His (data not shown) and alfa-galactosidase activity was detected (Figure 1B). Therefore, Ixr1 has a domain responsible for transcriptional activation through interactions with components of the transcriptional machinery. The protein depleted from the amino-end loses this capacity (Figure 1B), thus indicating that the eliminated sequence, consisting in the first 43 amino acids, is part

of an activation domain. Elimination of the carboxyl-end has the opposite effect upon transcriptional activation (Figure 1B), thus signaling this domain as repressor.

Ixr1 interacts with Ssn8 (Srb11)

Among the potential partners of Ixr1 in the transcriptional control of the *S. cerevisiae* aerobic-hypoxic regulon we have tested physical interactions by the Y2H method (James *et al.*, 1996) with Tup1, Cyc8 (Ssn6), and Ssn8 (Srb11). Considering that Ixr1 has a transcriptional activation domain, in order to avoid false positives, in the Y2H experiments Ixr1 was fused to the activation domain of Gal4 and preys were fused to the DNA-binding domain of Gal4. Data show that Ixr1 self-interacts (Figure 2), which has been attributed to oligomerization. We have found that among the tested targets, only Ssn8 (Srb11) is a positive prey (Figure 2).

This discards that in aerobiosis the repressor effect of Ixr1 on hypoxic genes is mediated by the general co-repressor complex Tup1-Cyc8.

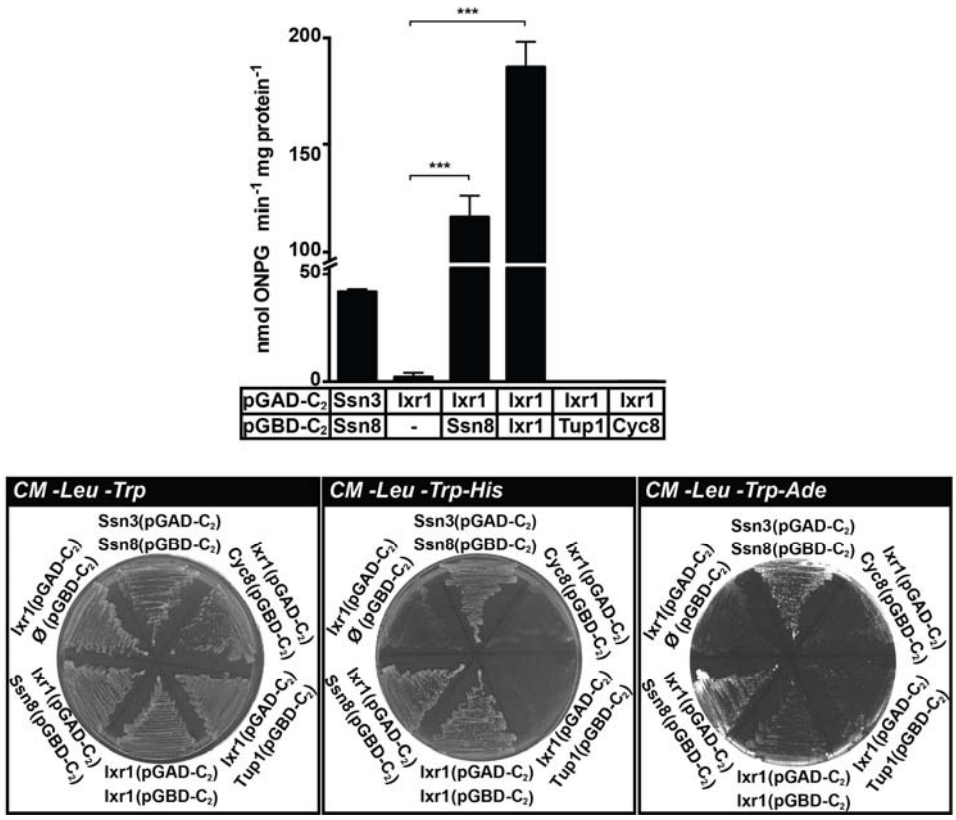

Figure 2. Two Hybrid assay of Ixr1 interactions with Ssn8, Tup1 and Cyc8. Beta-galactosidase reporter activity was measured in three biological replica and two technical duplicates of each. Statistical significance ($p < 0.01$) was evaluated by a t-student test.

In order to find data supporting that the mechanism of transcriptional regulation mediated by Ixr1 might depend on the four-subunit Cdk8 kinase module, through the detected physical interaction between Ixr1 and Ssn8, we have looked for genes previously identified under the control of the proteins of the Cdk8 kinase module (Ssn3, Ssn8, Med12 and Med13). Ixr1 regulated targets (Vizoso-Vazquez *et al.*, 2012) were compared with available data from Ssn3, Med12 and Med13-targets (Hu *et al.*, 2007).

Table 1. Co-regulated targets of Ixr1 and CDK8 complex subunits

Co-regulated genes			Hu Z, *et al*. (2007)		
			Ssn3	Med12	Med13
Vizoso-Vázquez A, *et al*. (2012)	Ixr1 targets	*ALE1*	+	-	-
		ARG1	+	-	-
		CWP1	+	+	-
		DDR2	-	+	+
		FIT3	-	+	+
		GCV2	-	-	+
		GLK1	-	+	+
		GRE1	-	+	-
		GSY1	-	-	+
		HSP12	-	+	-
		PTR2	-	+	+
		SPT1	-	+	+
		TPO4	-	+	+
		TSL1	+	+	+
		YCR013C	+	-	-
		YGP1	-	+	+
		ZRT1	-	+	+
CDK8 targets (positive/total)			(5/11)	(12/29)	(11/27)

The common targets obtained in these comparisons (Table 1) reveal that 40-45% of genes regulated by Ssn3, Med12 or Med13 are also regulated by Ixr1. As reference value, and according to similar calculations from previous data (Hu *et al.*, 2007), Med12 and Med13, which belong to the same complex, have 48.1% of common targets. Data from a large-scale genetic perturbations study that includes the four components of the Cdk8 kinase module (Kemmeren *et al.*, 2014) indicate that in aerobic conditions this subcomplex has a predominant repressor role on transcription. The data of Ixr1-repressed targets in aerobic conditions (Vizoso-Vazquez *et al.*, 2012) were compared with the data sets of aerobic repressed genes by Ssn3, Ssn8, Med12 and Med13 (Kemmeren *et al.*, 2014) and results are shown in Table 2. Also in this comparison it is possible to find common targets (Table 2), although the percentage is minor than in the previous one (Table 1).

Table 2. Co-repressed targets of Ixr1 and Cdk8 complex subunits during normoxia

Co-repressed genes			(Kemmeren *et al*., 2014) Ssn3 target	Ssn8 target	Med12 target	Med13 target
Vizoso-Vázquez A, *et al*. (2012)	Ixr1 targets	*ALD3*	+	+	+	+
		CTT1	+	+	+	+
		DAK1	+	-	-	-
		GRE1	+	+	+	+
		GSY2	+	+	-	+
		HMS1	+	+	+	-
		HOR7	+	+	+	+
		PAI3	+	+	+	+
		PBI2	+	+	-	+
		PTR2	+	+	+	+
		SIP18	+	+	+	+
		SPI1	+	+	+	+
		SSA4	+	+	+	+
		SSE2	+	-	-	-
		STF2	+	+	-	-
		TFS1	+	+	+	+
		TKL2	+	+	+	+
		UGP1	+	+	+	+
		YGP1	+	+	+	+
		YJR096W	+	+	-	+
		YLR149C	+	+	-	+
CDK8 targets (positive/total)			(21/128)	(19/99)	(14/82)	(17/88)

Identification of other proteins that interact with Ixr1 by co-purification and MS

We have also identified yeast proteins that co-purify with Ixr1 using two purification approaches, trying to find other partners, which may influence Ixr1 functions.

Ixr1 was cloned in the YEpFLAG-1 plasmid under the regulation of the inducible promoter *ADH2*. This approach allows high expression of Ixr1 in aerobiosis after glucose consumption. The bait protein and preys were purified by affinity using anti-Flag antibody. After purification, following the

protocols described in Materials and methods, the proteins in the sample were concentrated, digested with trypsin, and peptides identified by MALDI-TOF-TOF analysis. The results (Supplementary table 2) allowed the identification of 65 yeast Ixr1-binding proteins with at least two unique peptides detected. None of these proteins have been previously experimentally identified to bind Ixr1 according to STRING analysis and the majority clearly clusters in two groups. One related to ribosome components and other related to glycolysis/gluconeogenesis (Figure 3A).

Since the expression system usually conditions protein levels, and indirectly the possibility of artifacts in the detection of co-purified proteins, we performed a second strategy using the expression plasmid Ycplac33, in which Ixr1 transcription is under the control of the Ixr1 promoter. This approach guaranteed aerobic expression of Ixr1 at natural levels. Ixr1 and co-purified proteins were concentrated, digested with trypsin and peptides were identified by MALDI-TOF-TOF analysis. In this approach a total of 38 proteins were identified with at least two unique peptides detected (Supplementary table 3). None of these proteins were previously known to bind Ixr1 according to STRING analysis, and the majority clearly belongs to the cluster "ribosome components" or to the cluster "glycolysis/gluconeogenesis" (Figure 3B). The intersection of Ixr1 preys identified in the two approaches (high or low Ixr1 aerobic expression) gives 14 proteins, 7 related to glucose metabolism (Pgk1, Eno2, Tdh3, Eno1, Tdh1, Pdc1, Adh1), 2 related to stress (Ssa1, Hsc82), 2 ribosomal proteins (Rpp0, Rpl5), 1 translational elongation factor (Tef1), actin (Act1) and 1 related to cell division cycle (Cdc9).

.

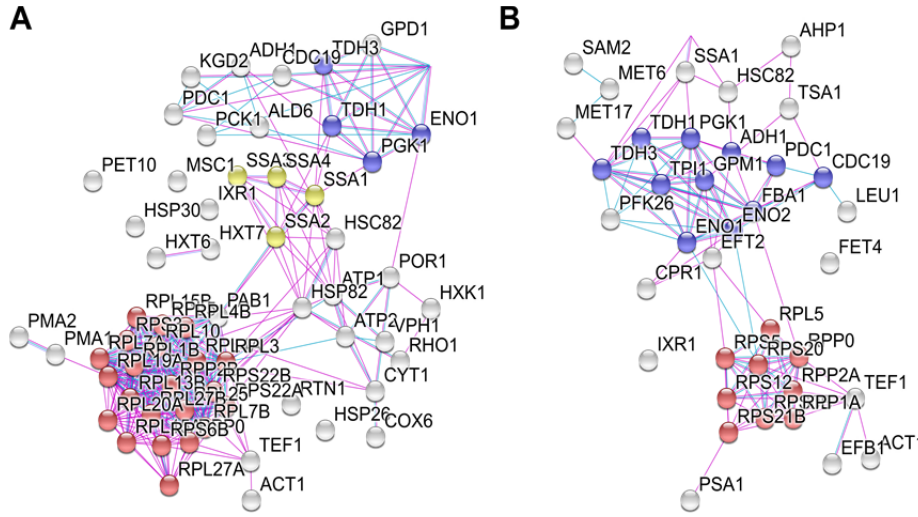

Figure 3. Interactome of Ixr1. Analysis for functional enrichment was done with STRING. (A) High aerobic over-expression of Ixr1 driven by the *ADH2* promoter; blue represents GO:0006094, gluconeogenesis, with a False Discovery Rate (FDR) of 3.8e-05; red represents GO:0022626, cytosolic ribosome, with FDR of 1.64e-18; yellow is IPR013126, Heat shock protein 70 family, with FDR of 0.00522. **(B)** Native aerobic expression driven by *IXR1* promoter; blue represents GO:00010, glycolysis/gluconeogenesis, with a FDR of 4.37e-13; red represents GO:0022626, cytosolic ribosome, with a FDR of 3.62e-05.

Modification of Ixr1 by phosphorylation differs in aerobic and hypoxic conditions

It has been previously suggested that Ixr1 is a highly phosphorylated protein (Tsaponina *et al.*, 2011), therefore we wanted to know the extension and localization of these modifications and whether they could be influenced by the aerobic/hypoxic conditions. Aerobic expression of Ixr1 for purification and identification of phosphorylated residues was performed using the construction of Ixr1 in the YEpFLAG-1 plasmid previously described. Hypoxic expression of Ixr1 was achieved from the genomic copy of Ixr1 expressed by its own promoter and COOH-tagged with HBH, which allows purification under denaturing conditions. In each approach the isolated protein was

further purified by electrophoresis in gel, eluted from the band and digested with trypsin or quimotrypsin. The second digestion was more adequate for identifying phosphorylated peptides. Positions identified are shown in Figure 4 and correspond to S6 and S83 in aerobic conditions or T45 and S559 in hypoxia.

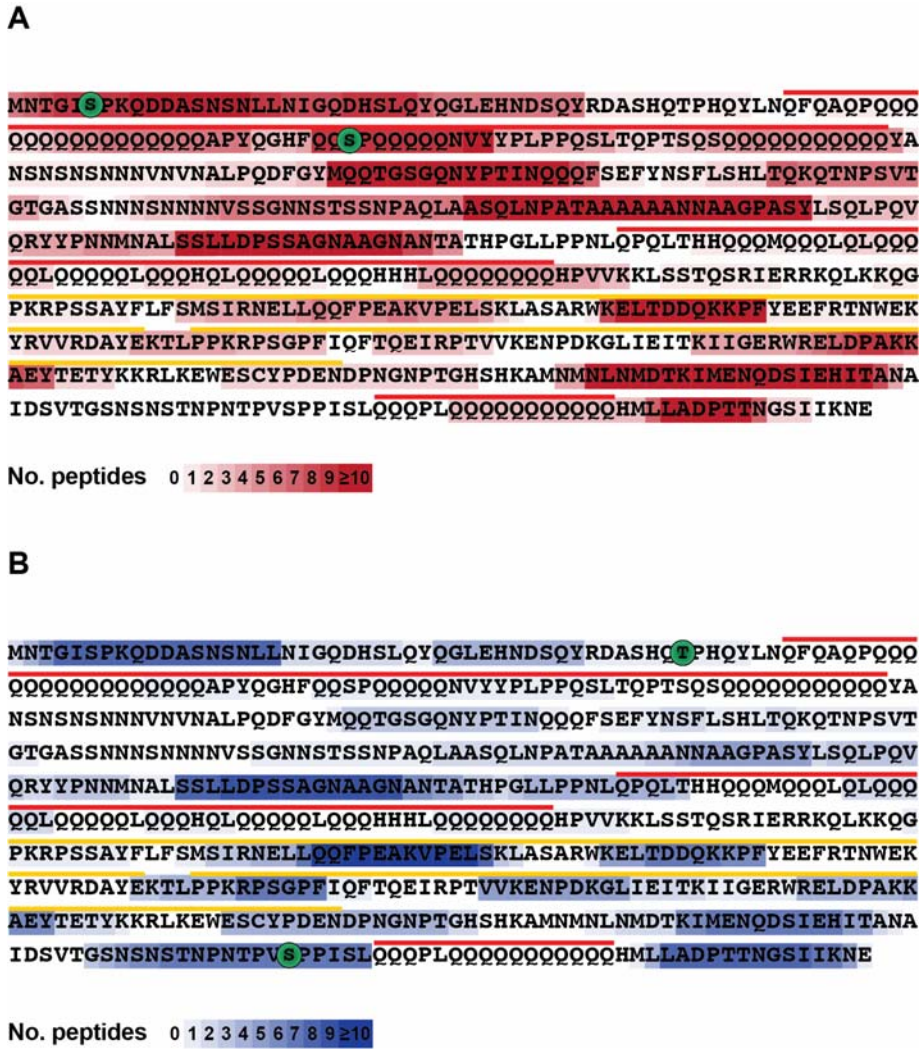

Figure 4. Phosphorylated sites in Ixr1 as shown by MS analysis. (A) Aerobic conditions. **(B)** Hypoxic conditions.

DISCUSSION

Although it is already known that Ixr1 can behave as a specific transcriptional factor controlling sub-sets of genes or regulons during hypoxia and oxidative stress (Lambert *et al.*, 1994; Bourdineaud *et al.*, 2000; Castro-Prego *et al.*, 2009; Vizoso-Vazquez *et al.*, 2012) the mechanisms affecting the basal transcriptional machinery had not been explored in detail. In aerobiosis the repressor function of Ixr1 on yeast promoters predominates over activation (Vizoso-Vazquez *et al.*, 2012). During hypoxia the expression of Ixr1 increases (Castro-Prego *et al.*, 2009), and the model changes; in this condition Ixr1 activates an increased number of genes, which are necessary at low oxygen levels (Vizoso-Vazquez *et al.*, 2012). The results presented here show that Ixr1 has an intrinsic activator capacity when artificially recruited to a promoter with a Gal4 binding site (Figure 1) and the NH_2-terminus of Ixr1 is necessary for this function (Figure 1). This mechanism might explain the activator function of Ixr1 upon a subset of genes.

Our data clearly show that Ixr1 interacts with Ssn8 (Srb11) in aerobic conditions (Figure 2). In *S. cerevisiae*, the Cdk8 kinase module has been associated with the Mediator coactivator and facilitates the recruitment, or stable association, of TBP to the *GAL1* promoter (Larschan and Winston, 2005). But at genome scale, the Cdk8 kinase module majorly mediates processes of transcriptional repression in *S. cerevisiae* (Kemmeren *et al.*, 2014), and it has been demonstrated that the general co-repressor Cyc8-Tup1 interacts *in vivo* with Ssn8, a subunit of this Cdk8 kinase module (Schuller and Lehming, 2003). Our data shows that Ixr1, although having a

repressor effect on several promoters (i.e. hypoxic genes during aerobiosis), does not interact with Cyc8 or Tup1. Genes in the Rox1 regulon need the interaction of the specific repressor Rox1 with the general co-repressor Cyc8-Tup1 complex to be down-regulated during aerobiosis (Zitomer, Carrico, *et al.*, 1997). However, genes in the Ixr1 regulon might have overpass this requirement by the existing direct interaction between Ixr1 and Ssn8, since we do not detect interaction with the Cyc8-Tup1 co-repressor components.

The connection of Ixr1 and the Mediator complex, via the Cdk8 kinase module, is interesting from the point of view that the Mediator has been considered as an antenna sensor for multiple environmental and cellular changes that affect transcription. The Mediator is generally targeted by specific transcription factors that control gene expression programs in response to developmental or environmental cues (Poss *et al.*, 2013). Ixr1 adequately fits in this general scheme, since it influences transcription of different gene clusters in response to oxygen availability (Vizoso-Vazquez *et al.*, 2012). Besides, in humans, it has been demonstrated that the Mediator also participates in DNA repair (Kikuchi *et al.*, 2015) and Ixr1, in yeast, also takes part in this process (McA'Nulty and Lippard, 1996; Tsaponina and Chabes, 2013).

We have also detected that Ixr1 interacts with Tdh3, encoding the enzyme glyceraldehyde-3-phosphate dehydrogenase. Interestingly, a previous report of a nuclear interaction of the human homologous protein with other HMGB proteins exists, since altogether with HSP70 and ERP60, glyceraldehyde-3-phosphate dehydrogenase forms a complex with HMGB1 and HMGB2 that is involved in a cytotoxic response to modified DNA

(Krynetski *et al.*, 2003). In *S. cerevisiae*, Tdh3 has nuclear functions unrelated to the glycolytic pathway, and it was demonstrated that Tdh3 interacts with Sir2, a NAD(+)-dependent histone deacetylase that regulates transcriptional silencing and rDNA recombination (Ringel *et al.*, 2013). It is possible to speculate that a part of the repressor effect of Ixr1 during aerobiosis might be dependent on Tdh3 silencing, thus explaining the existence of only partial overlap between the targets of Ixr1 and Cdk8 kinase module.

MS experiments demonstrate that Ixr1, besides participating in nuclear interactions related to DNA transcription and DNA repair, also interacts with other proteins mainly associated to ribosome, cytoplasm and plasma membrane (Figure 3A). Although many of these interactions are probably not physiological and could be attributed to experimental over-expression of Ixr1, our data clearly shows that, even when using conditions of low Ixr1 expression, it is possible to detect proteins of these functional groups interacting with Ixr1 (Figure 3B).

The complete picture about how Ixr1 controls positive or negative regulatory transcriptional responses in aerobiosis or anaerobiosis remains to be elucidated. From our results we conclude that Ixr1 has an activator domain that would explain its activator function by interaction with the transcriptional machinery. The repressor function of Ixr1 in aerobiosis does not depend on direct interaction with the Ccy8-Tup1 co-repressor. The new discovered Ixr1 interaction with Ssn8 probably affects the Mediator function or causes indirect recruitment of the Cyc8-Tup1 co-repressor, as previously supported by the reported binding between Ssn8 and the Cyc8-Tup1 complex (Schuller and Lehming, 2003). Ixr1 also interacts with Tdh3

that has been previously associated with transcriptional silencing by de-acetylation (Ringel *et al.*, 2013). Our findings showing that Ixr1 has specific phosphorylated residues in aerobic or anaerobic conditions suggest that interactions with other proteins related to mechanisms of transcriptional activation or repression might be conditioned by these post-translational modifications. Interestingly, Ser6 phosphorilated in aerobiosis is included in the NH_2-terminal region of Ixr1, which is involved in transcriptional activation; Ser559, phosphorylated in aerobiosis is included in the COOH-terminal region of Ixr1, which has been associated to repression. Further studies are needed to conclude whether these differential post-translational modifications of Ixr1 affect the interactions with Ssn8, Tdh3 or other transcriptional regulators.

REFERENCES

Abramova NE, Cohen BD, Sertil O, Kapoor R, Davies KJ, Lowry C V. 2001. Regulatory mechanisms controlling expression of the DAN/TIR mannoprotein genes during anaerobic remodeling of the cell wall in Saccharomyces cerevisiae. *Genetics*, **157**: 1169–1177.

Becerra M, Lombardia-Ferreira LJ, Hauser NC, Hoheisel JD, Tizon B, Cerdan ME. 2002. The yeast transcriptome in aerobic and hypoxic conditions: effects of hap1, rox1, rox3 and srb10 deletions. *Mol. Microbiol.*, **43**: 545–555.

Bourdineaud JP, De Sampaio G, Lauquin GJ. 2000. A Rox1-independent hypoxic pathway in yeast. Antagonistic action of the repressor Ord1 and activator Yap1 for hypoxic expression of the SRP1/TIR1 gene. *Mol. Microbiol.*, **38**: 879–890.

Bradford MM. 1976. A rapid and sensitive method for the quantitation of microgram quantities of protein utilizing the principle of protein-dye binding. *Anal. Biochem.*, **72**: 248–254.

Castro-Prego R, Lamas-Maceiras M, Soengas P, Carneiro I, Gonzalez-Siso I, Cerdan ME. 2009. Regulatory factors controlling transcription of

Saccharomyces cerevisiae IXR1 by oxygen levels: a model of transcriptional adaptation from aerobiosis to hypoxia implicating ROX1 and IXR1 cross-regulation. *Biochem. J.*, **425**: 235–243.

Castro-Prego R, Lamas-Maceiras M, Soengas P, Fernandez-Leiro R, Carneiro I, Becerra M, Gonzalez-Siso MI, Cerdan ME. 2010. Ixr1p regulates oxygen-dependent HEM13 transcription. *FEMS Yeast Res.*, **10**: 309–321.

Cohen BD, Sertil O, Abramova NE, Davies KJ, Lowry C V. 2001. Induction and repression of DAN1 and the family of anaerobic mannoprotein genes in Saccharomyces cerevisiae occurs through a complex array of regulatory sites. *Nucleic Acids Res.*, **29**: 799–808.

Deckert J, Khalaf RA, Hwang SM, Zitomer RS. 1999. Characterization of the DNA binding and bending HMG domain of the yeast hypoxic repressor Rox1. *Nucleic Acids Res.*, **27**: 3518–3526.

Deckert J, Perini R, Balasubramanian B, Zitomer RS. 1995. Multiple elements and auto-repression regulate Rox1, a repressor of hypoxic genes in Saccharomyces cerevisiae. *Genetics*, **139**: 1149–1158.

Gietz RD, Sugino A. 1988. New yeast-Escherichia coli shuttle vectors constructed with in vitro mutagenized yeast genes lacking six-base pair restriction sites. *Gene*, **74**: 527–534.

Guarente L. 1983. Yeast promoters and lacZ fusions designed to study expression of cloned genes in yeast. *Methods Enzymol.*, **101**: 181–191.

Hu Z, Killion PJ, Iyer VR. 2007. Genetic reconstruction of a functional transcriptional regulatory network. *Nat. Genet.*, **39**: 683–687.

James P, Halladay J, Craig EA. 1996. Genomic Libraries and a Host Strain Designed for Highly Efficient Two-Hybrid Selection in Yeast. *Genetics*, **144**: 1425–1436.

Kemmeren P, Sameith, K, van de Pasch, LA, Benschop, JJ, Lenstra, TL, Margaritis, T. 2014. Large-scale genetic perturbations reveal regulatory networks and an abundance of gene-specific repressors. *Cell*, **157**: 740–752.

Kikuchi Y et al. 2015. Human mediator MED17 subunit plays essential roles in gene regulation by associating with the transcription and DNA repair machineries. *Genes Cells*, **20**: 191–202.

Krynetski EY, Krynetskaia NF, Bianchi ME, Evans WE. 2003. A nuclear protein complex containing high mobility group proteins B1 and B2, heat shock cognate protein 70, ERp60, and glyceraldehyde-3-phosphate

dehydrogenase is involved in the cytotoxic response to DNA modified by incorporation of anticancer nucleoside. *Cancer Res.*, **63**: 100–106.

Lambert JR, Bilanchone VW, Cumsky MG. 1994. The ORD1 gene encodes a transcription factor involved in oxygen regulation and is identical to IXR1, a gene that confers cisplatin sensitivity to Saccharomyces cerevisiae. *Proc. Natl. Acad. Sci. U. S. A.*, **91**: 7345–7349.

Larschan E, Winston F. 2005. The Saccharomyces cerevisiae Srb8-Srb11 complex functions with the SAGA complex during Gal4-activated transcription. *Mol. Cell. Biol.*, **25**: 114–123.

Liu Y, Ranish JA, Aebersold R, Hahn S. 2001. Yeast nuclear extract contains two major forms of RNA polymerase II mediator complexes. *J. Biol. Chem.*, **276**: 7169–7175.

Lowry C V, Cerdan ME, Zitomer RS. 1990. A hypoxic consensus operator and a constitutive activation region regulate the ANB1 gene of Saccharomyces cerevisiae. *Mol. Cell. Biol.*, **10**: 5921–5926.

McA'Nulty MM, Lippard SJ. 1996. The HMG-domain protein Ixr1 blocks excision repair of cisplatin-DNA adducts in yeast. *Mutat. Res.*, **362**: 75–86.

Nuñez L, Gonzalez-Siso MI, Becerra M, Cerdan ME. 2007. Functional motifs outside the kinase domain of yeast Srb10p. Their role in transcriptional regulation and protein-interactions with Tup1p and Srb11p. *Biochim. Biophys. Acta*, **1774**: 1227–1235.

Petrenko N, Jin Y, Wong KH, Struhl K. 2016. Mediator Undergoes a Compositional Change during Transcriptional Activation. *Mol. Cell*, **64**: 443–454.

Poss ZC, Ebmeier CC, Taatjes DJ. 2013. The Mediator complex and transcription regulation. *Crit. Rev. Biochem. Mol. Biol.*, **48**: 575–608.

Qi D, Scholthof KB. 2008. A one-step PCR-based method for rapid and efficient site-directed fragment deletion, insertion, and substitution mutagenesis. *J. Virol. Methods*, **149**: 85–90.

Regnacq M, Alimardani P, El Moudni B, Berges T. 2001. SUT1p interaction with Cyc8p(Ssn6p) relieves hypoxic genes from Cyc8p-Tup1p repression in Saccharomyces cerevisiae. *Mol. Microbiol.*, **40**: 1085–1096.

Ringel AE, Ryznar R, Picariello H, Huang KL, Lazarus AG, Holmes SG. 2013. Yeast Tdh3 (glyceraldehyde 3-phosphate dehydrogenase) is a Sir2-interacting factor that regulates transcriptional silencing and rDNA

recombination. *PLoS Genet.*, **9**: e1003871.

Rodríguez-Lombardero S, Vizoso-Vázquez A, Rodríguez-Belmonte E, González-Siso MI, Cerdán ME. 2012. SKY1 and IXR1 interactions, their effects on cisplatin and spermine resistance in Saccharomyces cerevisiae. *Can. J. Microbiol.*, **58**: 184–188.

Schuller J, Lehming N. 2003. The cyclin in the RNA polymerase holoenzyme is a target for the transcriptional repressor Tup1p in Saccharomyces cerevisiae. *J. Mol. Microbiol. Biotechnol.*, **5**: 199–205.

Szklarczyk D et al. 2017. The STRING database in 2017: quality-controlled protein-protein association networks, made broadly accessible. *Nucleic Acids Res.*, **45**: D362–D368.

Tagwerker C, Zhang H, Wang X, Larsen LS, Lathrop RH, Hatfield GW, Auer B, Huang L, Kaiser P. 2006. HB tag modules for PCR-based gene tagging and tandem affinity purification in Saccharomyces cerevisiae. *Yeast*, **23**: 623–632.

Tsaponina O, Barsoum E, Astrom SU, Chabes A. 2011. Ixr1 is required for the expression of the ribonucleotide reductase Rnr1 and maintenance of dNTP pools. *PLoS Genet.*, **7**: e1002061.

Tsaponina O, Chabes A. 2013. Pre-activation of the genome integrity checkpoint increases DNA damage tolerance. *Nucleic Acids Res.*, **41**: 10371–10378.

Vizoso-Vazquez A, Lamas-Maceiras M, Becerra M, Gonzalez-Siso MI, Rodriguez-Belmonte E, Cerdan ME. 2012. Ixr1p and the control of the Saccharomyces cerevisiae hypoxic response. *Appl. Microbiol. Biotechnol.*, **94**: 173–184.

Vizoso-Vazquez A, Lamas-Maceiras M, Fernandez-Leiro R, Rico-Diaz A, Becerra M, Cerdan ME. 2017. Dual function of Ixr1 in transcriptional regulation and recognition of cisplatin-DNA adducts is caused by differential binding through its two HMG-boxes. *Biochim. Biophys. Acta*, **1860**: 256–269.

Zitomer RS, Carrico P, Deckert J. 1997. Regulation of hypoxic gene expression in yeast. *Kidney Int.*, **51**: 507–513.

Zitomer RS, Limbach MP, Rodriguez-Torres AM, Balasubramanian B, Deckert J, Snow PM. 1997. Approaches to the study of Rox1 repression of the hypoxic genes in the yeast Saccharomyces cerevisiae. *Methods*, **11**: 279–288.

ANNEXE TO CHAPTER 1

Supplementary table 1. Oligonucleotides used in this study.

Name	Sequence	Gene	S	RS
ECV410	ggg**ggatcc**ATCCGGGCGGTGAACAA	*CYC8*	W	*BamHI*
ECV411	ggg**gtcgac**CGTCGTAGTTTTCATCTTCTTCCA	*CYC8*	C	*Sal*I
ECV412	ggg**atcgac**CTGCCAGCGTTTCGAATAC	*TUP1*	W	*Cla*I
ECV413	ggg**ctgcag**TTGGCGCTATTTTTTTATACTTC	*TUP1*	C	*Pst*I
ECV352	ggg**ggatcc**CGGGGAGCTTCTGGACATC	*SSN8*	W	*BamH*I
ECV353	ggg**gtcgac**TTGCAGATGCTGGTCTAAGATACAA	*SSN8*	C	*Sal*I
ECV354	ggg**ggatcc**ATAATGGCAAGGATAGAGCACA	*SSN3*	W	*BamH*I
ECV355	ggg**gtcgac**TTCTGTTTTTCTTTCGAGATGG	*SSN3*	C	*Sal*I
ECV657	ggg**gtcgac**CATTTTTTATGATCGAACCATTTGTAGTGTAGTG	*IXR1*	W	*BamH*I
ECV658	ggg**gtcgac**CATTTTTTATGATCGAACCATTTGTAGTGTAGTG	*IXR1*	C	*Sal*I
AVV023	ctatatcgtaatacaccaagctcgacctcgcgATGAACACCGGTATCTC GCC	*IXR1*	W	-
AVV024	ggtcgacgggcccggatccatcgatagatctttTTATTCATTTTTTATGA TCGAACC	*IXR1*	C	-
ECV775AV	ggg**ggatcc**GGGAGCCTGTGTACAGACCTATG	*IXR1*	W	*BamHI*
ECV776AV	ggg**aagctt**TTAACTGGTTTGTCTAGGCAGGG	*IXR1*	C	*HindIII*
AVV241	gactacaaggatgacgatgacaagAACACCGGTATCTCGCCCAAAC	*IXR1*	W	-
AVV242	agcataatctggaacatcatatggataCATTGCAGTTGTGGGTACTGT TAG	*YEP-FLAG*	C	-
ABA1	CATGGAGGCC**GAATTC**ATGAACACCGGTATCTCGCCC	*IXR1*	W	*EcoRI*
ABA2	GCAG**GTCGAC**GGATCCTTATTCATTTTTTATGATCGAACCAT TTGT	*IXR1*	C	*SalI*
ABA1b	GCAG**GTCGAC**GGATCCTTAACCGGTTGGGTTACCGT	*IXR1ΔC*	W	*SalI*
ABA2b	CATGGAGGCC**GAATTC**ATGCAATACTTGAACCAGTTTCAAG CCC	*IXR1ΔN*	C	*EcoRI*

S: strand; **RS**: Restriction Site in bold

Supplementary table 2. Preys of Ixr1 purified from YEpFLAG-1 (over-expressed).

C	P	GENE	Accession	Name
74.7	73	IXR1	P33417	Intrastrand cross-link recognition protein
86.3	36	HSP71	P10591	Heat shock protein Ssa1
81.7	26	HSP72	P10592	Heat shock protein Ssa2
86.5	22	EF1A	P02994	Elongation factor 1-alpha
94.6	20	G3P3	P00359	Glyceraldehyde-3-phosphate dehydrogenase 3
90.6	20	HSP26	P15992	Heat shock protein 26 OS=Saccharomyces cerevisiae
85.6	19	PGK	P00560	Phosphoglycerate kinase
66.1	19	ADH1	P00330	Alcohol dehydrogenase 1
87.1	17	G3P1	P00360	Glyceraldehyde-3-phosphate dehydrogenase 1
68.9	16	PDC1	P06169	Pyruvate decarboxylase isozyme 1
77.1	15	HSP74	P22202	Heat shock protein Ssa4
87.4	14	ENO2	P00925	Enolase 2 OS=Saccharomyces cerevisiae
70.0	14	KPYK1	P00549	Pyruvate kinase 1 OS=Saccharomyces cerevisiae
87.0	13	ENO1	P00924	Enolase 1
72.1	12	HSP73	P09435	Heat shock protein Ssa3
74.7	11	PCKA	P10963	Phosphoenolpyruvate carboxykinase [ATP]
81.6	10	ATPB	P00830	ATP synthase subunit beta, mitochondrial
82.9	9	RPL4A	P10664	60S ribosomal protein L4-A
78.5	9	RPL4B	P49626	60S ribosomal protein L4-B
72.3	9	ATPA	P07251	ATP synthase subunit alpha, mitochondrial
54.5	9	VPH1	P32563	V-type proton ATPase subunit a, vacuolar isoform
61.3	8	PMA2	P19657	Plasma membrane ATPase 2
59.0	8	RPLA0	P05317	60S acidic ribosomal protein P0
63.4	7	PMA1	P05030	Plasma membrane ATPase 1
58.0	6	VDAC1	P04840	Mitochondrial outer membrane protein porin 1
39.6	6	RPL1B	P0CX44	60S ribosomal protein L1-B
39.6	6	RPL1A	P0CX43	60S ribosomal protein L1-A
82.7	5	RPL3	P14126	60S ribosomal protein L3
71.9	5	RPL13B	P40212	60S ribosomal protein L13-B
70.6	5	RPL15A	P05748	60S ribosomal protein L15-A

Supplementary table 2. Continuation

C	P	GENE	Accession	Name
63.2	5	PET10	P36139	Protein PET10
61.7	5	RPS3	P05750	40S ribosomal protein S3
58.2	5	RPL7B	Q12213	60S ribosomal protein L7-B
55.7	5	RPL7A	P05737	60S ribosomal protein L7-A
39.4	5	RPL10	P41805	60S ribosomal protein L10
69.5	4	RPS6B	P0CX38	40S ribosomal protein S6-B
69.5	4	RPS6A	P0CX37	40S ribosomal protein S6-A
67.8	4	MSC1	Q03104	Meiotic sister chromatid recombination protein 1
64.7	4	RPL27B	P0C2H7	60S ribosomal protein L27-B
63.7	4	RPL15B	P54780	60S ribosomal protein L15-B
58.4	4	HSC82	P15108	ATP-dependent molecular chaperone Hsc82
55.4	4	RPLA4	P02400	60S acidic ribosomal protein P2-beta
50.6	4	RPL20B	P0CX24	60S ribosomal protein L20-B
50.6	4	RPL20A	P0CX23	60S ribosomal protein L20-A
50.0	4	RPL27A	P0C2H6	60S ribosomal protein L27-A
48.8	4	ACT	P60010	Actin
45.6	4	HSP82	P02829	ATP-dependent molecular chaperone Hsp82
70.4	3	ODO2	P19262	Dihydrolipoyllysine-residue succinyltransferase component of 2-oxoglutarate dehydrogenase complex, mitochondrial
66.0	3	RPL5	P26321	60S ribosomal protein L5
52.4	3	HXKA	P04806	Hexokinase-1
45.0	3	GPD1	Q00055	Glycerol-3-phosphate dehydrogenase [NAD] 1
39.8	3	HSP30	P25619	30 kDa heat shock protein
90.1	2	RPL25	P04456	60S ribosomal protein L25
66.9	2	RPS22A	P0C0W1	40S ribosomal protein S22-A
65.4	2	RPS22B	Q3E7Y3	40S ribosomal protein S22-B
62.2	2	RHO1	P06780	GTP-binding protein Rho1
62.2	2	COX6	P00427	Cytochrome c oxidase subunit 6, mitochondrial
53.7	2	CY1	P07143	Cytochrome c1, heme protein, mitochondrial
53.2	2	ALDH6	P54115	Magnesium-activated aldehyde dehydrogenase, cytosolic
51.6	2	HXT6	P39003	High-affinity hexose transporter Hxt6

Supplementary table 2. Continuation

C	P	GENE	Accession	Name
51.2	2	RTN1	Q04947	Reticulon-like protein 1
47.9	2	HXT7	P39004	High-affinity hexose transporter Hxt6
46.8	2	PABP	P04147	Polyadenylate-binding protein, cytoplasmic and nuclear
45.0	2	RPL19B	P0CX83	60S ribosomal protein L19-B
45.0	2	RPL19A	P0CX82	60S ribosomal protein L19-A

C: % coverage; **P:** peptides (95%)

Supplementary table 3. Preys of Ixr1 purified from YCplac33 (low-expressed).

C	P	GENE	Accession	Name
63.8	18	CDC19	P00549	Pyruvate kinase 1
63.7	18	PGK1	P00560	Phosphoglycerate kinase
66.4	13	ENO2	P00925	Enolase 2
58.3	13	TEF1	P02994	Elongation factor 1-alpha
54	12	ADH1	P00330	Alcohol dehydrogenase 1
33.3	12	LEU1	P07264	3-isopropylmalate dehydratase
59	11	ENO1	P00924	Enolase 1
54	10	PDC1	P06169	Pyruvate decarboxylase isozyme 1
48.3	9	HSP71	P10591	Heat shock protein Ssa1
68.7	8	TDH3	P00359	Glyceraldehyde-3-phosphate dehydrogenase 3
41.4	8	HSP75	P11484	Heat shock protein Ssb1
36.8	8	FBA1	P14540	Fructose-bisphosphate aldolase
38.5	6	PMG1	P00950	Phosphoglycerate mutase 1
27.6	6	ETF1	P32324	Elongation factor 2
19.6	6	FET4	P40988	Low-affinity Fe(2+) transport protein
44.4	5	RSSA2	P46654	40S ribosomal protein S0-B
34.9	5	G3P1	P00360	Glyceraldehyde-3-phosphate dehydrogenase 1
26.9	5	MET6	P05694	5-methyltetrahydropteroyltriglutamate--homocysteine methyltransferase
23.5	5	PFK26	P40433	6-phosphofructo-2-kinase 1
51.9	4	CPR1	P14832	Peptidyl-prolyl cis-trans isomerase
38.7	4	TPI1	P00942	Triosephosphate isomerase
18.6	4	HSC82	P15108	ATP-dependent molecular chaperone Hsc82
17.3	4	IXR1	P33417	Intrastrand cross-link recognition protein
17.3	4	RPLA0	P05317	60S acidic ribosomal protein P0
29.6	3	AHP1	P38013	Peroxiredoxin type-2
24.5	3	ACT1	P60010	Actin
24.2	3	RPL5	P26321	60S ribosomal protein L5
16.7	3	METK2	P19358	S-adenosylmethionine synthase 2
58.6	2	RPS21B	Q3E754	40S ribosomal protein S21-B
45.5	2	RPS12	P48589	40S ribosomal protein S12

Supplementary table 3. Continuation

C	P	GENE	Accession	Name
43.4	2	RPLA1	P05318	60S acidic ribosomal protein P1-alpha
41.5	2	RPLA2	P05319	60S acidic ribosomal protein P2-alpha
27.7	2	MPG1	P41940	Mannose-1-phosphate guanyltransferase
27.7	2	EF1B	P32471	Elongation factor 1-beta
18.7	2	RPS5	P26783	40S ribosomal protein S5
18.4	2	TSA1	P34760	Peroxiredoxin Tsa1
10.7	2	RPS20	P38701	40S ribosomal protein S20
7.7	2	MET17	P06106	Protein Met17

C: % coverage; **P:** peptides (95%)

Chapter 2

Delineating the HMGB1 and HMGB2 interactome in prostate and ovary epithelial cells and its relationship with cancer

INTRODUCTION

Carcinomas are the most frequent types of cancer, in which epithelial cells lose their normal cell-to cell contacts, adopt a mesenchymal morphology and experiment a transformation to tumor cells (Berman, 2004). Adenocarcinomas are epithelial cancers arising in glandular tissues and they comprise the largest group of human epithelial malignancies that develop in different organs.

HMGB1 and HMGB2 are members of the High Mobility Group (HMG) protein superfamily that contain a DNA binding domain (HMG-Box), and their overexpression has been associated to main cancer hallmarks, tumor progression, metastasis formation and bad prognosis (Lange and Vasquez, 2009). The HMGB proteins are localized in the nucleus, cytoplasm and are also secreted to the extracellular milieu following either active secretion by immune cells or passive release from necrotic cells (Tang *et al.*, 2010). HMGB proteins are functionally related to cancer progression (Gnanasekar *et al.*, 2009; Chen, Liu, *et al.*, 2012; Chen, Xi, *et al.*, 2012; Zhao *et al.*, 2014) and overexpression of the *HMGB1* gene has been detected in cancerous cells from epithelial origin in prostate and ovary (Zhao *et al.*, 2014; Gatla *et al.*, 2014). In addition, HMGB proteins have increased affinity for platinated DNA (Jung and Lippard, 2003) and are also involved in sensitizing cells to platinum compounds used in the chemotherapy of prostate and ovary cancer (Huang *et al.*, 1994; Yusein-Myashkova *et al.*, 2016).

Protein interactions are ultimately responsible of cellular signaling and transformation; for this reason the identification of protein-protein interactions in ovarian and prostatic epithelial cells is crucial for the

understanding of carcinoma origin and evolution in these organs. In the present work we describe proteins interacting with human HMGB1 and HMGB2 in ovarian and prostatic epithelial cells. Prostate PNT2 cells were used in proteomic studies based on immunoprecipitation of HMGB1 and identification of co-immunoprecipitating proteins by mass spectrometry. Libraries constructed with RNA from epithelial cell lines from prostate and ovary as well as from healthy ovary tissue were used to perform yeast two-hybrid screening using HMGB1 and HMGB2 baits. The nature and functions of the identified binding partners were analyzed and correlated to cancerous processes.

MATERIALS AND METHODS

Yeast strains

Sacchacomyces cerevisiae strains used in this study were: Y187 (MATα, *ura3-52, his3-200, ade2-101, trp1-901, leu2-3, 112, gal4Δ, gal80Δ, met-, URA3::GALuas-GAL1TATA-LacZ MEL1*) and Y2HGold (MATa, *trp1-901, leu2-3, 112, ura3-52, his3-200, gal4Δ, gal80Δ, LYS2:: GAL1uas-Gal1TATA-His3, GAL2uas-Gal2TATA-Ade2 URA3:: MEL1UAS-Mel1TATA, AUR1-C MEL1*).

Library construction

cDNA libraries were constructed using Make Your Own “Mate&Plate” Library System (Clontech, CA). 1.0-2.0 μg of total RNA from HOSEpiC, and HPEpiC provided by Innoprot (Spain) and from healthy ovarian tissue provided by Biobanco de Andalucía (Spain) were used to construct each library. cDNA was generated using Clontech SMART technology following the manufacturer´s instructions. A degenerated oligo-dT primer: CDS III

Primer (5´-ATTCTAGAGGCCGAGGCGGCCGACATG-d(T)30VN-3´, where N=A, G, C or T and V=A, G or C) was used for first strand cDNA synthesis, after reverse transcription SMART III-modified Oligo (5´-AAGCAGTGGTATCAACGCAGAGTGGCCATTATGGCCGGG-3´) was incorporated to the cDNA. Double strand cDNA was amplified using Long Distance PCR (LD-PCR) after which ds cDNA molecules over 200 pb were purified with CHROMA SPIN^{TM}+ TE-400 Columns.

To prepare each library, competent Y187 yeast cells were cotransformed with 20µl of the ds cDNA (2-5µg) and 3µg of pGADT7-Rec (SmaI-linearalized) following the Yeastmaker Yeast Transformation System 2 (Clontech, CA, USA) protocol. pGADT7-Rec vector is suitable for expressing a protein fused to the GAL4 activation domain (AD) under the constitutive ADH1 promoter (PADH1). This vector contains LEU2 nutritional marker for selection in yeast (www.clontech.com/xxclt_ibcGetAttachment.jsp?cItemId=17643). Cells were plated on CM-Leu plates for selection and incubated at 30ºC for 3-4 days. All the colonies were harvested with freezing medium (YPDA/25% glycerol) and pooled together. The library was divided in 1 ml aliquots and stored at -80 ºC.

Bait construction

The bait clones were generated fusing the *HMGB1* or *HMGB2* genes to the *GAL4* DNA binding domain (DNA-BD) of the plasmid pGBKT7 (Clontech, CA, USA). This vector allows high level expression of fusion proteins due to the constitutive *ADH1* promoter (PADH1) and carries the *TRP1* gene that is used for auxotrofic selection in yeast

(www.clontech.com/xxclt_ibcGetAttachment.jsp?cItemId=17639). *HMGB1* and *HMGB2* were amplified from commercial vectors containing the *HMGB1* and *HMGB2* complete ORFs (OriGene, USA). Primers used to amplify the bait genes were designed with the following sequences: 5´-CATGGAGGCCGAATTCATGGGCAAAGGAGATCCTAAGAAG-3´ and 5´-GCAGGTCGACGGATCCTTATTCATCATCATCATCTTCTTCTTCATC-3´ for *HMGB1* and 5´-CATGGAGGCCCCGGGATGGGTAAAGGAGACCCCAACAAG-3´and 5´-GCAGGTCGACGGATCCTTATTCTTCATCTTCATCCTCTTC-3´ for *HMGB2*. *HMGB1* was cloned in the PGBKT7-BD plasmid using the In-Fusion Cloning Kit (Clontech, CA). *HMGB2* construct was obtained by digestion of both the PGBKT7-BD and the HMGB2 PCR product with SmaI and BamHI and subsequent ligation. The constructs were sequenced to confirm correct insertion of each gene. Y2HGold cells were transformed with pGBKT7-BD bait plasmids and plated in CM-Trp to select for selection of bait plasmids. Prior to the two-hybrid assays, both baits were tested for autoactivation to confirm that neither HMGB1 nor HMGB2 autonomously activate the reporter genes in Y2HGold.

Yeast two-hybrid library screening

HMGB1 and HMGB2 interacting partners were assessed using Matchmaker Gold Yeast Two-Hybrid System (Clontech, CA). For each Two-hybrid screening 1 ml of the library was combined with the Bait Strain following the manufacturer´s instructions. In short, the mating between both strains was performed in 2xYPDA medium during 24h at 30ºC with slow shaking. The efficiencies in the constructions of libraries were in the range recommended in the kit, although lower in ovarian tissue libraries than in HOSEpiC or HPEpiC cell libraries. After the mating, cells were plated in CM-

Trp-Leu-His. In each two hybrid assay more than 1 million clones (diploids) were screened, calculated as indicated by the kit. The clones growing in CM-Trp-Leu-His were tested in two more media: CM-Trp-Leu-Ade and CM-Trp-LeuX-α-Gal. Clones that could grow in all specific depleted media and displayed α-galactosidase activity contained the cDNA of a possible interacting partner in the pGADT7-Rec vector. In order to identify the encoded proteins the prey plasmid was rescued and amplified in bacteria, and the inserted cDNA was sequenced using the T7 sequencing primer (5´-TAATACGACTCACTATAGGG-3´). The sequences were analyzed using Blastn from the NCBI (https://blast.ncbi.nlm.nih.gov/Blast.cgi?PROGRAM=blastn&PAGE_TYPE=BlastSearch&LINK_LOC=blasthome).

Cell Culture

Immortalized human benign prostate epithelial cells PNT2 (kindly provided by Dr. Inés Díaz-Laviada Mauret) were grown in RPMI-1640 (Thermo Fisher Scientific, Inc., Waltham, MA, USA), supplemented with 10% fetal bovine serum (Thermo Fisher Scientific, Inc.) and 1% penicillin-streptomycin (Thermo Fisher Scientific, Inc.). All cells were maintained in standard cell culture conditions (37°C and 5% CO_2 in a humidified incubator). Cells were regularly tested for mycoplasma.

Immunoprecipitation

Total protein from PNT2 cells was extracted in lysis buffer (50mM Tri-HCl pH 8.0, 150mM NaCl, 0.1% NP-40, 1mM EDTA, 2mM MgCl2 and cOmplete™ Mini, EDTA-free Protease Inhibitor Cocktail (Roche) and incubated for 30 min at 4ºC with Benzonase®Nuclease (Sigma-Aldrich) to eliminate nucleic

acids from the lysates. Total protein was quantified using the Bradford reagent. Prior to the immunoprecipitation, Protein G-Dynal beads (Invitrogen) were crosslinked to 40 µg of HMGB1 antibody (Abcam, Cambridge, UK) or anti-rabbit IgG antibody (Millipore) as previously described (Pardo *et al.*, 2010). For each immunoprecipitation 2.5-3 mg of protein were incubated for 4 h at 4 ºC with the corresponding HMGB1 or control rabbit antibody-linked beads. Nonspecific binding proteins were removed by four washes with IPP150 buffer (10 mM Tris-HCl pH8.0, 150 mM NaCl and 0.1% NP-40) and four washes with 50 mM ammonium bicarbonate. On-bead digestion was carried out overnight at 37 ºC with trypsin (sequencing grade, Roche). Peptides were then collected, acidified with formic acid, filtered through Millipore Multiscreen HTS plates and dried in a Speed Vac (Thermo). Peptides were then resuspended in 20 mm TCEP and formic acid was added to a final concentration of 0.5%.

Mass Spectrometry and Data Analysis

Peptides were analysed with online nanoLC-MS/MS on an Orbitrap Velos mass spectrometer coupled with an Ultimate 3000 RSLCnano System. Samples were first loaded and desalted on a nanotrap (100 µm id x 2 cm) (PepMap C18, 5 µ) at 10 µl/min with 0.1% formic acid for 10 min and then separated on an analytical column (75 µm id x 25 cm) (PepMap C18, 2µ) over a 90 min linear gradient of 5 – 42% B (where B = 80% CH3CN/0.1% formic acid) at 300 nl/min, and the total cycle time was 120 min, or a 120 min linear gradient of 4 – 32% CH3CN/0.1% formic acid at 300 nl/min, and the total cycle time was 150 min. The Orbitrap Velos was operated in standard data-dependent acquisition. The survey scans (m/z 380-1500) were acquired in the Orbitrap at a resolution of 30,000 at m/z 400, and one

microscan was acquired per spectrum. The 10 most abundant multiply charged ions with a minimal intensity of 2000 counts were subject to MS/MS in the linear ion trap at an isolation width of 2 Th. Dynamic exclusion width was set at ± 10 ppm for 45 s. The automatic gain control target value was regulated at 1x106 for the Orbitrap and 5000 for the ion trap, with maximum injection time at 200 ms for Orbitrap and 100 ms for the ion trap, respectively.

The raw files were processed with Proteome Discoverer v1.4 (Thermo Fisher Scientific). Database searches were performed with Mascot (Matrix Science) against the human Uniprot database (2014, 77606 entries) and an in-house contaminant database. The search parameters were: trypsin/P digestion, 2 missed cleavages, 10 ppm mass tolerance for MS, 0.5 Da mass tolerance for MS/MS, with variable modifications of acetyl (N-terminal), carbamidomethyl (C), N-formylation (protein), oxidation (M), and pyro-glu (N-term Q). Database search results were refined through processing with Percolator (significance threshold < 0.05, FDR < 1%). Protein identification required at least one high-confidence peptide (FDR < 1%) with a minimum score of 20. External contaminants (albumin, casein, trypsin) were removed from protein lists before further analysis. Keratins were not removed, as they could potentially represent true interactors.

To discriminate specific from unspecific interactions, the identified proteins in each immunoprecipitation (HMGB1 and IgG antibody) were analyzed with the Significance Analysis of INTeractome (SAINT) score SAINTexpress (Choi *et al.*, 2012). Results from each experiment were analyzed using their corresponding negative control. Preys with SAINT probability score cut-off of 1 detected by at least two unique peptides were deemed high confidence

HMGB1 interacting proteins and further analyzed for functional significance. The mass spectrometry proteomics data have been deposited to the ProteomeXchange Consortium via the PRIDE (Vizcaíno *et al.*, 2016) partner repository with the dataset identifier PXD007867.

RESULTS AND DISCUSSION

Identification of HMGB1 interacting proteins in prostate epithelial cells by co-immunoprecipitation and mass spectrometry

To identify proteins interacting with HMGB1, cell lysates from PNT2 prostate epithelial cells were incubated with anti-HMGB1 antibody or anti-rabbit IgG antibody (negative control) and immunoprecipitated proteins were identified by mass spectrometry as described in the materials and methods section. Two replicate experiments were performed. HMGB1 was specifically detected in the experimental replicates and not in the negative controls (Supplementary table 1). We used SAINT analysis to derive a list of statistically significant true interactors. Preys with SAINT probability score cut-off of 1 detected by at least two unique peptides were deemed high confidence HMGB1 interacting proteins. The complete list of 159 proteins fulfilling these criteria is shown in Supplementary table S1. To explore if any of the identified HMGB1 associated proteins was already known to interact with it, the list was matched against published HMGB1 binding partners in the BioGRID database (Stark *et al.*, 2006). There are 89 of such proteins annotated in the database, including HMGB1, since it has been reported to form dimmers and tetramers (Anggayasti *et al.*, 2016). Six proteins from our list were annotated as HMGB1 interactors, validating our experimental approach: SUPT16H and SSRP1, the two subunits of the FACT complex, a

general chromatin remodeler that reorganizes nucleosomes; PARP1, the poly(ADP-ribose) polymerase 1; the H3 Family 3A histone; HNRNPK, the heterogeneous nuclear ribonucleoprotein K, and heat shock protein HSPA8.

We then analyzed the list of HMGB1 interacting proteins in detail to explore their functional significance. We first looked for functional protein association networks amongst the identified HMGB1 preys with STRING (Szklarczyk *et al.*, 2017). The majority of proteins clustered into 4 clearly differentiated groups (Figure 1). Cluster 1 included DNA binding proteins involved in DNA transcription or DNA repair and proteins involved in chromatin structure and remodeling. Cluster 2 included proteins from the spliceosome. Cluster 3 comprised ribosomal proteins and/or proteins related to ribosome biogenesis. Cluster 4 proteins were implicated in mitochondrial translation.

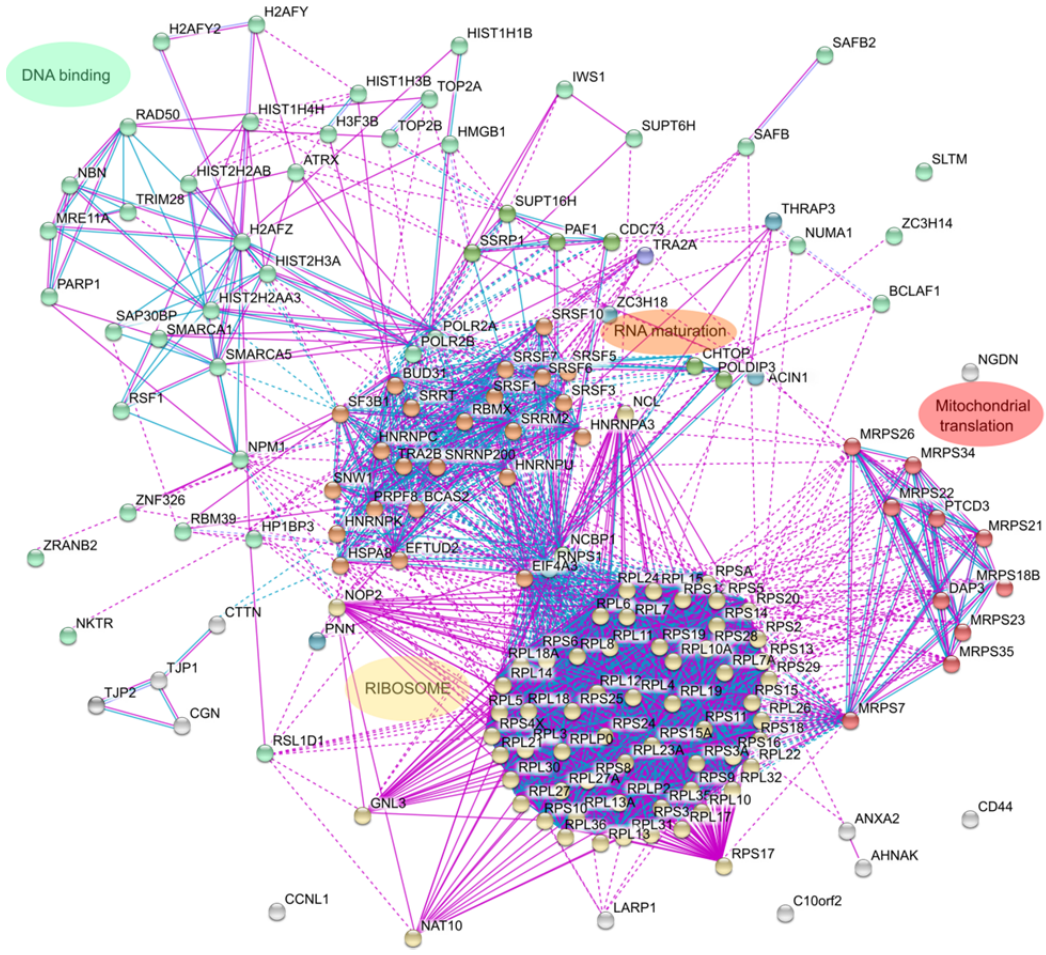

Figure 1. Clustering of proteins that interact with HMGB1 in PNT2 cells. The interactome of HMGB1 partners, reflecting only experimental or data-base recorded interactions, has been constructed with STRING.

The role of HMGB1 in the regulation of gene expression has been previously reported and is mediated by diverse mechanisms: modulation of DNA template accessibility (Štros, 2010; Thomas and Stott, 2012), interaction with the general transcriptional machinery (Das and Scovell, 2001; Thomas and Chiang, 2006) or control of the activity of specific transcriptional factors (Thomas and Stott, 2012; Banerjee and Kundu, 2003). In the nucleus HMGB1 binds DNA, which facilitates chromatin bending, an event required for its interaction with proteins engaged in transcription and DNA repair (Lange and Vasquez, 2009). Our interaction proteomics study suggests that HMGB1 might also participate in other co or post-transcriptional events that affect gene expression. These results hint that HMGB1 interactions with other proteins might control gene expression in a very complex way at different stages, from regulating DNA template availability for transcription, through RNA synthesis, maturation and export of RNA from the nucleus to the cytoplasm and protein synthesis. In addition, coordination of mitochondrial translation with ribosomal protein synthesis is important in terms of bioenergetic balance; HMGB1 regulates mitochondrial bioenergetics in tumor cells (Kang *et al.*, 2014) and HMGB1 binding proteins included in cluster 4 confirm this function.

Strikingly, in addition to proteins regulating gene expression, we also identified tight junction proteins TJP1 and TJP2 among HMGB1 interacting proteins. This is remarkable in light of HMGB1's role in metastasis (Karsch-Bluman *et al.*, 2017; Lv *et al.*, 2017) and points to potential players cooperating with HMGB1 to promote metastasis.

We then performed GO term enrichment analysis to functionally characterize the list (Figure 2). This showed that the clusters above coincided with statistically overrepresented terms. Regarding biological processes, enriched terms included

"Gene expression" and "Regulation of gene expression". Other overrepresented GO terms included chromatin/DNA modification, response to DNA damage, transcription mediated by RNA polymerase II, and RNA polymerase I, RNA export from nucleus, processing of mRNA, rRNA and ncRNA, and ribosome biogenesis. The GO term "SRP- dependent cotranslational protein targeting to membrane", associated with 55 proteins, refers to the intracellular protein transport of ribosomes and nascent polypeptides to the ER membrane. These findings suggest a cytoplasmic function of HMGB1 in the control of ribosome biogenesis and protein synthesis, which could affect the proliferative capacity of cells. In support of this function of HMGB1 in the control of cell proliferation, it has been reported that ethyl pyruvate, a potent inhibitor of HMGB1 transport from nucleus to cytoplasm, greatly reduces cancerous cell proliferation (M L Li *et al.*, 2012; Pellegrini *et al.*, 2017).

GO cellular component enriched terms included "nuclear part" and "ribosome", in agreement with GO biological process terms "gene expression" and "ribosome biogenesis". In addition, the term "extracellular exosome" was also over-represented. The 51 proteins annotated with this term included many ribosomal proteins. Extracellular vesicles are promising blood biomarkers since their cargoes may reflect the pathophysiological state in the cell of origin. The production of extracellular vesicles has been experimentally proven in PNT2 cells, and their mRNA content found to differ from that in exosomes from cancerous cells of epithelial origin (Lázaro-Ibáñez *et al.*, 2017). HMGB1 itself was recently detected in epithelial cells exosomes (Sheller-Miller *et al.*, 2017).

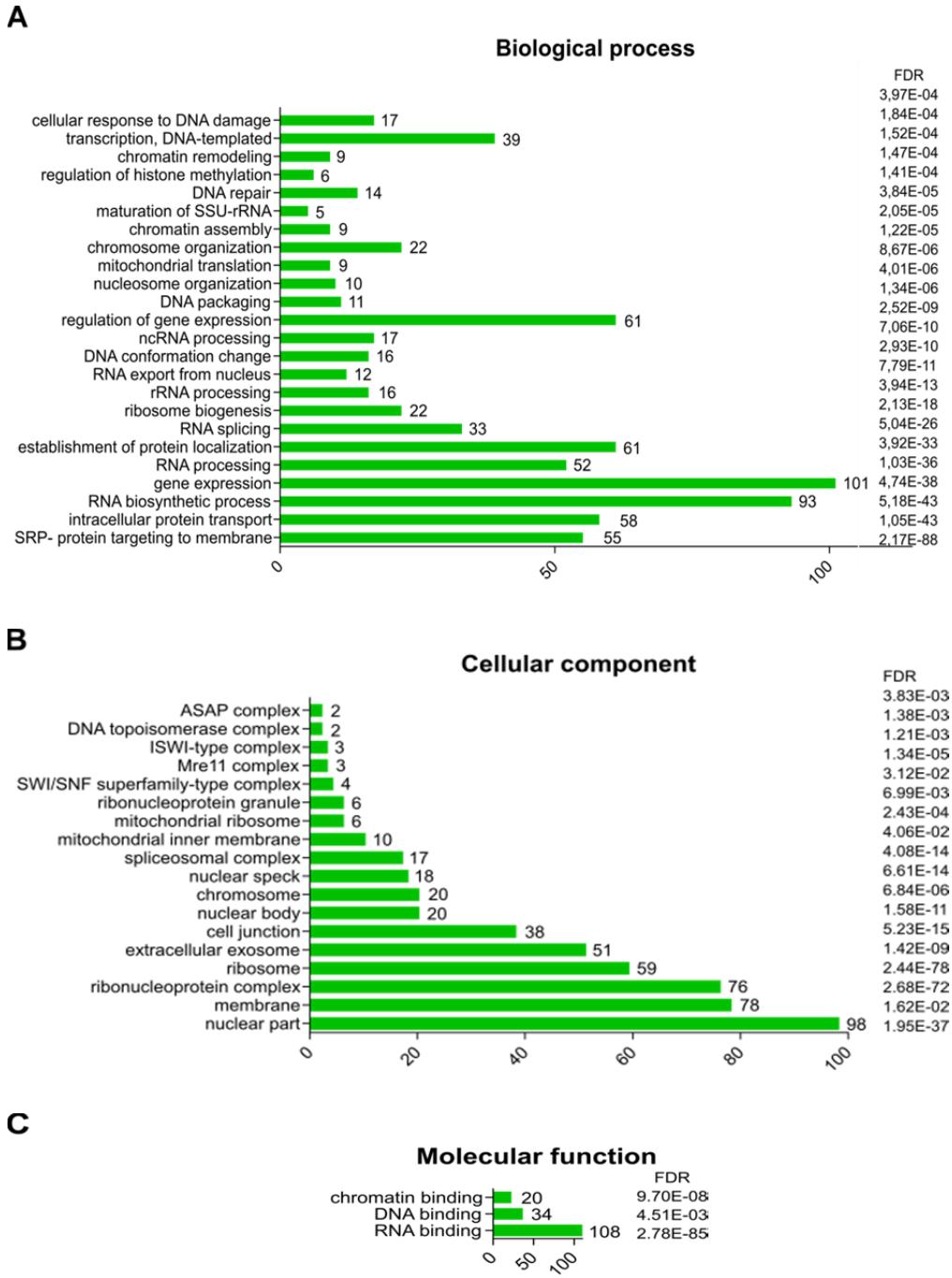

Figure 2. **GO Term enrichment analysis of proteins that interact with HMGB1 in PNT2 cells. (A)** Biological process enrichment. **(B)** Cellular component enrichment. **(C)** Molecular function.

Chapter 2

Identification of HMGB1 and HMGB2 binding proteins by yeast two-hybrid screening of cDNA libraries from human prostate and ovary epithelial cells

The identification of HMGB1 associated proteins based on co-immunoprecipitation and MS analysis was carried out in the non-cancerous, immortalized prostate epithelial cell line PNT2 containing a SV40 genome with a defective replication origin. To identify interactions in non-transformed cells, we then extended our analysis to human epithelial cells from prostate and ovary primary cultures (HPEpiC and HOSEpiC respectively). We generated cDNA libraries from RNA extracted from epithelial cells from prostate (HPEpiC) and ovary (HOSEpiC), and screened for interactions using HMGB1 and HMGB2 baits, as described in the Materials and methods section. We did not achieve saturation in the screen and there are probably other preys of HMGB1 and HMGB2 that were not captured.

HMGB1 binding proteins in HPEpiC and HOSEpic cells

The proteins identified as HMGB1 preys (Table 1) can be classified in several functional groups: a) components of the cytoskeletal system: KRT7, and NEXN; b) cellular signaling in response to growth factors: DPP9, ENAH, RPS20 and SPINT1; c) components of the cellular membrane and extracellular matrix and regulators of cell invasion and migration in tumoral cells: PCOLCE, HSPA5, UBE2I, RPL29, CTNNBL1 and ZNF428; d) apoptosis-related proteins: EIF1, CCAR1 and ACBD3. FIP1L1 was not included in any of the previous categories. None of these have previously been reported as HMGB1 interacting proteins.

Table 1. HMGB1 preys in HOSEpic and HPEpiC cells

Gene	N	Cells	Function	Relation to cancer
ACBD3	7	HOSEpiC	Apoptosis	Golgi resident protein GCP60 (GOCAP1) can interact with a golgin-160 fragment to regulate cell apoptosis (Fan *et al.*, 2010).
CCAR1	3	HOSEpiC	Apoptosis	Cell division cycle and apoptosis regulator protein 1 (CARP-1) regulates cell growth and apoptosis by serving as a co-activator of several genes including steroid nuclear receptors and tumour suppressor p53 (Kolostova *et al.*, 2016).
UBE2I	1	HPEpiC	Tumour progression	SUMO-conjugating enzyme UBC9, plays a major role in sumoylation (Schwarz *et al.*, 1998). UBE2I expression is increased in several cancers as in epithelial ovarian cancer (EOC) (Zhu and Yu, 2010), colon and prostate neoplasias and adenocarcinomas (Moschos *et al.*, 2010). Moreover, overexpression of UBE2I has also been related to migration, invasion and proliferation in a lung cancer cell line and in breast cancer (Li *et al.*, 2013; Xu *et al.*, 2016).
C1QBP	2	HOSEpiC	Cell motility	C1qBP protects the cells against staurosporine induced apoptosis and increases proliferation and cell migration in cancerous cells (McGee *et al.*, 2011). Predictor of tumor size in progesterone positive tumors and marker for proliferation in breast cancer (Scully *et al.*, 2015).
EIF1/SUI1	1	HPEpiC	Apoptosis	Eukaryotic translation initiation factor 1 (eIF1) is activated by oncogene *MCT-1* (Reinert *et al.*, 2006).
ENAH	2	HPEpiC	Cellular signalling	Protein enabled homolog. Involved in PI3K-dependent cell invasion induced by Platelet-derived growth factor in human breast cancer cells (Takahashi and Suzuki, 2011). Involved in human lung cancer metastasis and migration of breast cancer cells (Santiago-Medina and Yang, 2016).
HSPA5	1	HOSEpiC	Tumour progression	78 kDa glucose-regulated protein (GRP-78) or Heat shock 70 kDa protein 5 has been proposed as a potential biomarker for predicting high-risk endometrial carcinoma (Teng *et al.*, 2013), as well as positive regulator of cellular migration (Luo *et al.*, 2016).

Table 1. Continuation

Gene	N	Cells	Function	Relation to cancer
KRT7	19	HPEpiC	Cytoskeleton	Keratin, type II cytoskeletal 7. The keratin KRT7 gene has been found to be hyper-methylated in prostate cancer (Ibragimova *et al.*, 2010).
NEXN	11	HOSEpiC	Cytoskeleton Cell motility	Nexilin is an F-actin associated protein that stimulates cell motility (Wang *et al.*, 2005) and NEXN is down regulated after radiation of prostate adenocarcinoma cells (Suetens *et al.*, 2014).
PCOLCE	1	HOSEpiC	Tumour progression	Procollagen C-endopeptidase enhancer 1 (PCPE-1) binds procollagen, potentiating its cleavage by specific proteinases, and might be involved in tumour growth (Salza *et al.*, 2014).
SPINT1	2	HPEpiC	Cellular signalling	Kunitz-type protease inhibitor 1 (or hepatocyte growth factor activator inhibitor type 1, HAI-1) malfunction promotes intestinal carcinogenesis by activating NF-κB signalling (Sechler *et al.*, 2015). Low HAI-1 expression is a significant predictor for poor prognosis in prostate cancer (Hu *et al.*, 2014).
FIP1L1	1	HPEpiC	-	The fusion of the gene encoding the Pre-mRNA 3'-end-processing factor FIP, with the *PDGFRA* gene or the RARA gene generate a novel tyrosine kinase due to a interstitial chromosomal deletion (Cools *et al.*, 2003). These associations have been linked to the pathogenesis of leukemias (Iwasaki *et al.*, 2014).
RPS20	1	HOSEpiC	Cellular signalling	40S ribosomal protein S20 binds the RING-type E3 ubiquitin ligases Mdm2 and MdmX therefore regulating the Mdm2-p53-MdmX network (Daftuar *et al.*, 2013).
RPL29	2	HOSEpiC	Tumour progression	60S ribosomal protein L29 has been related to tumoral events as angiogenesis (Jones *et al.*, 2013) and cell proliferation (Chaodong Li *et al.*, 2012).
CTNNBL1	1	HOSEpiC	Tumour progression	The spliceosome-associated factor, Beta-catenin-like protein 1, is overexpressed in High-grade serous ovarian carcinomas. Moreover, this protein can promote proliferation and invasion in ovarian cancer cells (Li *et al.*, 2017).

Table 1. Continuation

Gene	N	Cells	Function	Relation to cancer
ZNF428	11	HOSEpiC	Tumour progression	Zinc finger protein 428 interacts with Bcl2-associated athanogene 3 (BAG3) protein, which is related to cancerous processes. BAG3 can modulate apoptosis, autophagy, mechanotransduction, cytoskeleton organization, and motility (De Marco *et al.*, 2017). Moreover, BAG3 regulates epithelial-mesenchymal transition (EMT) and angiogenesis and its knockdown reduced migration and invasion in cancerous cells (Xiao *et al.*, 2014).

N: repetitive identification during Y2H screening

Interestingly, all the identified HMGB1 binding proteins have been reported to be involved in cellular proliferation and cancer progression, as detailed in Table 1, some of them specifically in ovary or prostate cancer. This is the case for keratins KRT7 (Ibragimova *et al.*, 2010) and SPINT1, a membrane-bound serine protease inhibitor expressed on the epithelial cell surface (Sun *et al.*, 2016; Hu *et al.*, 2014; Warren *et al.*, 2009). Keratins form obligate heteropolymers between one type I and one type II keratin; the keratin prey found in our analyses is type II and the human *in vivo* partner from type I is KRT18 for KRT7. KRT18 has been proposed as biomarker in prostate carcinoma (Karantza, 2011). Since keratin expression is tissue-specific, they are extensively used as diagnostic tumor markers. Moreover, they are also active players in cancer progression and metastasis, as well as multifunctional regulators of epithelial tumorigenesis (Karantza, 2011). In prostate cancer, SPINT1 regulates matriptase, a membrane-associated serine protease that activates prostatin, through regulation of the matriptase endogenous inhibitor HAI-1 (Warren *et al.*, 2009). A recent study has demonstrated that ovarian cancer cell metastasis and invasion are dependent on upregulation of matriptase (Sun *et al.*, 2016).

HMGB2 binding proteins in HPEpiC and HOSEpiC cells

The proteins interacting with HMGB2 as detected by Y2H (Table 2) can be classified in several groups: a) apoptosis-related proteins: ZNF622, EIF1, SAMM50 and ZNF428; b) cell motility: C1QBP, MIEN1, and NEXN; c) cellular proliferation: NAP1L1, CACTIN, ARCN1, ZNF668, NCBP3, H3F3A, HDLBP, HACD3 and FEZ1. None of these interactors has previously been reported.

All these HMGB2 binding proteins have also been reported to be involved in cellular proliferation and cancer progression as detailed in Table 2, and in some cases specifically associated to ovary or prostate cancer. MIEN1 (c17crf37)

maintains the plasticity of the dynamic membrane-associated actin cytoskeleton, and its overexpression in prostate cancer functionally enhances migration and invasion of tumor cells (Dasgupta *et al.*, 2009). NAP1L1 (nucleosome-assembly-protein-I), a chaperone for histone exchange in nucleosomes, is the only ATP-dependent chromatin remodeler essential for transcription-coupled nucleotide excision DNA repair (Lee *et al.*, 2017) and it is a candidate biomarker identified in primary ovarian tumors that respond to cytotoxic gold compounds (Guidi *et al.*, 2012). SAMM50 has been linked to apoptosis through its role in the targeting of the mitochondrial channel VDAC (Kozjak-Pavlovic *et al.*, 2007). In addition, SAMM50 interacts with DRP1, a dynamin-like protein involved in apoptosis in prostate cancer cells (Kaddour-Djebbar *et al.*, 2010).

Table 2. HMGB2 preys in HOSEpic and HPEpiC cells.

Gene	N	Cells	Function	Relation to cancer
ARCN1	1	HPEpiC	Cell proliferation	*ARCN1* encodes the Coatomer subunit delta and its depletion inhibits growth of cancer cell lines without affecting normal cell growth and survival (Oliver *et al.*, 2017). It is functionally related to the retrograde transport mediating intracellular protein traffic (Kobayashi *et al.*, 2015). It is targeted by miR-361-5p (Chang *et al.*, 2016).
C1QBP	12	HPEpiC	Cell motility	Previously described in Table 1.
CACTIN	1	HPEpiC	Cell proliferation	Cactin forms part of a family of conserved eukaryotic proteins, which are required for multiple processes including cell proliferation and genome stability maintenance by allowing faithful splicing of specific pre-mRNAs (Zanini *et al.*, 2017) and it has been reported to inhibit NFκB- and TLR-mediated transcription (Suzuki *et al.*, 2016).
EIF1/SUI1	1	HPEpiC	Apoptosis	Previously described in Table 1.
LZTS1/ FEZ1	4	HOSEpiC	Cell proliferation	Leucine zipper putative tumor suppressor 1. The LZTS1 tumor suppressor gene 1 (FEZ1) inhibits cell proliferation and tumor growth in colorectal cancer cells, in part via suppression of AMT-mTOR (Zhou *et al.*, 2015).
MIEN1	1	HPEpiC	Cell motility	Migration and invasion enhancer 1 is involved jn filopodia formation and tumor cell migration. Differently expressed in normal and cancer cells (Kpetemey *et al.*, 2015). Related to prostate cancer (Dasgupta *et al.*, 2009).
NAP1L1	1	HPEpiC	Cell proliferation	Nucleosome assembly protein 1-like is a chaperone for histone exchange in nucleosomes and it promotes cell proliferation (Schimmack *et al.*, 2014).

Table 2. Continuation

Gene	N	Cells	Function	Relation to cancer
NCBP3	1	HOSEpiC	Cell Proliferation	Nuclear cap-binding protein subunit 3 associates with components of the mRNA processing machinery and contributes to poly(A) RNA export. With Nuclear cap-binding protein subunit 1 forms an alternative cap-binding complex in higher eukaryotes (Gebhardt *et al.*, 2015). Silencing of NCBP1 causes deregulated expression of several hundred genes and a reduction in the cell proliferation rate (Narita *et al.*, 2007).
NEXN	4	HOSEpiC	Cell motility Cytoskeleton	Previously described in Table 1.
SAMM50	2	HOSEpiC	Apoptosis	Sorting and assembly machinery component 50 homolog participates in mitochondrial respiratory chain complexes assembly and mitochondrial morphology. In apoptotic cells, mitochondrial fission requires the cytoplasmic dynamin-related protein, DRP1, a GTPase protein responsible for mitochondrial division that translocates to the nucleus(Liu *et al.*, 2016). Drp1 is involved in apoptosis in prostate cancer cells (Kaddour-Djebbar *et al.*, 2010).
H3F3A	1	HPEpiC	Cell proliferation	Mutations in the gene codifying Histone H3.3, have been associated to glioma (Sturm *et al.*, 2012). Moreover, overexpression of this chromatin remodeling protein has been associated with lung cancer progression and promotes cell migration by activating metastasis-related genes (Park *et al.*, 2016).
HDLBP	1	HOSEpiC	Cell proliferation	The high density lipoprotein-binding protein, VIgilin, may be involved in cell proliferation (Cao *et al.*, 2004) and in chromosomal condensation and segregation (Wei *et al.*, 2015). HDLBP is upregulated in hepatocellular carcinomas (Yang *et al.*, 2014).
HACD3	1	HOSEpiC	Cell proliferation	Very-long-chain (3R)-3-hydroxyacyl-CoA dehydratase 3, HACD3 plays a role in Rac1 signalling pathways (Courilleau *et al.*, 2000) a small GTPase widely related to tumoral processes (Mack *et al.*, 2011).

Table 2. Continuation

Gene	N	Cells	Function	Relation to cancer
ZNF428	15 1	HOSEpiC HPEpiC	Apoptosis	Previously described in Table 1
ZNF622	1	HPEpiC	Apoptosis	Zinc finger protein 622 is involved in apoptosis and regulation of JNK cascade. Interacts with Apoptosis signal-regulating kinase 1(ASK1); ASK family members are activated by a wide variety of stressors, and they regulate various cellular responses, such as cell proliferation, inflammation and apoptosis in cancer development (Seong *et al.*, 2011).
ZNF668	4	HPEpiC	Cell proliferation	Zinc finger protein 668 suppresses breast cancer cell proliferation. *ZNF668* is a breast tumor suppressor gene. Zinc finger protein 668 physically interacts with and regulates p53 stability (Hu *et al.*, 2011). It promotes H2AX acetylation after DNA damage and is a regulator of DNA repair (Hu *et al.*, 2013).

N: repetitive identification during Y2H screening

FEZ1 is a mitotic regulator implicated in cancer (Vecchione *et al.*, 2007) that is associated with microtubule components (Ishii *et al.*, 2001). It is a leucine-zipper protein, and its expression is undetectable in 60% of ephitelial human tumors, including prostate(Ishii *et al.*, 1999). It has been suggested as a tumor suppressor gene in prostate and other cancers (Cabeza-Arvelaiz *et al.*, 2001) and therefore its loss may contribute to tumor progression, as has been also found in ovarian carcinogenesis (Califano *et al.*, 2010).

Identification of HMGB1 binding proteins by Y2H screening of a healthy ovarian tissue library

Healthy ovarian tissue obtained after biopsy was used for RNA extraction and construction of a cDNA library. The library was screened for interactions using HMGB1 as bait, as described in the Materials and methods section. The efficiency obtained in the preparation of the tissue-based library was lower than that obtained from primary cells and the number of preys identified was lower too. As observed with HPEpiC and HOSEpiC libraries, HMGB1 binding proteins identified from healthy ovarian tissue libraries are also all involved in cellular proliferation and cancer progression, as detailed in Table 3. Four of them have been reported to be specifically related to ovary or prostate cancer, namely CCAR1 (Muthu *et al.*, 2015), KRT7 (Kolostova *et al.*, 2016), already identified with the other libraries, MT2A, a metallothionein that promotes the survival of human prostate cancer cells (Yamasaki *et al.*, 2007) and C3, Complement C3 protein, that contributes to ovarian tumoral cell proliferation, migration and invasion.

Table 3. HMGB1 Y2H preys in a library from ovarian tissue.

Gene	N	Function	Relation to cancer
CCAR1	3	Apoptosis	Cell division cycle and apoptosis regulator 1 regulates cell growth and apoptosis by serving as a co-activator of several genes including steroid nuclear receptors and tumor suppressor p53 (Muthu *et al.*, 2015).
KRT7	5	Cytoskeleton	KRT7 7, KRT18 and KRT19 are differentially expressed in circulating tumor cells in ovarian cancer patients (Kolostova *et al.*, 2016).
MT2A	1	Apoptosis	MT2A is upregulated in chemotherapy resistant ovarian tumors, and also in human prostate cell lines (Yamasaki *et al.*, 2007).
C3	1	Cell Proliferation	Secretion of Complement C3 protein in ovarian cancer cells promotes cell proliferation, invasion, and migration (Cho *et al.*, 2014).
RPS12	1	Cell Proliferation	RPS12 encodes the 40S ribosomal protein S12. RPS12 expression changes in breast cancer (Deng *et al.*, 2006).

N: repetitive identification during Y2H screening

Cross validation of HMGB1 and HMGB2 interactions identified by different strategies

In this study we used two complementary techniques and three epithelial cell lines to investigate HMGB1 and HMGB2 partners in the context of epithelial tissue. MS-based strategies are well-recognized methods to investigate interacting proteins or protein complexes (Gingras and Wong, 2016). However, this technique has several limitations, and the interactions detected could be direct or mediated by other interacting proteins. In addition, expression of the proteins involved in the interaction might be dependent of cell signaling pathways, which are not known *a priori* and therefore cannot be accounted for in the experimental design. By contrast, the Y2H technology allows the co-expression of the two partners of the interaction, independently of cellular signals, bypassing this limitation, but has other drawbacks, like heterologous

expression in yeast, or conditioned nuclear localization of bait and prey due to their fusion to a transcriptional factor. Interactions identified in this study that are cross-validated because they were detected either using both Co-IP/MS and Y2H approaches, or detected at least in two different epithelial cells include CCAR1, KRT7, H3F3A, RPS12, RPS20, and ZNF428.

The data obtained in our study reveal that, in epithelial cells, HMGB1 interacts with many nuclear proteins but also with proteins that form part of the cytoskeleton, cell-adhesion structures and others related to intracellular protein translocation, a process which is involved in diverse cellular functions including cellular migration, secretion, apoptosis and cell survival. Among HMGB1 interactions are nuclear proteins affecting gene expression, such as Cell division cycle and apoptosis regulator 1 (CCAR1) (Kim *et al.*, 2008). CCAR1 is a coactivator necessary for recruitment of the Mediator complex by nuclear receptors and it regulates expression of key proliferation inducing genes. CCAR1 also functions as a p53 coactivator, which explains its broader role in transcriptional regulation. Extra-nuclear proteins were also found, like Cytokeratin 7, one of the intermediate filament proteins that constitute the cytoskeleton of numerous types of epithelial cells (Pan *et al.*, 2013). CCAR1 and KRT7, were found to interact with HMGB1 in two different cell types, CCAR1 in HOSEpiC and healthy ovarian tissue cells, and KRT7 in HPEpiC and healthy ovarian tissue cells. Only one protein interacting with HMGB2 was cross-validated in our study, the Zinc Finger Factor 428 (ZNF428), an uncharacterized zinc finger protein detected by using HPEpiC and HOSEpiC cells in the Y2H strategy.

Since HGMB1 and HMGB2 have sequences with 82.3 % similarity, we expected that the two baits would have common targets, but we found only four, ZNF428, EIF1, C1QBP and Nelin (NEXN), an F-actin associated protein involved in cell

motility (Wang *et al.*, 2005). Previous data available in BioGRID also reveal that intersection of HMGB1 (89 hits) and HMGB2 (55 hits) interactions is limited to only 19 proteins, which suggests that the specificity of these proteins for their respective partners is high.

The proteins interacting with HMGB1 or HMGB2 in prostate and ovarian epithelial cells identified in our study are involved in cellular processes which are altered in cancerous cells, and hence provide a useful resource for further investigation of the complex roles of HMGB1/2 in cancer (He *et al.*, 2017). Our data should also be of interest in future clinical trials to identify potential biomarkers of cancer diagnosis and progression, as well as pharmacological targets for the development of new therapy approaches for cancers of epithelial origin.

REFERENCES

Anggayasti WL, Mancera RL, Bottomley S, Helmerhorst E. 2016. The effect of physicochemical factors on the self-association of HMGB1: A surface plasmon resonance study. *Biochim. Biophys. Acta*, **1864**: 1620–1629.

Banerjee S, Kundu TK. 2003. The acidic C-terminal domain and A-box of HMGB-1 regulates p53-mediated transcription. *Nucleic Acids Res.*, **31**: 3236–3247.

Berman JJ. 2004. Tumor taxonomy for the developmental lineage classification of neoplasms. *BMC Cancer*, **4**: 88.

Cabeza-Arvelaiz Y, Sepulveda JL, Lebovitz RM, Thompson TC, Chinault AC. 2001. Functional identification of LZTS1 as a candidate prostate tumor suppressor gene on human chromosome 8p22. *Oncogene*, **20**: 4169–4179.

Califano D, Pignata S, Pisano C, Greggi S, Laurelli G, Losito NS, Ottaiano A, Gallipoli A, Pasquinelli R, De Simone V, Cirombella R, Fusco A, Chiappetta G. 2010. FEZ1/LZTS1 protein expression in ovarian cancer. *J. Cell. Physiol.*, **222**: 382–386.

Cao WM, Murao K, Imachi H, Yu X, Abe H, Yamauchi A, Niimi M, Miyauchi A, Wong NCW, Ishida T. 2004. A Mutant High-Density Lipoprotein Receptor Inhibits Proliferation of Human Breast Cancer Cells. *Cancer Res.*, **64**: 1515–1521.

Chang JT, Wang F, Chapin W, Huang RS. 2016. Identification of MicroRNAs as Breast Cancer Prognosis Markers through the Cancer Genome Atlas. *PLoS One*, **11**: e0168284.

Chen J, Liu X, Zhang J, Zhao Y. 2012. Targeting HMGB1 inhibits ovarian cancer growth and metastasis by lentivirus-mediated RNA interference. *J. Cell. Physiol.*, **227**: 3629–3638.

Chen J, Xi B, Zhao Y, Yu Y, Zhang J, Wang C. 2012. High-mobility group protein B1 (HMGB1) is a novel biomarker for human ovarian cancer. *Gynecol. Oncol.*, **126**: 109–117.

Cho MS, Vasquez HG, Rupaimoole R, Pradeep S, Wu S, Zand B, Han H, Rodriguez-aguayo C, Bottsford-miller J, Miyake T, Choi H, Dalton HJ, Ivan C, Baggerly K, Lopez-Berestein G, Sood A k, Afshar-Kharghan V. 2014. Autocrine Effects of Tumor-Derived Complement. *Cell Rports*, **6**: 1085–1095.

Choi H, Liu G, Mellacheruvu D, Tyers M, Gingras AC, Nesvizhskii AI. 2012. Analyzing protein-protein interactions from affinity purification-mass spectrometry data with SAINT. *Curr. Protoc. Bioinforma.*, **Chapter 8**: Unit8.15.

Cools J, DeAngelo D, Gotlib J, Stover E, Legare R, Cortes J, Kutok J, Clark J, Galinsky I, Griffin J. 2003. A Tyrosine Kinase Created by Fusion of the PDGFRA and FIP1L1 Genes as a Therapeutic Target of Imatinib in Idiopathic Hypereosinophilic Syndrome. *New Engl. J. od Med.*, **348**: 1201–1214.

Courilleau D, Chastre E, Sabbah M, Redeuilh G, Atfi A, Mester J. 2000. B-ind1, a novel mediator of Rac1 signaling cloned from sodium butyrate- treated fibroblasts. *J. Biol. Chem.*, **275**: 17344–17348.

Daftuar L, Zhu Y, Jacq X, Prives C. 2013. Ribosomal Proteins RPL37, RPS15 and RPS20 Regulate the Mdm2-p53-MdmX Network. *PLoS One*, **8**: e68667.

Das D, Scovell WM. 2001. The binding interaction of HMG-1 with the TATA-binding protein/TATA complex. *J. Biol. Chem.*, **276**: 32597–32605.

Dasgupta S, Wasson LM, Rauniyar N, Prokai L, Borejdo J, Vishwanatha JK. 2009. Novel gene C17orf37 in 17q12 amplicon promotes migration and invasion of prostate cancer cells. *Oncogene*, **28**: 2860–2872.

Deng SS, Xing TY, Zhou HY, Xiong RH, Lu YG, Wen B, Liu SQ, Yang HJ. 2006. Comparative proteome analysis of breast cancer and adjacent normal breast tissues in human. *Genomics. Proteomics Bioinformatics*, **4**: 165–172.

Fan J, Liu J, Culty M, Papadopoulos V. 2010. Acyl-coenzyme A binding domain containing 3 (ACBD3; PAP7; GCP60): an emerging signaling molecule. *Prog. Lipid Res.*, **49**: 218–234.

Gatla HR, Singha B, Persaud V, Vancurova I. 2014. Evaluating cytoplasmic and nuclear levels of inflammatory cytokines in cancer cells by western blotting. *Methods Mol. Biol.*, **1172**: 271–283.

Gebhardt A, Habjan M, Benda C, Meiler A, Haas DA, Hein MY, Mann A, Mann M, Habermann B, Pichlmair A. 2015. mRNA export through an additional cap-binding complex consisting of NCBP1 and NCBP3. *Nat. Commun.*, **6**: 8192.

Gingras AC, Wong CJ. 2016. Proteomics approaches to decipher new signaling pathways. *Curr. Opin. Struct. Biol.*, **41**: 128–134.

Gnanasekar M, Thirugnanam S, Ramaswamy K. 2009. Short hairpin RNA (shRNA) constructs targeting high mobility group box-1 (HMGB1) expression leads to inhibition of prostate cancer cell survival and apoptosis. *Int. J. Oncol.*, **34**: 425–431.

Guidi F, Puglia M, Gabbiani C, Landini I, Gamberi T, Fregona D, Cinellu MA, Nobili S, Mini E. 2012. 2D-DIGE analysis of ovarian cancer cell responses to cytotoxic gold compounds. *Mol. Biosyst.*, **8**: 985–993.

He S, Cheng J, Feng X, Yu Y, Tian L, Huang Q. 2017. The dual role and therapeutic potential of high-mobility group box 1 in cancer. *Oncotarget*.

Hu C, Jiang N, Wang G, Zheng J, Yang W, Yang J. 2014. Expression of hepatocyte growth factor activator inhibitor-1 (HAI-1) gene in prostate cancer: clinical and biological significance. *J. B.U.ON. Off. J. Balk. Union Oncol.*, **19**: 215–220.

Hu R, Peng G, Dai H, Breuer EK, Stemke-Hale K, Li K, Gonzalez-Angulo AM, Mills GB, Lin SY. 2011. ZNF668 functions as a tumor suppressor by regulating p53 stability and function in breast cancer. *Cancer Res.*, **71**: 6524–6534.

Hu R, Wang E, Peng G, Dai H, Lin SY. 2013. Zinc finger protein 668 interacts with Tip60 to promote H2AX acetylation after DNA damage. *Cell Cycle*, **12**: 2033–2041.

Huang JC, Zamble DB, Reardon JT, Lippard SJ, Sancar A. 1994. HMG-domain proteins specifically inhibit the repair of the major DNA adduct of the anticancer drug cisplatin by human excision nuclease. *Proc. Natl. Acad. Sci. U. S. A.*, **91**: 10394–10398.

Ibragimova I, Ibanez de Caceres I, Hoffman AM, Potapova A, Dulaimi E, Al-Saleem T, Hudes GR, Ochs MF, Cairns P. 2010. Global reactivation of epigenetically silenced genes in prostate cancer. *Cancer Prev. Res. (Phila).*, **3**: 1084–1092.

Ishii H, Baffa R, Numata SI, Murakumo Y, Rattan S, Inoue H, Mori M, Fidanza V, Alder H, Croce CM. 1999. The FEZ1 gene at chromosome 8p22 encodes a leucine-zipper protein, and its expression is altered in multiple human tumors. *Proc. Natl.*

Acad. Sci. U. S. A., **96**: 3928–3933.

Ishii H, Vecchione A, Murakumo Y, Baldassarre G, Numata S, Trapasso F, Alder H, Baffa R, Croce CM. 2001. FEZ1/LZTS1 gene at 8p22 suppresses cancer cell growth and regulates mitosis. *Proc. Natl. Acad. Sci. U. S. A.*, **98**: 10374–10379.

Iwasaki J, Kondo T, Darmanin S, Ibata M, Onozawa M, Hashimoto D, Sakamoto N, Teshima T. 2014. FIP1L1 presence in FIP1L1-RARA or FIP1L1-PDGFRA differentially contributes to the pathogenesis of distinct types of leukemia. *Ann. Hematol.*, **93**: 1473–1481.

Jones DT, Lechertier T, Reynolds LE, Mitter R, Robinson SD, Kirn-Safran CB, Hodivala-Dilke KM. 2013. Endogenous ribosomal protein L29 (RPL29): a newly identified regulator of angiogenesis in mice. *Dis. Model. Mech.*, **6**: 115–24.

Jung Y, Lippard SJ. 2003. Nature of full-length HMGB1 binding to cisplatin-modified DNA. *Biochemistry*, **42**: 2664–2671.

Kaddour-Djebbar I, Choudhary V, Brooks C, Ghazaly T, Lakshmikanthan V, Dong Z, Kumar M V. 2010. Specific mitochondrial calcium overload induces mitochondrial fission in prostate cancer cells. *Int. J. Oncol.*, **36**: 1437–1444.

Kang R, Tang D, Schapiro N, Loux T, Livesey K, Billiar T, Wang H, Van Houten B, Lotze M, Zeh H. 2014. The HMGB1/RAGE inflammatory pathway promotes pancreatic tumor growth by regulating mitochondrial bioenergetics. *Oncogene*, **33**: 567–577.

Karantza V. 2011. Keratins in health and cancer: more than mere epithelial cell markers. *Oncogene*, **30**: 127–138.

Karsch-Bluman A, Amoyav B, Friedman N, Shoval H, Schwob O, Ella E, Wald O, Benny O. 2017. High mobility group box 1 antagonist limits metastatic seeding in the lungs via reduction of cell − cell adhesion. *Oncotarget*, **8**: 32706–32721.

Kim JH, Yang CK, Heo K, Roeder RG, An W, Stallcup MR. 2008. CCAR1, a key regulator of mediator complex recruitment to nuclear receptor transcription complexes. *Mol. Cell*, **31**: 510–519.

Kobayashi H, Nishimura H, Matsumoto K, Yoshida M. 2015. Identification of the determinants of 2-deoxyglucose sensitivity in cancer cells by shRNA library screening. *Biochem. Biophys. Res. Commun.*, **467**: 121–127.

Kolostova K, Pinkas M, Jakabova A, Pospisilova E, Svobodova P, Spicka J, Cegan M, Matkowski R, Bobek V. 2016. Molecular characterization of circulating tumor cells in ovarian cancer. *Am. J. Cancer Res.*, **6**: 973–980.

Kozjak-Pavlovic V, Ross K, Benlasfer N, Kimmig S, Karlas A, Rudel T. 2007.

Conserved roles of Sam50 and metaxins in VDAC biogenesis. *EMBO Rep.*, **8**: 576–582.

Kpetemey M, Dasgupta S, Rajendiran S, Das S, Gibbs LD, Shetty P, Gryczynski Z, Vishwanatha JK. 2015. MIEN1, a novel interactor of Annexin A2, promotes tumor cell migration by enhancing AnxA2 cell surface expression. *Mol. Cancer*, **14**: 156–158.

Lange SS, Vasquez KM. 2009. HMGB1: the jack-of-all-trades protein is a master DNA repair mechanic. *Mol. Carcinog.*, **48**: 571–580.

Lázaro-Ibáñez E, Lunavat TR, Jang SC, Escobedo-Lucea C, Oliver-De La Cruz J, Siljander P, Lötvall J, Yliperttula M. 2017. Distinct prostate cancer-related mRNA cargo in extracellular vesicle subsets from prostate cell lines. *BMC Cancer*, **17**: 92.

Lee JY, Lake RJ, Kirk J, Bohr VA, Fan HY, Hohng S. 2017. NAP1L1 accelerates activation and decreases pausing to enhance nucleosome remodeling by CSB. *Nucleic Acids Res.*, **45**: 4696–4707.

Li C, Ge M, Yin Y, Luo M, Chen D. 2012. Silencing expression of ribosomal protein L26 and L29 by RNA interfering inhibits proliferation of human pancreatic cancer PANC-1 cells. *Mol. Cell. Biochem.*, **370**: 127–139.

Li HUI, Niu H, Peng Y, Wang J, He P. 2013. Ubc9 promotes invasion and metastasis of lung cancer cells. *Oncol. reportseports*, **29**: 1588–1594.

Li ML, Wang XF, Tan ZJ, Dong P, Gu J, Lu JH, Wu XS, Zhang L, Ding QC, Wu WG. 2012. Ethyl pyruvate administration suppresses growth and invasion of gallbladder cancer cells via downregulation of HMGB1-RAGE axis. *Int. J. Immunopathol. Pharmacol.*, **25**: 955–965.

Li Y, Guo H, Jin C, Qiu C, Gao M, Zhang L, Liu Z, Kong B. 2017. Spliceosome-associated factor CTNNBL1 promotes proliferation and invasion in ovarian cancer. *Exp. Cell Res.*, **357**: 124–134.

Liu S, Gao Y, Zhang C, Li H, Pan S, Wang X, Du S, Deng Z, Wang L, Song Z, Chen S. 2016. SAMM50 Affects Mitochondrial Morphology through the Association of Drp1 in Mammalian Cells. *FEBS Lett.*, **590**: 1313–1323.

Luo X, Yao J, Nie P, Yang Z, Feng H, Chen P, Shi X, Zou Z. 2016. FOXM1 promotes invasion and migration of colorectal cancer cells partially dependent on HSPA5 transactivation. *Oncotarget*, **7**: 26480–26495.

Lv G, Wu M, Wang M, Jiang X, Du J, Zhang K, Li D, Ma N, Peng Y, Wang L, Zhou L, Zhao W, Jiao Y, Gao X, Hu Z. 2017. miR-320a regulates high mobility group box 1 expression and inhibits invasion and metastasis in hepatocellular carcinoma. *Liver Int. Off. J. Int. Assoc. study liver*, **37**: 1354–1364.

Mack NA, Whalley HJ, Castillo-Lluva S, Malliri A. 2011. The diverse roles of Rac signaling in tumorigenesis. *Cell Cycle*, **10**: 1571–1581.

De Marco M, Basile A, Iorio V, Festa M, Falco A, Ranieri B, Pascale M, Sala G, Remondelli P, Capunzo M, Firpo MA, Pezzilli R, Marzullo L, Cavallo P, De Laurenzi V, Turco MC, Rosati A. 2017. Role of BAG3 in cancer progression: A therapeutic opportunity. *Semin. Cell Dev. Biol.*

McGee AM, Douglas DL, Liang Y, Hyder SM, Baines CP. 2011. The mitochondrial protein C1qbp promotes cell proliferation, migration and resistance to cell death. *Cell Cycle*, **10**: 4119–4127.

Moschos SJ, Jukic DM, Athanassiou C, Bhargava R, Dacic S, Wang X, Kuan S-F, Fayewicz SL, Galambos C, Acquafondata M, Dhir R, Becker D. 2010. Expression analysis of Ubc9 , the single small ubiquitin-like modifier (SUMO) E2 conjugating enzyme , in normal and malignant tissues. *Hum. Pathol.*, **41**: 1286–1298.

Muthu M, Cheriyan VT, Rishi AK. 2015. CARP-1/CCAR1: a biphasic regulator of cancer cell growth and apoptosis. *Oncotarget*, **6**: 6499–6510.

Narita T, Yung TM, Yamamoto J, Tsuboi Y, Tanabe H, Tanaka K, Yamaguchi Y, Handa H. 2007. NELF interacts with CBC and participates in 3' end processing of replication-dependent histone mRNAs. *Mol. Cell*, **26**: 349–365.

Oliver D, Ji H, Liu P, Gasparian A, Gardiner E, Lee S, Zenteno A, Perinskaya LO, Chen M, Buckhaults P, Broude E, Wyatt MD, Valafar H, Pena E, Shtutman M. 2017. Identification of novel cancer therapeutic targets using a designed and pooled shRNA library screen. *Sci. Rep.*, **7**: 43023.

Pan X, Hobbs RP, Coulombe PA. 2013. The expanding significance of keratin intermediate filaments in normal and diseased epithelia. *Curr. Opin. Cell Biol.*, **25**: 47–56.

Pardo M, Lang B, Yu L, Prosser H, Bradley A, Babu MM, Choudhary J. 2010. An Expanded Oct4 Interaction Network: Implications for Stem Cell Biology, Development, and Disease. *Cell Stem Cell*, **6**: 382–395.

Park SM, Choi EY, Bae M, Kim S, Park JB, Yoo H, Choi JK, Kim YJ, Lee SH, Kim IH. 2016. Histone variant H3F3A promotes lung cancer cell migration through intronic regulation. *Nat. Commun.*, **7**: 12914.

Pellegrini L, Xue J, Larson D, Pastorino S, Jube S, Forest KH, Saad-Jube ZS, Napolitano A, Pagano I, et al. 2017. HMGB1 targeting by ethyl pyruvate suppresses malignant phenotype of human mesothelioma. *Oncotarget*, **8**: 22649–22661.

Reinert LS, Shi B, Nandi S, Mazan-Mamczarz K, Vitolo M, Bachman KE, He H,

Gartenhaus RB. 2006. MCT-1 protein interacts with the cap complex and modulates messenger RNA translational profiles. *Cancer Res.*, **66**: 8994–9001.

Salza R, Peysselon F, Chautard E, Faye C, Moschcovich L, Weiss T, Perrin-Cocon L, Lotteau V, Kessler E, Ricard-Blum S. 2014. Extended interaction network of procollagen C-proteinase enhancer-1 in the extracellular matrix. *Biochem. J.*, **457**: 137–149.

Santiago-Medina M, Yang J. 2016. MENA Promotes Tumor-Intrinsic Metastasis through ECM Remodeling and Haptotaxis. *Cancer Discov.*, **6**: 474–476.

Schimmack S, Taylor A, Lawrence B, Alaimo D, Schmitz-Winnenthal H, Buchler MW, Modlin IM, Kidd M. 2014. A mechanistic role for the chromatin modulator, NAP1L1, in pancreatic neuroendocrine neoplasm proliferation and metastases. *Epigenetics Chromatin*, **7**: 15–8935–7–15. eCollection 2014.

Schwarz SyE, Matuschewski K, Liakopoulos D, Scheffner M, Jentsch S. 1998. The ubiquitin-like proteins SMT3 and SUMO-1 are conjugated by the UBC9 E2 enzyme. *Proc. Natl. Acad. Sci. U. S. A.*, **95**: 560–564.

Scully OJ, Yu Y, Salim A, Thike AA, Yip GW-C, Baeg GH, Tan P-H, Matsumoto K, Bay BH. 2015. Complement component 1, q subcomponent binding protein is a marker for proliferation in breast cancer. *Exp. Biol. Med.*, **240**: 846–853.

Sechler M, Borowicz S, Van Scoyk M, Avasarala S, Zerayesus S, Edwards MG, Kumar Karuppusamy Rathinam M, Zhao X, Wu PY, Tang K, Bikkavilli RK, Winn RA. 2015. Novel Role for gamma-Catenin in the Regulation of Cancer Cell Migration via the Induction of Hepatocyte Growth Factor Activator Inhibitor Type 1 (HAI-1). *J. Biol. Chem.*, **290**: 15610–15620.

Seong HA, Jung H, Manoharan R, Ha H. 2011. Positive regulation of apoptosis signal-regulating kinase 1 signaling by ZPR9 protein, a zinc finger protein. *J. Biol. Chem.*, **286**: 31123–31135.

Sheller-Miller S, Urrabaz-Garza R, Saade G, Menon R. 2017. Damage-Associated molecular pattern markers HMGB1 and cell-Free fetal telomere fragments in oxidative-Stressed amnion epithelial cell-Derived exosomes. *J. Reprod. Immunol.*, **123**: 3–11.

Stark C, Breitkreutz BJ, Reguly T, Boucher L, Breitkreutz A, Tyers M. 2006. BioGRID: a general repository for interaction datasets. *Nucleic Acids Res.*, **34**: D535-9.

Štros M. 2010. HMGB proteins: Interactions with DNA and chromatin. *Biochim. Biophys. Acta*, **1799**: 101–113.

Sturm D, Witt H, Hovestadt V, Khuong-Quang DA, Jones DTW, Konermann C,

Pfaff E, Tönjes M, Sill M, Bender S, et al. 2012. Hotspot Mutations in H3F3A and IDH1 Define Distinct Epigenetic and Biological Subgroups of Glioblastoma. *Cancer Cell*, **22**: 425–437.

Suetens A, Moreels M, Quintens R, Chiriotti S, Tabury K, Michaux A, Gregoire V, Baatout S. 2014. Carbon ion irradiation of the human prostate cancer cell line PC3: a whole genome microarray study. *Int. J. Oncol.*, **44**: 1056–1072.

Sun P, Jiang Z, Chen X, Xue L, Mao X, Ruan G, Song Y, Mustea A. 2016. Decreasing the ratio of matriptase/HAI1 by downregulation of matriptase as a potential adjuvant therapy in ovarian cancer. *Mol. Med. Rep.*, **14**: 1465–1474.

Suzuki M, Watanabe M, Nakamaru Y, Takagi D, Takahashi H, Fukuda S, Hatakeyama S. 2016. TRIM39 negatively regulates the NFkappaB-mediated signaling pathway through stabilization of Cactin. *Cell. Mol. Life Sci.*, **73**: 1085–1101.

Szklarczyk D, Morris JH, Cook H, Kuhn M, Wyder S, Simonovic M, Santos A. 2017. The STRING database in 2017: quality-controlled protein-protein association networks, made broadly accessible. *Nucleic Acids Res.*, **45**: D362–D368.

Takahashi K, Suzuki K. 2011. WAVE2, N-WASP, and Mena facilitate cell invasion via phosphatidylinositol 3-kinase-dependent local accumulation of actin filaments. *J. Cell. Biochem.*, **112**: 3421–3429.

Tang D, Kang R, Zeh 3rd HJ, Lotze MT. 2010. High-mobility group box 1 and cancer. *Biochim. Biophys. Acta*, **1799**: 131–140.

Teng Y, Ai Z, Wang Y, Wang J, Luo L. 2013. Proteomic identification of PKM2 and HSPA5 as potential biomarkers for predicting high-risk endometrial carcinoma. *J. Obstet. Gynaecol. Res.*, **39**: 317–325.

Thomas JO, Stott K. 2012. H1 and HMGB1: modulators of chromatin structure. *Biochem. Soc. Trans.*, **40**: 341–346.

Thomas MC, Chiang CM. 2006. The general transcription machinery and general cofactors. *Crit. Rev. Biochem. Mol. Biol.*, **41**: 105–178.

Vecchione A, Croce CM, Baldassarre G. 2007. Fez1/Lzts1 a new mitotic regulator implicated in cancer development. *Cell Div.*, **2**: 24.

Vizcaíno JA, Csordas A, Del-Toro N, Dianes JA, Griss J, Lavidas I, Mayer G, Perez-Riverol Y. 2016. 2016 update of the PRIDE database and its related tools. *Nucleic Acids Res.*, **44**: D447–D456.

Wang W, Zhang W, Han Y, Chen J, Wang Y, Zhang Z, Hui R. 2005. NELIN, a new F-actin associated protein, stimulates HeLa cell migration and adhesion. *Biochem.*

Biophys. Res. Commun., **330**: 1127–1131.

Warren M, Twohig M, Pier T, Eickhoff J, Lin CY, Jarrard D, Huang W. 2009. Protein expression of matriptase and its cognate inhibitor HAI-1 in human prostate cancer: a tissue microarray and automated quantitative analysis. *Appl. Immunohistochem. Mol. Morphol. AIMM*, **17**: 23–30.

Wei L, Xie X, Li J, Li R, Shen W, Duan S, Zhao R, Yang W, Liu Q, Fu Q, Qin Y. 2015. Disruption of human vigilin impairs chromosome condensation and segregation. *Cell Biol. Int.*, **39**: 1234–1241.

Xiao H, Cheng S, Tong R, Lv Z, Ding C, Du C, Xie H, Zhou L, Wu J, Zheng S. 2014. BAG3 regulates epithelial-mesenchymal transition and angiogenesis in human hepatocellular carcinoma. *Lab. Invest.*, **94**: 252–261.

Xu J, Footman A, Qin Y, Aysola K, Black S, Reddy V, Singh K, Grizzle W, You S. 2016. BRCA1 Mutation Leads to Deregulated Ubc9 Levels which Triggers Proliferation and Migration of Patient-Derived High Grade Serous Ovarian Cancer and Triple Negative Breast Cancer Cells. *Int. J. Chronic Dis.*, **2**: 31–38.

Yamasaki M, Nomura T, Sato F, Mimata H. 2007. Metallothionein is up-regulated under hypoxia and promotes the survival of human prostate cancer cells. *Oncol. Rep.*, **18**: 1145–1153.

Yang WL, Wei L, Huang WQ, Li R, Shen WY, Liu JY, Xu JM, Li B, Qin Y. 2014. Vigilin is overexpressed in hepatocellular carcinoma and is required for HCC cell proliferation and tumor growth. *Oncol. Rep.*, **31**: 2328–2334.

Yusein-Myashkova S, Stoykov I, Gospodinov A, Ugrinova I, Pasheva E. 2016. The repair capacity of lung cancer cell lines A549 and H1299 depends on HMGB1 expression level and the p53 status. *J. Biochem.*, **160**: 37–47.

Zanini IM, Soneson C, Lorenzi LE, Azzalin CM. 2017. Human cactin interacts with DHX8 and SRRM2 to assure efficient pre-mRNA splicing and sister chromatid cohesion. *J. Cell Sci.*, **130**: 767–778.

Zhao CB, Bao JM, Lu YJ, Zhao T, Zhou XH, Zheng DY, Zhao SC. 2014. Co-expression of RAGE and HMGB1 is associated with cancer progression and poor patient outcome of prostate cancer. *Am. J. Cancer Res.*, **4**: 369–377.

Zhou W, He MR, Jiao HL, He LQ, Deng DL, Cai JJ, Xiao ZY, Ye YP, Ding YQ,. 2015. The tumor-suppressor gene LZTS1 suppresses colorectal cancer proliferation through inhibition of the AKT-mTOR signaling pathway. *Cancer Lett.*, **360**: 68–75.

Zhu H, Yu JJ. 2010. Gene expression patterns in the histopathological classification of epithelial ovarian cancer. *Exp. Ther. Med.*, **1**: 187–192.

ANNEX TO CHAPTER 2

Supplementary table. HMGB1 interacting partners in PNT2 with a SP=1 from two independent experiments.

	First experiment							Second experiment						
	HMGB1 IP			Rabbit IP			SP	HMGB1 IP			Rabbit IP			SP
GENE	C	P	S	C	P	S		C	P	S	C	P	S	
SMARCA5	12,83	12	21				1	2,57	3	5				1
NBN	33,29	14	57				1	11,14	5	10				1
H2AFY	27,42	6	50	5,91	1	3	1	31,99	7	98				1
SRSF10	23,66	5	25				1	20,99	4	22				1
SF3B1	11,96	8	19				1	8,13	5	11				1
SNRNP200	10,96	15	49				1	9,78	11	39				1
BCAS2	48,44	7	17				1	34,22	4	8				1
RSL1D1	20,61	7	14				1	24,29	10	50				1
ZRANB2	6,06	2	2				1	10	3	5				1
RPLP2	55,65	3	18				1	70,43	4	20				1
RPLP0	28,71	5	16				1	31,23	9	35				1
NPM1	62,59	13	184	19,73	2	4	1	59,18	9	108	24,83	3	9	1
ANXA2	52,21	14	53	9,14	3	6	1	45,72	11	70	30,38	7	12	1
HNRNPC	8,82	2	8				1	12,42	5	16				1
RPSA	18,31	4	9				1	50,85	10	60				1
HMGB1	42,33	13	176				1	27,44	10	171				1
PARP1	36,88	26	106	1,48	1	2	1	32,25	21	106	2,76	2	3	1
H2AFZ	53,91	6	139	53,91	5	25	1	45,31	5	145	28,13	2	25	1
RPS17L	51,85	5	20				1	47,41	6	58				1
HSPA8	20,43	10	32	6,19	3	4	1	18,89	9	30	8,98	4	10	1
TOP2A	12,41	14	43				1	11,89	15	35				1
RPS2	25,94	7	39	7,85	2	6	1	32,42	9	74	4,1	1	5	1
CD44	8,49	4	15	2,16	1	1	1	3,91	2	5				1
HIST1H1B	25,66	7	24	10,18	2	2	1	26,11	9	53	21,68	5	8	1

Supplementary table. Continuation

GENE	First experiment						SP	Second experiment						SP
	HMGB1 IP			Rabbit IP				HMGB1 IP			Rabbit IP			
	C	P	S	C	P	S		C	P	S	C	P	S	
RPL7	37,9	10	45	4,44	1	2	1	41,53	11	74	14,92	3	10	1
RPL17	23,37	4	15	5,43	1	1	1	38,59	5	18				1
NCL	34,93	30	571	24,93	13	42	1	33,24	25	578	18,73	8	32	1
RPS3	56,79	12	101	5,35	1	3	1	65,84	14	194	28,4	5	10	1
POLR2A	3,76	5	8				1	1,62	2	4				1
RPS12	62,88	7	47	16,67	1	5	1	57,58	7	96	30,3	2	7	1
RPL13	35,55	7	16	14,69	3	5	1	40,28	9	39	30,33	6	13	1
RPL10	19,16	3	21				1	40,19	8	49	6,54	1	2	1
SMARCA1	4,36	5	5				1	2,56	3	5				1
RPL12	24,85	3	7	5,45	1	1	1	32,12	4	19	9,7	1	2	1
NKTR	3,97	4	7				1	1,98	2	6				1
POLR2B	6,56	4	9				1	2,47	2	2				1
RPL22	39,06	3	10				1	63,28	6	33				1
RPL4	37,7	17	60				1	44,5	19	154	17,33	4	13	1
RBMX	29,92	12	94	5,63	2	3	1	39,13	15	92	9,97	3	7	1
EIF4A3	37,96	17	73				1	40,39	13	85	3,16	1	2	1
RPS19	44,83	7	34	6,21	1	1	1	52,41	10	82	15,17	2	4	1
RPL3	22,58	7	40				1	41,19	15	107	11,91	2	2	1
RPL13A	23,15	6	21	5,91	1	1	1	24,14	5	37				1
BUD31	20,14	2	4				1	13,89	2	3				1
RPL35	21,95	3	16				1	22,76	4	49	21,95	3	5	1
NOP2	5,3	3	5				1	18,84	8	13				1
ATRX	6,06	9	20				1	1,89	4	7				1
RPL27A	32,43	4	20	7,43	1	2	1	36,49	6	53	23,65	3	14	1

Supplementary table. Continuation.

	First experiment							Second experiment						
	HMGB1 IP			Rabbit IP			SP	HMGB1 IP			Rabbit IP			SP
GENE	C	P	S	C	P	S		C	P	S	C	P	S	
RPL5	24,24	8	34				1	29,97	7	29				1
RPL21	27,5	3	23				1	31,25	4	38	31,87	4	10	1
RPS9	26,8	7	22	8,76	2	2	1	32,47	8	30	9,28	2	3	1
RPS5	36,76	5	23				1	35,29	9	74	11,76	1	1	1
RPS10	32,73	4	14				1	47,27	9	86	13,94	2	3	1
MRE11A	43,36	24	148				1	23,31	9	31				1
RPL14	16,28	3	11				1	10,7	2	10				1
DAP3	15,33	5	11				1	8,54	2	7				1
HNRNPA3	14,29	3	8				1	10,05	2	4				1
RPS20	31,09	5	39	9,24	1	1	1	34,45	6	95	25,21	2	8	1
RPS3A	40,53	10	49	3,03	1	1	1	54,55	14	79	15,53	3	5	1
RPL26	15,86	2	10				1	17,24	2	13				1
RPL15	20,1	4	9				1	25,98	5	17				1
RPL27	43,38	5	18	6,62	1	1	1	35,29	4	24	7,35	1	1	1
HNRNPK	11,02	3	8				1	5,62	2	3				1
RPS8	42,79	8	52	11,54	2	4	1	51,92	12	108	23,08	4	12	1
RPS15A	23,08	3	10				1	26,92	4	29				1
RPS16	52,05	10	80	15,75	2	3	1	47,95	10	99	15,75	2	3	1
RPS14	31,79	6	30	24,5	3	4	1	33,77	7	77	31,79	3	7	1
RPS18	47,37	9	61	20,39	3	5	1	58,55	13	165	42,11	5	12	1
RPS29	46,43	3	9				1	26,79	2	8	14,29	1	2	1
RPS13	43,05	7	27	4,64	1	1	1	41,06	7	73	14,57	2	5	1
RPS11	38,61	5	13	11,39	2	2	1	39,87	6	31	24,68	3	10	1
RPL7A	34,59	11	55	9,02	2	4	1	34,96	12	83	24,81	5	14	1

Supplementary table. Continuation

	First experiment							Second experiment						
	HMGB1 IP			Rabbit IP			SP	HMGB1 IP			Rabbit IP			SP
GENE	C	P	S	C	P	S		C	P	S	C	P	S	
RPS4X	20,53	4	15				1	27,76	8	49				1
RPL23A	23,08	5	14	13,46	2	4	1	33,33	6	39	16,03	2	6	1
RPS6	29,32	7	33	6,02	1	2	1	25,7	7	81	12,85	2	8	1
HIST1H4A	64,08	13	891	53,4	8	65	1	65,05	16	1062	63,11	12	163	1
RPS15	36,55	3	42				1	40	5	77	15,17	1	5	1
RPS24	21,05	4	17				1	25,56	3	17				1
RPS25	28	4	18	15,2	2	4	1	24	3	15				1
RPS28	34,78	3	14				1	59,42	6	29	31,88	2	4	1
RPL30	40,87	3	11				1	50,43	4	29				1
RPL31	18,4	2	7				1	33,6	3	11	14,4	2	3	1
RPL10A	23,5	4	13				1	29,49	6	27				1
RPL32	22,22	3	9				1	20,74	3	20				1
RPL11	21,35	4	13	14,61	2	3	1	26,97	5	22	14,61	2	4	1
RPL8	12,06	3	12				1	28,79	5	29	4,28	1	1	1
TRA2B	24,31	6	27				1	6,94	2	7				1
HIST1H3A	58,09	11	115	44,12	6	38	1	58,82	12	375	50,74	6	83	1
MRPS22	14,72	4	10	3,33	1	1	1	8,61	3	8				1
MRPS35	18,27	3	9				1	11,46	2	8				1
MRPS21	29,89	2	4				1	29,89	2	5				1
MRPS34	11,01	2	4				1	12,39	2	3				1
RPL24	19,75	4	11				1	21,02	5	12	11,46	2	2	1
RPL19	22,45	5	29	8,67	1	3	1	13,78	3	35	9,18	2	5	1
SRSF3	28,66	4	31				1	23,17	3	10				1
H3F3A	58,09	11	159	19,85	4	18	1	58,82	11	262	50	5	40	1

Supplementary table. Continuation

	First experiment						SP	Second experiment						SP
	HMGB1 IP			Rabbit IP				HMGB1 IP			Rabbit IP			
GENE	C	P	S	C	P	S		C	P	S	C	P	S	
HNRNPU	20,48	10	40	3,88	1	3	1	14,42	6	19	6,55	2	5	1
RPL18A	11,36	2	7				1	18,18	4	10	7,39	1	2	1
RPL6	31,94	8	41				1	48,96	15	60	5,9	2	2	1
TOP2B	9,1	10	28				1	6,21	7	19				1
RPL18	31,91	7	32				1	30,32	8	49	12,77	2	3	1
TJP1	53,43	63	575				1	38,79	44	352	0,57	1	1	1
SRSF1	36,69	7	30				1	35,89	6	23				1
SSRP1	14,53	6	21				1	20,87	11	42				1
NCBP1	5,32	3	7				1	5,57	3	5				1
AHNAK	47,37	133	527				1	29,32	75	275				1
SRSF5	5,88	2	4				1	8,46	2	6				1
SRSF6	12,5	4	12				1	9,01	3	17				1
TRIM28	14,01	5	9				1	6,11	2	5				1
SNW1	33,96	10	20				1	11,94	3	10				1
TRA2A	9,93	3	5				1	18,44	3	9				1
SAFB2	16,05	9	27				1	3,88	3	5				1
CTTN	13,64	4	12				1	10	2	10	6,36	1	1	1
RBM39	8,11	3	8				1	4,91	2	6				1
NUMA1	5,72	6	9				1	1,37	2	3				1
EFTUD2	25,72	13	49				1	8,64	4	7				1
RNPS1	25,57	6	53	4,92	1	2	1	22,62	5	50				1
SAFB	18,14	10	38				1	10,49	7	20				1
SRSF7	15,97	4	28				1	22,27	5	34				1
ZNF326	11,51	4	5				1	7,04	3	4				1

Supplementary table. Continuation

GENE	First experiment						SP	Second experiment						SP
	HMGB1 IP			Rabbit IP				HMGB1 IP			Rabbit IP			
	C	P	S	C	P	S		C	P	S	C	P	S	
HP1BP3	11,57	3	6				1	17,36	6	43	2,35	1	1	1
HIST2H2AA3	68,46	10	633	40,77	5	31	1	66,15	12	1512	56,15	8	174	1
CDC73	23,73	10	23				1	26,18	12	42				1
PRPF8	18,03	24	72				1	9,04	10	24				1
ZC3H14	7,61	3	5				1	8,56	4	6				1
LARP1	17,06	9	23				1	22,99	10	29				1
HIST2H3A	58,09	11	217	44,12	5	19	1	58,82	11	461	50,74	6	53	1
SUPT6H	18,19	16	38				1	6,32	6	10				1
ZC3H18	12,28	6	17				1	8,6	6	11				1
HIST2H2AB	40,77	5	69	29,23	2	13	1	66,92	8	297	45,38	2	10	1
PAF1	25,05	9	30				1	19,02	8	26				1
NGDN	10,16	2	4				1	10,16	2	4				1
RAD50	35,9	43	230				1	16,01	16	57				1
PTCD3	10,89	5	8				1	15,38	6	13				1
TWNK	21,2	8	27				1	19,15	8	24				1
IWS1	8,18	4	14				1	6,72	3	11				1
RSF1	20,61	19	64				1	6,52	5	8				1
GNL3	14,94	5	10				1	20,4	6	15				1
SRRT	4	2	3				1	6,05	3	4				1
POLDIP3	30,64	7	18				1	19,48	5	18				1
MRPS26	12,68	2	7				1	18,54	4	14				1
NAT10	2,63	2	3				1	7,51	3	9				1
PNN	16,88	9	42				1	15,48	10	53				1
SLTM	7,16	6	17				1	3,68	3	9				1

Supplementary table. Continuation

GENE	First experiment						SP	Second experiment						SP
	HMGB1 IP			Rabbit IP				HMGB1 IP			Rabbit IP			
	C	P	S	C	P	S		C	P	S	C	P	S	
BCLAF1	32,83	26	114				1	24,67	20	89				1
H2AFY2	22,04	5	24				1	15,59	3	19				1
CGN	17,21	11	27				1	8,02	5	6				1
TJP2	33,11	25	127				1	28,24	20	101				1
SAP30BP	11,04	2	6				1	8,44	2	3				1
CCNL1	6,65	2	6				1	6,65	2	4				1
ACIN1	19,69	15	44				1	13,72	11	48				1
SRRM2	11,12	19	64	1,02	2	2	1	6,87	14	44	0,51	1	2	1
MRPS7	20,25	4	6				1	9,5	2	5				1
THRAP3	25,45	23	155	2,09	1	2	1	23,25	21	212	3,35	2	4	1
MRPS23	15,79	3	5				1	13,68	3	5				1
RPL36	20	3	7				1	22,86	4	27	8,57	1	4	1
CHTOP	11,69	2	9				1	11,69	2	7				1
SUPT16H	22,45	18	47				1	19,77	15	53				1
MRPS18B	40,7	6	13				1	28,29	3	7				1

C: coverage; **P**: peptides; **S**: spectra

Chapter 3

Novel HMGB1 and HMGB2 interacting partners in prostate and ovarian tumoral cells

INTRODUCTION

In a recent review we have described the role of human HMGB proteins in cancerous processes related to oxidative stress, with special reference to ovarian and prostate cancer (Barreiro-Alonso *et al.*, 2016). Human HMGB proteins, HMGB1, 2, 3, and 4 are differentially expressed in diverse tissues (Barreiro-Alonso *et al.*, 2016). These differences might be correlated with binding to tissue-specific protein partners. Remarkably, abnormal mRNA and protein levels of these proteins have been detected in numerous cancers, including ovarian and prostate (Y Li *et al.*, 2014; Srinivasan *et al.*, 2014; Li *et al.*, 2012). Likewise, different studies linked HMGB1 to the principal cancer hallmarks as epithelial-mesenchymal transition, invasion, migration and angiogenesis (Chandrasekaran *et al.*, 2016; Beijnum *et al.*, 2012; Liu *et al.*, 2017). The role of HMGB2 in these processes has also been reported although is less studied (Wang *et al.*, 2013; Tang *et al.*, 2017; Wu *et al.*, 2013).

Since HMGB proteins are multifunctional and are also necessary in healthy cells, probably the modulation of their role during cancer onset and progression is caused by changes in specific interactions with other proteins. The identification of HMGB partners, which could be specifically involved in malignant cell transformation, is a field of interest for ongoing translational cancer research. Interactome strategies are outstanding for the development of these research lines.

In the preceding chapter we have analyzed by proteomic strategies specific partners of HMGB1 and HMGB2 in epithelial cells from ovary and prostate. In this chapter we extend the use of yeast two hybrid methods to find

proteins that interact with HMGB1 and HMGB2 in cancer cell lines of prostate and ovary derived from epithelial cells. Validation of the data set by analysis of co-immunoprecipitation, sub-cellular co-localization and co-regulated expression is also presented for KRT7 which is a new HMGB1 interacting partner.

MATERIALS AND METHODS

Cell culture

PC-3 cell line (human prostate adenocarcinoma) was grown in RPMI-1640 (Thermo Fisher Scientific, Inc.) supplemented with 10% heat-inactivated fetal bovine serum (Thermo Fisher Scientific, Inc.) and 1% penicillin-streptomycin (Thermo Fisher Scientific, Inc.) respectively. Cells were cultured at 37ºC, 5% CO_2 in a humidified incubator. Cells were tested regularly for mycoplasma contamination.

Yeast strains

Sacchacomyces cerevisiae strains used in this study are Y187 (MATα, *ura*3-52, *his3*-200, *ade2*-101*, trp1*-901, *leu*2-3, 112, *gal*4Δ, *gal*80Δ, *met*-, *URA3*::*GAL*uas-*GAL1*TATA-*LacZ MEL*1) and Y2HGold (MATa, *trp*1-901, *leu*2-3, 112, *ura*3-52, *his*3-200, *gal*4Δ, *gal*80Δ, *LYS2::GAL1*uas-*GAl1*TATA-His3, *GAL2*uas-Gal2TATA-Ade2 URA3:: MEL1UAS-Mel1TATA, AUR1-C MEL1).

Library construction, bait construction and Yeast two-hybrid library screening

Total RNA from the ovary adenocarcinoma cell line SKOV-3 and from the prostate cancer cell line PC-3 (Sigma-Aldrich) were used to construct cDNA

libraries. Library construction, bait construction and Yeast two-hybrid library screening were assessed as described in Chapter 2.

Quantitative real-time polymerase chain reaction (qRT-PCR)

Total RNA from the tumor cell lines PC-3 and SKOV-3 (Sigma Aldrich) and from Human prostate or ovary epithelial cells (Innoprot, Spain), HPEpiC and HOSEpiC repectively, was transcribed into cDNA and labeled with the KAPA SYBR FAST universal one-step qRT-PCR kit (Kappa Biosystems, Inc, Woburn, Massachusetts, USA). Reaction conditions for thermal cycling were: 42 ºC for 5 min, 95 ºC for 5 s, 40 cycles of 95 ºC for 3 s and finally 60 ºC for 20 s. The list of primers is provided in Table 1. The ECO Real-Time PCR System was used for the experiments (Illumina, Inc., San Diego, California, USA) and calculations were made by the $2^{-\Delta\Delta Ct}$ method (Livak and Schmittgen, 2001). A t-test was applied to evaluate the statistically significant differences between samples with a p-value lower than 0.05. The relative mRNA levels of the experimentally selected genes (target-genes) were calculated by referring to the mRNA levels of the housekeeping gene *GADPH*. It was previously verified that this gene is expressed constitutively in the assayed conditions. For valid quantification using the $2^{-\Delta\Delta Ct}$ method, it is crucial that target and housekeeping PCR amplification efficiencies are approximately equal. To determine if the target and reference primer pairs have comparable PCR efficiencies, the ratios of Ct (reference gene versus analyzed gene) were plotted versus the logarithm of input RNA template (0.01, 0.1, 1 and 10 ng). It was verified that the absolute value of the slope of the regression line is lower than 0.15 and, therefore, the efficiencies of the two PCR reactions differ less than 10%. At least six independent replicas were made for each sample.

Table 1. Primer pairs for qRT-PCR.

Gene Name	Sequence 5`-3`	Tm (ºC)	Product size (pb)
HMGB1	F: TCAAAGGAGAACATCCTGGCC	57.1	86
	R: GCTTGTCATCTGCAGCAGTGTT	58	
KRT7	F: TGAATGATGAGATCAACTTCCTCAG	55	75
	R: RTGTCGGAGATCTGGGACTGC	58.1	
GADPH	F: AGCGCAACCCACTCCTCCAC	61.7	147
	R: TCCCCAGCAGTGAGGGTCTC	61.2	
HOXA10	F: CTCCCACACTCGCCATCTC	58.13	180
	R: CAAACCCAGCCCAGTCAGG	60.85	

Immunoprecipitation

-Using Protein G Plus-Agarose

100 µl of Protein G Plus-Agarose immunoprecipitation Reagent (Santa Cruz) were coupled with 2.5/4 µg anti-HMGB1 antibody (Santa Cruz, sc-74085) or anti-mouse antibody (Molecular Probes, A10534) in PBS for 1 hour at 4ºC in rotation. PC-3 cells were lysated in 20 mM Tris/HCl, 150 mM, 1% Triton X-100, 1X PMSF and protease inhibitor cocktail (Sigma-Aldrich) and incubated for 30 minutes at 4 ºC in rotation. 500 µg of total proteins were incubated with the antibody-agarose beads overnight and eluted by incubation in 1× LDS loading buffer containing 350 mM beta-mercaptoethanol at 95 ºC for 10 min.

- Using Dynabeads Protein G

PC-3 cells were lysed in 50 mM Tris-HCl pH 8.0, 150 mM NaCl, 0.1% NP-40, 1 mM EDTA, 2 mM $MgCl_2$ and cOmplete™ Mini, EDTA-free Protease Inhibitor Cocktail (Roche) and incubated with Benzonase®Nuclease (Sigma-Aldrich) for 30 min at 4 ºC to eliminate nucleic acids from the lysates. 25 µl of beads were coupled with 5 µg of anti-HMGB1 antibody (Abcam, ab18256) and

Millipore Normal Rabbit IgG Polyclonal (12-360) was used as the negative control. 1 mg of total protein was used for each immunoprecipitation. Proteins were eluted by incubation in 1× LDS loading buffer (Life Technologies) containing 350 mM beta-mercaptoethanol at 95 ºC for 10 min.

Western blot analysis

Samples were run on 10% SDS-PAGE gels at 80 V for 20 minutes and at 200 V for the next 45-60 minutes, proteins were then transferred onto a PVDF membrane at 0.2 A for 1 hour. Membranes were blocked by incubating with 5% nonfat dry milk for 1 hour at room temperature (RT) and then incubated with primary antibodies: anti-HMGB1 (Santa Cruz, sc-74085) or anti-Cytokeratin 7 (Abcam, ab181598) in PBST (containing 0.1% Tween 20) overnight at 4º C. After incubation with the corresponding horseradish peroxidase–conjugated secondary antibody: ECL Anti-mouse IgG (NXA931, GE Healthcare Sciences) or ECL Anti-rabbit IgG (NA934, GE Healthcare Sciences), protein bands were detected using Luminata^{TM}Crescendo Western HRP Substrate (Millipore) according to manufacturer´s instructions, Bio-Rad ChemiDocTM imager were used for chemiluminescence detection.

Immunofluorescence and confocal microscopy

PC-3 cells were plated in 6-well plates each of them containing 4 sterile 13mm glass coverslips. When 80% confluence was achieved, cells were fixed using 4% para-formaldehyde in PBS for 15 minutes at room temperature. Cells were washed three times with PBS (137 mM NaCl, 2,7 mM KCl, 10 mM Na_2HPO_4, 2 mM KH_2PO_4) and permeabilized in 0.1% Triton/PBS for 15

minutes at room temperature. Afterwards, they were blocked in 1% BSA in PBS for one hour at room temperature. Primary antibodies: anti-HMGB1 (Santa Cruz, sc-74085), anti-HOXA10 (Santa Cruz, sc-28602) or anti-Cytokeratin 7 (Abcam, ab181598) were diluted in 1% BSA in PBS. Cells were incubated with the correspondent primary antibodies overnight at 4 ºC followed by three washes with PBS and staining with the secondary antibodies modified with Alexa Fluor 488 for HMGB1 and Alexa Fluor 568 for Cytokeratin 7 and HOXA10 (Invitrogen), previously diluted in 1% BSA in PBS, for one hour at RT in the dark. After secondary antibody incubation wells were washed three times and stained with Hoechst (Life Technologies) for five minutes at room temperature in the dark. Cells were washed once with PBS and once with sterile-distilled water. Each coverslip was mounted on a clean slide using ProLong™ Gold Antifade Mountant (Invitrogen). Once dried, the slides were stored at 4 ºC in the dark until confocal microscopy was carried out.

RESULTS

HMGB1 and HMGB2 interacting partners found by Y2H assays using as bait cDNA libraries from the prostate cancer cell line PC-3 and the ovarian carcinoma cell line SKOV-3

To obtain greater insight into the role of HMGB1 in the development of prostate and ovarian cancer, cDNA libraries were constructed using total RNA from the cancer cell lines SKOV-3 and PC-3 and yeast two-hybrid assays were carried out using a full-length HMGB1 as the bait. 10 HMGB1 preys were identified in the assays performed with the PC-3 cDNA library while 5

were found using the SKOV-3 library (Figure 1A). Two of the proteins found were common to both libraries, KRT7 and UHRF2.

Moreover a long non-coding RNA, MALAT1, was identified. Functions of found proteins are associated to cell cycle progression (UHRF2), microtubule structure (DNAAF2, WDR60), proteasome/protein degradation (UBE2E3, UBXN1) and transcription factors (HOXA10, ZNF428), among others (Figure 1C). None of HMGB1 interactions found in these assays have been previously reported in STRING or BioGRID at the time this chapter was written.

HMGB2 has high homology with HMGB1 so not surprisingly they have common functions as playing a role in inflammation (Pusterla *et al.*, 2009) and chromatin remodeling activity (Ugrinova *et al.*, 2009). Common interacting proteins for these two HMGB proteins have been described but,as HMGB2 has been less studied than HMGB1, the number of known interactions for the former is considerably lower. In this study we wanted to find new HMGB2 partners in relation to prostate and ovarian cancer to unveil new HMGB2 roles in the development and progression of these tumors. Therefore the same approach used for HMGB1 was carried out for HMGB2.

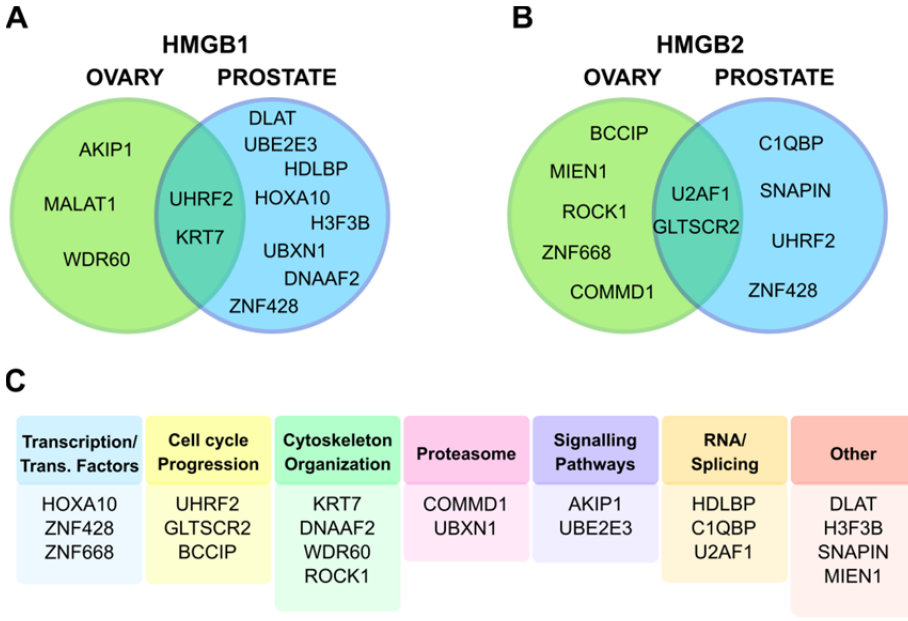

Figure 1. (A) Venn diagram showing HMGB1 interacting partners found in Y2H assays using SKOV-3 (ovary tumoral cells) or PC-3 (prostate tumoral cells) libraries and common proteins to both cell types. **(B)** Venn diagram showing HMGB2 interacting partners found in Y2H assays using SKOV-3 (ovary tumoral cells) or PC-3 (prostate tumoral cells) libraries and common proteins to both cell types. **(C)** Functions associated to HMGB1 and HMGB2 interacting proteins.

The results from the yeast two-hybrid assays showed 6 HMGB2 interacting partners in PC-3 prostate cancer cells and 7 interacting proteins in the ovarian carcinoma cell line, SKOV-3 (Figure 1B); 2 of them, GLTSCR2 and U2AF1, were found in both libraries. As for HMGB1, all the interactions found for HMGB2 in these experiments had not been described before in the databases STRING and BioGRID. Among the proteins found, some of them are associated to the cell cycle (UHRF2, GLTSCR2, BCCIP), to RNA splicing (U2AF1, C1QBP) or to the endosomal-lysosomal system (SNAPIN) (Figure 1C).

If the results of the yeast two-hybrid assay from HMGB2 are compared to the ones obtained for HMGB1 only UHRF2 and ZNF428 are common to both proteins.

HMGB1 and HMGB2 binding partners and their relation to cancer

Due to the objective of this study, finding HMGB interacting proteins in relation to prostate and ovarian cancer, we look for the role of the found preys in these specific cancers or other cancer-associated processes. Relevant available information relative to each found HMGB1 or HMGB2 preys is summarized in the Annex to this chapter. In Table 2 we summarized this information considering implication in miss-regulation of cellular processes related to malignant cell transformation and Table 3 shows their deregulation in cancer of different origins.

Among the preys found in our work, we considered highly relevant for further research those previously related to prostate or ovary cancers. Among HMGB1 preys, the Homeobox protein HOXA10 is a transcriptional factor that regulates the formation of the adult female reproductive tract during development (Du and Taylor, 2015). Interestingly HOXA10 has been associated to both prostate and ovarian cancer. HOXA10 was shown to be related to proliferation, migration, and invasion of ovarian clear cell adenocarcinoma (OCCA) (Li *et al.*, 2009). Similar results were obtained in cell lines from epithelial ovary (EOC), since downregulation of HOXA10 expression by miR-135a inhibited cell proliferation, promoted apoptosis and it also decreased cell adhesion ability (Tang *et al.*, 2014).

Table 2. HMGB1 and HMGB2 preys with associated functional processes related to cancer development.

Protein	Signalling pathways	Angiogenesis	Invasion/ Metastasis	Telomerase /Chromosome integrity	Cell proliferation/ growth	Cell cycle progression	Migration /Cell motility	EMT	Tumor suppressor	Genomic integrity	Metabolism disruption	Apoptosis	DNA damage response
AKIP1	*	*	*				*						
DLAT					*								
HDLBP					*	*							
HOXA10			*		*		*						
MALAT1			*		*		*	*					
UBXN1	*		*				*	*	*				
UHRF2			*				*	*	*				
BCCIP					*	*			*	*			
C1QBP			*			*	*				*		
COMMD1			*		*								
GLTSCR2	*		*	*	*	*			*			*	
MIEN1			*		*								
ROCK1		*	*		*		*					*	
ZNF668									*				*

EMT: epithelial mesenchymal transition

Table 3. Expression of HMGB1 and HMGB2 preys in different cancers.

Protein	Prostate	Ovary	Breast	Escc	Lung	Colorectal	Gastric	Glioblastoma	Hepatocellular	Oral	Pancreatic	Endometrial	Others (Glioma, lymphoma, cervical …)
AKIP1	*		*	*									
DLAT							*						
H3F3B								*					*
HDLBP									*				
HOXA10	*	*	*				*			*	*		
KRT7	*												
MALAT1		*											
UBE2E3	*												
UBXN1							*		*		*	*	*
C1QBP	*	*	*			*							
MIEN1	*	*	*		*					*			
BCCIP		*							*				
ROCK1	*	*											
SNAPIN									*				

Escc: esophageal squamous cell carcinoma

Regarding prostate cancer, Li and colleagues evaluated HOXA10 expression in prostate cancer cell lines and observed that its expression was higher in prostate cancer cell lines than in a control cell line (Baoxiu Li *et al.*, 2014). The overexpression of HOXA10 was associated to higher cell proliferation whereas silencing of HOXA10 decreased cell proliferation (Baoxiu Li *et al.*, 2014). KRT7 has been related to prostate cancer (Ibragimova *et al.*, 2010; Kolostova *et al.*, 2016) and has been proposed as a diagnostic marker (Thomas *et al.*, 2016). Although we have found MALAT1 as a HMGB1 prey, this DNA is considered to transcribe a long non-coding RNA (lncRNA) that is tightly related to a wide range of cancers including ovarian cancer (Liu *et al.*, 2016; Wu *et al.*, 2017) and prostate cancer (Wang *et al.*, 2015). In the ovarian cancer cell line SKOV-3 downregulation of MALAT1 decreased viability, proliferation, migration and invasion (Zou *et al.*, 2016).

Among HMGB2 preys we also find proteins related to prostate or ovarian cancers. Complement component 1 Q subcomponent-binding protein, C1QBP, is overexpressed in prostate cancer (Amamoto *et al.*, 2011) and ovarian cancer (Yu and Wang, 2013). COMM domain-containing protein 1 influences increased ovarian cell sensitivity to the antitumoral drug cisplatin (Fedoseienko *et al.*, 2016). GLTSCR2 seems to behave as a tumor suppressor and knock down of the gene, in LNCaP prostatic cancer cell line, lead to an increase in the invasiveness of these cells (Kim *et al.*, 2013). Migration and invasion enhancer 1 (MIEN1) is upregulated in prostate cancer (Dasgupta *et al.*, 2009) and ovarian cancer (Leung *et al.*, 2013) and it has been suggested that affects chemo-resistance to cisplatin treatment (Leung *et al.*, 2013). Rho-associated protein kinase 1, plays a role in prostate cancer (Zhang *et al.*, 2014; Xu *et al.*, 2015) and in ovarian cancer (Tocci *et al.*, 2016).

Validation of HOXA10 and KRT7 interactions with HMGB1

Among the HMGB1 and HMGB2 identified in this study we select HOXA10 and KRT7 for validation of the data set. In a recent review (Vizoso-Vázquez *et al.*, 2017) we have shown the interplay between HMGB proteins and HOX transcriptional factors. Therefore we were particularly interested in HOXA10, also because being a regulator of transcription, this interaction could extend present knowledge about nuclear functions of HMGB1. Our interest for KRT7 came from the fact that, although connection of KRT7 with prostate and ovarian cancers is known, the molecular mechanisms involved are completely unexplored.

To further validate HOXA10 and KRT7 interactions with HMGB1 we carried out studies of co-immunoprecipitation and co-localization in PC-3 cells and studies of co-regulation in PC-3 and SKOV-3 cells. Results are exposed in the following sections.

HMGB1 interacts with KRT7 in prostate cancer cells

Two-hybrid assays pointed KRT7 as a possible HMGB1 interacting partner. As above mentioned, KRT7 pathways still remain quite unknown; no previous physical interaction between HMGB1 and any cytokeratin had been described. Due to the implication of both proteins in cancer development we wanted to validate the interaction between these two proteins by *in vivo* assays. In order to do so, co-immunoprecipitation and co-localization experiments were carried out in the PC-3 cell line.

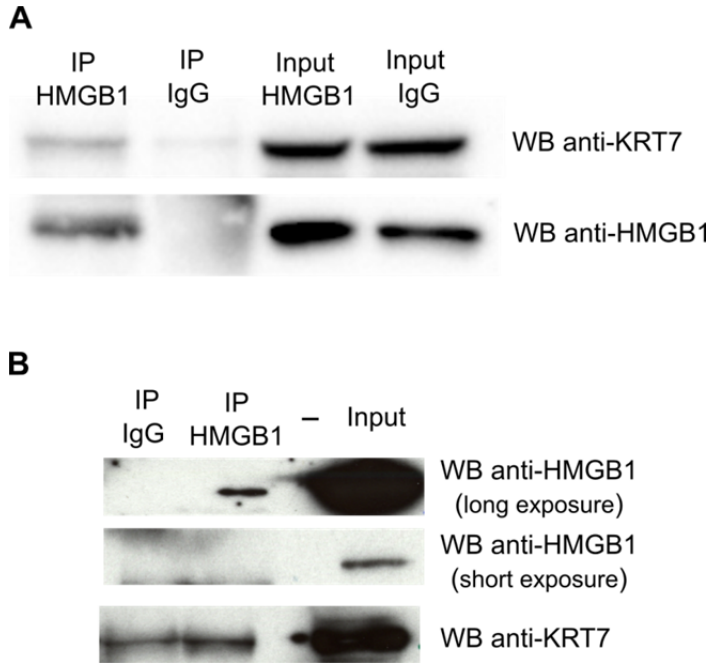

Figure 2. HMGB1 and KRT7 physical interaction. (A) PC-3 lysates were immunoprecipitated with anti-HMGB1 antibody (Santa Cruz, sc-74085) or normal mouse IgG (Molecular Probes, A10534) and immunoblotted with antibodies to KRT7 and HMGB1. **(B)** PC-3 lysates were immunoprecipitated with anti-HMMGB1 antibody (Abcam, ab18256) or normal rabbit IgG (Millipore, 12-360) and immunoblotted with antibodies to KRT7 and HMGB1.

Results from the immunoprecipitation of HMGB1 (Figure 2A) reveal an enrichment of KRT7 in the immunoprecipitation with anti-HMGB1 antibody (Santa Cruz, sc-74085) when compared to the control immunoprecipitation using an immunoglobulin isotype control. It is important to take into account that due to the size of KRT7, around 50 kDa, a band of the same size in the negative control is expected, which corresponds to the heavy chain of the antibody used for the control immunoprecipitation. Although Protein G HRP labelled was used as a secondary antibody to minimize the signal given by the light and heavy chains of the immunoprecipitation antibody, we have not been able to inhibit completely this signal. Despite

this downside, repeated HMGB1 immunoprecipitation showed the same enrichment in KRT7 and it was quantified by image analysis. This analysis showed that KRT7 signal in HMGB1 immunoprecipitation was approximately 4,5 times higher than the one obtained in the negative control. Moreover, to dismiss the possibility of this enrichment being an experimental artifact we performed HMGB1 immunoprecipitation using a different anti-HMGB1 (Abcam, ab18256), a different control immunoglobulin and a different protocol. The results (Figure 2B) from these experiments show an enrichment of KRT7 in HMGB1 immunoprecipitation in all the tested conditions, supporting the previous results.

The interaction between KRT7 and HMGB1 was further confirmed via confocal fluorescent microscopy. Results from the immunofluorescent analysis show HMGB1 localization both in the nucleus and in the cytoplasm, being the nuclear localization preferential over the cytoplasmic localization (Figure 3). However, co-localization of HMGB1 and KRT7 is observed in the cytoplasm of PC-3 (Figure 4).

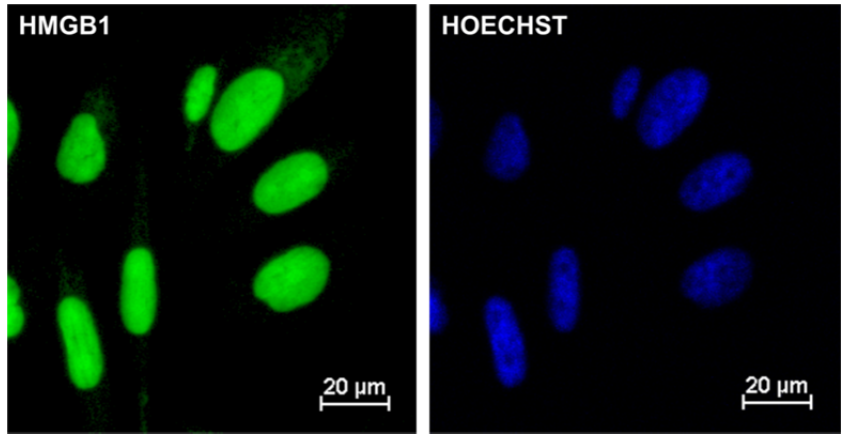

Figure 3. HMGB1 localization in PC-3 cells. Immunofluorescence staining of HMGB1 (green) and nuclear staining with Hoechst (blue) show that HMGB1 localizes mainly within the nucleus while lower HMGB1 levels are seen in the cytoplasm.

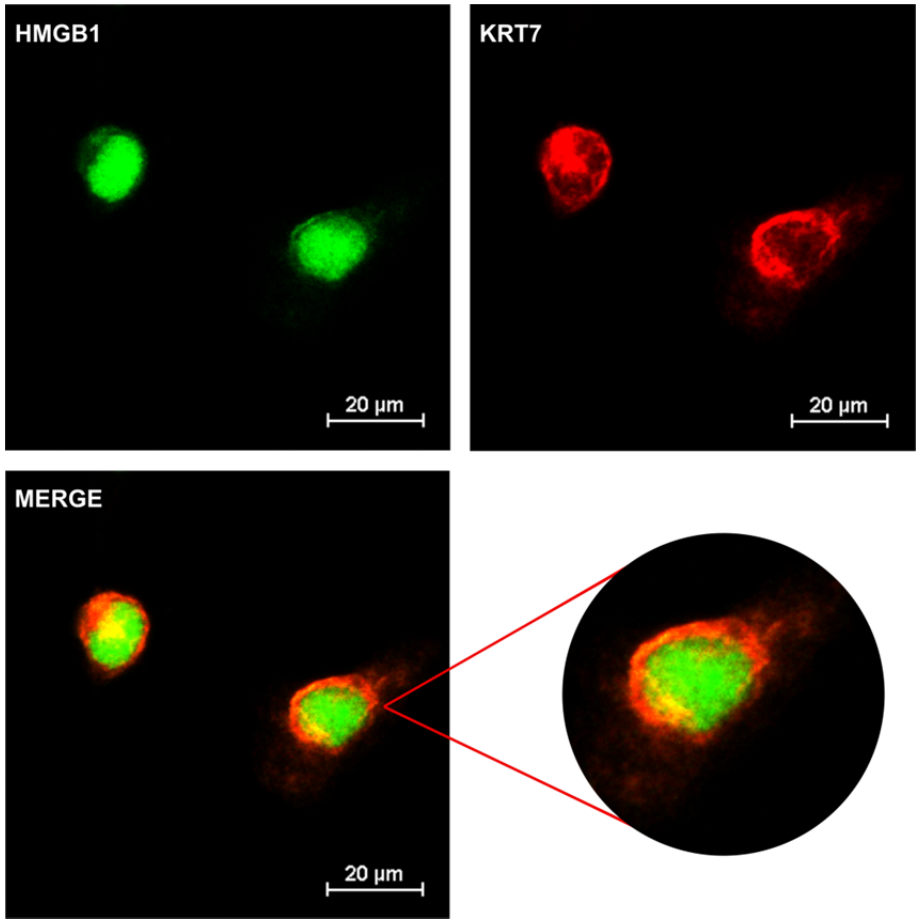

Figure 4. HMGB1 and KRT7 colocalize in the cytoplasm of PC-3 cells. Immunofluorescent staining of HMGB1 and KRT7 in PC-3 cells. HMGB1 is shown in green and KRT7 in red. Co-localization of HMGB1 and KRT7 in the cytoplasm is seen as yellow staining.

Taken together, these results validate that there is a physical interaction of HMGB1 and KRT7 in prostate cancer cells that physiologically takes place in the cytoplasm and it is perinuclear.

HMGB1 colocalizes in the nucleus with HOXA10 in prostate cancer cells

Zappavigna and collaborators, reported protein-protein interaction between HMGB1 and members from the *HOX* gene family (HOXD11, HOXD10, HOXD9, HOXD3, HOXC6, HOXB3 and HOXB1) through their

respective HMG box domains and the HOX homeodomain (Zappavigna *et al.*, 1996). HOXA10 was one of the HMGB1 interacting partners found in the Y2H assays using PC-3 cDNA library, however, no previous direct interaction between HMGB1 and proteins from the HOXA cluster had been described. We could not confirm this interaction by immunoprecipitation, since we obtained negative results. Going back to sequence data of the obtained clone in the Y2H assay, we realized that the clone contained a non-coding DNA sequence and therefore the positive effect observed in the screening could not be explained by protein-protein interaction.

However,co-localization studies suggest a physical interaction between HMGB1 and HOXA10 in specific zones of the nucleus (Figure 5).

Future experiments will be needed to clarify this issue.

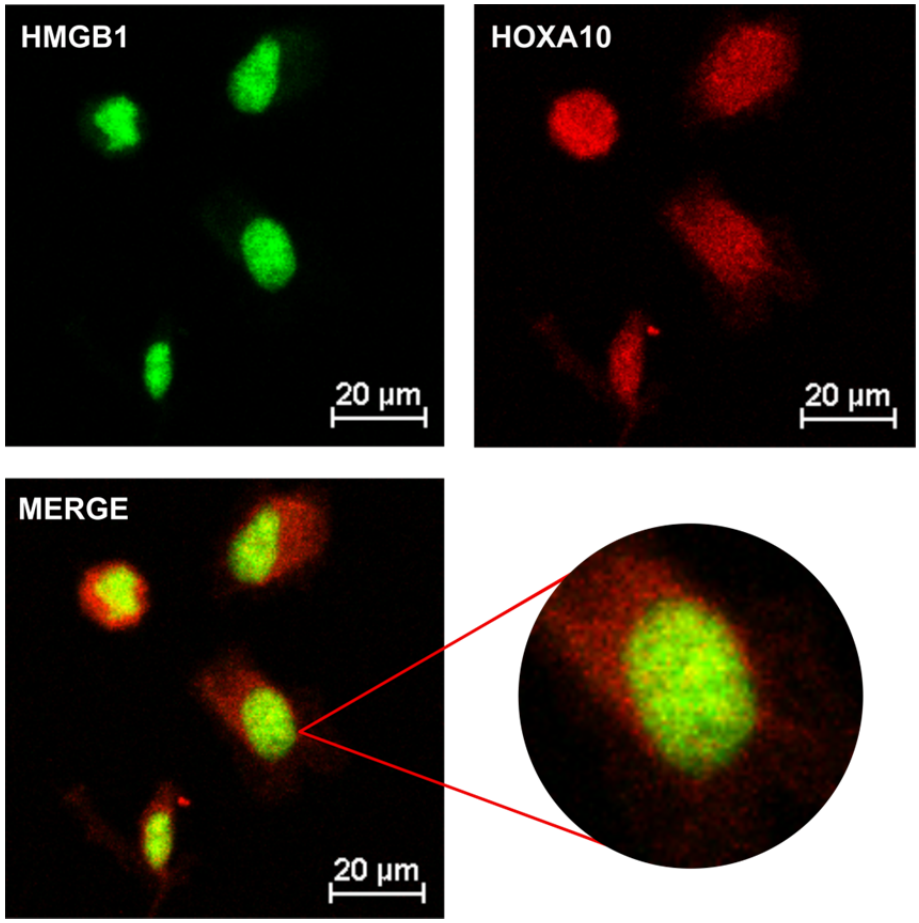

Figure 5. HMGB1 and HOXA10 colocalize in the nucleus of PC-3 cells. Immunofluorescent staining of HMGB1 and HOXA10 in PC-3 cells. HMGB1 is shown in green and HOXA10 in red. Co-localization of HMGB1 and HOXA10 in the nucleus is seen as yellow staining.

Evaluation of HOXA10, HMGB1, HMGB2 and KRT7 expression levels

In order to find differential mRNA co-expression of HOXA10, KRT7 and HMGB1 in tumor cells, retrotranscription of RNA from the human cancer cell lines, PC-3 and SKOV-3 and non-tumor epithelial cells HPEpiC and HOSEpiC was coupled to quantitative real-time polymerase chain reaction (qRT-PCR). The expression fold change for these genes comparing cancer

cells to non-cancerous cells was calculated using the $2^{-\Delta\Delta Ct}$ analysis (Livak and Schmittgen, 2001). Our data show that these three genes are overexpressed in the ovarian cancer cells (Figure 6A). HMGB1 and KRT7 expression was more than ten times higher in SKOV-3 cells than in ovarian noncancerous cells, HOSEpiC, whereas HOXA10 had a slightly lower than two-fold increase. Results obtained from the comparison between prostate cancer cells, PC-3, and prostate epithelial cells, HPEpiC, showed opposite results. HOXA10 and HMGB1 are overexpressed in PC-3 (Figure 6B), being the increased expression of the first gene more than ten-fold higher in this tumoral cell line, while HMGB1 doubled its expression in PC-3. Oppositely, KRT7 expression was decreased in PC-3 in comparison to HPEpiC.

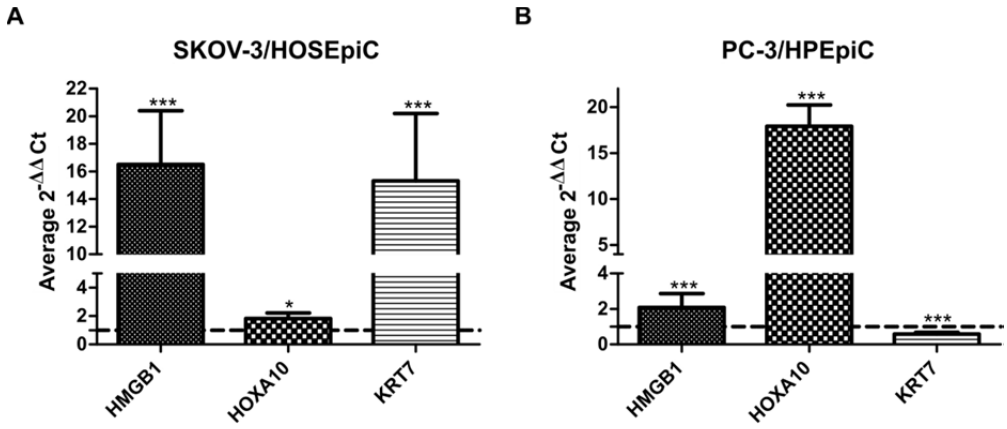

Figure 6. HMGB1, HOXA10 and KRT7 expression analysis by RT-qPCR. Data represent the difference between the expression of the genes in tumoral cells and normal cells. Values over 1 (discontinuous line in the graphics) indicate higher expression of the gene in tumoral cells than in normal cells (mean ± S.D.). At last 6 independent experiments were done for each gene. *P<0.05; ***P<0.001. **(A)** Expression analysis of HMGB1, HOXA10 and KRT7 genes in ovarian tumoral /non tumoral cells. **(B)** Expression analysis of HMGB1, HOXA10 and KRT7 genes in prostate tumoral /non tumoral cells.

Taken together, these results report an increase in the expression of HMGB1 and HOXA10 in ovarian and prostate cell lines while KRT7 is overexpressed in ovarian cancer cells but its expression is decreased in the prostate cancer cell line.

DISCUSSION

The unveiling of protein interactions is a key point to understand the role of such proteins in the development of disease. Although HMGB1 and HMGB2 have already been related to the onset and progression of cancer, being involved in events such as the evasion of apoptosis (Liu *et al.*, 2014), telomere homeostasis (Ke *et al.*, 2015) and cell growth and invasion (Tang *et al.*, 2017), the mechanisms underlining these processes still remain unknown. In this study we search for novel proteins interacting with HMGB1 and HMGB2 in relation to ovarian and prostate cancer. To carry out this search yeast-two hybrid assays were performed using cDNA libraries from ovarian and prostate cancer cell lines, SKOV-3 and PC-3.

Our results show a new subset of HMGB1 and HMGB2 interacting partners (shown in Figure 1) that had not been described previously and that conform a new panel of candidates for searching diagnosis and therapeutic targets in prostate and ovarian cancers. Functions associated to these proteins are quite diverse, as transcription, RNA metabolic processes, proteasome and cytoskeleton reorganization, among others. Considering the diversity of functions, it is however remarkable that the preys found using cancer cell lines had been in many instances related directly to these cancers, which reinforces the adequacy of the methodology used.

Using primary antibodies and secondary antibodies labeled with fluorescent green or red dyes and using Hoechst as a nuclear marker, we observed that HMGB1 is mainly located in the nucleus of PC-3 cells while a more faint HMGB1 signal was seen in the cytoplasm of PC-3 cells. This result is in concordance with the described shuttling of HMGB1 from the nucleus to the cytoplasm due to different stimuli and posttranslational modifications (Tang *et al.*, 2010; Youn and Shin, 2006). Although many studies associate the translocation of HMGB1 from the nucleus to the cytoplasm within cells from the immune system for its release out of the cell, Mosevitsky *et al*., described HMGB1 distribution in the cytoplasm of cells from spleen and testis rat tissue among others (Mosevitsky *et al.*, 1989) and Cheng *et al*., showed HMGB1 mainly localized in the cytoplasm of cervical cancer cells (Cheng *et al.*, 2017). Our confocal data also show that HMGB1-KRT7 interaction is observed in the cytoplasm. This indicates that HMGB proteins participate in multiple functions in the cell and that the sequential changes that are required to control HMGB1 switching between nucleus and cytoplasm are important clues to study cell malignization. The significance of this new panel of proteins that bind to HMGB1 and/or HMGB2 is increased by validation of the interaction of HMGB1 with KRT7 by different approaches like co-inmunoprecipitation and co-localization as reported in the Results section. It is important to remark that, KRT7 interaction with HMGB1 is also produced in healthy epithelial cells of the same origin, as reported in the previous chapter of this Thesis. This might indicate that the interaction between HMGB1 and KRT7 is of general relevance in the cell, and being KRT7 a cytoskeleton protein it is tempting to speculate that could be related to nuclear transport of HMGB1.

About the validated HMGB1 prey, Keratin 7, it had been previously linked to cancer diagnosis (Bournet *et al.*, 2012), although the mechanism of its participation was unknown. Our results indicate that it is probably associated to a HMGB1-related function in the cytoplasm where the two proteins co-localize in PC-3 cancer cells. However, the result of KRT7 regulated expression in PC-3 and SKOV-3 cells against normal prostate or ovarian cells is contradictory. KRT7 showed a different pattern of expression, while its expression significantly increased in SKOV-3 cells, KRT7 lowered its expression in PC-3 cells. However it is interesting to note that even though KRT7 expression diminishes in PC-3 cells, it is still possible to detect the interaction with HMGB1 in them.

It has been suggested that HMGB1 and HMGB2 may have redundant roles in several processes, as cleavage during V(D)J recombination (Gent *et al.*, 1997; Swanson, 2002) and human development (Bagherpoor *et al.*, 2017). However, in our study only two common interacting partners for HMGB1 and HMGB2 were found, UHRF2 and ZNF428, which reflects the specificity of these proteins and their interactions to contribute to cellular functions. Several studies have brought into light specific functions for each protein. While HMGB1 is expressed ubiquitously in adult organs, HMGB2 expression pattern is more restricted, mainly being found in the thymus and in certain immune cells (Barreiro-Alonso *et al.*, 2016), thus giving an idea of the different roles of these two proteins (Ronfani *et al.*, 2001). Reinforcing their different functions,, HMGB1 deficiency in mice leads to their death in a 24 hour period due to hypoglycaemia (Calogero *et al.*, 1999); while HMGB2 null mice are viable and their lifespan is not shortened, although reduced fertility and alterations in spermatogenesis result from the loss of HMGB2

(Ronfani *et al.*, 2001). A study carried out by Polanská and collaborators suggests an opposite role of these proteins in telomerase activity (Polanská *et al.*, 2012).

Zappavigna and collaborators evidenced the interactions between HMGB1 and protein members of the HOX family from clusters B and D (Zappavigna *et al.*, 1996). HMGB1 and HOXA10 have been related to the progression of different cancers (Yang *et al.*, 2016; Shah *et al.*, 2016) among them is prostate cancer, where HOXA10 has been suggested to be involved in cell proliferation (Baoxiu Li *et al.*, 2014). Our results also confirm that cancer cells from prostate epithelial origin over-express both HMGB1 and HOXA10 genes and similar results are obtained using ovary cancer cells from epithelial origin. These results are in accordance with other studies showing that HMGB1 and HOXA10 genes are up-regulated in different tumors (Abe *et al.*, 2006; Feng *et al.*, 2016; Zhu *et al.*, 2015). These results open the opportunity of proving the capacity of tumor generation by conjunct over-expression of HMGB1 and HOXA10 and also of clinical trials of prostate and ovary cancer diagnosis based in over-expression of these two markers.

In summary, in this study we have reported novel HMGB1 and HMGB2 interacting partners in ovarian and prostate cancer cells. The different functions as well as the cellular localizations associated to these protein preys reveal the complexity that is associated to HMGB1 and HMGB2 functions. Focusing in HMGB1 interactions, we have validated the cytoplasmic interaction of this protein with the cytoskeleton protein, KRT7.

REFERENCES

Abe M, Hamada J-I, Takahashi O, Takahashi Y, Tada M, Miyamoto M, Morikawa T, Kondo S, Moriuchi T. 2006. Disordered expression of HOX genes in human non-small cell lung cancer. *Oncol Reports.*, **15**: 797–802.

Amamoto R, Yagi M, Song Y, Oda Y, Tsuneyoshi M, Naito S, Yokomizo A, Kuroiwa K, Tokunaga S, Uchiumi T. 2011. Mitochondrial p32/C1QBP is highly expressed in prostate cancer and is associated with shorter prostate-specific antigen relapse time after radical prostatectomy. *Cancer Sci.*, **102**: 639–647.

Bagherpoor AJ, Dolezalova D, Barta T, Kučírek M, Sani SA, Ešner M, Bosakova, Michaela Kunova Vinarský V, Peskova L, Hampl A, Štros M. 2017. Properties of Human Embryonic Stem Cells and their Differentiated Derivatives Depend on Non-histone DNA-Binding HMGB1 and HMGB2 Proteins. *Stem Cells Dev.*, **26**: 328–340.

Barreiro-Alonso A, Lamas-Maceiras M, Rodríguez-Belmonte E, Vizoso-Vázquez Á, Quindós M, Cerdán ME. 2016. High Mobility Group B Proteins, Their Partners, and Other Redox Sensors in Ovarian and Prostate Cancer. *Oxid. Med. Cell. Longev.*, **2016**.

Beijnum JR Van, Boezem E Van Den, Hautvast P, Buurman WA, Griffioen AW. 2012. Tumor angiogenesis is enforced by autocrine regulation of high-mobility group box 1. *Oncogene*, **32**: 363–374.

Bournet B, Pointreau A, Souque A, Oumouhou N, Muscari F, Lepage B, Senesse P, Barthet M, Lesavre N, Hammel P, Buscail L. 2012. Gene expression signature of advanced pancreatic ductal adenocarcinoma using low density array on endoscopic ultrasound-guided fine needle aspiration samples. *Pancreatology*, **12**: 27–34.

Calogero S, Grassi F, Aguzzi A, Voigtländer T, Ferrier P, Ferrari S, Bianchi ME. 1999. The lack of chromosomal protein Hmg1 does not disrupt cell growth but causes lethal hypoglycaemia in newborn mice. *Nat. Genet.*, **22**: 276–280.

Chandrasekaran KS, Sathyanarayanan A, Karunagaran D. 2016. Downregulation of HMGB1 by miR-34a is sufficient to suppress proliferation, migration and invasion of human cervical and colorectal cancer cells. *Tumor Biol.*, **37**: 13155–13166.

Cheng H, Wang W, Zhang Y, Zhang B, Cheng J, Teng P, Tang X. 2017. Expression levels and clinical significance of hepsin and HMGB1 proteins in

cervical carcinoma. *Oncol. Lett.*, **14**: 159–164.

Dasgupta S, Wasson LM, Rauniyar N, Prokai L, Borejdo J, Vishwanatha JK. 2009. Novel gene C17orf37 in 17q12 amplicon promotes migration and invasion of prostate cancer cells. *Oncogene*, **28**: 2860–2872.

Du H, Taylor HS. 2015. The Role of Hox Genes in Female Reproductive Tract Development, Adult Function, and Fertility. *Cold Spring Harb. Perspect. Med.*, **6**: a023002.

Fedoseienko A, Wieringa HW, Wisman GBA, Duiker E, Reyners AKL, Hofker MH, Van Der Zee AGJ, Van De Sluis B, Van Vugt MATM. 2016. Nuclear COMMD1 is associated with cisplatin sensitivity in ovarian cancer. *PLoS One*, **11**: 1–21.

Feng A, Tu Z, Yin B. 2016. The effect of HMGB1 on the clinicopathological and prognostic features of non-small cell lung cancer. *Oncotarget*, **7**: 20507–19.

Gent DC Van, Hiom K, Paull TT, Gellert M. 1997. Stimulation of V (D) J cleavage by high mobility group proteins. *EMBO J.*, **16**: 2665–2670.

Ibragimova I, Ibáñez De Cáceres I, Hoffman AM, Potapova A, Dulaimi E, Al-Saleem T, Hudes GR, Ochs MF, Cairns P. 2010. Global reactivation of epigenetically silenced genes in prostate cancer. *Cancer Prev. Res.*, **3**: 1084–1092.

Ke S, Zhou F, Yang H, Wei Y, Gong J, Mei Z, Wu L, Yu H, Zhou Y. 2015. Downregulation of high mobility group box 1 modulates telomere homeostasis and increases the radiosensitivity of human breast cancer cells. *Int. J. Oncol.*, **46**: 1051–1058.

Kim JY, Cho YE, Kim GY, Lee HL, Lee S, Park JH. 2013. Down-regulation and aberrant cytoplasmic expression of GLTSCR2 in prostatic adenocarcinomas. *Cancer Lett.*, **340**: 134–140.

Kolostova K, Pinkas M, Jakabova A, Pospisilova E, Svobodova P, Spicka J, Cegan M, Matkowski R, Bobek V. 2016. Molecular characterization of circulating tumor cells in ovarian cancer. *Am. J. Cancer Res.*, **6**: 973–980.

Leung TH-Y, Wong SC-S, Chan KK-L, Chan DW, Cheung AN-Y, Ngan HY-S. 2013. The interaction between C35 and ΔNp73 promotes chemo-resistance in ovarian cancer cells. *Br. J. Cancer*, **109**: 965–975.

Li B, Cao X, Weng C, Wu Y, Fang X, Zhang X, Liu G. 2014. HoxA10 induces proliferation in human prostate carcinoma PC-3 cell line. *Cell Biochem.*

Biophys., **70**: 1363–1368.

Li B, Jin H, Yu Y, Gu C, Zhou X, Zhao N, Feng Y. 2009. HOXA10 is overexpressed in human ovarian clear cell adenocarcinoma and correlates with poor survival. *Int. J. Gynecol. Cancer*, **19**: 1347–1352.

Li T, Gui Y, Yuan T, Liao G, Bian C, Jiang Q, Huang S, Liu B, Wu D. 2012. Overexpression of high mobility group box 1 with poor prognosis in patients after radical prostatectomy. *Br. J. Urol. Int.*, **110**: E1125-30.

Li Y, Tian J, Fu X, Chen Y, Zhang W, Yao H, Hao Q. 2014. Serum high mobility group box protein 1 as a clinical marker for ovarian cancer. *Neoplasma*, **61**: 579–584.

Liu K, Huang J, Xie M, Yu Y, Zhu S, Kang R, Cao L, Tang D, Duan X. 2014. MIR34A regulates autophagy and apoptosis by targeting HMGB1 in the retinoblastoma cell. *Autophagy*, **10**: 442–452.

Liu P-L, Liu W-L, Chang J-M, Chen Y-H, Liu Y-P, Kuo H-F, Hsieh C-C, Ding Y-S, Chen W-W, Chong I-W. 2017. MicroRNA-200c inhibits epithelial-mesenchymal transition, invasion, and migration of lung cancer by targeting HMGB1 Ahmad A. (ed). *PLoS One*, **12**: e0180844.

Liu S, Jiang X, Li W, Cao D, Shen K, Yang J. 2016. Inhibition of the long non-coding rna malat1 suppresses tumorigenicity and induces apoptosis in the human ovarian cancer skov3 cell line. *Oncol. Lett.*, **11**: 3686–3692.

Livak KJ, Schmittgen TD. 2001. Analysis of Relative Gene Expression Data Using Real-Time Quantitative PCR and the 2−ΔΔCT Method. *Methods*, **25**: 402–408.

Mosevitsky MI, Novitskaya VA, Iogannsen MG, Zabezhinsky MA. 1989. Tissue specificity of nucleo-cytoplasmic distribution of HMG1 and HMG2 proteins and their probable functions. *Eur. J. Biochem.*, **185**: 303–310.

Polanská E, Dobšáková Z, Dvořáčková M, Fajkus J, Štros M. 2012. HMGB1 gene knockout in mouse embryonic fibroblasts results in reduced telomerase activity and telomere dysfunction. *Chromosoma*, **121**: 419–431.

Pusterla T, de Marchis F, Palumbo R, Bianchi ME. 2009. High mobility group B2 is secreted by myeloid cells and has mitogenic and chemoattractant activities similar to high mobility group B1. *Autoimmunity*, **42**: 308–310.

Ronfani L, Ferraguti M, Croci L, Ovitt CE, Schöler HR, Consalez GG, Bianchi ME. 2001. Reduced fertility and spermatogenesis defects in mice lacking chromosomal protein Hmgb2. *Development*, **128**: 1265–1273.

Shah CA, Bei L, Wang H, Altman JK, Platanias LC, Eklund EA. 2016. Cooperation between αvβ3 integrin and the fibroblast growth factor receptor enhances proliferation of Hox-overexpressing acute myeloid leukemia cells. *Oncotarget*, **7**: 1–13.

Srinivasan M, Banerjee S, Palmer A, Zheng G, Chen A, Bosland MC, Kajdacsy-Balla A, Kalyanasundaram R, Munirathinam G. 2014. HMGB1 in Hormone-Related Cancer: A Potential Therapeutic Target. *Horm. Cancer*, **5**: 127–139.

Swanson PC. 2002. Fine structure and activity of discrete RAG-HMG complexes on V(D)J recombination signals. *Mol. Cell. Biol.*, **22**: 1340–51.

Tang C, Yang Z, Chen D, Xie Q, Peng T, Wu J, Qi S. 2017. Downregulation of miR-130a promotes cell growth and epithelial to mesenchymal transition by activating HMGB2 in glioma. *Int. J. Biochem. Cell Biol.*, **In Press,**.

Tang D, Kang R, Livesey KM, Cheh CW, Farkas A, Loughran P, Hoppe G, Bianchi ME, Tracey KJ, Zeh HJ, Lotze MT. 2010. Endogenous HMGB1 regulates autophagy. *J. Cell Biol.*, **190**: 881–892.

Tang W, Jiang Y, Mu X, Xu L, Cheng W, Wang X. 2014. MiR-135a functions as a tumor suppressor in epithelial ovarian cancer and regulates HOXA10 expression. *Cell. Signal.*, **26**: 1420–1426.

Thomas BC, Kay JD, Menon S, Vowler SL, Dawson SN, Bucklow LJ, Luxton HJ, Johnston T, Massie CE, Pugh M, Whitaker HC. 2016. Whole blood mRNA in prostate cancer reveals a four-gene androgen regulated panel. *Endocr. Relat. Cancer*, **23**: 797–812.

Tocci P, Caprara V, Cianfrocca R, Sestito R, Di Castro V, Bagnato A, Rosanò L. 2016. Endothelin-1/endothelin A receptor axis activates RhoA GTPase in epithelial ovarian cancer. *Life Sci.*, **159**: 49–54.

Ugrinova I, Pashev IG, Pasheva EA. 2009. Nucleosome binding properties and co-remodeling activities of native and in vivo acetylated HMGB-1 and HMGB-2 proteins. *Biochemistry*, **48**: 6502–6507.

Vizoso-Vázquez A, Barreiro-Alonso A, Rico-Díaz A, Lamas-Maceiras M, Rodríguez-Belmonte E, Becerra M, González-Siso M., Cerdán M. 2017. HMGB proteins from yeast to human. Gene regulation, DNA repair and beyond. In *Old Yeasts - New Questions*,.

Wang D, Ding L, Wang L, Zhao Y, Sun Z, Karnes RJ, Zhang J, Huang H. 2015. LncRNA MALAT1 enhances oncogenic activities of EZH2 in castration-resistant prostate cancer. *Oncotarget*, **6**: 41045–41055.

Wang W, Jiang H, Zhu H, Zhang H, Gong J, Zhang L, Ding Q. 2013. Overexpression of high mobility group box 1 and 2 is associated with the progression and angiogenesis of human bladder carcinoma. *Oncol. Lett.*, **5**: 884–888.

Wu L, Wang X, Guo Y. 2017. Long non-coding RNA MALAT1 is upregulated and involved in cell proliferation, migration and apoptosis in ovarian cancer. *Exp. Ther. Med.*, **13**: 3055–3060.

Wu ZB, Cai L, Lin SJ, Xiong ZK, Lu JL, Mao Y, Yao Y, Zhou LF. 2013. High-mobility group box 2 is associated with prognosis of glioblastoma by promoting cell viability, invasion, and chemotherapeutic resistance. *Neuro. Oncol.*, **15**: 1264–1275.

Xu B, Huang Y, Niu X, Tao T, Jiang L, Tong N, Chen S, Liu N, Zhu W, Chen M. 2015. Hsa-miR-146a-5p modulates androgen-independent prostate cancer cells apoptosis by targeting ROCK1. *Prostate*, **75**: 1896–1903.

Yang B, Li SZ, Ma L, Liu HL, Liu J, Shao JJ. 2016. Expression and mechanism of action of miR-196a in epithelial ovarian cancer. *Asian Pac. J. Trop. Med.*, **9**: 1105–1110.

Youn JH, Shin J-S. 2006. Nucleocytoplasmic Shuttling of HMGB1 Is Regulated by Phosphorylation That Redirects It toward Secretion. *J. Immunol.*, **177**: 7889–7897.

Yu G, Wang J. 2013. Significance of hyaluronan binding protein (HABP1/P32/gC1qR) expression in advanced serous ovarian cancer patients. *Exp. Mol. Pathol.*, **94**: 210–215.

Zappavigna V, Falciola L, Helmer-Citterich M, Mavilio F, Bianchi ME. 1996. HMG1 interacts with HOX proteins and enhances their DNA binding and transcriptional activation. *Embo Jour*, **15**: 4981–4991.

Zhang C, Zhang S, Zhang Z, He J, Xu Y, Liu S. 2014. ROCK has a crucial role in regulating prostate tumor growth through interaction with c-Myc. *Oncogene*, **33**: 5582–5591.

Zhu L, Li X, Chen Y, Fang J, Ge Z. 2015. High-mobility group Box 1: A novel inducer of the epithelial-mesenchymal transition in colorectal carcinoma. *Cancer Lett.*, **357**: 527–534.

Zou A, Liu R, Wu X. 2016. Long non-coding RNA MALAT1 is up-regulated in ovarian cancer tissue and promotes SK-OV-3 cell proliferation and invasion. *Neoplasma*, **63**: 865–872.

ANNEX TO CHAPTER 3

ANNEX TO CHAPTER 3

Available information about HMGB1 and HMGB2 preys found in this study in PC-3 or SKOV-3 cells.

HMGB1 PREYS		
PREY	**CELL LINE**	**Available information**
AKIP1	SKOV-3	Transcription A-kinase-interacting protein 1, is a nuclear protein implicated in different signaling pathways tightly related to NF-κB pathway, as it enhances its activity (Gao *et al.*, 2008). AKIP1 was first discovered in breast and prostate cancer tissue were this protein was overexpressed (Kitching *et al.*, 2003). Lin and colleagues also observed overexpression of AKIP1 in esophageal squamous cell carcinoma (ESCC) (Lin *et al.*, 2015). Overexpression of this protein is related to tumoral processes as angiogenesis (Lin *et al.*, 2015), cell motility and invasion (Mo *et al.*, 2016).
DLAT	PC-3	Dihydrolipoyl-lysine acetyltransferase component of pyruvate dehydrogenase complex, mitochondrial, also known as PDC-E2, is a mitochondrial protein that is part of the pyruvate dehydrogenase complex. This enzyme plays a key role in mitochondria metabolism, specifically in the conversion of pyruvate to acetyl-CoA. DLAT is also well characterized for being the immunodominant autoantigen of primary biliary cirrhosis (Mao *et al.*, 2011). DLAT was identified through mass spectrometry assays as an upregulated protein in 8 out of 11 gastric cancer cell lines (Goh *et al.*, 2015). Moreover, the same study also suggests that DLAT knock down can reduce cell proliferation in gastric carcinoma cells.
H3F3B	PC-3	Histone H3.3, is a histone that replaces canonical H3 when chromatin assembly occurs at a different time than DNA replication. This histone is mainly localized in transcriptionally active chromatin (Mito *et al.*, 2005). Mutation of H3.3 have been linked to the development of glioblastomas in children and young adults (Bjerke *et al.*, 2013).
HDLBP	PC-3	Vigilin, is a High density lipoprotein-binding protein, and is related to sterol metabolism. Vigilin is a multi-KH domain protein, likewise is involved in several RNA processes such as RNA cytoplasmic transport, mRNAs metabolism, tRNA export (Vollbrandt *et al.*, 2004), and translation regulation of certain proteins (Mobin *et al.*, 2016). Vigilin has also been related to cell cycle progression as Wei and colleagues suggest that Vigilin may play a role in chromatin condensation and segregation (Wei *et al.*, 2015). Vigilin expression is increased in human hepatocellular carcinoma cells. Depletion of Vigilin in this type of cells has been associated to attenuated cell proliferation, clonogenicity and migration (Yang *et al.*, 2014). Moreover, cells lacking Vigilin, have less ability to induce xenograft tumors in nude mice (Yang *et al.*, 2014).
HOXA10	PC-3	Homeobox protein Hox-A10, acts as a transcription factor that has a role in embryonic development processes and is implicated in the regulation of the adult female reproductive tract and female fertility (Du and Taylor, 2015). HOXA10 is overexpressed in several cancers as oral cancer (Libório-

		Kimura *et al.*, 2015), gastric cancer (Han *et al.*, 2015)and pancreatic cancer (Mao *et al.*, 2017). HOXA10 has been associated to tumoral processes as invasion, proliferation and migration in oral cancers (Carrera *et al.*, 2015), gastric cancer (Han *et al.*, 2015), pancreatic cancer (Cui *et al.*, 2014). Unexpectedly, HOXA10 has the opposite effect in breast and endometrial cancer. An study carried out by Chu and colleagues suggests that HOXA10 expression decreases invasiveness in breast cancer cells (Chu *et al.*, 2004). Moreover, HOXA10 mRNA expression is lower in endometrial cancer tissue compared to normal tissue and overexpression of HOXA10 in endometrial cancer cell lines arrested cells in G1 phase and the proliferative activity of these cells decreased when HOXA10 levels were increased (Lin Zhang *et al.*, 2014). Interestingly HOXA10 has been associated to the development of both prostate (Li *et al.*, 2014) and ovarian cancer. (Li *et al.*, 2009; Tang *et al.*, 2014)(Tang *et al.*, 2014).
KRT7	PC-3 SKOV-3	Keratin, type II cytoskeletal 7, is one of the keratins which are mainly expressed in simple (single layer) epithelia (Omary *et al.*, 2009). Although a great number of studies have been done relating KRT7 to disease, mainly cancer, the functional role *in vivo* is still not very well characterized. Keratins have been used as tools for tumors detections, KRT7 included. KRT7 has been proposed to be an oncogene promoting bladder cancer (Ichimi *et al.*, 2009) and KRT7 has been involved in prostate cancer (Ibragimova *et al.*, 2010).
MALAT1	SKOV-3	Metastasis-associated lung adenocarcinoma transcript 1, is a long non-coding RNA (lncRNA) that is tightly related to a wide range of cancers. It was one of the first lncRNA associated to cancer. MALAT1 has been linked to main cancer hallmarks as epithelial-mesenchymal transition, cell migration, metastasis in different types of tumors (L Li *et al.*, 2016; Huang *et al.*, 2016; Dong *et al.*, 2015; Sun *et al.*, 2016; Ji *et al.*, 2013; Gutschner *et al.*, 2014). Relation of MALAT1 with the development of ovarian cancer has been shown by different research groups. Zou *et al.*, showed that downregulation of MALAT 1 in the ovarian cancer cell line SKOV-3 decreased viability, proliferation, migration and invasion (Zou *et al.*, 2016). Similar results were achieved by Liu *et al.*, and Wu *et al.*, (Liu *et al.*, 2016; Wu *et al.*, 2017). Migration and invasion of prostate cancer cells has also been related to this lncRNA (Wang *et al.*, 2015).
UBE2E3	PC-3	Ubiquitin-conjugating enzyme E2 E3, UBE2E3, Is involved in Nrf2-mediated redox homeostasis (Plafker *et al.*, 2010) and in the epithelial Na+ channel regulation (Debonneville and Staub, 2004). Bull and collaborators associated UBE2E3 to prostate cancer, highlighting its possible diagnostic potential (Bull *et al.*, 2001).
UBXN1	PC-3	UBX domain-containing protein 1, is an Ubiquitin-binding protein that mediates proteasome protein degradation**.** Huang *et al.*, reported that UBXN1 negatively regulates NF-κB activity in glioma cells and its expression associates to good prognosis of glioma patients (Huang *et al.*, 2017).
UHRF2	PC-3 SKOV-3	Cell cycle regulation E3 ubiquitin-protein ligase UHRF2, UHRF2, is a E3 ubiquitin ligase that plays an important role in cell cycle (Mori *et al.*, 2011). UHRF2 protein levels are downregulated in several cancers such as gastric, liver, pancreatic, lymphoma, cervical, endometrial, squamous cell

		carcinoma, and head and neck cancers (Lu *et al.*, 2016). Moreover, UHRF2 has been suggested to be a tumor suppressor (Mori *et al.*, 2011). However different studies show contradictory results as proteome profiling studies carried out by Lia et al., in gastric cells overexpressing UHRF2 show that there is an upregulation of transcription factors that are related to ephitelial mesenquimal transition (EMT). Moreover UHRF2 silencing induced a decrease in migration and invasion in *in vitro* cell invasion experiments (Lai *et al.*, 2016).
DNAAF2	PC-3	Protein kintoun, is a protein involved in cell motility of cilia and flagella, playing an important role in pre-assembly of dynein arm (Omran *et al.*, 2008). No information for direct implication of DNAAF2 with cancer was available at the time this thesis was written.
ZNF428	PC-3	No information for direct implication of ZNF428 with cancer was available at the time this thesis was written.
WDR60	SKOV-3	WD repeat-containing protein 60, although this protein functions are still not very well characterized, Asante and collaborators showed an association between cytoplasmic dynein 2 and WDR60 (Asante *et al.*, 2014), Ishikawa *et al*., also related WDR60 to cilia formation (Ishikawa *et al.*, 2012). No information for direct implication of WDR60 with cancer was available at the time this thesis was written.
ATF7IP	SKOV-3	ATF7IP, Activating transcription factor 7-interacting protein 1, is a transcription cofactor that has been related to MBD1-mediated transcriptional repression and heterochromatin formation (Ichimura *et al.*, 2005). ATF7IP interacts with Sp1, and the resulting complex is necessary for telomerase activity, as both genes are upregulated in several cancers this upregulation has been associated with telomerase maintenance, one of the hallmarks of cancer (Liu *et al.*, 2009). This protein is overexpressed in cancers such as stomach cancer, breast cancer and lung cancer (Liu *et al.*, 2009).

HMGB2 PREYS		
PREY	**CELL LINE**	**Available information**
BCCIP	PC-3	BRCA2 and CDKN1A-interacting protein, is a protein that has been seen to participate in essential cellular processes like control of the cell cycle and cellular growth (Meng *et al.*, 2004) and maintenance of genomic integrity (Meng *et al.*, 2007). Liu *et al*., showed how BCCIP has a tumor suppression role in breast and brain cancer as it inhibits cell growth (Liu *et al.*, 2001). BCCIP is down-regulated in several cancers as ovarian cancer (Liu *et al.*, 2013) and hepatocellular carcinoma (Lin *et al.*, 2016).
C1QBP	SKOV-3	Complement component 1 Q subcomponent-binding protein, is a protein which mainly localizes in the mitochondria. This protein has been associated to different roles as in RNA splicing (Petersen-Mahrt *et al.*, 1999), ribosome biogenesis. Expression pattern of BCCIP in hepatocellular carcinoma is correlated with poor prognosis and enhanced cell

		proliferation. Several groups have seen an overexpression of this protein in cancer cells as breast cancer (Zhang *et al.*, 2013; Scully *et al.*, 2015), prostate cancer (Amamoto *et al.*, 2011), ovarian cancer (Yu and Wang, 2013) and colon cancer (Kim *et al.*, 2017). Metastasis, (Zhang *et al.*, 2013), migration (Scully *et al.*, 2015) and normal metabolism disruption (Fogal *et al.*, 2010) are some of the tumoral events in which C1QBP may play a role in. C1QBP overexpression in prostate cancer cells has been associated with cell migration and cell cycle control (Amamoto *et al.*, 2011).
COMMD1	SKOV-3	COMM domain-containing protein 1, has a crucial role in copper metabolism (Phillips-Krawczak *et al.*, 2015), regulates Na(+) transport through the epithelial sodium channel (Ke *et al.*, 2010) and ubiquitination (Maine *et al.*, 2007). Other works associate COMMD1 expression with cell growth suppression (Mu *et al.*, 2017), lower pro-inflammatory response (Yeh *et al.*, 2016) and inhibition of tumor cell invasion (van de Sluis *et al.*, 2010). Moreover, nuclear expression of COMMD1 has been associated to increased ovarian cell sensitivity to the antitumoral drug, cisplatin (Fedoseienko *et al.*, 2016).
GLTSCR2	PC-3 SKOV-3	Ribosome biogenesis protein NOP53. Lee and colleagues demonstrated that GLTSCR2 can directly regulate p53 expression, having thus an important role in cell cycle (Lee *et al.*, 2012). The same study showed that downregulation of GLTSCR reduces cell proliferation on a p53-dependent manner. The study carried out by Moon *et al*., also reveal GLTSCR2 activity as a tumor suppressor. In this research they observed that GLTSCR expression is downregulated in breast cancer and how overexpressing GLTSCR2 in breast cancer cells reduced the invasiveness ability of those cells (Moon *et al.*, 2013). Similar results were obtained by Okahara *et al*., as their study show how downregulation of GLTSCR2 in HeLa cells increased cell proliferation and decreased apoptosis in a PTEN-dependent way (Okahara *et al.*, 2006). Even though GLTSCR2 behaves as a tumor suppressor in the development of different cancers, some studies also bring to light an oncogenic role of this protein. Likewise, a study carried out in gastric cancer revealed that GLTSCR2 depletion induced an inhibition in cell growth on a p53 dependent way (Uchi *et al.*, 2013), and Kim *et al*., suggested that GLTSCR2 is involved in the positive regulation of telomerase and chromosome stability (Kim *et al.*, 2016). Regarding prostate cancer, GLTSCR2 seems to behave as a tumor suppressor, since knock down of this gene in LNCaP prostatic cancer cells lead to an increase in the invasiveness of these cells (Kim *et al.*, 2013).
MIEN1	SKOV-3	Migration and invasion enhancer 1, is a protein not detectable or of low expression in normal human tissues, but it is up-regulated in prostate cancer (Dasgupta *et al.*, 2009), ovarian cancer (Leung *et al.*, 2013), breast cancer (Evans *et al.*, 2006), oral cancer cell lines (Rajendiran *et al.*, 2015) and non-small cell lung cancer (Dongmei Li *et al.*, 2016). Cell proliferation, invasion and metastasis are tumoral events that have been related to MIEN1 overexpression in cancer cells (Rajendiran *et al.*, 2014, 2015; Kpetemey *et al.*, 2016). Leung and collaborators also showed that MIEN1 may be involved in chemo-resistance to cisplatin treatment in cancer cells (Leung *et al.*, 2013).

ROCK1	SKOV-3	Rho-associated protein kinase 1, is implicated in different functions, as in actin organization, apoptosis, cell proliferation, cytokinesis and may also play a role in developing embryos (Julian and Olson, 2014). A review carried out by Wei and colleagues explains the implication of ROCK1 in key events during cancer development such as cell migration, angiogenesis and metastasis (Wei *et al.*, 2016). Among the cancers where ROCK1 has been seen to play a role in are prostate cancer (C Zhang *et al.*, 2014; Xu *et al.*, 2015) and ovarian cancer (Tocci *et al.*, 2016).
SNAPIN	PC-3	SNARE-associated protein Snapin, is part of the Biogenesis of lysosome-related organelles complex-1 (BLOC-1), which plays a key role in the endosomal-lysosomal system (Starcevic and Dell'Angelica, 2004). SNAPIN is also necessary for the correct working of the synaptic vesicle cycle (Yu *et al.*, 2013). A study published by Inagaki and collaborators suggest that SNAPIN may be overexpressed in hepatocellular carcinoma and this overexpression may be linked to the development or progression of this type of cancer (Inagaki *et al.*, 2008).
U2AF1	PC-3 SKOV-3	Splicing factor U2AF 35 kDa subunit, plays a critical role in splicing mechanisms. Its activity is necessary for the correct function of constitutive splicing as well as for enhancer-dependent splicing (Zuo and Maniatis, 1996). Mutation in genes of the splicing machinery such as U2AF1 may be involved in de development of hematologic tumors (Je *et al.*, 2013).
UHRF2	PC-3	Previously described in the table of HMGB1 interactants.
ZNF428	PC-3	Previously described in the table of HMGB1 interactants.
ZNF668	SKOV-3	Zinc finger protein 668, is a member of the krüppel C2H2-type zinc finger protein family. Although not many studies have been done with this protein and its functions are still quite unknown, Hu *et al.*, demonstrated a functional interaction with p53 and MDM2 and they identify ZNF688 as a novel tumor suppressor (Hu *et al.*, 2011). The same group suggest in another study that this protein may play an important role in the later stages of DNA damage response (Hu *et al.*, 2016).

REFERENCES

Amamoto R, Yagi M, Song Y, Oda Y, Tsuneyoshi M, Naito S, Yokomizo A, Kuroiwa K, Tokunaga S, Kato S, Hiura H, Samori T, Kang D, Uchiumi T. 2011. Mitochondrial p32/C1QBP is highly expressed in prostate cancer and is associated with shorter prostate-specific antigen relapse time after radical prostatectomy. *Cancer Sci.*, **102**: 639–647.

Asante D, Stevenson NL, Stephens DJ. 2014. Subunit composition of the human cytoplasmic dynein-2 complex. *J. Cell Sci.*, **127**: 4774–4787.

Bjerke L, Mackay A, Nandhabalan M, Burford A, Jury A, Popov S, Bax DA, Carvalho D, Taylor KR, Vinci M, Bajrami I, Mcgonnell IM, Lord CJ, Reis RM, Hargrave D, Ashworth A, Workman P, Jones C. 2013. Histone H3 . 3 mutations drive paediatric glioblastoma through upregulation of MYCN. *Cancer Discov.*, **3**: 512–519.

Bull JH, Ellison G, Patel a, Muir G, Walker M, Underwood M, Khan F, Paskins L. 2001.

Identification of potential diagnostic markers of prostate cancer and prostatic intraepithelial neoplasia using cDNA microarray. *Br. J. Cancer*, **84**: 1512–9.

Carrera M, Bitu CC, Oliveira CE De, Cervigne NK, Graner E, Salo T, Coletta RD. 2015. HOXA10 controls proliferation , migration and invasion in oral squamous cell carcinoma. *Int. J. Clin. Exp. Pathol.*, **8**: 3613–3623.

Chu MC, Selam FB, Taylor HS. 2004. HOXA10 regulates p53 expression and matrigel invasion in human breast cancer cells. *Cancer Biol. Ther.*, **3**: 568–572.

Cui XP, Qin CK, Zhang ZH, Su ZX, Liu X, Wang SK, Tian XS. 2014. HOXA10 promotes cell invasion and MMP-3 expression via TGF??2-mediated activation of the p38 MAPK pathway in pancreatic cancer cells. *Dig. Dis. Sci.*, **59**: 1442–1451.

Dasgupta S, Wasson LM, Rauniyar N, Prokai L, Borejdo J, Vishwanatha JK. 2009. Novel gene C17orf37 in 17q12 amplicon promotes migration and invasion of prostate cancer cells. *Oncogene*, **28**: 2860–2872.

Debonneville C, Staub O. 2004. Participation of the Ubiquitin-Conjugating Enzyme UBE2E3 in Nedd4-2-Dependent Regulation of the Epithelial Na+ Channel. *Mol. Cell. Biol.*, **24**: 2397–2409.

Dong Y, Liang G, Yuan B, Yang C, Gao R, Zhou X. 2015. MALAT1 promotes the proliferation and metastasis of osteosarcoma cells by activating the PI3K/Akt pathway. *Tumor Biol.*, **36**: 1477–1486.

Du H, Taylor HS. 2015. The Role of Hox Genes in Female Reproductive Tract Development, Adult Function, and Fertility. *Cold Spring Harb. Perspect. Med.*, **6**: a023002.

Evans EE, Henn AD, Jonason A, Paris MJ, Schiffhauer LM, Borrello MA, Smith ES, Sahasrabudhe DM, Zauderer M. 2006. C35 (C17orf37) is a novel tumor biomarker abundantly expressed in breast cancer. *Mol Cancer Ther*, **5**: 2919–2930.

Fedoseienko A, Wieringa HW, Wisman GBA, Duiker E, Reyners AKL, Hofker MH, Van Der Zee AGJ, Van De Sluis B, Van Vugt MATM. 2016. Nuclear COMMD1 is associated with cisplatin sensitivity in ovarian cancer. *PLoS One*, **11**: 1–21.

Fogal V, Richardson AD, Karmali PP, Scheffler IE, Smith JW, Ruoslahti E. 2010. Mitochondrial p32 Protein Is a Critical Regulator of Tumor Metabolism via Maintenance of Oxidative Phosphorylation. *Mol. Cell. Biol.*, **30**: 1303–1318.

Gao N, Asamitsu K, Hibi Y, Ueno T, Okamoto T. 2008. AKIP1 enhances NF-κB-dependent gene expression by promoting the nuclear retention and phosphorylation of p65. *J. Biol. Chem.*, **283**: 7834–7843.

Goh WQJ, Ow GS, Kuznetsov VA, Chong S, Lim YP. 2015. DLAT subunit of the pyruvate dehydrogenase complex is upregulated in gastric cancer-implications in cancer therapy. *Am. J. Transl. Res.*, **7**: 1140–1151.

Gutschner T, Hämmerle M, Eißmann M, Hsu J, Kim Y, Hung G, Revenko A, Arun G, Stentrup M, Groß M, Zörnig M, Macleod AR, Spector DL, Diederichs S. 2014. The non-coding RNA MALAT1 is a critical regulator of the metastasis phenotype of lung cancer cells. **73**: 1180–1189.

Han Y, Lu S, Wen YG, Yu FD, Zhu XW, Qiu GQ, Tang HM, Peng ZH, Zhou CZ. 2015.

Overexpression of HOXA10 promotes gastric cancer cells proliferation and HOXA10+/CD44+ is potential prognostic biomarker for gastric cancer. *Eur. J. Cell Biol.*, **94**: 642–652.

Hu R, Peng G, Dai H, Breuer EK, Stemke-Hale K, Li K, Gonzalez-Angulo AM, Mills GB, Lin SY. 2011. ZNF668 functions as a tumor suppressor by regulating p53 stability and function in breast cancer. *Cancer Res.*, **71**: 6524–6534.

Hu R, Wang E, Peng G, Dai H, Lin S. 2016. Zinc finger protein 668 interacts with Tip60 to promote H2AX acetylation after DNA damage Zinc finger protein 668 interacts with Tip60 to promote H2AX acetylation after DNA damage. *Cell Cycle*, **12**: 2033–2041.

Huang J-K, Ma L, Song W-H, Lu B-Y, Huang Y-B, Dong H-M, Ma X-K, Zhu Z-Z, Zhou R. 2016. MALAT1 promotes the proliferation and invasion of thyroid cancer cells via regulating the expression of IQGAP1. *Biomed Pharmacother*, **83**: 1–7.

Huang K, Yang C, Wang Q xue, Li Y sheng, Fang C, Tan Y li, Wei J wei, Wang Y fei, Li X, Zhou J hu, Zhou B cong, Yi K kai, Zhang K liang, Li J, Kang C sheng. 2017. The CRISPR/Cas9 system targeting EGFR exon 17 abrogates NF-κB activation via epigenetic modulation of UBXN1 in EGFRwt/vIII glioma cells. *Cancer Lett.*, **388**: 269–280.

Ibragimova I, Ibanez de Caceres I, Hoffman AM, Potapova A, Dulaimi E, Al-Saleem T, Hudes GR, Ochs MF, Cairns P. 2010. Global reactivation of epigenetically silenced genes in prostate cancer. *Cancer Prev. Res. (Phila).*, **3**: 1084–1092.

Ichimi T, Enokida H, Okuno Y, Kunimoto R, Chiyomaru T, Kawamoto K, Kawahara K, Toki K, Kawakami K, Nishiyama K, Tsujimoto G, Nakagawa M, Seki N. 2009. Identification of novel microRNA targets based on microRNA signatures in bladder cancer. *Int. J. Cancer*, **125**: 345–352.

Ichimura T, Watanabe S, Sakamoto Y, Aoto T, Pujita N, Nakao M. 2005. Transcriptional repression and heterochromatin formation by MBD1 and MCAF/AM family proteins. *J. Biol. Chem.*, **280**: 13928–13935.

Inagaki Y, Yasui K, Endo M, Nakajima T, Zen K, Tsuji K, Minami M, Tanaka S, Taniwaki M, Itoh Y, Arii S, Okanoue T. 2008. CREB3L4, INTS3, and SNAPAP are targets for the 1q21 amplicon frequently detected in hepatocellular carcinoma. *Cancer Genet. Cytogenet.*, **180**: 30–36.

Ishikawa H, Thompson J, Yates JR, Marshall WF. 2012. Proteomic analysis of mammalian primary cilia. *Curr. Biol.*, **22**: 414–419.

Je EM, Yoo NJ, Kim YJ, Kim MS, Lee SH. 2013. Mutational analysis of splicing machinery genes SF3B1, U2AF1 and SRSF2 in myelodysplasia and other common tumors. *Int. J. Cancer*, **133**: 260–265.

Ji Q, Liu X, Fu X, Zhang L, Sui H, Zhou L, Sun J, Cai J, Qin J, Ren J, Li Q. 2013. Resveratrol inhibits invasion and metastasis of colorectal cancer cells via MALAT1 mediated Wnt/β-catenin signal pathway. *PLoS One*, **8**.

Julian L, Olson MF. 2014. Rho-associated coiled-coil containing kinases (ROCK). *Small GTPases*, **5**: e29846.

Ke Y, Butt AG, Swart M, Liu YF, Mcdonald FJ. 2010. COMMD1 downregulates the epithelial sodium channel through Nedd4 – 2. *Am. J. Physiol. Renal Physiol.*, **298**: 1445–1456.

Kim JY, An YM, Park JH. 2016. Role of GLTSCR2 in the regulation of telomerase activity and

chromosome stability. *Mol. Med. Rep.*, **14**: 1697–1703.

Kim JY, Cho YE, Kim GY, Lee HL, Lee S, Park JH. 2013. Down-regulation and aberrant cytoplasmic expression of GLTSCR2 in prostatic adenocarcinomas. *Cancer Lett.*, **340**: 134–140.

Kim K, Kim M-J, Kim K-H, Ahn S-A, Kim JH, Cho JY, Yeo S-G. 2017. C1QBP is upregulated in colon cancer and binds to apolipoprotein A-I. *Exp. Ther. Med.*, **13**: 2493–2500.

Kitching R, Li H, Wong MJ, Kanaganayakam S, Kahn H, Seth A. 2003. Characterization of a novel human breast cancer associated gene (BCA3) encoding an alternatively spliced proline-rich protein. *Biochim. Biophys. Acta*, **1625**: 116–121.

Kpetemey M, Chaudhary P, Van Treuren T, Vishwanatha JK. 2016. MIEN1 drives breast tumor cell migration by regulating cytoskeletal-focal adhesion dynamics. *Oncotarget*, **7**: 54913–54924.

Lai M, Liang L, Chen J, Qiu N, Ge S, Ji S, Shi T, Zhen B, Liu M, Ding C, Wang Y, Qin J. 2016. Multidimensional Proteomics Reveals a Role of UHRF2 in the Regulation of Epithelial-Mesenchymal Transition (EMT). *Mol. Cell. Proteomics*, **15**: 2263–2278.

Lee S, Kim J-Y, Kim Y-J, Seok K-O, Kim J-H, Chang Y-J, Kang H-Y, Park J-H. 2012. Nucleolar protein GLTSCR2 stabilizes p53 in response to ribosomal stresses. *Cell Death Differ.*, **19**: 1613–1622.

Leung TH-Y, Wong SC-S, Chan KK-L, Chan DW, Cheung AN-Y, Ngan HY-S. 2013. The interaction between C35 and ΔNp73 promotes chemo-resistance in ovarian cancer cells. *Br. J. Cancer*, **109**: 965–975.

Li B, Cao X, Weng C, Wu Y, Fang X, Zhang X, Liu G. 2014. HoxA10 induces proliferation in human prostate carcinoma PC-3 cell line. *Cell Biochem. Biophys.*, **70**: 1363–1368.

Li B, Jin H, Yu Y, Gu C, Zhou X, Zhao N, Feng Y. 2009. HOXA10 is overexpressed in human ovarian clear cell adenocarcinoma and correlates with poor survival. *Int. J. Gynecol. Cancer*, **19**: 1347–1352.

Li D, Wei Y, Wang D, Gao H, Liu K. 2016. MicroRNA-26b suppresses the metastasis of non-small cell lung cancer by targeting MIEN1 via NF-κB/MMP-9/VEGF pathways. *Biochem. Biophys. Res. Commun.*, **472**: 465–470.

Li L, Chen H, Gao Y, Wang YW, Zhang GQ, Pan SH, Ji L, Kong R, Wang G, Jia YH, Bai XW, Sun B. 2016. Long Noncoding RNA MALAT1 Promotes Aggressive Pancreatic Cancer Proliferation and Metastasis via the Stimulation of Autophagy. *Mol Cancer Ther*, **15**: 2232–2243.

Libório-Kimura TN, Jung HM, Chan EKL. 2015. MiR-494 represses HOXA10 expression and inhibits cell proliferation in oral cancer. *Oral Oncol.*, **51**: 151–157.

Lin C, Song L, Liu A, Gong H, Lin X, Wu J, Li M, Li J. 2015. Overexpression of AKIP1 promotes angiogenesis and lymphangiogenesis in human esophageal squamous cell carcinoma. *Oncogene*, **34**: 384–393.

Lin Z, Hu B, Ni W, Mao X, Zhou H, Lv J, Yin B, Shen Z, Wu M, Ding W, Xiao M, Ni R. 2016. Expression pattern of BCCIP in hepatocellular carcinoma is correlated with poor prognosis and enhanced cell proliferation. *Tumor Biol.*, **37**: 16305–16315.

Liu J, Yuan Y, Huan J, Shen Z. 2001. Inhibition of breast and brain cancer cell growth by BCCIPalpha, an evolutionarily conserved nuclear protein that interacts with BRCA2. *Oncogene*, **20**: 336–345.

Liu L, Ishihara K, Ichimura T, Fujita N, Hino S, Tomita S, Watanabe S, Saitoh N, Ito T, Nakao M. 2009. MCAF1/AM is involved in Sp1-mediated maintenance of cancer-associated telomerase activity. *J. Biol. Chem.*, **284**: 5165–5174.

Liu S, Jiang X, Li W, Cao D, Shen K, Yang J. 2016. Inhibition of the long non-coding rna malat1 suppresses tumorigenicity and induces apoptosis in the human ovarian cancer skov3 cell line. *Oncol. Lett.*, **11**: 3686–3692.

Liu X, Cao L, Ni J, Liu N, Zhao X, Wang Y, Zhu L, Wang L, Wang J, Yue Y, Cai Y, Jin J. 2013. Differential BCCIP gene expression in primary human ovarian cancer, renal cell carcinoma and colorectal cancer tissues. *Int. J. Oncol.*, **43**: 1925–1934.

Lu H, Bhoopatiraju S, Wang H, Schmitz NP, Wang X, Freeman MJ, Forster CL, Verneris MR, Linden MA, Hallstrom TC. 2016. Loss of UHRF2 expression is associated with human neoplasia , promoter hypermethylation , decreased 5-hydroxymethylcytosine , and high proliferative activity. *Oncotarget*, **7**: 76047–76061.

Maine GN, Mao X, Komarck CM, Burstein E. 2007. COMMD1 promotes the ubiquitination of NF-κB subunits through a cullin-containing ubiquitin ligase. *EMBO J.*, **26**: 436–447.

Mao TK, Davis PA, Odin JA, Coppel RL, Gershwin ME. 2011. Sidechain biology and the immunogenicity of PDC-E2, the major autoantigen of primary biliary cirrhosis. *Hepatology*, **40**: 1241–1248.

Mao Y, Shen J, Lu Y, Lin K, Wang H, Li Y, Chang P, Walker MG, Li D. 2017. RNA sequencing analyses reveal novel differentially expressed genes and pathways in pancreatic cancer. *Oncotarget*, **8**: 42537–42547.

Meng X, Fan J, Shen Z. 2007. Roles of BCCIP in chromosome stability and cytokinesis. *Oncogene*, **26**: 6253–6260.

Meng X, Liu J, Shen Z. 2004. Inhibition of G 1 to S Cell Cycle Progression by BCCIPβ. *Cell Cycle*, **3**: 343–348.

Mito Y, Henikoff JG, Henikoff S. 2005. Genome-scale profiling of histone H3.3 replacement patterns. *Nat. Genet.*, **37**: 1090–1097.

Mo D, Li X, Li C, Liang J, Zeng T, Su N, Jiang Q, Huang J. 2016. Overexpression of AKIP1 predicts poor prognosis of patients with breast carcinoma and promotes cancer metastasis through Akt / GSK-3β / Snail pathway. *Am. J. Transl. Res.*, **8**: 4951–4959.

Mobin MB, Gerstberger S, Teupser D, Campana B, Charisse K, Heim MH, Manoharan M, Tuschl T, Stoffel M. 2016. The RNA-binding protein vigilin regulates VLDL secretion through modulation of Apob mRNA translation. *Nat. Commun.*, **7**: 12848.

Moon A, Lim SJ, Jo YH, Lee S, Kim JY, Lee J, Park JH. 2013. Downregulation of GLTSCR2 expression is correlated with breast cancer progression. *Pathol. Res. Pract.*, **209**: 700–704.

Mori T, Ikeda DD, Fukushima T, Takenoshita S, Kochi H. 2011. NIRF constitutes a nodal point in the cell cycle network and is a candidate tumor suppressor. *Cell Cycle*, **10**: 3284–3299.

Mu P, Akashi T, Lu F, Kishida S, Kadomatsu K. 2017. A novel nuclear complex of DRR1, F-actin and COMMD1 involved in NF-κB degradation and cell growth suppression in neuroblastoma. *Oncogene*, 1–12.

Okahara F, Itoh K, Nakagawara A, Murakami M, Kanaho Y, Maehama T. 2006. Critical Role of PICT-1, a Tumor Suppressor Candidate, in Phosphatidylinositol 3,4,5-Trisphosphate Signals and Tumorigenic Transformation. *Mol. Biol. Cell*, **17**: 4888–4895.

Omary MB, Ku NO, Strnad P, Hanada S. 2009. Toward unraveling the complexity of simple epithelial keratins in human disease. *J. Clin. Invest.*, **119**: 1794–1805.

Omran H, Kobayashi D, Olbrich H, Tsukahara T, Loges NT, Hagiwara H, Zhang Q, Leblond G, Eileen O, Hara C, Mizuno H, Kawano H, Fliegauf M, Yagi T, Koshida S, Miyawaki A, Zentgraf H, Seithe H, Reinhardt R, Watanabe Y, Mitchell DR, Takeda H. 2008. Ktu/PF13 is required for cytoplasmic pre-assembly of axonemal dyneins. *Nature*, **456**: 611–616.

Petersen-Mahrt SK, Estmer C, Öhrmalm C, Matthews DA, Russell WC, Akusjärvi G. 1999. The splicing factor-associated protein, p32, regulates RNA splicing by inhibiting ASF/SF2 RNA binding and phosphorylation. *EMBO J.*, **18**: 1014–1024.

Phillips-Krawczak CA, Singla A, Starokadomskyy P, Deng Z, Osborne DG, Li H, Dick CJ, Gomez TS, Koenecke M, Zhang J-S, Dai H, Sifuentes-Dominguez LF, Geng LN, Kaufmann SH, Hein MY, Wallis M, McGaughran J, Gecz J, Sluis B v. d., Billadeau DD, Burstein E. 2015. COMMD1 is linked to the WASH complex and regulates endosomal trafficking of the copper transporter ATP7A. *Mol. Biol. Cell*, **26**: 91–103.

Plafker KS, Nguyen L, Barneche M, Mirza S, Crawford D, Plafker SM. 2010. The ubiquitin-conjugating enzyme UbcM2 can regulate the stability and activity of the antioxidant transcription factor Nrf2. *J. Biol. Chem.*, **285**: 23064–23074.

Rajendiran S, Kpetemey M, Maji S, Gibbs LD, Dasgupta S, Mantsch R, Hare RJ, Vishwanatha JK. 2015. MIEN1 promotes oral cancer progression and implicates poor overall survival. *Cancer Biol. Ther.*, **16**: 876–885.

Rajendiran S, Parwani A V, Hare RJ, Dasgupta S, Roby RK, Vishwanatha JK. 2014. MicroRNA-940 suppresses prostate cancer migration and invasion by regulating MIEN1. *Mol. Cancer*, **13**: 250.

Scully OJ, Yu Y, Salim A, Thike AA, Yip GW-C, Baeg GH, Tan P-H, Matsumoto K, Bay BH. 2015. Complement component 1, q subcomponent binding protein is a marker for proliferation in breast cancer. *Exp. Biol. Med.*, **240**: 846–853.

van de Sluis B, Mao X, Zhai Y, Groot AJ, Vermeulen JF, van der Wall E, van Diest PJ, Hofker MH, Wijmenga C, Klomp LW, Cho KR, Fearon ER, Vooijs M, Burstein E. 2010. COMMD1 disrupts HIF-1alpha/beta dimerization and inhibits human tumor cell invasion. *J. Clin. Invest.*, **120**: 2119–30.

Starcevic M, Dell'Angelica EC. 2004. Identification of Snapin and three novel proteins (BLOS1, BLOS2, and BLOS3/reduced pigmentation) as subunits of biogenesis of lysosome-related organelles complex-1 (BLOC-1). *J. Biol. Chem.*, **279**: 28393–28401.

Sun R, Qin C, Jiang B, Fang S, Pan X, Peng L, Liu Z, Li W, Li Y, Li G. 2016. Down-regulation of MALAT1 inhibits cervical cancer cell invasion and metastasis by inhibition of epithelial–mesenchymal transition. *Mol. Biosyst.*, **12**: 952–962.

Tang W, Jiang Y, Mu X, Xu L, Cheng W, Wang X. 2014. MiR-135a functions as a tumor suppressor in epithelial ovarian cancer and regulates HOXA10 expression. *Cell. Signal.*, **26**: 1420–1426.

Tocci P, Caprara V, Cianfrocca R, Sestito R, Di Castro V, Bagnato A, Rosanò L. 2016. Endothelin-1/endothelin A receptor axis activates RhoA GTPase in epithelial ovarian cancer. *Life Sci.*, **159**: 49–54.

Uchi R, Kogo R, Kawahara K, Sudo T, Yokobori T, Eguchi H, Sugimachi K, Maehama T, Mori M, Suzuki A, Komune S, Mimori K. 2013. PICT1 regulates TP53 via RPL11 and is involved in gastric cancer progression. *Br. J. Cancer*, **109**: 2199–2206.

Vollbrandt T, Willkomm D, Stossberg H, Kruse C. 2004. Vigilin is co-localized with 80S ribosomes and binds to the ribosomal complex through its C-terminal domain. *Int. J. Biochem. Cell Biol.*, **36**: 1306–1318.

Wang D, Ding L, Wang L, Zhao Y, Sun Z, Karnes RJ, Zhang J, Huang H. 2015. LncRNA MALAT1 enhances oncogenic activities of EZH2 in castration-resistant prostate cancer. *Oncotarget*, **6**: 41045–41055.

Wei L, Surma M, Shi S, Lambert-Cheatham N, Shi J. 2016. Novel Insights into the Roles of Rho Kinase in Cancer. *Arch. Immunol. Ther. Exp. (Warsz).*, **64**: 259–278.

Wei L, Xie X, Li J, Li R, Shen W, Duan S, Zhao R, Yang W, Liu Q, Fu Q, Qin Y. 2015. Disruption of human vigilin impairs chromosome condensation and segregation. *Cell Biol. Int.*, **39**: 1234–1241.

Wu L, Wang X, Guo Y. 2017. Long non-coding RNA MALAT1 is upregulated and involved in cell proliferation, migration and apoptosis in ovarian cancer. *Exp. Ther. Med.*, **13**: 3055–3060.

Xu B, Huang Y, Niu X, Tao T, Jiang L, Tong N, Chen S, Liu N, Zhu W, Chen M. 2015. Hsa-miR-146a-5p modulates androgen-independent prostate cancer cells apoptosis by targeting ROCK1. *Prostate*, **75**: 1896–1903.

Yang WL, Wei L, Huang WQ, Li R, Shen WY, Liu JY, Xu JM, Li B, Qin Y. 2014. Vigilin is overexpressed in hepatocellular carcinoma and is required for HCC cell proliferation and tumor growth. *Oncol. Rep.*, **31**: 2328–2334.

Yeh D-W, Chen Y-S, Lai C-Y, Liu Y-L, Lu C-H, Lo J-F, Chen L, Hsu L-C, Luo Y, Xiang R, Chuang T-H. 2016. Downregulation of COMMD1 by miR-205 promotes a positive feedback loop for amplifying inflammatory- and stemness-associated properties of cancer cells. *Cell Death Differ.*, **23**: 841–852.

Yu G, Wang J. 2013. Significance of hyaluronan binding protein (HABP1/P32/gC1qR) expression in advanced serous ovarian cancer patients. *Exp. Mol. Pathol.*, **94**: 210–215.

Yu SC, Klosterman SM, Martin AA, Gracheva EO, Richmond JE. 2013. Differential Roles for Snapin and Synaptotagmin in the Synaptic Vesicle Cycle. *PLoS One*, **8**.

Zhang C, Zhang S, Zhang Z, He J, Xu Y, Liu S. 2014. ROCK has a crucial role in regulating prostate tumor growth through interaction with c-Myc. *Oncogene*, **33**: 5582–5591.

Zhang L, Wan Y, Jiang Y, Ma J, Liu J, Tang W, Wang X, Cheng W. 2014. Upregulation HOXA10 homeobox gene in endometrial cancer: Role in cell cycle regulation. *Med. Oncol.*, **31**.

Zhang X, Zhang F, Guo L, Wang Y, Zhang P, Wang R, Zhang N, Chen R. 2013. Interactome analysis reveals that C1QBP (complement component 1, q subcomponent binding protein) is associated with cancer cell chemotaxis and metastasis. *Mol. Cell. proteomics MCP*, **12**: 3199–209.

Zou A, Liu R, Wu X. 2016. Long non-coding RNA MALAT1 is up-regulated in ovarian cancer tissue and promotes SK-OV-3 cell proliferation and invasion. *Neoplasma*, **63**: 865–872.

Zuo P, Maniatis T. 1996. The splicing factor U2AF35 mediates critical protein-protein interactions in constitutive and enhancer-dependent splicing. *Genes Dev.*, **10**: 1356–1368.

Chapter 4

Nuclear and cytoplasmic interactions of HMGB1 in prostate and ovarian tumoral cells identified by an Immunoprecipitation/MS approach

INTRODUCTION

HMGB1 was first described as a non-histone DNA binding protein which highly increases thermal stabilization of this molecule (Yu *et al.*, 1977). Originally HMGB1 functions were related to DNA and nuclear functions such as acting as a DNA/chromatin chaperone, V(D)J recombination (Schatz and Swanson, 2011) and DNA replication and repair (Yuan *et al.*, 2004; Prasad *et al.*, 2007) among others. Nevertheless, nowadays HMGB1 is known to have key roles in the cytoplasm and in the extracellular milieu such as activating autophagy (Tang *et al.*, 2010) or behaving as a damage-associated molecular pattern (DAMP) that triggers inflammatory processes once released to the extracellular matrix (Yang and Wang, 2015). HMGB1 localization, post-translational modifications and redox states are crucial to its proper function.

HMGB1 has been tightly associated to the development of a wide range of cancers including prostate and ovary (reviwed in Barreiro-Alonso *et al.*, 2016). Likewise, different studies link HMGB1 to the principal cancer hallmarks as angiogenesis (Beijnum *et al.*, 2012), epithelial-mesenchymal transition, invasion, and migration (Chandrasekaran *et al.*, 2016; Liu *et al.*, 2017).

Expression of HMGB1 in prostate tumoral cells increases (Gnanasekar *et al.*, 2009; Li *et al.*, 2012). Moreover due to its role in prostate cancer progression HMGB1 has been proposed as a therapeutic target for this type of cancer (Gnanasekar *et al.*, 2013). HMGB1 is also overexpressed in ovarian carcinomas and its expression has been associated to development of ovarian cancer (Zhang *et al.*, 2014). Moreover, several studies consider

HMGB1 as a promising marker for ovarian cancer (Li *et al.*, 2014; Wang *et al.*, 2015; Paek *et al.*, 2016).

Studying and identifying the physical interactions of proteins is vital to understand their implication in a certain malignancy. Currently, the mass spectrometry (MS) technology is of widespread use in proteomic studies as it allows the precise identification of a huge number of proteins. In this study HMGB1 large scale immunoprecipitation assays coupled to MS analysis are used as a start point to identify novel HMGB1 interactions in ovarian and prostate cancer cells. In addition, experiments carried out after cellular fractionation has allowed the identification of specific nuclear or extranuclear interactions. The more promising interactions have been studied in more detail.

MATERIALS AND METHODS

Cell culture

PC-3 (human prostate cancer) and SKOV-3 (human ovarian cancer) were grown in RPMI-1640 (Thermo Fisher Scientific, Inc.) and McCoy's 5a Modified Medium (Thermo Fisher Scientific, Inc.) supplemented with 10% heat-inactivated fetal bovine serum (Thermo Fisher Scientific, Inc.) and 1% penicillin-streptomycin (Thermo Fisher Scientific, Inc.) respectively. For cells harboring the Tag-*HMGB1* and β-*lactamase* PC-3 clones, culture media was supplemented with either 400 μg/ml or 200 μg/ml of G418 and penicillin-streptomycin was omitted. Cells were cultured at 37 ºC, 5% CO_2 in a humidified incubator. Cells were tested regularly for mycoplasma contamination.

Generation of N-terminal tag *HMGB1* constructs

The complete *HMGB1* coding sequence was cloned in frame in the pDsRed-Monomer-C1-Vector (Clontech) as follows. The DsRed-Monomer was removed from the plasmid by double digestion with *Age*I and *Sal*I. The FTAP containing 3xFLAG-2xTEV-CBP designed by Pardo and collaborators (Pardo *et al.*, 2010), modified as required for this construction and designed to include the TAG in the N-terminal *HMGB1* coding region, was synthesized by NZYTtech (Figure 1A). The PCR product and vector were digested with *Age*I and *Sal*I and ligated . A parallel construction was made expressing the bacterial β-*lactamase* gene in frame with the epitope in the pDsRed-Monomer-C1-Vector lacking the DsRed-Monomer. The complete constructions were sequenced for verification.

Generation of PC-3 clones expressing tagged HMGB1

PC-3 cells were transfected with 1 or 2 μg of either tag-HMGB1 vector or pDsRed-Monomer-C1-Vector using Lipofectamine®2000 (Invitrogen) following the manufacturer´s instructions. 48 hours after transfection, cells were incubated with 400 μg/ml G418 for selection of drug-resistant colonies over more than 3 weeks. Small cloning cylinders were used to encircle single colonies and grow them inside until a sufficient number of cells grew and they could be harvested and expanded using a lower dose of antibiotic, 200 μg/ml, thus generating stable clones expressing the tagged HMGB1. The same procedure was followed to obtain clones expressing β-lactamase tagged with the same epitope, but pooled colonies were used instead of isolating single colonies.

Large-scale immunoprecipitation

PC-3 and SKOV-3 cells were lysed in 50 mM Tri-HCl pH 8.0, 150 mM NaCl, 0.1% NP-40, 1 mM EDTA, 2 mM $MgCl_2$ and complete™ Mini, EDTA-free Protease Inhibitor Cocktail (Roche) and incubated with 1,5:1000 (v/v) Benzonase®Nuclease (Sigma-Aldrich) for 30 min at 4 ºC to eliminate nucleic acids from the lysates. Total protein was quantified using the Bradford method. 40 µg of HMGB1 antibody (Abcam, ab 18256, Cambridge, UK), THOC5 (Abcam, ab86070, Cambridge, UK) or anti-rabbit IgG antibody (Millipore) were crosslinked to 50 µl of Protein G-Dynal beads (Invitrogen) as previously described (Pardo *et al.*, 2010). For each immunoprecipitation 2.5-3 mg of total protein were incubated with antibody-coupled beads for 4 h at 4 ºC and beads were then washed four times with IPP150 buffer (10 mM Tris-HCl pH 8.0, 150 mM NaCl and 0.1% NP-40) and four times with 50 mM ammonium bicarbonate. On-bead digestion was carried out overnight at 37 ºC with trypsin (sequencing grade, Roche). Peptides were then collected, filtered through Millipore Multiscreen plates to remove remnant beads, and dried in a Speed Vac (Thermo). Prior to MS analysis peptides were solved in 20 mM TCEP and formic acid was added to a final concentration of 0.5%.

Affinity purification

Whole-cell extracts from clone 7 and clone 8 expressing HMGB1 and the pool expressing β-galacosidase were obtained and incubated with Protein G-Dynal beads (Invitrogen). Beads were crosslinked to M2 FLAG antibody (Sigma) beforehand. Cell lysis, bead crosslinking, incubation with the crosslinked beads, washes and elution were performed as explained for

large scale immunoprecipitation with two exceptions: the lysis buffer also contained 1 mM DTT and the incubation of the lysate with the cross-linked beads was maintained during two hours instead of four.

Mass spectrometry and data analysis

Peptides were analyzed with online nanoLC-MS/MS on an Orbitrap Velos mass spectrometer coupled with an Ultimate 3000 RSLCnano System. Samples were first loaded and desalted on a nanotrap (100 µm id x 2 cm) (PepMap C18, 5 µ) at 10 µl/min with 0.1% formic acid for 10 min and then separated on an analytical column (75 µm id x 25 cm) (PepMap C18, 2µ) over a 120 min linear gradient of 4-32% CH_3CN/0.1% formic acid at 300 nl/min, and the total cycle time was 150 min. The Orbitrap Velos was operated in standard data-dependent acquisition. The survey scans (m/z 380-1500) were acquired in the Orbitrap at a resolution of 30000 at m/z 400, and one micro-scan was acquired per spectrum. The 10 most abundant multiply charged ions with a minimal intensity of 2000 counts were subject to MS/MS in the linear ion trap at an isolation width of 2 Th. Dynamic exclusion width was set at ± 10 ppm for 45 s. The automatic gain control target value was regulated at $1x10^6$ for the Orbitrap and 5000 for the ion trap, with maximum injection time at 200 ms for Orbitrap and 100 ms for the ion trap, respectively.

The raw files were processed with Proteome Discoverer v1.4 (Thermo Fisher Scientific). Database searches were performed with Mascot (Matrix Science) against the human Uniprot database (2014, 77606 entries) and an in-house contaminant database. The search parameters were: trypsin/P digestion, 2 missed cleavages, 10 ppm mass tolerance for MS, 0.5 Da mass

tolerance for MS/MS, with variable modifications of acetyl (N-terminal), carbamidomethyl (C), N-formylation (protein), oxidation (M), and pyro-glu (N-term Q). Database search results were refined through processing with Percolator (significance threshold < 0.05, FDR < 1%). Protein identification required at least one high-confidence peptide (FDR < 1%) with a minimum score of 20. External contaminants (albumin, casein, trypsin,) were removed from protein lists before further analysis. Keratins were not removed, as they could potentially represent true interactors.

To discriminate specific from non-specific interactions, the identified proteins in each immunoprecipitation (HMGB1 antibody as experiment and IgG antibody as negative control) were analyzed with the Significance Analysis of INTeractome (SAINT) score SAINTexpress (Choi *et al.*, 2012). Results from each experiment were analyzed using their corresponding negative control. Preys with SAINT probability score cut-off of 1 detected by at least two unique peptides were deemed high confidence HMGB1 interacting proteins and further analyzed for biological significance. The mass spectrometry proteomics data have been deposited to the ProteomeXchange Consortium via the PRIDE (Vizcaino *et al.*, 2016).

Small scale immunoprecipitation

SKOV-3 and PC-3 lysates were obtained as described above. 25 µl of beads were coupled with 5 µg of antibody. Antibodies were not crosslinked to protein G-Dynal beads (Invitrogen). Immunoprecipitations were carried out with Abcam antibodies to THOC5 (ab86070), THOC2 (ab129485), Rab11 (ab3612), and Millipore Normal Rabbit IgG Polyclonal (12-360) was used as the negative control. 1 mg of total protein was used for each

immunoprecipitation. Proteins were eluted by incubation in 1× LDS loading buffer (Life Technologies) containing 350 mM beta-mercaptoethanol at 95 ºC for 10 min.

Subcellular fractionation

Confluent SKOV-3 and PC-3 cells were pelleted down by centrifugation at 1000 rpm for 5 (Centrifuge 5804R, A-4-44 rotor, Eppendorf) min and cell fractionation was performed immediately. Each pellet was resuspended in Lysis Buffer (10 mM Tris-HCl pH 8.0, 10 mM NaCl, 1.5 mM $MgCl_2$, 0.05% NP-40) supplemented with Halt™Protease and Phosphatase Inhibitor Single-Use Cocktail (Thermo Scientific) and 1mM DTT just prior to use, and incubated 10 min on ice. The lysate was then added carefully onto an equal volume of sucrose cushion (10 mM Tris-HCl pH 8.0, 10 mM NaCl, 1.5 mM $MgCl_2$, 1 mM DTT, 0.05% NP-40, 1.2 M sucrose, Halt™Protease and Phosphatase Inhibitor Single-Use Cocktail (Thermo Scientific) and centrifuged at 4000 rpm (Centrifuge 5804R, A-4-44 rotor, Eppendorf) for 10 min at 4 ºC. After centrifugation, the supernatant containing the cytoplasmic fraction was transferred to a clean tube. The nuclear pellet was resuspended in Nuclear Extraction Buffer (50mM Tris-HCl pH 8.0, 450 mM NaCl, 1.5 mM $MgCl_2$, 0. 2% NP-40, 10% glycerol) supplemented with Halt™Protease and Phosphatase Inhibitor Single-Use Cocktail (Thermo Scientific) and 1mM DTT just prior to use, and incubated with rotation for 30 minutes at 4 ºC. If the lysate was going to be used for immunoprecipitation 1.5:1000 (v/v) Benzonase®Nuclease (Sigma-Aldrich) was added to the Nuclear Extraction Buffer to eliminate nucleic acids. After the incubation, the nuclear lysates were centrifuged at 13000 rpm (Centrifuge 5804R, FA-45-30-11 rotor, Eppendorf) at 4 ºC for 10 minutes.

The supernatant (soluble nuclear fraction) was transferred to a new tube and the pellet (chromatin and membrane debris) was also stored. To analyze protein localization, lysis buffer was added to the different cellular fractions to equalize the volumes. Subcellular fractions were also used for HMGB1 immunoprecipitation as described above.

Western blot analysis

Protein samples were run on NuPAGE™ 4-12% Bis-Tris Protein Gels (Novex, Thermo Fisher Scientific) for 50 minutes at 200 V and transferred onto a nitrocellulose or PVDF membrane at 30V for 1 hour. Membranes were blocked with PBS-0.1% Tween-20 (PBST) (137 mM NaCl, 2,7 mM KCl, 10mM Na_2HPO_4, 2 mM KH_2PO_4, 0,1% Tween-20) containing 5% non-fat milk for 1 hour at room temperature or at 4 ºC overnight. Membranes were then incubated with the primary antibody: anti-GAPDH (Santa Cruz Biotechnology sc-25778, 1/2000), anti-Rbbp4 (Abcam ab1765, 1/4000), anti-Histone3-Lys14acetylated (Millipore 07-353, 1/2000), anti-THOC5 (Abcam ab86070, 1/1000), anti-THOC2 (Abcam ab129485, 1/1000), anti-SEPT7 (Abcam ab186021, 1/1000), anti-SEPT2 (Abcam ab18020, 1/1000) for 1 hour at RT or with anti-HMGB1 (Santa Cruz Biotechnology sc-74085, 1/1000) and anti-Rab11 (Abcam ab3612, 1/1000), at 4 ºC overnight. After washing with PBST, membranes were probed with the corresponding horseradish peroxidase-conjugated secondary antibodies: anti-protein G, HRP conjugate (Millipore, 18-161, 1/5000) or anti-rabbit HRP (1/2000). After washing the membranes with PBST, chemiluminescence analysis was performed using Amershan™ECL™Prime Western Blotting Detection reagents according to the manufacturer´s instructions. X-ray films or Bio-Rad ChemiDoc™ imager were used for chemiluminescence detection.

HMGB1 and RBBP7 constructs and yeast two-hybrid assays

HMGB1 and *RBBP7* genes were amplified from commercial clones using the following primers: 5'-ATCGAATTCCCGGGGATCGGCAAAGGAGATCCTAAGAAGCC-3' and 5'-CTCTGCAGGTCGACATCGTTAATCATCATCATCATCTTCTTCTTC-3' for *HMGB1* and 5'-CCGGAATTCCCGGGGATCGCGAGTAAAGAGATGTTTGAAGATAC-3' and 5'- CTCTGCAGGTCGACATCGTTAAGATCCTTGTCCCTCCAGTTC-3' for *RBBP7*. Once amplified, the genes were cloned in pGAD-C2 and pGBD-C2 vectors (James *et al.*, 1996) respectively. These vectors allow expression of *HMGB1* and *RBBP7* fused to the *Gal4*-AD (Activation domain) or the *Gal4*-BD (DNA binding domain). The expression of the fused genes is controlled by the *ADH1* promoter. For yeast-two hybrid assays both constructs were co-transformed into the two-hybrid host strain PJ69-4A (*MATa trpl-901 leu2-3,112 ura3-52 his3-200 ga14Δ gal80Δ LYS2::GAL1-HIS3 GAL2-ADE2 met2::GAL7-lacZ*) developed by James et al. (1996), which allows the use of three reporter genes induced by Gal4 (*LYSZ::GALI-HIS3, GAL2-ADE2, mt2::GAL7-**lacZ***) that assess protein-protein interactions. Yeast transformants were selected in complete medium CM without Trp and Leu and positive candidates were selected after growing them in CM without His and CM without Ade and testing them for *β*-galactosidase activity.

β-*galactosidase* activity assay

β-*galactosidase* activity was measured following the method developed by Rose and Botstein (Rose and Botstein, 1983) using ONPG as substrate. 150 µl of total protein was mixed with 850 µl of Z Buffer (40 mM Na_2HPO_4, 60 mM NaH_2PO_4, 10 mM KCl, 1 mM $MgSO_4$, 50 mM 2-Mercaptoethanol). After

incubation at 28 ºC for 5 minutes 200 µl of 4 mg/ml ONPG in Z buffer were added. Reaction was stopped by addition of 500 µl 1M Na_2CO_3 when a color change was spotted and reaction time was written down. Absorbance measures were taken at 420 nm. Specific activity was calculated as: (A_{420} x 1,7)/ (0,0045 x protein concentration x extract volume x time). Protein concentration is measured in mg/ml, extract volume in ml and time in minutes. The interaction between the yeast proteins Ixr1 and Swi6 was used as a positive control.

RESULTS

Generation of PC-3 cells expressing a tagged *HMGB1*

In order to broaden the knowledge of HMGB1 interactions we decided to perform double-affinity purifications of a tagged HMGB1. To carry out these experiments HMGB1 was tagged with a modified FTAP, which consists in 3× FLAG epitope and a calmodulin binding peptide (CBP) separated by two TEV cleavage sites (Pardo *et al.*, 2010). This tag was fused in the NH_2 terminus to HMGB1, inverting the order of the tags regarding the one previously published (Pardo *et al.*, 2010), being the CBP in the free NH_2 terminal end (Figure 1A). The modified *HMGB1* construction was cloned in a pDsRed-Monomer-C1 vector (Clontech) where the DsRed-Monomer gene had been previously removed and its expression was under the control of the cytomegalovirus promoter. PC-3 cells were transfected with the modified plasmid and single colonies were isolated to obtain different clones expressing the tagged HMGB1. Expression of the tagged protein was analyzed in 6 different clones by western blotting. As shown in figure 1B, 4 of these clones expressed the

tagged HMGB1 protein, although its expression in one of them was very low.

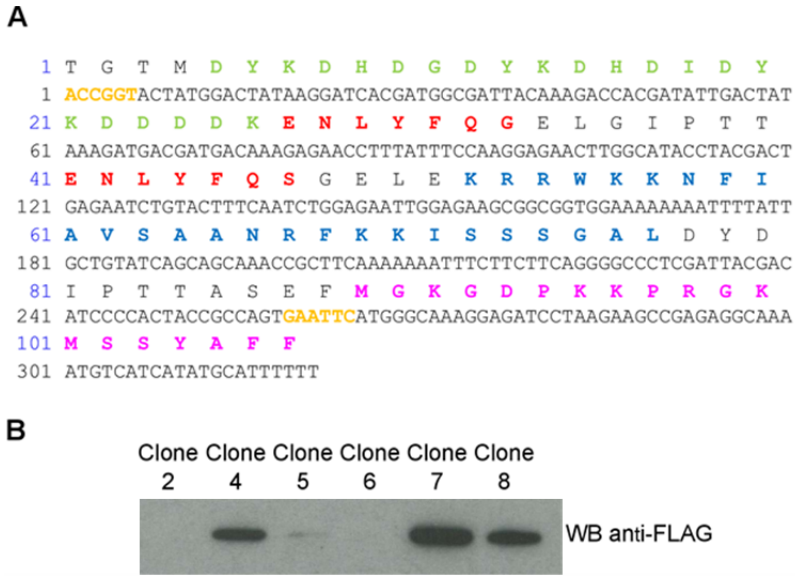

Figure 1. (A) DNA and amino acid sequence of the N-terminal tag of *HMGB1*, 3xFLAG in green, 2xTEV in red, CBP (calmodulin binding peptide) in blue and *HMGB1* N-terminal sequence in pink. Restriction sites for *AgeI* and *SalI* are indicated in yellow. **(B)** Western blot showing tagged-*HMGB1* in 6 different clones using anti-FLAG antibody.

Identification of HMGB1 partners by epitope-tagging affinity purification in PC3 cells

Two different clones expressing the tagged HMGB1, clones 7 and 8, were selected to accomplish the affinity purifications. Although HMGB1 had been tagged with a tandem affinity tag that allows double-affinity purifications, considering that the expression of the tagged protein was not very high we decided to perform single-affinity purifications using the Flag antibody. Three independent purifications were carried out and in each purification HMGB1 was purified from lysates coming from clone 7

and clone 8; FTAP-β-galactosidase PC-3 lysate was used as a negative control. Purifications were carried out as detailed in the materials and methods section. Eluates from the purification were analyzed by mass spectrometry. Surprisingly, the number of proteins identified in each purification was very low. Data from the MS/MS experiments was analyzed using the CRAPome computational tools (www.crapome.org) in order to distinguish between possible HMGB1 partners and unspecific binding proteins, SAINTexpress was run along this analysis so that only proteins with a SP (SAINT Probability of proteins co-purifying with HMGB1) higher than 0.7 were taken into account. Only three proteins with a SP higher than 0.7 were common to both clones (MYLK2, HMGB1, ZCCHC17) in the first purification assay, six (ICT1, RPL39, C1orf35, HMGB1, MYLK2, HMGB3) in the second approach and three (HMGB1, MYLK2 and CALM1) in the last purification. As expected, HMGB1 was found in all the experiments but only one protein purified along with HMGB1 was found in both clones and in the three experiments: Myosin light chain kinase 2 (MYLK2). The low number of HMGB1 interacting proteins identified in these approaches suggested that the epitope added to the amino-terminal region of HMGB1 was interfering the binding with its partners. The strategy to overcome this problem was to use HMGB1 immunoprecipitations of the native untagged protein directly from PC-3 or SKOV-3 cells.

Identification of HMGB1 binding partners in SKOV-3

In order to profile the interactome of HMGB1 in ovarian tumoral cells, three independent immunoprecipitations of HMGB1 coupled to MS-based proteomics were carried out using whole-cell SKOV-3 extracts. Control immunoprecipitations using a rabbit IgG were performed in parallel to

HMGB1 immunoprecipitations. HMGB1 interacting proteins were analyzed by MS/MS. A total of 555 proteins were identified in the three experiments, including HMGB1. SAINTexpress was run along this analysis so that only proteins with a SP higher than 0.7 were taken into account. 109 proteins were over this threshold (Table 1) including HMGB1. When comparing this list with the already known HMGB1 interacting partners covered by the STRING and BioGRID databases four of them, the FACT complex proteins, SSRP1 and SUPT16H, histone H1FX and PARP1 had been already described to interact with HMGB1.

Table 1. HMGB1 interacting partners in SKOV-3 with a SP> 0.7 from three independent experiments.

	First experiment						Second experiment						Third experiment						
	HMGB1 IP			Rb IP			HMGB1 IP			Rb IP			HMGB1 IP			Rb IP			SP
GENE	C	P	S	C	P	S	C	P	S	C	P	S	C	P	S	C	P	S	
CTTN	31,82	13	51				40,00	18	66				42,55	17	91				1
SEPT6	36,64	11	49				31,11	11	28				18,89	8	41				1
POLDIP3	22,33	5	15				34,20	8	16				22,57	6	15	3,09	1	1	1
THOC5	15,81	7	19				15,23	4	11				5,71	2	16				1
ZCCHC8	6,51	3	8				15,13	5	14				8,06	3	6				1
SNRNP200	24,86	38	105				15,68	16	38				6,84	8	27				1
ASCC3	4,59	6	11				8,81	10	21				2,45	4	7				1
TRIM28	16,05	7	20	5,39	2	2	21,68	9	22				15,45	6	17	3,71	1	1	1
ACACA	1,45	2	3				4,09	5	9				4,82	7	14				1
GRAMD3	33,10	9	57				52,08	18	83				46,99	15	79				1
RBBP6	6,53	7	20				8,48	9	20				6,92	7	14				1
RPS15	55,86	5	65	36,55	3	22	58,62	6	97	36,55	3	14	39,31	4	71	23,45	2	27	1
EIF4A3	42,82	15	61	16,55	5	14	38,93	15	41				29,93	10	81				1
TCOF1	12,97	15	40				8,27	7	14				3,29	3	10				1
SNRPD1	27,73	2	13	16,81	1	1	27,73	2	10				16,81	1	6				1
MATR3	14,76	8	32	1,77	1	2	25,15	11	46	2,95	1	2	26,33	11	63	5,43	2	5	1
THOC2	7,28	9	22				2,64	3	4				2,45	3	9				1

Table 1. Continuation

	First experiment						Second experiment						Third experiment						SP
	HMGB1 IP			Rb IP			HMGB1 IP			Rb IP			HMGB1 IP			Rb IP			
GENE	**C**	**P**	**S**	**C**	**P**	**S**	**C**	**P**	**S**	**C**	**P**	**S**	**C**	**P**	**S**	**C**	**P**	**S**	
PRPF4B	5,66	4	10				9,63	7	21				5,46	3	3				1
PRPF4B	5,66	4	10				9,63	7	21				5,46	3	3				1
SEPT7	41,88	14	81				49,43	23	165				45,31	21	245				1
YTHDC1	13,34	6	18				5,36	3	12				6,19	4	5				1
SART1	18,00	9	17				25,50	15	32	1,13	1	2	19,63	12	37	1,13	1	2	1
HDLBP	5,91	5	11				4,65	3	5				5,36	4	7				1
ZNF512B	16,59	10	22				11,21	7	13				3,59	2	7				1
SRRT	7,08	4	10				13,81	6	21				16,78	6	12				1
PAF1	6,97	3	5	2,45	1	1	13,75	5	12				11,86	4	11				1
SRSF10	23,28	5	22				23,66	6	17				10,69	2	9				1
BCLAF1	19,13	16	67	5,43	5	11	24,67	19	75				15,00	11	50				1
HP1BP3	10,31	5	24	6,33	2	4	17,36	8	35				17,54	6	17	6,87	3	5	1
RPS10	23,64	4	32	14,55	3	9	46,67	10	51	15,15	2	7	29,70	4	35	20,00	3	11	1
HMGB1	**22,33**	**6**	**39**				**27,44**	**11**	**75**				**33,49**	**14**	**189**				**1**
RPS25	24,00	4	23	24,00	3	8	29,60	5	20	20,00	3	4	31,20	5	20	16,00	2	5	1
MAGOH	36,99	4	8				43,15	5	8				21,23	3	6				1
SEPT11	39,39	14	58				31,70	16	53				19,81	10	58				1

Table 1. Continuation

	First experiment						Second experiment						Third experiment						SP
	HMGB1 IP			Rb IP			HMGB1 IP			Rb IP			HMGB1 IP			Rb IP			
GENE	C	P	S	C	P	S	C	P	S	C	P	S	C	P	S	C	P	S	
SEPT10	33,48	9	35				37,22	13	41				27,97	10	40				1
AHNAK	33,96	78	192				24,89	51	129				29,39	62	231				1
RBMX	19,95	6	60	19,95	6	16	41,18	16	71	11,00	3	6	30,69	11	56	22,51	6	18	1
MSL1	10,42	3	4				4,40	1	3				6,35	2	9				1
MVP	14,89	6	10				16,13	6	12				12,43	4	17	3,25	1	2	1
PNN	12,13	7	35	4,18	2	7	16,46	9	30				16,32	11	45				1
SEPT5	5,15	1	3				5,96	1	3				5,96	1	4				1
THRAP3	19,06	15	102	5,55	4	13	23,35	20	95	1,99	1	2	17,80	14	82	6,81	4	10	1
CDC73	14,69	6	11				7,53	3	7				11,86	5	10				1
HNRNPUL2	1,87	1	3				10,44	4	10				1,87	1	3				1
HNRNPA3	20,90	5	17				15,34	3	6				10,05	2	3				1
THOC1	14,61	6	20				14,92	6	19				18,72	8	21				1
SEPT8	36,02	11	38				38,10	15	55				25,05	10	51				1
RPS7	38,66	4	10				43,30	6	24	5,67	1	2	26,29	6	49	11,86	1	1	1
SEPT9	36,18	16	109				62,63	37	187				68,94	50	504				1
SKIV2L2	8,35	5	11				10,84	8	14				8,83	5	7				1
LARP1	2,37	2	3				14,05	6	16				13,23	6	15				1

Table 1. Continuation

	First experiment						Second experiment						Third experiment						SP
	HMGB1 IP			Rb IP			HMGB1 IP			Rb IP			HMGB1 IP			Rb IP			
GENE	C	P	S	C	P	S	C	P	S	C	P	S	C	P	S	C	P	S	
SEPT2	51,52	12	83				71,19	26	177				63,16	23	315				1
ASCC2	4,76	2	3				8,32	4	14				3,83	1	5				1
GRAMD1A	12,43	5	11				24,31	10	27				20,30	10	39				1
MAGOHB	37,16	4	7				37,16	4	7				15,54	2	4				1
RBM7	6,77	1	3				13,91	2	7				22,93	4	7				1
RNPS1	20,33	4	18	4,92	1	3	25,57	6	38				16,72	5	21	7,54	2	3	1
TRA2A	20,57	3	8				4,96	1	3				8,16	2	4				1
BCAS2	41,78	6	17				23,56	2	4				12,44	1	4				1
POGZ	5,82	5	10	1,06	1	1	9,50	7	15				2,48	2	4				1
LUZP1	10,59	8	13				24,81	18	31				15,61	10	26				1
RASAL2	12,82	10	30				15,36	9	21				10,80	7	53				1
IWS1	5,25	3	7				6,72	3	8				4,03	2	4				1
PARP1	34,32	27	91	14,69	11	19	27,22	18	58	5,72	4	6	20,32	16	62	12,62	9	19	1
MISP	9,57	4	9				21,21	7	13				13,40	5	9				1
THOC6	8,80	2	6				10,26	2	8				14,37	3	7				1
SUGP2	8,69	7	15				17,65	7	15				5,36	3	7				1
PRPF8	24,67	37	120	1,28	2	2	15,20	17	52				6,08	7	11				1

Table 1. Continuation

	First experiment						Second experiment						Third experiment						SP
	HMGB1 IP			Rb IP			HMGB1 IP			Rb IP			HMGB1 IP			Rb IP			
GENE	C	P	S	C	P	S	C	P	S	C	P	S	C	P	S	C	P	S	
RPLP1	74,56	3	8	14,04	1	3	94,74	4	18				66,67	3	12	14,91	1	1	0,99
PRRC2C	0,97	2	2				6,35	6	9				5,80	8	20				0,99
ZNF326	2,75	1	3				2,75	1	3				2,75	1	2				0,99
MSL2	5,20	2	4				9,01	3	4				2,95	1	2				0,99
RBM39	4,91	2	4				11,89	4	9				2,83	1	2				0,99
RALY	9,80	2	5				21,57	4	11				3,92	1	2				0,99
SNW1	27,99	9	27	4,66	1	1	4,66	1	3				7,28	2	4				0,99
RBBP4	11,29	3	8				3,29	1	2				3,29	1	4				0,99
CCNL2	11,54	2	3				4,04	1	2				4,04	1	2				0,99
EFTUD2	29,63	18	49	1,34	1	2	19,24	10	19				3,91	2	5				0,99
SUPT16H	15,19	12	31	6,59	6	10	14,33	10	25				15,28	11	33	7,26	4	7	0,99
RPS29	33,93	2	10	33,93	2	3	33,93	2	13	14,29	1	2	33,93	2	20	33,93	2	4	0,99
PRPF38A	15,71	3	11				6,73	1	4				3,85	1	2				0,99
RBBP7	4,94	2	4				3,06	1	2				3,06	1	2				0,99
ZC3H18	5,88	3	10	4,51	2	4	8,29	6	15				13,12	9	19				0,99
SRRM2	15,92	28	88	4,98	9	18	11,88	21	47				8,25	16	34				0,99
HNRNPM	16,30	7	16	2,19	1	2	25,07	9	30				12,47	5	14	8,36	3	6	0,98

Table 1. Continuation

	First experiment						Second experiment						Third experiment						SP
	HMGB1 IP			Rb IP			HMGB1 IP			Rb IP			HMGB1 IP			Rb IP			
GENE	C	P	S	C	P	S	C	P	S	C	P	S	C	P	S	C	P	S	
RPL9	34,38	5	22	15,63	2	6	45,83	8	28				22,40	3	63	35,42	5	10	0,98
SERBP1	13,73	5	9				12,50	3	5				9,07	3	8	5,15	1	2	0,98
ACIN1	16,93	17	54	9,77	9	19	19,16	19	54				12,83	13	26				0,97
RPSA	26,78	5	13	10,51	3	6	41,36	7	21				28,14	5	13	5,42	1	2	0,97
SRSF7	23,53	6	23	18,49	4	6	19,75	3	13				15,97	2	10				0,97
SRSF9	27,15	6	11	9,50	2	2	33,48	6	16				10,86	2	4				0,97
NAP1L1	7,42	2	10				4,60	1	6				13,81	3	11	4,60	1	3	0,97
RBM8A	25,86	3	15	19,54	2	5	55,17	6	26				10,92	1	7				0,96
HSPA5	12,54	6	13	2,45	1	3	6,57	3	5				10,40	5	7				0,95
SRSF3	23,17	3	14	8,54	1	2	28,66	3	24				12,80	1	3				0,95
RPS27A	16,03	2	10	10,26	1	2	7,69	1	10				17,95	2	10	23,72	3	5	0,94
FYTTD1	27,67	8	17	6,60	2	4	19,81	5	6				10,69	3	7				0,94
SRSF6	12,50	4	7	2,62	1	2	9,01	3	6				2,62	1	3				0,94
H1FX	18,78	3	7				14,08	2	5				18,78	3	10	13,15	2	4	0,92
HNRNPL	7,64	2	12				4,92	1	5				4,92	1	6	4,92	1	4	0,91
SRSF4	4,25	2	6	1,82	1	2	1,82	1	3				1,82	1	3				0,89
SRSF5	12,50	3	5	3,31	1	2	3,31	1	3				3,31	1	3				0,88

Table 1. Continuation

	First experiment						Second experiment						Third experiment						SP
	HMGB1 IP			Rb IP			HMGB1 IP			Rb IP			HMGB1 IP			Rb IP			
GENE	**C**	**P**	**S**	**C**	**P**	**S**	**C**	**P**	**S**	**C**	**P**	**S**	**C**	**P**	**S**	**C**	**P**	**S**	
TRA2B	19,79	5	50	12,85	3	5	22,57	8	32				12,50	3	4				0,86
RPS15A	23,85	3	7	6,15	1	1	59,23	8	40	6,15	1	1	43,85	7	41	21,54	3	6	0,84
RSL1D1	2,45	1	2				26,94	11	33				22,04	7	13	9,18	3	3	0,83
SAFB	13,11	8	23	7,32	3	8	6,78	3	7				10,27	4	11				0,83
HNRNPH1	14,25	4	11				11,14	3	5				3,79	1	3	3,79	1	4	0,79
RPS17L	40,74	4	28	32,59	2	6	56,30	8	41	23,70	2	8	63,70	10	80	46,67	5	16	0,75
SQSTM1	13,18	3	11	4,77	1	3	14,32	3	9				5,91	1	3	5,91	1	2	0,73
SSRP1	16,08	9	26	4,09	3	6	5,08	2	6				7,62	4	16	5,36	2	3	0,71

C: coverage; **P**: peptides; **S**: spectra

The novel HMGB1 binding partners discovered in our study were analyzed for GO term enrichment. Results show that the biological processes with the lowest false discovery rates (FDR) are mainly related to RNA. Half of the HMGB1 binding proteins found in these studies (55 out of 108) are included within the mRNA metabolic process pathway (GO:0016071); 42 are associated to RNA splicing (GO:0008380), 30 are included in mRNA splicing, via spliceosome (GO:0000398) and 22 are involved in mRNA transport (GO:0051028). Analysis of the molecular function shows similar results Poly (A) RNA binding (GO:0044822) and RNA binding (GO:0003723) have the lowest false discovery rates, each group including 68 and 73 proteins respectively. When analyzing the cellular component, 88 are associated to the nucleus (GO:0005634). When the proteins are clustered in cellular complexes (Figure 2) 21 of them belong to the spliceosomal complex (GO:0005681), 11 proteins form part of the small ribosomal subunit (GO:0044391), 4 proteins belong to the THO complex, which is part of the transcript export complex (GO:0000445). Finally, 22 proteins cluster in different groups which are associated to the nucleolus (GO:0005730).

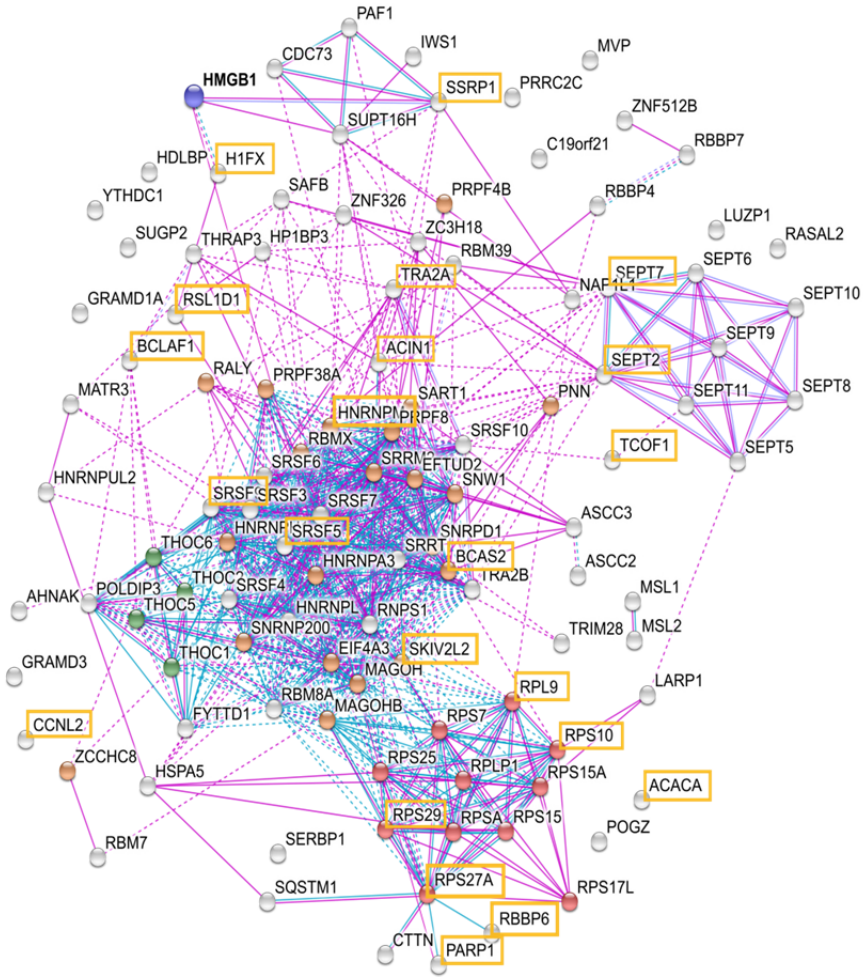

Figure 2. HMGB1 network in SKOV-3 cells found by immunoprecipitation assays. HMGB1 interacting proteins identified in three independent immunoprecipitations and with a Saint probability score (SP) higher than 0.7 were analyzed with STRING. Previously described interactions (in experiments or databases) are shown with purple and blue lines. Proteins are clustered based on their function. Red nodes represent proteins from the small ribosomal subunit, green nodes are members of the THO complex, orange nodes are proteins from the spliceosomal complex and orange boxes mark proteins related to the nucleolus. HMGB1 is highlighted as a bigger blue node.

Identification of HMGB1 binding partners in PC-3

Following the same criteria and methods already outlined for SKOV-3, the interactome of HMGB1 in the PC-3 cell line was determined. After selection of the specific HMGB1 partners 49 proteins were identified with a SAINT score over 0.7 (Table2). None of the proteins found in these experiments were previously known to interact with HMGB1 in public databases.

When analyzing GO enrichment for the biological processes, molecular function and cellular component, it is obvious that most of the proteins found in this study are related to RNA metabolism. Considering biological processes, 25 proteins are included within RNA metabolic process (GO:0016070) and gene expression (GO:0010467). Results of molecular function enrichment show similar outcome being the RNA binding term (GO:0003723) the one with the lowest FDR. Analyzing the cellular component enrichment also gives a general idea of the different complexes in which the identified proteins are included. As displayed in Figure 3, 11 proteins belong to the catalytic step 2 spliceosome (GO:0071013), 5 are included in the transcript export complex (GO:0000346) and at the same time 4 of them are included in the THO complex (GO:0000445). In addition, 14 proteins are related to cytoskeleton (GO:0005856) and 9 are related to the nucleolus (GO:0005730).

Table 2. HMGB1 interacting partners in PC-3 with a SP> 0.7 from three independent experiments.

	First experiment						Second experiment						Third experiment						SP
	HMGB1 IP			Rb IP			HMGB1 IP			Rb IP			HMGB1 IP			Rb IP			
GENE	C	P	S	C	P	S	C	P	S	C	P	S	C	P	S	C	P	S	
CTTN	40,91	19	79			0	32,36	14	54			0	52,36	18	64			0	1
SEPT6	33,41	11	33			0	30,41	11	42			0	26,50	8	32			0	1
SEPT9	57,51	37	272			0	35,67	18	112			0	82,94	51	307			0	1
THOC5	14,06	4	13			0	12,45	5	20			0	17,13	5	21			0	1
ZCCHC8	8,06	3	11			0	9,62	4	12			0	5,66	3	5			0	1
SNRNP200	7,07	7	25			0	12,22	14	34	0,70	1	1	2,34	3	7			0	1
ACACA	6,35	9	18			0	2,00	3	5			0	7,76	9	18			0	1
GRAMD3	22,22	9	26			0	25,69	6	16			0	21,30	6	18			0	1
RBBP6	2,90	4	8			0	4,85	5	9			0	3,24	3	4			0	1
TCOF1	3,90	4	9			0	5,65	6	13			0	8,74	8	14			0	1
RAB11A	25,46	4	15			0	27,31	3	7			0	40,74	6	25			0	1
MATR3	19,72	9	23	2,95	1	3	10,27	5	16			0	17,12	6	13			0	1
THOC2	4,46	6	15			0	5,27	6	20			0	6,84	5	14			0	1
SEPT7	41,42	23	214			0	45,54	13	66			0	51,72	22	123			0	1
ZNF512B	14,13	8	18			0	16,59	9	17			0	11,43	7	12			0	1
RAB11FIP5	17,15	5	19			0	19,14	6	19			0	37,98	13	33			0	1
PLIN4	25,72	19	64			0	21,81	15	47			0	25,42	15	42			0	1

Table 2. Continuation

	First experiment						Second experiment						Third experiment						SP
	HMGB1 IP			Rb IP			HMGB1 IP			Rb IP			HMGB1 IP			Rb IP			
GENE	C	P	S	C	P	S	C	P	S	C	P	S	C	P	S	C	P	S	
GRAMD1B	26,96	12	44			0	19,78	12	45			0	13,28	5	15			0	1
HMGB1	27,44	10	71			0	22,33	6	40			0	43,72	10	63			0	1
EFTUD2	11,93	5	9			0	12,86	9	25			0	10,49	3	6			0	1
C10orf2	27,19	14	65			0	29,97	12	49			0	42,40	19	75			0	1
SEPT11	28,90	15	44			0	29,84	10	40			0	31,00	14	37			0	1
SEPT10	39,43	18	87			0	24,89	7	36			0	52,64	21	65			0	1
AHNAK	8,73	11	27			0	6,69	5	10			0	12,51	15	28			0	1
MSL1	7,82	2	4			0	2,77	1	3			0	6,84	2	4			0	1
SEPT5	13,01	3	6			0	8,94	2	3			0	5,96	1	3			0	1
CEP55	12,93	4	8			0	10,99	4	10			0	11,21	2	5			0	1
THOC1	26,94	12	34			0	14,76	7	15			0	27,25	9	26			0	1
SEPT8	27,12	9	25			0	10,97	4	6			0	20,91	7	17			0	1
SNRNP40	22,97	4	5			0	11,20	2	4			0	10,92	1	5			0	1
SEPT2	66,76	25	247			0	41,27	10	68			0	69,25	22	151			0	1
GRAMD1A	8,84	4	12			0	14,92	6	10			0	6,22	3	7			0	1
SYF2	11,93	1	5			0	11,52	1	3			0	11,93	1	4			0	1
THOC6	14,66	3	9			0	13,49	3	7			0	11,14	2	5			0	1
CLK3	3,13	1	3			0	4,23	2	4			0	3,13	1	3			0	1

Table 2. Continuation

	First experiment						Second experiment						Third experiment						SP
	HMGB1 IP			Rb IP			HMGB1 IP			Rb IP			HMGB1 IP			Rb IP			
GENE	C	P	S	C	P	S	C	P	S	C	P	S	C	P	S	C	P	S	
PRPF4B	8,54	6	20	2,18	1	1	6,95	5	11	2,18	1	3	3,77	2	9			0	0.99
PRPF8	10,02	11	28	2,06	2	2	8,99	11	32	1,88	2	4	2,78	3	12			0	0.99
C1QBP	10,64	1	5			0	19,86	2	3			0	10,64	1	2			0	0.98
PRRC2A	2,50	2	3			0	2,41	3	4			0	1,44	1	2			0	0.98
SRRM2	7,99	14	29	3,05	6	11	8,10	14	32	3,56	7	10	8,98	14	29	3,20	5	9	0.98
SART1	17,00	10	18	1,13	1	2	10,25	5	8	1,13	1	3	10,63	5	9	1,13	1	1	0.97
RBBP7	3,06	1	2			0	12,24	3	5			0	3,06	1	2			0	0.97
SRRT	20,09	8	22	9,59	3	6	13,93	8	32	6,39	3	10	19,52	9	23	10,16	4	7	0.96
SF3B1	11,89	7	13			0	7,98	5	10	3,07	2	2	3,91	2	4			0	0.94
NCBP1	4,68	3	5			0	4,05	2	6	2,66	1	2	2,66	1	4			0	0.89
CHTOP	11,69	2	9	11,69	2	5	12,10	3	12			0	16,94	3	7			0	0.85
SKIV2L2	6,33	4	4			0	8,54	5	14	1,92	1	3	5,47	3	6			0	0.84
BCLAF1	17,07	14	51	7,61	4	7	15,33	11	36	6,63	5	14	15,11	11	26	4,78	3	5	0.81
YTHDC1	9,63	4	7	3,30	2	2	3,44	2	6			0	3,99	2	2			0	0.79
RBBP4	3,29	1	3	3,29	1	2	12,71	3	4			0	3,29	1	3			0	0.71

C: coverage; **P**: peptides; **S**: spectra

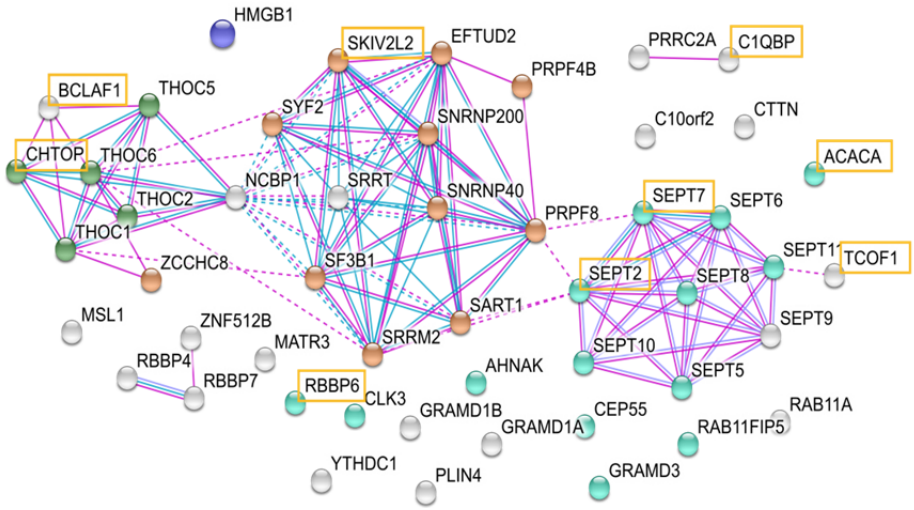

Figure 3. HMGB1 network in PC-3 cells found by immunoprecipitation assays. HMGB1 interacting proteins identified in three independent HMGB1 immunoprecipitations and with a Saint probability score (SP) higher than 0.7 were analyzed with STRING. Previously described interactions (in experiments or databases) are shown with purple and blue lines. Proteins are clustered based on their function. Light blue nodes represent proteins related to the cytoskeleton, green nodes are members of the THO complex, orange nodes are proteins from the spliceosomal complex and orange boxes mark proteins related to the nucleolus. HMGB1 is highlighted as a bigger blue node.

Comparison of HMGB1 binding partners in SKOV-3 and PC-3

As PC-3 and SKOV-3 are both cancerous cell lines from epithelial origin it would be fair to expect that, when comparing the results obtained, common HMGB1 partners should be found. As described above, the obtained number of HMGB1 interacting proteins in SKOV-3 cell line was two-fold higher than in PC-3. Both lists were compared and 35 proteins were found in both cell lines, 73 proteins were only detected in SKOV-3 and 14 proteins only appeared in the experiments carried out using PC-3 lysates.

Proteins found in all the immunoprecipitation experiments are presented in Figure 4. The fact that these proteins immunoprecipitated in six independent replica in two different cell lines increases their probability of being HMGB1 specific interacting partners. Among these proteins are the THO complex proteins, THOC1, THOC2, THOC5 and THOC6, key proteins for mRNA transcription, processing and export; spliceosome proteins SKIV2L2, SNRNP200, SART1, PRPF8, PRPF4B, EFTUD2, SRRM2, YTHDC1 and ZCCHC8; cytoskeleton reorganization proteins, SEPT10, SEPT7, SEPT2, SEPT6, SEPT11, SEPT5, SEPT9 and SEPT8; and proteins RBBP4 and RBBP7 from the NuRD complex, a chromatin remodeling complex that regulates cancer biology (Lai and Wade, 2011).

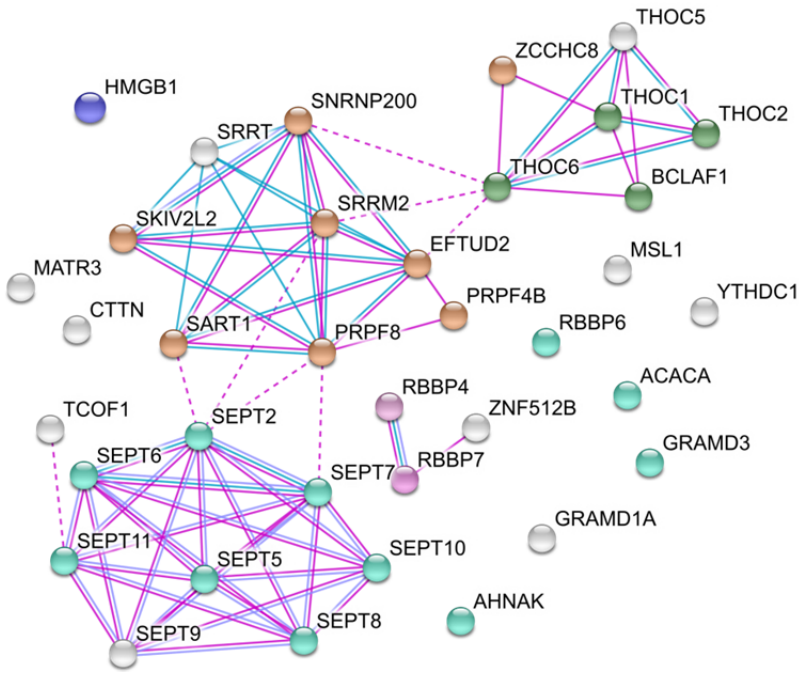

Figure 4. Common HMGB1 interactors in SKOV-3 and PC-3 cells. In blue, proteins related to the cytoskeleton; in orange, spliceosome proteins; in green, THO complex proteins and in purple, NuRD complex proteins. Previously described interactions are depicted with lines.

One of most obvious differences between the results obtained with SKOV-3 and PC-3 cells, is that the ribosomal proteins are only present in the SKOV-3 data set. Although proteins that play a role in RNA metabolic processes are found in the six experiments, a higher number of proteins associated to RNA processing, mainly related to splicing, are found in SKOV3.

HMGB1 localization in ovarian and prostate cancer cells

HMGB1 is mainly localized in the nucleus of normal cells but it has been demonstrated that this protein is also found in the cytoplasm and in the extracellular milieu of immune cells (Tang *et al.*, 2016) where it carries out important roles. In order to evaluate HMGB1 localization in PC-3 and SKOV-3 cell lines a subcellular fractionation approach was performed as explained in the materials and methods section. The localization of RBBP4 and Nucleolin, two proteins mainly located in the nucleus, Histone 3, a chromatin binding protein, and the cytoplasmic protein GAPDH were evaluated simultaneously to HMGB1 to verify the correct nucleus-cytoplasm fractionation.

According to western blot results, HMGB1 has a predominant cytoplasmic localization, being almost undetectable in the nuclear fraction and in the pellet obtained from PC-3 and SKOV-3 cell lines (Figure 5). Even though this result could seem contradictory to previous knowledge (Gatla *et al.*, 2014), control proteins are localized in the expected fraction validating the cell fractionation procedure. This experiment was repeated 4 times obtaining the same outcome thus reinforcing the obtained results. Data

obtained by immunoprecipitation from the nuclear and the cytoplasmic fractions separately and identification by mass spectrometry analysis show that the protein is also present in the nucleus. If the number of spectra found for this protein is considered as an indirect measure of the relative amount of protein in the two fractions, HMGB1 immunoprecipitated in the nucleus is much lower (four times lower in PC-3 and 14 times lower in SKOV-3 cells) than in the cytoplasm of these cells (Supplementary tables 1, 2, 3 and 4).

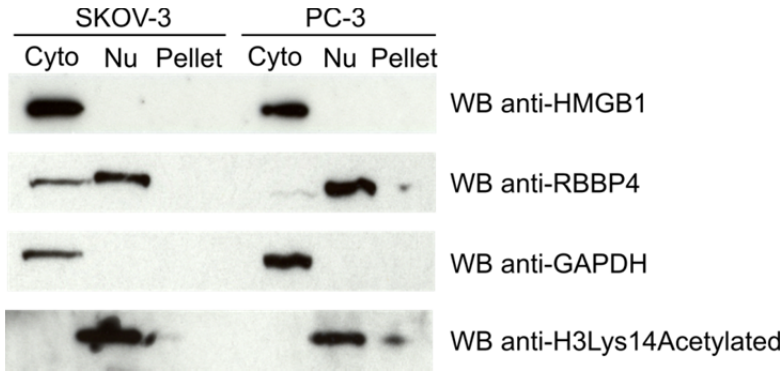

Figure 5. SKOV-3 and PC-3 subcellular fractionation. Equivalent amounts of cytoplasmic (Cyto) or nuclear (Nu) extracts prepared from SKOV-3 and PC-3 were analyzed by western blot (WB). HMGB1 subcellular localization was studied using an anti-HMGB1 antibody. Anti-GAPDH was used as a marker of the cytoplasm and anti-RBBP4 and anti-H3Lys14Acetilated were used as nuclear markers.

It is also important to highlight that in the cell lines used in this study p53 is not functional (Isaacs *et al.*, 1991; Vikhanskaya *et al.*, 1994) and it has been reported that absence of p53 induces translocation of HMGB1 to the cytoplasm (Livesey *et al.*, 2012). Therefore the possibility that the antibody fails to detect very low levels of HMGB1 in the nucleus should not be dismissed either. Strikingly, in the previous chapter and using confocal microscopy, a predominant localization of HMGB1 in the nucleus was

observed in the prostate cancer cells PC-3. Discrepancies in relative distribution between nucleus and cytoplasm using different approaches may be due to technical commitments, which may be detecting diverse isoforms or posttranslational modifications of HMGB1 with different sensitivity. The presence of HMGB1 in both compartments is functional (Tang *et al.*, 2010) and nucleo-cytoplasmic shuttling of HMGB1 conditioned by external stimuli and redox state has been observed in different cells (Bonaldi *et al.*, 2003; Hoppe *et al.*, 2006; Ito *et al.*, 2007; Stros, 2010).

HMGB1 interacting partners in nucleus and cytoplasm in SKOV-3 and PC-3

While performing immunoprecipitation of HMGB1 from total lysates brings to light new HMGB1 interacting partners, it is also interesting to locate such interactions within the cell. Immunoprecipitation of HMGB1 coupled to cell fractionation not only allows to map such interactions in the cellular compartments but also enables to detect a higher number of HMGB1 interacting partners as nucleus and cytoplasm are analyzed separately.

Following the procedure explained in the materials and methods section nuclear and cytoplasmic fractions were isolated from SKOV-3 and PC-3 cell lines and used for HMGB1 immunoprecipitation. HMGB1 interacting proteins were identified through MS/MS analysis. Supplementary tables 1, 2, 3 and 4 list the proteins with a SAINT (probability) score higher than 0.7 after analyzing the data in CRAPome (www.crapome.org). From this data, 76 and 117 proteins were specifically identified in the cytoplasmic fraction of PC-3 and SKOV-3 respectively; a higher number of proteins were

identified in the nuclear fraction, 117 and 306, in PC-3 and SKOV-3 respectively.

Firstly, a search for HMGB1 already known partners was made using STRING and BioGRID. A total of 21 of the identified proteins had already been described as HMGB1 interacting proteins (Table 3).

Table 3. Already described HMGB1 interactions identified in our HMGB1 immunoprecipitations in PC-3 and SKOV-3 cells

PC3		SKOV3	
NUCLEUS	**CYTOPLASM**	**NUCLEUS**	**CYTOPLASM**
HMGA1	HNRNPK	H3F3	CAPZA1
H3F3A		HSPA8	HSPA8
HSPA8		LRIF1	
PARP1		PARP1	
SSRP1		SP100	
SUPT16H		SSRP1	
H1F0		SUPT16H	
H1FX		ACTB	
H2AFZ		H1FX	
HIST1H1C		H2AFZ	
HIST1H1D		HIST1H1A	
HIST1H1E		HIST1H1B	
		HIST1H1E	
		POLR2A	

Only three of these interactions were found in the cytoplasmic fractions, HNRNPK, Heterogeneous nuclear ribonucleoprotein K, involved in chromatin remodeling and RNA processing that is a cofactor of p53, another protein interacting with HMGB1 (Moumen *et al.*, 2005); CAPZA1, a F-acting-capping protein and the chaperone HSPA8 which was also

identified in the cytoplasmic fraction of PC-3 cells. Nuclear HMGB1 already known interactions include SSRP1, SUPT16H and PARP1 which had also been identified in the previous SKOV-3 HMGB1 immunoprecipitations; not surprisingly half of the interacting nuclear partners are histones: H3F3, H3F3A, H2AFZ, H1FX, HIST1H1A, HIST1H1B, HIST1H1E, H1F0, HIST1H1C, HIST1H1D. Also included in this fraction are Polymerase POLR2A, tumor suppressor SP100, replication/repair protein LRIF1, actin ACTB and a member of the HMG superfamily, HMGA.

For further analysis SKOV-3 and PC-3 cell fractionation immunoprecipitation results were separately compared to those from SKOV-3 and PC-3 total lysate HMGB1 immunoprecipitations.

- SKOV-3 cell fractionation

After doing the intersection between the results from HMGB1 immunoprecipitations in SKOV-3 total lysates and the proteins identified in the cell fractionations, 23 proteins from total lysate HMGB1 immunoprecipitation were found in the cytoplasmic fraction (Figure 6A). This list includes 6 proteins from the small ribosomal subunit, several proteins related to cytoskeleton such as 8 proteins of the septin family and CTTN, MVP a major protein in the vault particle, the Ras pathway protein RASAL2 and the giant protein AHNAK. In the cytoplasmic fraction 94 more proteins immunoprecipitated with HMGB1 but were not present within the proteins found in the total lysates immunoprecipitations, more than a half are ribosomal proteins from either the small or the large subunit.

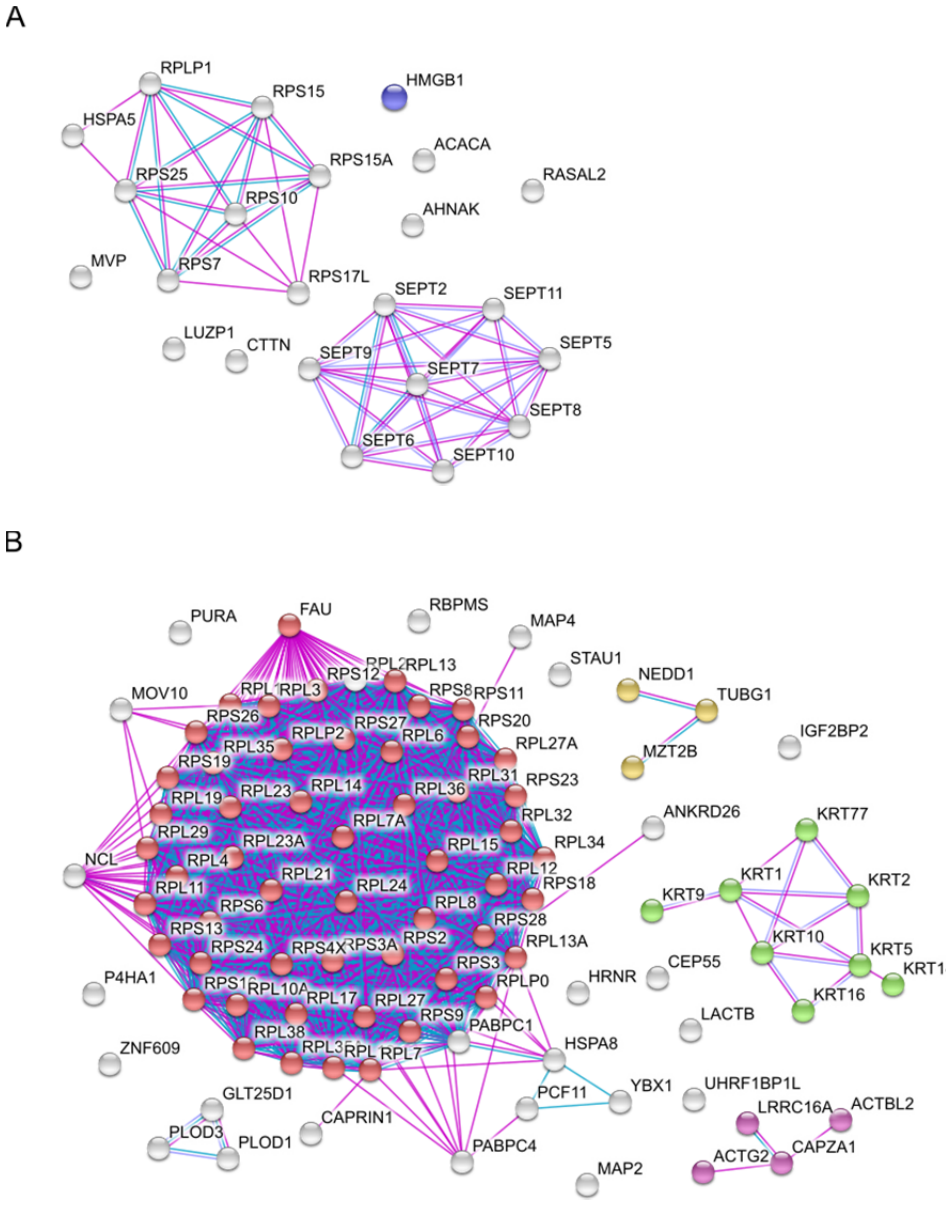

Figure 6. HMGB1 immunoprecipitation in SKOV-3 cytoplasmic fraction. (A) HMGB1 interacting proteins identified both in the cytoplasmic fraction of SKOV-3 cells and in whole SKOV-3 lysates **(B)** HMGB1 interacting proteins identified only in SKOV-3 cytoplasmic fraction and not in whole lysates. In red, ribosomal proteins; in green, keratins; in yellow microtubule organization proteins; in purple, actin polymerization proteins and HMGB1 is highlighted in dark blue.

Several clusters of proteins related to cytoskeleton were also identified in this fraction including a subset of 8 keratins (KRT1, KRT10, KRT14, KRT16, KRT2, KRT5, KRT77, KRT9), microtubule organization proteins (NEDD1, TUBG1, MZT2B) and actin and actin polymerization proteins (CAPZA1, ACTGA, ACTBL2, LRRC16A) (Figure 6B).

The comparison between HMGB1 immunoprecipitation in total SKOV-3 lysate and SKOV-3 nuclear fraction show that 68 of HMGB1 interactions detected in the immunoprecipitations from total lysates take place in the nucleus (Figure 7A). As expected almost half of the interacting proteins, 29, have functions related to RNA splicing as serine/arginine-rich splicing factors SRSF3, SRSF7 and SRSF5. 6 ribosomal proteins from the small ribosomal subunit and RPLP1 form the large subunit also interact with HMGB1 in the nucleus. Septins were also found in the nuclear fraction with the exception of SEPT5 and SEPT11 that only appear in the cytoplasmic interactions. Results from HMGB1 nuclear fraction immunoprecipitation show the nuclear-located interaction of HMGB1 with the nucleosome-remodeling and histone-deacetylase multiprotein complex (NuRD complex) proteins RBBP4 and RBBP7, and the Zinc finger protein ZNF512B which has also been related to the NuRD complex (Kloet *et al.*, 2015). As previously described, HMGB1 interaction with the FACT complex proteins SUPT16H and SSRP1, and histone H1FX also takes place in the nucleus.

238 proteins, displayed in Figure 7B, were found to interact with HMGB1 only in the cytoplasmic fraction of SKOV-3 cells but were not identified in total lysates from these cells. Among these proteins are a high number of ribosomal proteins, proteins related to RNA processing and DNA binding proteins as chromatin organization and modification proteins. Moreover,

proteins related to mitochondrial organization and translation were also identified within this subset of proteins.

One important difference between the immunoprecipitation of HMGB1 in cell fractions and total lysates was the absence of THO proteins, THOC1, THOC2, THOC5 and THOC6, in both the nuclear and the cytoplasmic fractions. This loss may be due to the high concentration of salt, 450 mM of NaCl, present in the Nuclear Extraction Buffer, as these complexes would likely be found within the nucleus. Nevertheless, MS/MS analysis revealed the presence of THO subunit 4, THOC4 (alias ALYREF), in the nuclear HMGB1 immunoprecipitation while this protein had not been identified in total lysates neither from SKOV-3 nor PC-3.

A

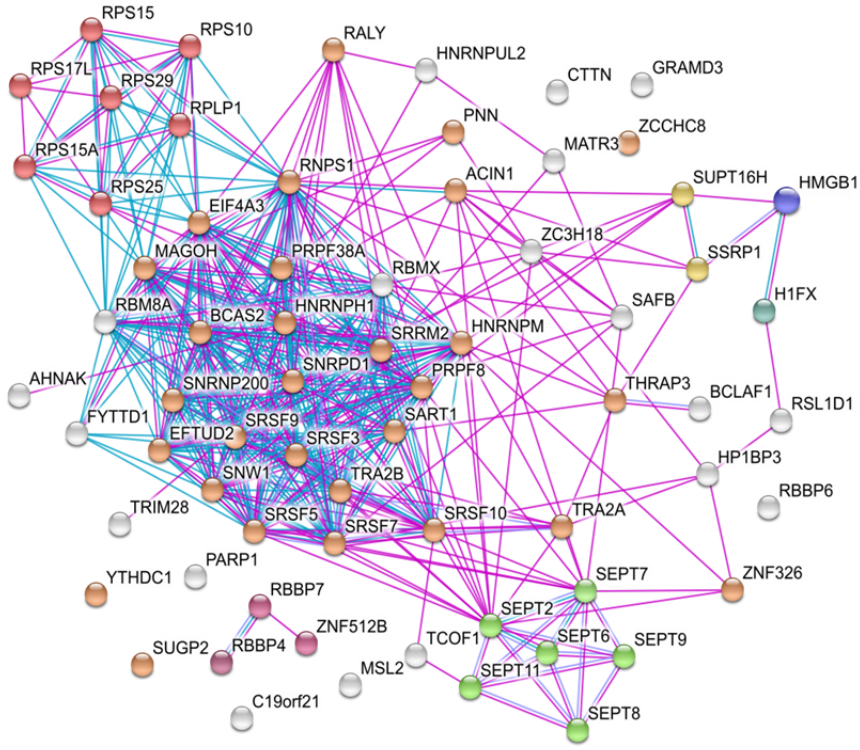

B

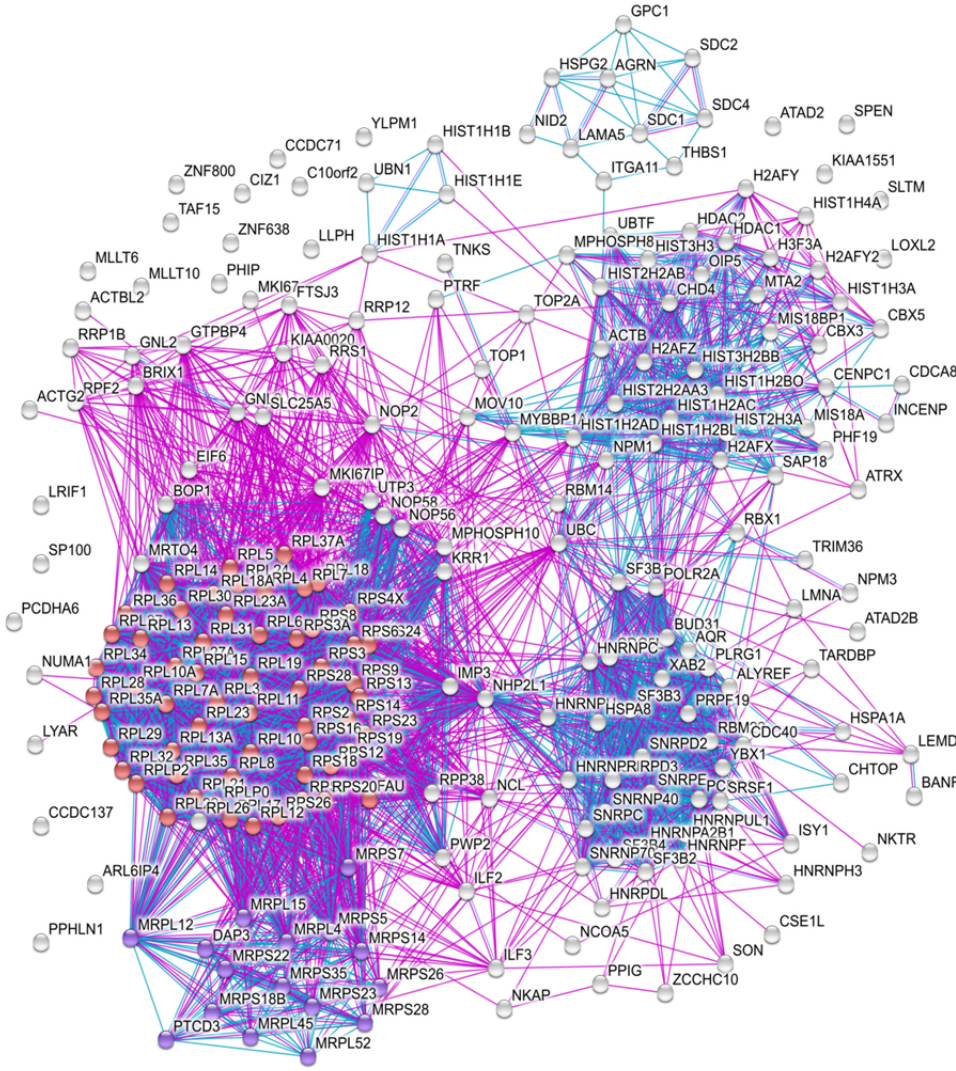

Figure 7. HMGB1 immunoprecipitation in SKOV-3 nuclear fraction. (A) HMGB1 interacting proteins identified both in the nuclear fraction of SKOV-3 cells and in whole SKOV-3 lysates **(B)** HMGB1 interacting proteins identified only in SKOV-3 nuclear fraction and not in whole lysates. In red, ribosomal proteins; in pink, NuRD complex proteins; in green, septins; in orange, RNA splicing related proteins; in yellow, FACT complex proteins; in purple, mitochondrial organization and translation related proteins; H1FX is marked in light blue and HMGB1 is highlighted in dark blue.

- PC-3 cell fractionation

13 of the 49 proteins identified in the immunoprecipitation of HMGB1 from total PC-3 lysates were found in the cytosolic fraction of PC-3. All these proteins were also found in the SKOV-3 cell fractionation immunoprecipitation, among them are septins, AHNAK, ACACA, CAP55 and PLIN4 (Figure 8A). 62 proteins were identified in HMGB1 immunoprecipitation in the cytoplasmic fraction but not in total PC-3 lysates (Figure 8B). Ribosomal proteins were the most abundant proteins in this set. Several proteins related to membrane remodeling mechanisms as the Endosomal Sorting Complex Required for protein transport, ESCRT complex, VPS37B, TSG101, CHMP4B, VPS28 and FAM125A, the CCR4-NOT complex proteins, CNOT1, CNOT2, CNOT3 and the related protein PABPC1 were identified. As described in the SKOV-3 cytoplasmic-fraction, in PC-3 microtubule organization proteins (NEDD1, TUBG1, MZT2B) immunoprecipitated with HMGB1.

25 proteins common to HMGB1 total lysate immunoprecipitation were identified in the nucleus of PC3 (Figure 9A). Septins and mRNA splicing proteins are the most abundant ones, although SEPT5 is missing in the nuclear fraction immunoprecipitation and the number of splicing related proteins is much higher in the nuclear fraction alone. The 3 proteins that belong to the NuRD complex isolated in the total lysates were also identified in the nuclear fractions (ZNF512B, RBBP7 and RBBP4). 10 more proteins, not previously found in total lysate immunoprecipitation, were seen to interact with HMGB1 in the nucleus (Figure 9B).

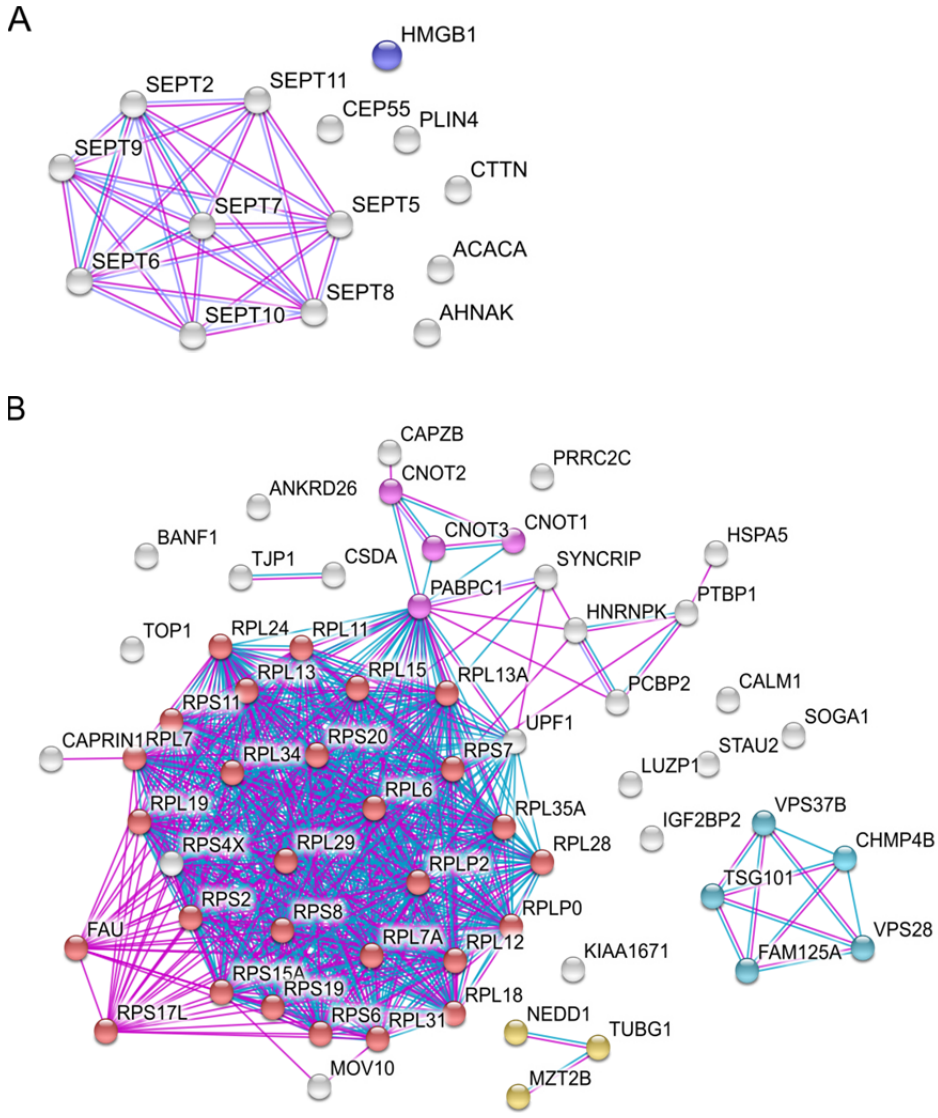

Figure 8. HMGB1 immunoprecipitation in PC-3 cytoplasmic fraction. (A) HMGB1 interacting proteins identified both in the cytoplasmic fraction of PC-3 cells and in whole PC-3 lysates. **(B)** HMGB1 interacting proteins identified only in SKOV-3 cytoplasmic fraction and not in whole lysates. In red, ribosomal proteins; in yellow microtubule organization proteins; in pink, CCR4-NOT complex proteins; in light blue, ESCRT complex proteins and HMGB1 is highlighted in dark blue.

A large number (263) of interactions were found only in the HMGB1 immunoprecipitation of the nuclear fraction. A high amount of these proteins have functions related to ribosomes, ribosomal biogenesis and translation processes, RNA metabolic processes as splicing and chromatin organization, assembly and remodeling.

As in the HMGB1 immunoprecipitation in SKOV-3 subcellular fractions, the THO complex proteins identified in the immunoprecipitations from PC-3 total lysates were not identified in the cell fractionation immunoprecipitations. As above described for SKOV-3 ALYREF was only identified in the nuclear fraction of PC-3.

A

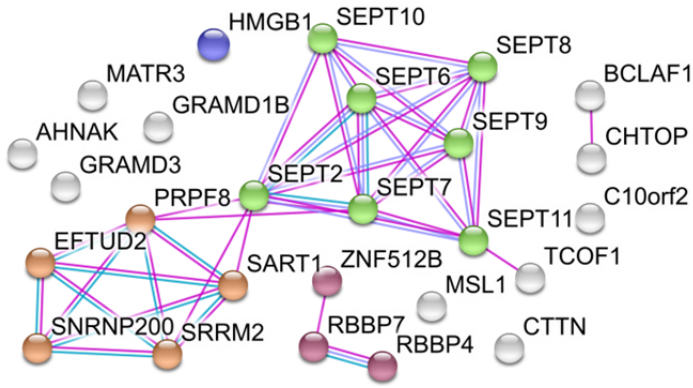

B

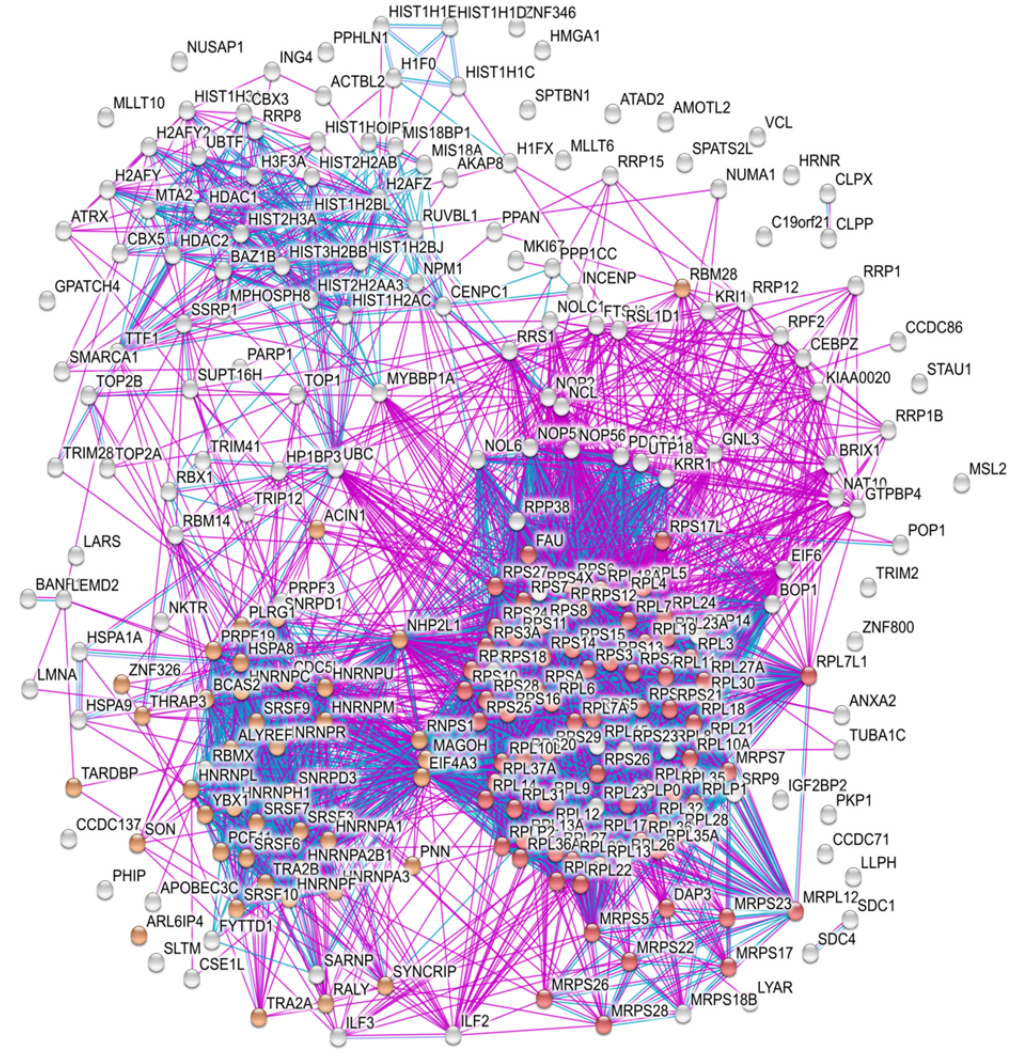

Figure 9. HMGB1 immunoprecipitation in PC-3 nuclear fraction. (A) HMGB1 interacting proteins identified both in the nuclear fraction of PC-3 cells and in whole PC-3 lysates **(B)** HMGB1 interacting proteins identified only in PC-3 nuclear fraction and not in whole lysates. In red, ribosomal proteins; in pink, NuRD complex proteins; in green, septins; in orange, RNA splicing related proteins and HMGB1 is highlighted in dark blue.

RBBP7 and HMGB1

In the immunoprecipitation assays we have isolated RBBP4 and RBBP7, two proteins that are part of the NuRD complex. This complex has been associated to transcriptional processes, chromatin assembly mechanisms, cell cycle progression and genomic stability (Lai and Wade, 2011). Moreover, two histone deacetylases, HDAC1 and HDAC2, and Metastasis-associated protein, MTA2, also components of the NuRD complex, were immunoprecipitated along with HMGB1 in the nuclear fraction of PC-3 and SKOV-3. In addition, Chromodomain-helicase-DNA-binding protein 4, CHD4, another component of the NuRD complex was identified in the nuclear fraction of SKOV-3 cells after immunoprecipitation with HMGB1. No previous interaction among HMGB1 and the NuRD complex proteins has been reported. Due to the interest of a possible relationship between HMGB1 and the components of the NuRD complex the possible direct interaction between HMGB1 and RBBP7 was analyzed using direct two hybrid assays. Results from direct yeast two hybrid and β-galactosidase assays show that there is direct interaction between HMGB1 and the NuRD protein, RBBP7 (Figure 10).

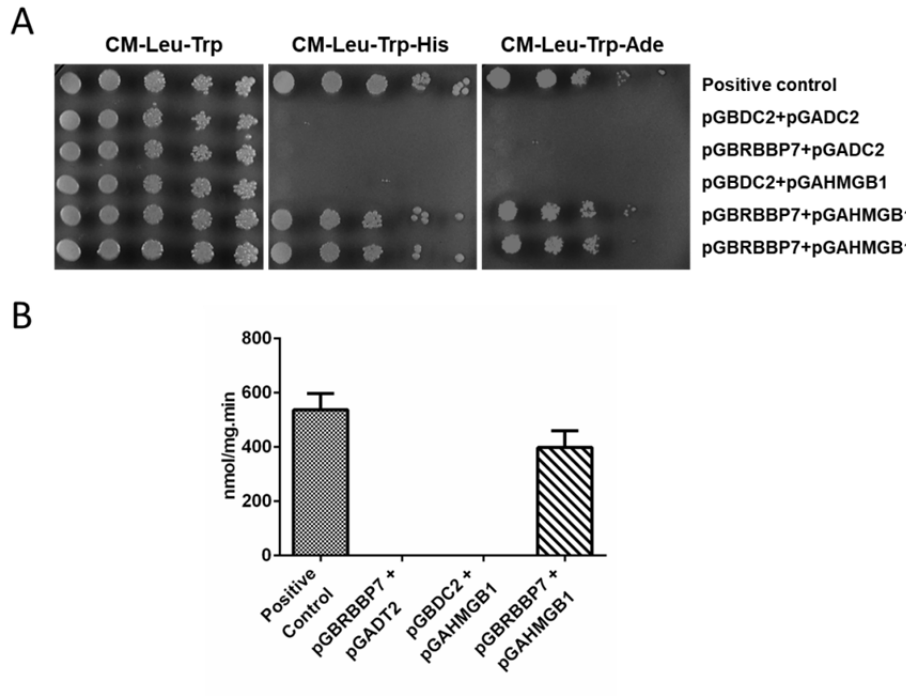

Figure 10. HMGB1 interacts with RBBP7. (A) PJ69-4A cells transformed with different constructions and incubated at 30 ºC in CM-Leu-Trp (positive growth), CM-Leu-Trp-His or CM-Leu-Trp-Ade plates. **(B)** β-galactosidase enzyme mesurements of PJ69-4A cells extracts carrying different constructions. Ixr1 and Swi6 interaction was used as a positive control.

Septins, the THOC complex and Rab11 interplay

Among the proteins identified in the large scale HMGB1 immunoprecipitations, two interesting subsets of proteins arised: Septins (SEPT6, SEPT9, SEPT7, SEPT11, SEPT10, SEPT8, SEPT2) cytoskeleton GTP binding proteins (Mostowy and Cossart, 2012), and proteins from the THOC complex (THOC1, THOC6, THOC5, THOC2) that are part of the "transcription/export" complex (TREX complex) (Masuda *et al.*, 2005). To study in depth these interactions a large scale THOC5 immunoprecipitation was performed, carried out in PC-3 cells following the same procedure as

for HMGB1 immunoprecipitations. 282 proteins were identified as THOC5 interacting proteins after analyzing the results from the immunoprecipitation with the SAINTexpress algorithm and selecting interactions with a higher SP of 0.7 (Supplementary table 5). Among those interacting partners are found other THO proteins (THOC1, THOC2, THOC3, THOC6 and THOC7) as expected as well as septin proteins (SEPT2, SEPT7, SEPT9 and SEPT11).

In order to verify these interactions small scale immunoprecipitations carried out using PC-3 cell lysates and antibodies against THOC5, THOC2, SEPT2, SEPT7. Results from this immunoprecipitations validate the physical interactions among THO proteins and septins. Moreover, small immunoprecipitation showed a third participant in these interactions, the small GTPase, Rab11 that also immunoprecipitated with HMGB1 and THOC5 in prostate cancer cells (Figure 11). Results from these experiments also prove the interactions between Rab11 and proteins from the THO complex and Septins.

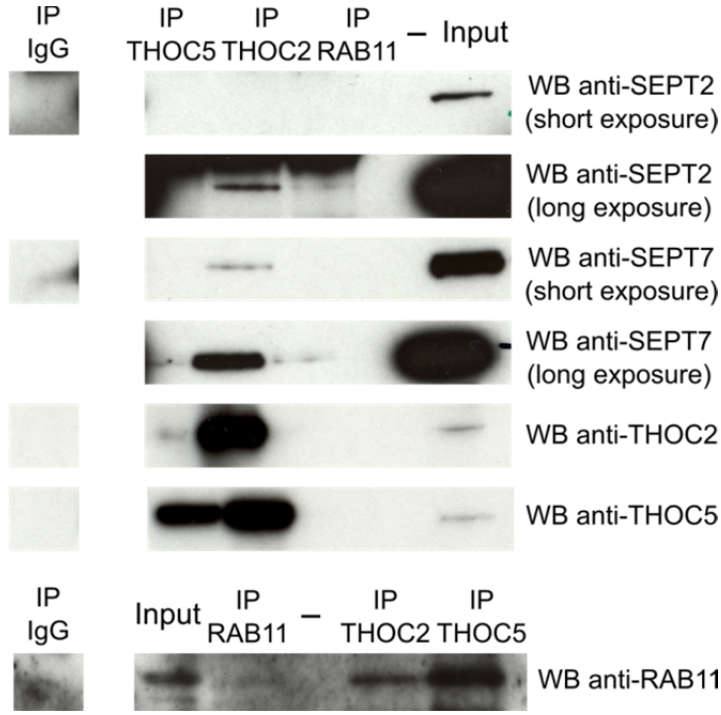

Figure 11. Interplay among Septins, THO proteins and RAB11. PC-3 lysates were immunoprecipitated with anti-THOC5 (ab86070), anti-THOC2 (ab129485), anti-Rab11 (ab3612) and Millipore Normal Rabbit IgG Polyclonal (12-360) and immunoblotted with antibodies to SEPT2, SEPT7, THOC2, THOC5 and RAB11.

DISCUSSION

Although HMGB1 is a protein that has been extensively studied and related to cancer (Kang *et al.*, 2013) many of its functional interactions still remain unknown. In the previous chapter we approached the study of HMGB1 interactions in ovarian and prostate cancer cells using two hybrid assays. To complete the study, large scale purification together with subcellular fractionation experiments were carried out to unveil a wider range of associated proteins and depict HMGB1 interactome in prostate and ovarian cells.

From data previous to our study, proteins interacting with HGMB1 were associated to the immune response, as toll-like receptor pathways; as well as to processes related to nuclear functions, such as chromatin organization and regulation of gene expression. However, our results strongly associate HMGB1 and binding partners with RNA metabolic processes, such as RNA splicing and mRNA transport in prostate and ovarian cancer cells. This processes have great importance in cell proliferation, differentiation, cell survival, and tumorigenesis (Corkery *et al.*, 2015) Among these proteins are found proteins from the THO subcomplex (THOC1, THOC2, THOC5 and THOC6) that were seen to interact with HMGB1 in both cells lines and had been related to cancer development. In particular THOC1 has been associated to prostate cancer aggressiveness (Chinnam *et al.*, 2014; Li *et al.*, 2007; Tran *et al.*, 2016).

Our results also associate HMGB1 to proteins from the small and the large subunit of the ribosome in the nucleus and the cytoplasm of PC-3 and SKOV-3 cell lines. Remarkably, some of the associated HMGB1 proteins identified in our studies were also related to the ribosome biogenesis as they cluster within nucleolar proteins, showing a possible role of HMGB1 in ribosomal gene transcription and ribosome assembly. As cancer development demands a higher rate of cell division and metabolism, an increase in protein synthesis is needed, and alteration in ribosomal proteins networks may play a role in tumor development. Accordingly, mutations of some of the ribosomal proteins found to interact with HMGB1 in PC-3 and SKOV-3, as RPL22 and RPL5, had been associated to tumor development (Ferreira *et al.*, 2014; Goudarzi and Lindström, 2016).

Although HMGB1 has not been linked to direct cytoskeleton reorganization, HMGB1 indirectly modulates the cytoskeleton throughout its interaction with other proteins, such as the two well characterized HMGB1 partners, the receptor for advanced glycation end products (RAGE) (Rauvala and Rouhiainen, 2010) and heat shock protein β-1 (HSPB1/HSP27), a cytoskeleton regulator needed during autophagy and mitophagy (Kang *et al.*, 2011). Our results show interaction of HMGB1 with several cytoskeleton proteins like septins, microtubule organization proteins, actin polymerization proteins and keratins in prostate and ovarian tumoral cells. The results reinforce the direct implication of HMGB1 in cell division, motility and differentiation, which are altered in cancer and tumor progression (Fife *et al.*, 2014; Yilmaz and Christofori, 2009).

The most important result validated in our study is the nuclear HMGB1 interaction with two components of the nucleosome remodeling and histone deacetylation (NuRD) complex. RBBP4 and RBBP7 immunoprecipitated with HMGB1 in PC-3 and SKOV-3 cell lines. Results from direct two hybrid assays validate the direct physical interaction between HMGB1 and RBBP7. Other proteins of the NuRD complex as HDAC1, HDAC2 and MTA2 were also identified as HMGB1 interacting proteins in the nuclear compartment. Due to the role of the NuRD complex in transcriptional regulation, this complex has been associated to pro-tumoral events through silencing of tumor suppressor genes (Cai *et al.*, 2014).

In this study we also reveal for the first time a link between proteins from the THO complex, septins and the small GTPase Rab11. Although it has not

been reported an interaction between Rab11 and septins, due to the functions of the former one in vesicle trafficking and recycling and in cytokinesis, an interaction between these proteins would be plausible. Moreover, studies carried out by Kouranti and collaborators and Chesneau and colleagues showed a conection between other member of the Rab GTPase family, Rab35, and septins (Chesneau *et al.*, 2012; Kouranti *et al.*, 2006). Due to the fact that THO proteins are involved in RNA export (Chi *et al.*, 2013) interaction of these proteins with septins and Rab11 could be somehow related to this trafficking. Functional analysis are needed to stablish the nature of this interaction.

As a whole, results from our study show that HMGB1 is an important actor in a wide range of cellular pathways in ovarian and prostate cancer cells.

REFERENCES

Barreiro-Alonso A, Lamas-Maceiras M, Rodríguez-Belmonte E, Vizoso-Vázquez Á, Quindós M, Cerdán ME. 2016. High Mobility Group B Proteins, Their Partners, and Other Redox Sensors in Ovarian and Prostate Cancer. *Oxid. Med. Cell. Longev.*, **2016**: 5845061.

Beijnum JR Van, Boezem E Van Den, Hautvast P, Buurman WA, Griffioen AW. 2012. Tumor angiogenesis is enforced by autocrine regulation of high-mobility group box 1. *Oncogene*, **32**: 363–374.

Bonaldi T, Talamo F, Scaffidi P, Ferrera D, Porto A, Bachi A, Rubartelli A, Agresti A, Bianchi ME. 2003. Monocytic cells hyperacetylate chromatin protein HMGB1 to redirect it towards secretion. *EMBO J.*, **22**: 5551–5560.

Cai Y, Geutjes E-J, Lint K de, Roepman P, Bruurs L, Yu L-R, Wang W, Blijswijk J van, Mohammad H, Baylin S. 2014. The NuRD complex cooperates with DNMTs to maintain silencing of key colorectal tumor suppressor genes. *Oncogene*, **33**: 2157–2168.

Chandrasekaran KS, Sathyanarayanan A, Karunagaran D. 2016. Downregulation of HMGB1 by miR-34a is sufficient to suppress

proliferation, migration and invasion of human cervical and colorectal cancer cells. *Tumor Biol.*, **37**: 13155–13166.

Chesneau L, Dambournet D, MacHicoane M, Kouranti I, Fukuda M, Goud B, Echard A. 2012. An ARF6/Rab35 GTPase cascade for endocytic recycling and successful cytokinesis. *Curr. Biol.*, **22**: 147–153.

Chi B, Wang Q, Wu G, Tan M, Wang L, Shi M, Chang X, Cheng H. 2013. Aly and THO are required for assembly of the human TREX complex and association of TREX components with the spliced mRNA. *Nucleic Acids Res.*, **41**: 1294–1306.

Chinnam M, Wang Y, Zhang X, Gold DL, Khoury T, Nikitin AY, Foster BA, Li Y, Bshara W, Morrison CD, Goodrich DW. 2014. The Thoc1 ribonucleoprotein and prostate cancer progression. *J. Natl. Cancer Inst.*, **106**: 1–8.

Choi H, Liu G, Mellacheruvu D, Tyers M, Gingras AC, Nesvizhskii AI. 2012. Analyzing protein-protein interactions from affinity purification-mass spectrometry data with SAINT. *Curr. Protoc. Bioinforma.*, **Chapter 8**: Unit8.15.

Corkery DP, Holly AC, Lahsaee S, Dellaire G. 2015. Connecting the speckles: Splicing kinases and their role in tumorigenesis and treatment response. *Nucleus*, **6**: 279–288.

Ferreira AM, Tuominen I, van Dijk-Bos K, Sanjabi B, van der Sluis T, van der Zee AG, Hollema H, Zazula M, Sijmons RH, Aaltonen LA, Westers H, Hofstra RMW. 2014. High frequency of RPL22 mutations in microsatellite-unstable colorectal and endometrial tumors. *Hum. Mutat.*, **35**: 1442–1445.

Fife CM, McCarroll JA, Kavallaris M. 2014. Movers and shakers: Cell cytoskeleton in cancer metastasis. *Br. J. Pharmacol.*, **171**: 5507–5523.

Gatla HR, Singha B, Persaud V, Vancurova I. 2014. Evaluating cytoplasmic and nuclear levels of inflammatory cytokines in cancer cells by western blotting. *Methods Mol. Biol.*, **1172**: 271–283.

Gnanasekar M, Kalyanasundaram R, Zheng G, Chen A, Bosland MC, Kajdacsy-Balla A. 2013. HMGB1: A Promising Therapeutic Target for Prostate Cancer. *Prostate Cancer*.

Gnanasekar M, Thirugnanam S, Ramaswamy K. 2009. Short hairpin RNA (shRNA) constructs targeting high mobility group box-1 (HMGB1) expression leads to inhibition of prostate cancer cell survival and apoptosis. *Int. J. Oncol.*, **34**: 425–431.

Goudarzi KM, Lindström MS. 2016. Role of ribosomal protein mutations in tumor development (Review). *Int. J. Oncol.*, **48**: 1313–1324.

Hoppe G, Talcott KE, Bhattacharya SK, Crabb JW, Sears JE. 2006. Molecular basis for the redox control of nuclear transport of the structural chromatin protein Hmgb1. *Exp. Cell Res.*, **312**: 3526–3538.

Isaacs WB, Carter BS, Ewing CM. 1991. Wild-Type p53 Suppresses Growth of Human Prostate Cancer Cells Containing Mutant p53 Alleles. *Cancer Res.*, **51**: 4716–4721.

Ito I, Fukazawa J, Yoshida M. 2007. Post-translational methylation of high mobility group box 1 (HMGB1) causes its cytoplasmic localization in neutrophils. *J. Biol. Chem.*, **282**: 16336–16344.

James P, Halladay J, Craig EA. 1996. Genomic Libraries and a Host Strain Designed for Highly Efficient Two-Hybrid Selection in Yeast. *Genetics*, **144**: 1425–1436.

Kang R, Livesey KM, Zeh HJ, Lotze MT, Tang D. 2011. Metabolic regulation by HMGB1-mediated autophagy and mitophagy. *Autophagy*, **7**: 1256–1258.

Kang R, Qiuhong Z, Zeh III HJ, Lotze MT, Tang D. 2013. HMGB1 in Cancer: Good, Bad, or Both? *Clin Cancer Res*, **19**: 4046–4057.

Kloet SL, Baymaz HI, Makowski M, Groenewold V, Jansen PWTC, Berendsen M, Niazi H, Kops GJ, Vermeulen M. 2015. Towards elucidating the stability, dynamics and architecture of the nucleosome remodeling and deacetylase complex by using quantitative interaction proteomics. *FEBS J.*, **282**: 1774–1785.

Kouranti I, Sachse M, Arouche N, Goud B, Echard A. 2006. Rab35 Regulates an Endocytic Recycling Pathway Essential for the Terminal Steps of Cytokinesis. *Curr. Biol.*, **16**: 1719–1725.

Lai AY, Wade PA. 2011. NuRD: A multi-faceted chromatin remodeling complex in regulating cancer biology. *Nat Rev Cancer*, **11**: 588–596.

Li T, Gui Y, Yuan T, Liao G, Bian C, Jiang Q, Huang S, Liu B, Wu D. 2012. Overexpression of high mobility group box 1 with poor prognosis in patients after radical prostatectomy. *BJU Int.*, **110**: E1125-30.

Li Y, Lin1 AW, Zhang X, Wang Y, Wang X, Goodrich DW. 2007. Cancer cells and normal cells differ in their requirements for Thoc1. *Cancer Res.*, **67**: 6657–6664.

Li Y, Tian J, Fu X, Chen Y, Zhang W, Yao H, Hao Q. 2014. Serum high mobility group box protein 1 as a clinical marker for ovarian cancer. *Neoplasma*, **61**: 579–584.

Liu P-L, Liu W-L, Chang J-M, Chen Y-H, Liu Y-P, Kuo H-F, Hsieh C-C, Ding Y-S, Chen W-W, Chong I-W. 2017. MicroRNA-200c inhibits epithelial-mesenchymal transition, invasion, and migration of lung cancer by targeting HMGB1 Ahmad A. (ed). *PLoS One*, **12**: e0180844.

Livesey KM, Kang R, Vernon P, Buchser W, Loughran P, Watkins SC, Zhang L, Manfredi JJ, Iii HJZ, Li L, Lotze MT, Tang D. 2012. p53/HMGB1 Complexes Regulate Autophagy and Apoptosis. *Cancer Res.*, **72**: 1996–2005.

Masuda S, Das R, Cheng H, Hurt E, Dorman N, Reed R. 2005. Recruitment of the human TREX complex to mRNA during splicing. *Genes Dev.*, **19**: 1512–1517.

Mostowy S, Cossart P. 2012. Septins: the fourth component of the cytoskeleton. *Nat. Rev. Mol. Cell Biol.*, **13**: 183–194.

Moumen A, Masterson P, O'Connor MJ, Jackson SP. 2005. hnRNP K: An HDM2 target and transcriptional coactivator of p53 in response to DNA damage. *Cell*, **123**: 1065–1078.

Paek J, Lee M, Nam EJ, Kim SW, Kim YT. 2016. Clinical impact of high mobility group box 1 protein in epithelial ovarian cancer. *Arch. Gynecol. Obstet.*, **293**: 645–650.

Pardo M, Lang B, Yu L, Prosser H, Bradley A, Babu MM, Choudhary J. 2010. An Expanded Oct4 Interaction Network: Implications for Stem Cell Biology, Development, and Disease. *Cell Stem Cell*, **6**: 382–395.

Prasad R, Liu Y, Deterding LJ, Poltoratsky VP, Padmini S, Horton JK, Kanno S, Asagoshi K, Hou EW, Khodyreva N, Wilson SH. 2007. HMGB1 is a Co-factor in Mammalian Base Excision Repair Rajendra. *Mol Cell*, **27**: 829–841.

Rauvala H, Rouhiainen A. 2010. Physiological and pathophysiological outcomes of the interactions of HMGB1 with cell surface receptors. *Biochim. Biophys. Acta - Gene Regul. Mech.*, **1799**: 164–170.

Rose M, Botstein D. 1983. Construction and use of gene fusions to lacZ (beta-galactosidase) that are expressed in yeast. *Methods Enzymol.*, **101**: 167–180.

Schatz DG, Swanson PC. 2011. V(D)J Recombination: Mechanisms of Initiation. *Annu. Rev. Genet.*, **45**: 167–202.

Stros M. 2010. HMGB proteins: interactions with DNA and chromatin. *Biochim. Biophys. Acta*, **1799**: 101–113.

Tang D, Kang R, Livesey KM, Cheh CW, Farkas A, Loughran P, Hoppe G, Bianchi ME, Tracey KJ, Zeh HJ, Lotze MT. 2010. Endogenous HMGB1 regulates autophagy. *J. Cell Biol.*, **190**: 881–892.

Tang Y, Zhao X, Antoine D, Xiao X, Wang H, Andersson U, Billiar TR, Tracey KJ, Lu B. 2016. Regulation of Posttranslational Modifications of HMGB1 During Immune Responses. *Antioxid. Redox Signal.*, **24**: 620–34.

Tran DDH, Saran S, Koch A, Tamura T. 2016. MRNA export protein THOC5 as a tool for identification of target genes for cancer therapy. *Cancer Lett.*, **373**: 222–226.

Vikhanskaya F, Erba E, D'Incalci M, Broggini M. 1994. Introduction of wild-type p53 in a human ovarian cancer cell line not expressing endogenous p53. *Nucleic Acids Res.*, **22**: 1012–7.

Vizcaino JA, Csordas A, Del-Toro N, Dianes JA, Griss J, Lavidas I, Mayer G, Perez-Riverol Y, Reisinger F, Ternent T, Hermjakob H. 2016. 2016 update of the PRIDE database and its related tools. *Nucleic Acids Res.*, **44**: 11033.

Wang H, Li Z, Sun Y, Xu Z, Han J, Song B, Song W, Qin C, Yin L. 2015. Relationship between high-mobility group box 1 overexpression in ovarian cancer tissue and serum : a meta-analysis. *Onco targets Ther.*, **8**: 3523–3531.

Yang H, Wang H. 2015. High Mobility Group Box Protein 1 (HMGB1): The Prototypical Endogenous Danger Molecule. *Mol. Med.*, **21**: S6–S12.

Yilmaz M, Christofori G. 2009. EMT, the cytoskeleton, and cancer cell invasion. *Cancer Metastasis Rev.*, **28**: 15–33.

Yu SS, Li HJ, Goodwin GH, Johns EW. 1977. Interaction of Non-histone Chromosomal Proteins HMG1 and HMG2 with DNA. *Eur. J. Biochem.*, **78**: 497–502.

Yuan F, Gu L, Guo S, Wang C, Li GM. 2004. Evidence for involvement of HMGB1 protein in human DNA mismatch repair. *J. Biol. Chem.*, **279**: 20935–20940.

Zhang W, Tian J, Hao Q. 2014. HMGB1 combining with tumor-associated macrophages enhanced lymphangiogenesis in human epithelial ovarian cancer. *Tumor Biol.*, **35**: 2175–2186.

ANNEX TO CHAPTER 4

Supplementary table 1. HMGB1 interacting proteins in the nuclear fraction of SKOV-3 cells.

GENE	HMGB1 IP			Rabbit IP			SP
	Coverage	Peptides	Spectra	Coverage	Peptides	Spectra	
RPL36	23,81	5	62				1
TRIM36	0,82	1	2				1
RPS6	18,88	6	29	15,26	3	6	1
RPL23A	16,67	4	17			0	1
HIST2H2AB	66,15	8	309	29,23	2	10	1
CTTN	30,36	13	48				1
NKAP	10,84	2	8				1
POLR2A	1,73	2	3				1
MRPS7	9,50	2	4				1
HNRNPC	41,18	12	97				1
ZNF800	3,46	1	3				1
H2AFZ	56,25	7	423	35,16	3	9	1
INCENP	6,21	4	7				1
LMNA	2,11	1	2				1
RPL13A	38,42	10	92				1
MRPS18B	12,79	1	3				1
SEPT6	3,92	2	3				1
HIST2H2BD	19,51	4	83				1
RPLP1	51,75	2	5				1
RPLP2	80,00	10	38				1
RPLP0	31,23	9	62				1
RPP38	3,89	1	2				1
RBX1	17,59	1	3				1
MPHOSPH10	4,70	1	2				1
NOP56	15,99	5	11				1
CDC40	13,64	4	9				1
RSL1D1	27,96	13	49				1
HNRNPM	47,53	21	171				1
YBX1	25,00	3	15				1
MPHOSPH8	6,05	2	10				1
PCBP1	25,00	4	26				1
PRPF19	43,45	13	48				1
RPL3	39,70	12	152				1
SRSF9	15,84	3	7				1
SF3B1	8,21	5	9				1
BANF1	29,21	2	15				1
SNRNP70	5,95	2	4				1
HIST1H4A	65,05	16	1379	41,75	5	21	1
MTA2	5,84	3	3				1
MOV10	8,08	5	10				1
RPL10	6,54	2	12				1

Supplementary table 1. Continuation.

GENE	HMGB1 IP			Rabbit IP			SP
	Coverage	Peptides	Spectra	Coverage	Peptides	Spectra	
HIST1H2BL	64,29	12	590	19,84	2	12	1
ZNF326	13,92	5	18				1
HSPA8	22,14	11	31				1
HIST2H3A	60,29	13	271	6,62	1	1	1
ITGA11	0,84	1	3				1
KRR1	10,50	2	4				1
ZCCHC10	7,29	1	2				1
RPL31	25,60	3	9				1
RPL35A	23,64	3	15				1
HNRNPUL1	5,49	3	7				1
RPS23	16,08	3	17	15,38	2	3	1
RPS14	26,49	6	23				1
RPS18	41,45	8	39				1
ZCCHC8	3,11	1	4				1
HSPG2	5,42	16	48				1
SNRNP200	19,94	22	85				1
H1FX	13,62	3	5				1
NPM1	63,95	13	356				1
RBM8A	38,51	5	26				1
SSRP1	10,30	5	18				1
CHTOP	11,69	2	8	5,24	1	2	1
RPL6	48,61	17	216			0	1
FYTTD1	16,67	4	5			0	1
SRSF1	13,31	2	3			0	1
MRPS28	5,35	1	2			0	1
H2AFY	35,22	7	82			0	1
RPF2	38,56	10	45			0	1
ACTB	24,80	6	20	12,00	3	4	1
GRAMD3	27,78	7	25			0	1
RBBP6	6,70	6	10			0	1
PTCD3	1,74	1	2			0	1
RPS15	28,28	2	32			0	1
RPL27	54,41	9	58			0	1
RPS24	30,08	5	26			0	1
EIF4A3	40,63	18	111			0	1
HIST2H2AA3	71,54	13	1167	63,08	6	22	1
SNRPD3	15,08	2	4			0	1
TCOF1	6,32	6	15			0	1
SNRPD2	15,25	1	2			0	1
SNRPD1	27,73	2	8			0	1
MYBBP1A	1,28	1	3			0	1
MSL2	2,95	1	2			0	1

Supplementary table 1. Continuation.

GENE	HMGB1 IP			Rabbit IP			SP
	Coverage	Peptides	Spectra	Coverage	Peptides	Spectra	
ZNF638	1,92	1	2			0	1
ARL6IP4	8,55	3	16			0	1
RPS17L	42,96	4	18			0	1
ACIN1	8,13	8	17			0	1
LOXL2	3,23	2	5			0	1
MRPS23	5,26	1	2			0	1
TRA2B	13,89	4	33			0	1
SEPT7	9,84	3	10			0	1
HIST3H2BB	60,32	9	592	11,90	1	8	1
YTHDC1	3,30	2	2			0	1
TAF15	14,02	5	20			0	1
HIST1H1A	31,63	7	63	7,44	4	20	1
MRPS26	8,78	1	3			0	1
RPL19	26,02	6	36			0	1
SP100	4,32	2	6			0	1
PWP2	1,74	1	2			0	1
NPM3	8,99	1	2			0	1
BRIX1	44,76	12	102			0	1
CSE1L	0,82	1	73			0	1
RBM22	7,14	2	3			0	1
SLC25A5	14,43	3	5	3,02	1	1	1
CDCA8	15,71	3	3			0	1
RPL18A	24,43	6	41			0	1
GNL2	4,79	2	3			0	1
LLPH	23,26	2	8			0	1
THBS1	4,27	3	4			0	1
RPL15	34,31	7	140			0	1
MRTO4	14,23	2	5			0	1
KIAA1551	2,18	3	5			0	1
RALY	41,18	11	75			0	1
TRIM28	20,36	9	34			0	1
RPS2	29,01	8	31			0	1
CIZ1	8,46	3	4			0	1
ZNF512B	18,50	9	27			0	1
RPL35	22,76	4	19	8,13	1	2	1
HNRNPA2B1	17,00	3	7			0	1
CCDC137	6,23	1	2			0	1
NCOA5	26,94	8	20			0	1
LAMA5	0,43	1	3			0	1
MIS18A	10,73	2	4			0	1
SRSF10	19,47	4	15			0	1
HIST1H1B	31,42	10	64	23,89	5	10	1

Supplementary table 1. Continuation.

GENE	HMGB1 IP			Rabbit IP			SP
	Coverage	Peptides	Spectra	Coverage	Peptides	Spectra	
RPS4X	24,71	5	23			0	1
SAFB	11,15	6	15			0	1
SF3B4	5,42	1	2			0	1
HIST1H3A	60,29	13	345	30,15	2	13	1
PPIG	4,77	2	6			0	1
RPS13	38,41	7	28	4,64	1	1	1
MKI67	2,83	6	7			0	1
RPS29	33,93	2	11			0	1
MRPL45	15,69	2	3			0	1
UBN1	2,65	1	2			0	1
RBBP4	19,53	5	12			0	1
BCLAF1	13,04	8	47			0	1
LRIF1	9,36	4	5			0	1
RIOX1	9,83	3	6			0	1
HP1BP3	8,86	3	19			0	1
BOP1	3,49	1	2			0	1
RPS12	34,09	4	19			0	1
RPS10	14,55	2	16			0	1
RPS5	18,63	3	14			0	1
RPS9	36,60	12	33	3,61	1	1	1
RPL13	44,55	10	54	20,38	4	12	1
MRPS14	11,72	1	2			0	1
MRPL15	8,45	1	3			0	1
TNKS	0,60	1	2			0	1
CDC5L	22,57	9	22			0	1
MRPL52	26,83	1	2			0	1
CBX3	23,50	3	10			0	1
HMGB1	16,28	4	13			0	1
MATR3	32,82	15	77			0	1
GNL3	17,85	5	13			0	1
MRPS35	8,36	1	3			0	1
MRPS5	3,26	1	2			0	1
RPS25	24,00	3	10			0	1
HSPA1A	4,52	2	5			0	1
RPL17	32,07	7	22			0	1
MAGOH	49,32	6	22			0	1
RPS28	21,74	2	9			0	1
HIST1H2AC	71,54	11	834	54,62	5	22	1
ISY1	11,23	2	5			0	1
HNRNPF	13,25	4	20			0	1
HIST1H2AD	71,54	13	1182	63,08	6	26	1
RPL32	18,52	4	28			0	1

Supplementary table 1. Continuation.

GENE	HMGB1 IP			Rabbit IP			SP
	Coverage	Peptides	Spectra	Coverage	Peptides	Spectra	
RPL11	15,73	3	27			0	1
RPL8	28,02	5	21			0	1
HNRNPH1	23,16	7	41			0	1
HNRNPH3	4,91	1	3			0	1
EFTUD2	19,96	12	41			0	1
SAP18	32,03	2	10			0	1
SNRPE	29,35	2	7			0	1
TWNK	11,40	4	12			0	1
ALYREF	17,51	2	3			0	1
ATAD2	26,55	24	78			0	1
PPHLN1	12,23	5	7			0	1
RPS3	52,26	12	58			0	1
RPL22	19,53	3	12			0	1
SUPT16H	15,09	11	33			0	1
ATAD2B	2,47	2	3			0	1
SDC2	7,46	1	6			0	1
MIS18BP1	8,13	4	7			0	1
DAP3	17,34	4	7			0	1
SNW1	31,16	10	26			0	1
PCDHA6	0,84	2	2			0	1
RPL26	22,07	5	11			0	1
UTP3	6,47	1	2			0	1
NUMA1	11,73	13	33			0	1
AHNAK	30,05	66	173			0	1
NKTR	4,65	4	11			0	1
RBMX	32,99	12	72			0	1
PNN	13,11	8	47			0	1
PHIP	22,24	26	92			0	1
MRPL12	35,86	3	10			0	1
RPL18	36,70	9	66			0	1
HNRNPDL	8,33	1	3			0	1
THRAP3	18,95	12	74			0	1
AGRN	9,92	10	21			0	1
MRPL4	11,25	2	2			0	1
TOP1	9,15	5	9			0	1
H2AFY2	38,71	8	54			0	1
RRP1B	24,27	10	17			0	1
TOP2A	9,41	10	21			0	1
RPL23	13,57	3	11			0	1
HNRNPUL2	5,62	3	8			0	1
SON	17,19	23	87			0	1
PTRF	4,36	1	2			0	1

Supplementary table 1. Continuation.

GENE	HMGB1 IP			Rabbit IP			SP
	Coverage	Peptides	Spectra	Coverage	Peptides	Spectra	
GTPBP4	22,56	10	26			0	1
SEPT8	3,52	2	3			0	1
RPL14	14,88	3	42			0	1
YLPM1	3,49	4	5			0	1
RPL37A	19,57	1	13			0	1
PLRG1	10,12	2	5			0	1
HDAC1	10,17	4	8			0	1
RPS8	28,37	5	48	5,29	1	2	1
RPS15A	10,00	1	2			0	1
RPS16	53,42	11	50			0	1
SEPT9	18,43	6	20			0	1
PRPF38A	8,97	2	3			0	1
RPL7	51,21	18	147			0	1
CENPC	3,18	2	2			0	1
UBTF	6,02	3	5			0	1
SNRNP40	11,48	2	4			0	1
SLTM	4,74	4	8			0	1
SDC1	11,94	2	11			0	1
NIFK	26,96	4	7			0	1
RPL7A	37,22	13	105			0	1
RPL12	45,45	4	44			0	1
NOP58	12,67	4	6			0	1
H3F3A	60,29	13	145	6,62	1	1	1
RPL10A	31,80	9	89			0	1
RPL24	19,11	3	10	10,83	2	3	1
FAU	18,64	2	17			0	1
NCL	27,32	21	114			0	1
H2AFX	55,24	9	622	31,47	3	13	1
GPC1	5,73	2	3			0	1
SF3B3	2,14	2	2			0	1
SEPT2	19,94	4	14			0	1
KIAA0020	3,86	1	2			0	1
RBM14	15,70	8	18			0	1
SPEN	3,77	6	10			0	1
CBX5	6,81	1	4			0	1
RBBP7	14,82	5	7			0	1
RPS19	36,55	7	28			0	1
ZC3H18	2,62	1	2			0	1
ATRX	2,01	3	5			0	1
HDAC2	13,52	5	11			0	1
TARDBP	15,22	4	13			0	1
NHP2L1	9,38	1	3			0	1

Supplementary table 1. Continuation.

GENE	HMGB1 IP			Rabbit IP			SP
	Coverage	Peptides	Spectra	Coverage	Peptides	Spectra	
MLLT6	2,84	2	4			0	1
CHD4	2,88	3	4			0	1
NOP2	5,42	3	6			0	1
RNPS1	22,62	5	51			0	1
MLLT10	10,96	5	21			0	1
RPS3A	21,97	6	22			0	1
UBC	28,91	2	4			0	1
TRA2A	12,06	3	10			0	1
RPL30	10,43	1	24			0	1
BCAS2	34,22	5	15			0	1
RPS20	25,21	4	29			0	1
SRSF7	19,75	4	20			0	1
BUD31	13,89	1	3			0	1
EIF6	26,94	4	33			0	1
RPL34	13,68	3	11			0	1
RRP12	5,17	4	5			0	1
ILF3	5,26	4	6			0	1
ILF2	7,69	2	4			0	1
IMP3	8,15	1	2			0	1
NID2	21,82	15	48			0	1
CCDC71	4,50	2	3			0	1
XAB2	1,99	1	2			0	1
SDC4	19,19	3	7			0	1
HNRNPR	12,01	5	10			0	1
HIST1H2BO	60,32	9	612	11,90	1	8	1
PARP1	15,38	8	20			0	1
SRRM2	13,34	23	80			0	1
RRS1	44,11	16	91			0	1
HNRNPU	15,76	7	24			0	1
SRSF5	3,31	1	3			0	1
SEPT11	11,42	4	6			0	1
OIP5	7,86	1	2			0	1
MRPS22	8,89	2	3			0	1
SART1	14,63	7	12			0	1
HIST3H3	58,09	11	99	6,62	1	1	1
LYAR	9,50	2	3			0	1
SNRPC	13,21	1	3			0	1
SF3B2	5,36	2	4			0	1
FTSJ3	21,49	10	23			0	1
LEMD2	9,74	2	5			0	1
MISP	33,43	12	40			0	1
AQR	5,52	4	11			0	1

Supplementary table 1. Continuation.

GENE	HMGB1 IP			Rabbit IP			SP
	Coverage	Peptides	Spectra	Coverage	Peptides	Spectra	
RPL4	35,83	21	201			0	1
RPL27A	32,43	4	24	7,43	1	3	1
RPL5	30,30	9	36			0	1
SUGP2	11,92	5	13			0	1
RPL21	33,13	5	76	27,50	3	7	1
RPL28	7,30	1	26	8,03	1	2	1
PRPF8	25,44	39	101			0	1
SRSF3	28,66	4	14			0	1
ACTG2	9,31	3	7	7,18	2	2	0.99
ACTBL2	6,38	2	5	7,18	2	2	0.94
RPS26	13,04	1	5	13,04	1	2	0.94
RPL29	9,43	1	7	9,43	1	3	0.89
HIST1H1E	33,33	14	123	26,48	9	49	0.71

Supplementary table 2. HMGB1 interacting proteins in the cytoplasmic fraction of SKOV-3 cells.

GENE	HMGB1 IP			Rabbit IP			SP
	Coverage	Peptides	Spectra	Coverage	Peptides	Spectra	
KRT16	30,02	11	25	5,92	3	4	1
RPL17	18,48	3	5			0	1
RPS26	13,04	1	3			0	1
RPS28	17,39	1	2			0	1
RPL36	21,90	3	5			0	1
RPS17L	23,70	2	4			0	1
LACTB	4,20	2	3			0	1
RPL7A	29,32	8	20	4,89	1	1	1
RPL12	9,70	1	5			0	1
PABPC1	10,69	6	11			0	1
HRNR	1,26	2	32			0	1
KRT9	56,82	32	394	41,73	15	64	1
MAP2	2,57	3	4			0	1
RPS6	18,07	5	11			0	1
SEPT7	66,13	32	403			0	1
CTTN	44,55	29	225			0	1
RPL10A	17,97	4	11			0	1
RPL24	13,38	2	3			0	1
PURA	27,64	2	5			0	1
RPS3	23,05	4	8	5,35	1	1	1
FAU	18,64	2	8			0	1
RPL19	13,27	3	10			0	1
NCL	11,69	6	15			0	1
SEPT2	80,33	27	484			0	1
PLOD3	9,21	5	12			0	1
LRRC16A	7,08	7	13			0	1
TUBG1	26,83	6	17			0	1
RPL13A	15,27	3	9			0	1
SEPT6	36,87	18	108			0	1
KRT2	49,61	24	161	40,69	19	61	1
RPLP1	14,04	1	3			0	1
RPLP0	25,87	5	10			0	1
RPS19	22,76	3	4			0	1
RPL32	11,11	1	3			0	1
SEPT9	70,82	50	488			0	1
RPL27A	7,43	1	3			0	1
IGF2BP2	24,71	11	25	2,00	1	1	1
RPS11	18,99	3	9			0	1
RPL26	6,21	1	2			0	1

Supplementary table 2. Continuation.

GENE	HMGB1 IP			Rabbit IP			SP
	Coverage	Peptides	Spectra	Coverage	Peptides	Spectra	
YBX1	33,95	5	28	15,12	2	6	1
RPL11	12,92	2	5			0	1
MZT2B	35,44	3	7			0	1
ZNF609	5,24	4	7			0	1
SEPT10	52,42	18	103			0	1
NEDD1	22,27	9	29			0	1
RPL8	4,28	1	2			0	1
AHNAK	39,46	95	259			0	1
P4HA1	8,99	2	2			0	1
RPL3	15,88	5	21	6,70	1	3	1
CAPRIN1	5,92	1	2			0	1
RPL15	13,73	3	6			0	1
MVP	21,05	9	20			0	1
SEPT5	12,20	3	7			0	1
RPS3A	12,50	3	7			0	1
UHRF1BP1L	3,55	3	6			0	1
KRT10	42,64	29	179	32,71	15	61	1
MOV10	4,99	3	5			0	1
RPL10	6,54	2	7			0	1
RPS23	7,69	1	2			0	1
RPL18	25,00	4	11			0	1
RPS20	19,33	2	3			0	1
RPS7	32,47	3	10			0	1
HSPA8	15,48	7	16	2,01	1	2	1
RPS2	11,60	3	6			0	1
PCF11	0,58	1	2			0	1
CEP55	13,58	4	15			0	1
RPL35	21,95	3	7			0	1
RPL34	6,84	1	3			0	1
LUZP1	17,38	14	35			0	1
RPLP2	42,61	2	9			0	1
RASAL2	1,14	1	2			0	1
PABPC4	11,02	5	9			0	1
RPL31	18,40	2	5			0	1
RPL35A	9,09	1	2			0	1
RPL23A	13,46	2	5			0	1
PLOD1	28,47	15	60			0	1
RPS18	19,08	3	8			0	1
RPL23	12,86	1	6			0	1
MAP4	3,13	3	6			0	1
RPS4X	13,69	3	4			0	1
ACACA	22,63	37	88			0	1

Supplementary table 2. Continuation.

GENE	HMGB1 IP			Rabbit IP			SP
	Coverage	Peptides	Spectra	Coverage	Peptides	Spectra	
SEPT11	50,82	27	203			0	1
RPS13	12,58	2	5			0	1
RPL6	37,85	9	18			0	1
SEPT8	47,62	20	168			0	1
STAU1	6,07	2	3			0	1
RPL14	14,88	3	6			0	1
COLGALT1	8,36	4	9			0	1
RPL29	9,43	1	3			0	1
RPS12	22,73	2	4			0	1
RPS10	5,45	1	2			0	1
RPS9	21,13	5	6			0	1
RPL13	24,17	5	13	5,21	1	2	1
RPS8	18,75	3	10			0	1
RPL4	19,44	6	13			0	1
RPS15A	6,92	1	2			0	1
RPS16	30,82	5	7			0	1
KRT14	31,99	12	37	13,35	5	10	1
CAPZA1	8,39	2	3			0	1
RPS15	15,17	1	8			0	1
RPL27	27,94	4	8			0	1
RPS24	9,02	2	2			0	1
KRT1	61,80	45	598	48,29	23	102	1
RPL21	27,50	3	8			0	1
RBPMS	22,96	3	6			0	1
RPL7	35,89	8	23			0	1
HMGB1	27,91	14	193			0	1
HSPA5	15,29	7	11			0	1
ANKRD26	3,22	5	7			0	1
RPS25	15,20	2	5	8,00	1	1	0.99
KRT5	27,29	16	51	14,41	9	19	0.99
ACTBL2	9,04	2	5	4,26	1	1	0.99
KRT77	5,36	4	65	5,36	4	25	0.96
P02668	16,57	2	4	5,92	1	1	0.96
ACTG2	8,51	2	4	4,26	1	1	0.96
RPL38	18,57	1	3	14,29	1	1	0.89
RPS27	29,76	2	5	15,48	1	2	0.79

Supplementary table 3. HMGB1 interacting proteins in the nuclear fraction of PC-3 cells.

GENE	HMGB1 IP			Rabbit IP			SP
	Coverage	Peptides	Spectra	Coverage	Peptides	Spectra	
TRIM41	4,60	2	3			0	1
RPL36	31,43	7	148	23,81	2	3	1
RPS6	26,91	8	92	20,88	6	23	1
RPL23A	35,90	8	39	8,33	1	3	1
HDAC2	11,27	5	14			0	1
HIST2H2AB	72,31	8	227	29,23	2	10	1
CTTN	27,09	10	49			0	1
MRPS17	6,92	1	2			0	1
MRPS7	9,09	2	3			0	1
HNRNPC	31,37	10	112	5,23	1	2	1
ZNF800	4,82	2	15			0	1
H2AFZ	56,25	6	278	53,91	5	17	1
INCENP	3,16	2	3			0	1
LMNA	3,77	2	3			0	1
RPL13A	36,45	10	120	22,66	6	12	1
MRPS18B	12,79	1	2			0	1
SEPT6	13,36	4	18			0	1
RPLP1	14,04	1	13			0	1
RPLP2	80,00	8	64	28,70	1	4	1
RPLP0	40,69	9	166	11,04	3	6	1
RPP38	3,89	1	4			0	1
RBX1	17,59	2	5			0	1
SEPT11	11,66	5	23			0	1
NOP56	11,95	5	13			0	1
ANXA2	10,91	3	11			0	1
RSL1D1	23,27	9	27			0	1
HNRNPM	40,14	16	234	13,70	7	10	1
YBX1	9,26	1	8			0	1
RPL11	21,35	4	47	22,47	4	8	1
TTF1	1,33	1	4			0	1
PRPF19	36,51	10	35			0	1
TRIP12	1,51	2	5			0	1
RPL3	32,51	12	386	24,81	7	15	1
BANF1	26,97	1	20			0	1
HNRNPA1	4,30	1	4			0	1
RPL7L1	5,69	1	2			0	1
HIST1H4A	65,05	14	1199	57,28	10	56	1
MTA2	7,04	4	7			0	1
RPL10	22,90	6	72	15,42	4	12	1
HIST1H2BL	57,14	11	632	27,78	4	25	1
RPS21	19,28	2	5			0	1
ZNF326	6,01	2	2			0	1

Supplementary table 3. Continuation.

GENE	HMGB1 IP			Rabbit IP			SP
	Coverage	Peptides	Spectra	Coverage	Peptides	Spectra	
HSPA8	16,25	7	25			0	1
HIST2H3A	66,91	15	278	24,26	4	11	1
KRR1	17,85	5	9			0	1
RPL31	33,60	4	29	17,60	2	4	1
RPL35A	32,73	5	23			0	1
RPS23	16,08	3	32	16,08	2	4	1
RPS14	41,72	8	126	25,17	3	8	1
RPS18	59,21	11	146	41,45	7	18	1
SNRNP200	2,06	4	6			0	1
H1FX	8,45	1	3			0	1
NPM1	47,28	12	303	36,39	5	17	1
SSRP1	5,08	2	19			0	1
ACTBL2	11,17	3	8	4,26	1	2	1
NAT10	19,32	13	47			0	1
CHTOP	16,94	3	8	6,45	1	2	1
RPL6	52,08	19	260	30,21	8	26	1
NEFL	1,66	1	5			0	1
FYTTD1	6,92	2	2			0	1
MRPS28	5,35	1	2			0	1
RRP1	5,42	2	2			0	1
H2AFY	27,42	5	49	2,42	1	1	1
RPF2	15,69	4	8			0	1
GRAMD3	13,66	3	11			0	1
RPS15	37,24	4	65	15,17	1	9	1
RPL27	49,26	7	90	20,59	3	4	1
RPS24	39,85	7	91	15,04	3	5	1
EIF4A3	28,47	10	37	3,16	1	2	1
NUSAP1	5,67	2	2			0	1
VCL	1,32	1	3			0	1
HIST2H2AA3	70,77	11	851	57,69	7	39	1
SNRPD3	15,08	2	2			0	1
TCOF1	4,17	5	9			0	1
SNRPD1	16,81	1	5			0	1
MYBBP1A	10,54	8	22			0	1
MSL2	7,28	3	8			0	1
MATR3	27,27	12	63			0	1
ARL6IP4	4,51	1	3			0	1
RPS17L	45,93	6	65	7,41	1	1	1
ACIN1	1,34	1	2			0	1
HDAC1	11,41	5	15			0	1
MRPS23	7,37	2	3			0	1
TRA2B	14,93	3	14			0	1

Supplementary table 3. Continuation

GENE	HMGB1 IP			Rabbit IP			SP
	Coverage	Peptides	Spectra	Coverage	Peptides	Spectra	
SEPT7	25,17	8	62			0	1
HIST3H2BB	55,56	8	513	26,19	4	24	1
MRPS26	8,78	1	6			0	1
PKP1	6,56	4	8			0	1
RPL19	22,96	6	101	17,86	3	7	1
NOL6	11,78	7	19			0	1
BRIX1	45,61	10	126			0	1
RPL10L	23,36	3	27	5,14	1	1	1
CSE1L	0,82	1	23			0	1
SART1	7,00	3	7			0	1
RPL18A	32,39	8	39	9,66	2	4	1
LLPH	23,26	2	12			0	1
CLPX	22,27	9	17			0	1
RPL15	34,31	7	179	25,98	5	10	1
SPATS2L	13,08	5	21			0	1
HNRNPL	10,87	2	5			0	1
SRP9	22,09	2	7			0	1
TRIM28	25,15	11	55			0	1
RPS2	26,28	10	71	11,60	3	8	1
ZNF512B	15,81	10	25			0	1
RPL35	22,76	5	82	21,95	3	12	1
HNRNPA2B1	20,96	4	28	12,75	3	4	1
CCDC137	9,69	2	3			0	1
RALY	31,70	7	47			0	1
MIS18A	4,29	1	4			0	1
BAZ1B	2,49	3	3			0	1
HMGA1	23,36	1	12			0	1
SRSF10	10,69	2	13			0	1
HSPA9	2,06	1	2			0	1
SYNCRIP	6,74	5	13			0	1
RPS4X	46,39	13	190	22,81	5	9	1
HIST1H1D	32,13	12	169	26,70	9	52	1
HIST1H3A	66,91	15	297	47,79	5	17	1
RPS13	46,36	9	83	31,13	5	12	1
MKI67	3,78	8	13			0	1
RPS29	33,93	2	9	14,29	1	2	1
C7orf50	35,57	3	6			0	1
RRP8	3,51	1	2			0	1
CEBPZ	2,18	2	4			0	1
RBBP4	13,18	4	9			0	1
BCLAF1	7,50	4	5			0	1
SRP14	20,59	2	14			0	1

Supplementary table 3. Continuation.

GENE	HMGB1 IP			Rabbit IP			SP
	Coverage	Peptides	Spectra	Coverage	Peptides	Spectra	
HP1BP3	18,08	7	20	6,33	2	2	1
BOP1	1,34	1	2			0	1
SPTBN1	0,42	1	2			0	1
RPS11	38,61	6	47	27,85	4	12	1
RPS12	37,12	6	56	22,73	2	8	1
RPS10	43,03	8	53	24,24	4	10	1
RPS5	21,08	5	15			0	1
RPS9	42,27	13	79	15,46	4	5	1
RPL13	45,50	11	119	45,02	11	31	1
GRAMD1B	2,98	1	4			0	1
MPHOSPH8	8,14	4	6			0	1
CDC5L	14,84	7	12			0	1
CCDC71	5,35	2	4			0	1
CBX3	8,74	1	2			0	1
HMGB1	23,26	10	78			0	1
GNL3	8,56	3	11	3,10	1	1	1
MRPS5	3,26	1	2			0	1
RPS25	24,00	3	25	7,20	1	2	1
RPL17	41,30	9	114	21,20	4	9	1
MAGOH	19,18	2	3			0	1
RPS26	13,04	1	15	20,87	2	5	1
RPS28	59,42	7	28	34,78	2	5	1
HIST1H2AC	70,77	9	724	57,69	7	34	1
HNRNPF	7,23	2	7			0	1
RPL32	25,19	6	60	12,59	2	6	1
HIST1H2BJ	57,14	9	553	26,19	4	24	1
RPL8	26,85	9	65			0	1
HNRNPH1	14,25	5	19			0	1
EFTUD2	1,34	1	2			0	1
C10orf2	30,70	17	134			0	1
ALYREF	28,40	6	26			0	1
ATAD2	20,29	19	80			0	1
PPHLN1	5,46	3	3			0	1
RPS3	62,14	14	298	40,74	7	15	1
RPL22	62,50	7	68	19,53	2	6	1
SUPT16H	19,20	15	44			0	1
RPL9	28,13	5	75	5,73	1	4	1
SRSF9	10,86	2	4			0	1
RPL7A	37,22	15	192	21,80	7	13	1
RPL26	42,76	9	63	11,72	2	3	1
NUMA1	13,85	17	46			0	1
RRP15	3,90	1	2			0	1

Supplementary table 3. Continuation.

GENE	HMGB1 IP			Rabbit IP			SP
	Coverage	Peptides	Spectra	Coverage	Peptides	Spectra	
ING4	11,24	2	5			0	1
SEPT10	6,83	3	8			0	1
RBM28	4,08	2	4			0	1
AHNAK	15,69	34	82			0	1
NKTR	7,46	7	26			0	1
RBMX	22,76	9	70			0	1
MSL1	5,70	2	9			0	1
PNN	12,41	6	36	2,37	1	2	1
PHIP	21,03	26	192			0	1
TOP2B	10,89	12	31			0	1
MRPL12	40,91	4	8			0	1
PPAN	5,29	2	3			0	1
RPL18	41,49	11	111	28,72	5	12	1
THRAP3	5,45	3	16	2,09	1	2	1
RPS27	30,95	3	12	15,48	1	2	1
TOP1	28,50	18	168	2,09	1	2	1
H2AFY2	22,58	4	28	2,42	1	1	1
RRP1B	26,12	10	28	1,45	1	1	1
TOP2A	11,95	13	33			0	1
DAP3	3,77	1	2			0	1
RPSA	18,31	4	18	2,71	1	1	1
RPL23	19,29	5	66	19,29	4	10	1
H1F0	19,07	4	32	19,59	4	8	1
HNRNPA3	10,05	2	4			0	1
SON	5,65	7	12			0	1
LARS	0,85	1	2			0	1
GTPBP4	3,47	2	4			0	1
SEPT8	3,52	2	10			0	1
RPL14	31,63	7	116	19,53	3	7	1
SARNP	13,81	2	3			0	1
RPL37A	29,35	2	40	19,57	1	3	1
PLRG1	10,12	2	3			0	1
RPS7	51,03	11	182	5,67	1	2	1
RPS8	39,90	8	91	32,69	6	15	1
RPS15A	43,85	7	50	6,92	1	2	1
RPS16	58,22	11	140	42,47	7	18	1
CCDC86	32,22	7	15			0	1
SEPT9	36,01	17	104			0	1
GPATCH4	1,79	1	2			0	1
RPL7	50,00	17	188	23,39	7	14	1
HIST1H1C	33,33	12	176	27,70	10	61	1
CENPC	2,23	2	4			0	1

Supplementary table 3. Continuation.

GENE	HMGB1 IP			Rabbit IP			SP
	Coverage	Peptides	Spectra	Coverage	Peptides	Spectra	
UBTF	4,45	3	8	2,36	1	2	1
SLTM	4,74	4	9			0	1
SDC1	17,74	4	10			0	1
HIST1H1E	36,53	13	179	26,94	10	62	1
RPL12	24,24	3	196	18,79	2	7	1
HRNR	2,88	2	10			0	1
NOP58	4,73	2	3			0	1
H3F3A	66,91	15	218	24,26	4	11	1
RPL10A	36,87	11	261	23,96	5	15	1
RPL24	29,94	7	49	21,66	4	10	1
UTP18	2,34	1	2			0	1
FAU	20,34	4	18	18,64	2	5	1
NCL	31,27	18	178	24,23	13	37	1
SEPT2	30,19	9	50			0	1
KIAA0020	2,47	1	2			0	1
RBM14	12,26	6	18			0	1
TUBA1C	7,35	2	4			0	1
CBX5	4,19	1	2			0	1
RBBP7	12,94	4	9			0	1
RUVBL1	5,04	2	3			0	1
RPS19	55,86	10	74	20,00	3	6	1
AMOTL2	1,16	1	2			0	1
IGF2BP2	4,84	2	4			0	1
ATRX	3,57	6	10			0	1
SMARCA1	3,42	4	5			0	1
AKAP8	1,59	1	3			0	1
TARDBP	6,52	2	5			0	1
NHP2L1	9,38	1	3			0	1
MLLT6	3,02	2	3			0	1
HSPA1A	4,52	2	7			0	1
NOP2	19,21	9	21			0	1
RNPS1	7,54	2	4			0	1
MLLT10	6,46	3	8			0	1
RPS3A	47,73	16	78	20,83	6	12	1
UBC	43,36	4	7			0	1
TRA2A	4,96	1	6			0	1
RPL30	10,43	2	65	10,43	1	4	1
BCAS2	44,00	6	12			0	1
RPS20	25,21	3	71	22,69	2	4	1
SRSF7	19,75	3	20			0	1
PCF11	0,90	1	3			0	1
EIF6	26,94	4	15			0	1

Supplementary table 3. Continuation.

GENE	HMGB1 IP			Rabbit IP			SP
	Coverage	Peptides	Spectra	Coverage	Peptides	Spectra	
RPL36A	28,30	3	6			0	1.0
RPL34	14,53	4	19	6,84	1	3	1.0
KRI1	8,39	4	6			0	1.0
RRP12	4,47	4	6			0	1.0
ILF3	23,94	15	122			0	1.0
ILF2	20,77	6	35			0	1.0
SDC4	18,69	3	6			0	1.0
PRPF3	10,25	4	10			0	1.0
HNRNPR	16,90	11	51			0	1.0
POP1	4,00	3	7			0	1.0
PARP1	30,18	21	93			0	1.0
SRRM2	5,27	9	18			0	1.0
RRS1	16,71	3	24			0	1.0
HNRNPU	29,82	24	310			0	1.0
SRSF6	5,23	2	5			0	1.0
MIS18BP1	6,36	3	8			0	1.0
ZNF346	4,42	1	3			0	1.0
OIP5	13,97	2	3			0	1.0
MRPS22	3,33	1	3			0	1.0
PDCD11	2,62	5	8			0	1.0
STAU1	2,77	1	2			0	1.0
LYAR	3,69	1	2			0	1.0
PPP1CC	7,43	2	4			0	1.0
FTSJ3	19,36	11	42			0	1.0
LEMD2	12,13	3	4			0	1.0
MISP	1,62	1	2			0	1.0
RPL4	38,17	21	310	23,65	9	23	1.0
RPL27A	39,86	7	67	23,65	4	13	1.0
RPL5	30,30	13	98	4,71	1	3	1.0
RPL21	33,13	4	80	21,25	4	13	1.0
RPL28	29,93	3	38	15,33	2	5	1.0
NOLC1	6,72	4	6	1,57	1	1	1.0
APOBEC3C	17,89	3	22	6,32	1	2	1.0
PRPF8	4,03	4	4			0	1.0
CLPP	16,61	2	3			0	1.0
SRSF3	28,66	3	8			0	1.0
RPL29	9,43	1	9	9,43	1	3	0.99

Supplementary table 4. HMGB1 interacting proteins in the cytoplasmic fraction of PC-3 cells.

GENE	HMGB1 IP			Rabbit IP			SP
	Coverage	Peptides	Spectra	Coverage	Peptides	Spectra	
RPS17L	16,30	1	3				1
RPL7A	12,03	3	7	4,89	1	1	1
PABPC1	28,62	13	36	4,09	3	4	1
SEPT7	70,71	37	686				1
CTTN	53,27	36	312				1
RPL24	13,38	2	3				1
FAU	18,64	2	6				1
MVB12A	13,19	2	5			0	1
SEPT2	81,72	28	715			0	1
TUBG1	21,95	6	10			0	1
RPL13A	15,27	3	3				1
SEPT6	43,55	23	184			0	1
RPLP2	28,70	1	3			0	1
RPLP0	7,26	2	3			0	1
SEPT9	70,48	58	1007			0	1
IGF2BP2	35,06	17	75	4,17	2	3	1
PCBP2	17,53	3	6			0	1
TSG101	17,44	4	9			0	1
SEPT10	68,06	25	263			0	1
NEDD1	17,42	6	16			0	1
AHNAK	31,66	70	163			0	1
PRRC2C	1,48	3	4			0	1
CAPRIN1	12,27	5	12			0	1
SEPT5	21,14	7	26			0	1
RPL18	18,09	3	4			0	1
RPS7	32,47	3	8			0	1
CEP55	49,78	20	134			0	1
TJP1	9,73	11	16			0	1
LUZP1	5,86	4	7			0	1
YBX3	30,11	7	14	6,18	2	3	1
KIAA1671	9,75	11	21				1
PLIN4	20,56	14	51			0	1
VPS37B	35,79	5	17			0	1
SYNCRIP	6,10	3	5			0	1
ACACA	12,87	21	46			0	1
SEPT11	52,91	31	282			0	1
RPL6	9,03	3	5			0	1
SEPT8	36,65	16	119			0	1
CAPZB	7,22	1	3			0	1
RPL29	9,43	1	3			0	1
CNOT1	1,18	2	3			0	1

Supplementary table 4. Continuation.

GENE	HMGB1 IP			Rabbit IP			SP
	Coverage	Peptides	Spectra	Coverage	Peptides	Spectra	
VPS28	30,77	4	12			0	1
RPL13	20,38	4	10			0	1
RPL7	23,79	5	8			0	1
CALM1	20,13	1	3			0	1
HMGB1	32,09	13	306			0	1
HSPA5	17,74	8	15	1,68	1	2	1
ANKRD26	10,77	13	21			0	1
CNOT2	3,15	1	2			0	0.99
RPL12	9,70	1	2			0	0.99
HNRNPK	3,67	1	2			0	0.99
RPL19	8,67	1	2			0	0.99
RPL11	5,06	1	2			0	0.99
MZT2B	13,92	1	2			0	0.99
CHMP4B	6,25	1	2			0	0.99
RPL15	6,86	1	2			0	0.99
BANF1	26,97	1	6			1	0.99
MOV10	2,89	2	2			0	0.99
RPL34	6,84	1	2			0	0.99
RPL31	7,20	1	2			0	0.99
RPL35A	9,09	1	2			0	0.99
TOP1	2,09	1	2			0	0.99
PTBP1	2,07	1	2			0	0.99
RPS4X	12,17	2	2			0	0.99
RPS15A	13,85	2	2			0	0.99
RPL28	8,03	1	2			0	0.99
SOGA1	1,34	2	2			0	0.99
CNOT3	2,52	1	2			0	0.99
STAU2	4,04	2	2			0	0.99
UPF1	4,69	3	4			1	0.91
RPS8	12,50	2	4	7,21	1	1	0.91
RPS6	15,26	3	9	9,24	2	3	0.9
RPS19	27,59	4	9	12,41	2	3	0.9
RPS11	11,39	2	6	6,96	1	2	0.84
RPS20	22,69	2	6	12,61	1	2	0.84
RPS2	11,60	3	8	4,10	1	3	0.72

Supplementary table 5. THOC5 interacting proteins in PC-3.

GENE	THOC5 IP			Rabbit IP			SP
	Coverage	Peptides	Spectra	Coverage	Peptides	Spectra	
TUBA4A	34,38	11	46	12,28	3	13	1
CCT6A	7,72	3	5				1
TPT1	27,33	1	5				1
KRT9	44,46	19	73	22,63	7	20	1
HNRNPK	21,60	7	19	4,97	1	3	1
CTTN	6,36	1	4				1
TUBB6	13,45	6	17	5,38	2	4	1
EIF4G1	1,19	1	2				1
PSMD2	3,52	2	3				1
SRP68	7,02	2	6				1
PRDX6	39,73	6	14	4,02	1	1	1
HNRNPC	16,01	4	7				1
KRT6B	43,26	23	99	1,60	1	1	1
RPLP2	28,70	1	3				1
RPLP0	19,87	5	8				1
HNRNPM	20,27	10	19	4,25	2	3	1
TMSB4X	31,82	1	3				1
PCBP1	14,33	4	6				1
GLRX3	7,76	1	2				1
SF3B1	1,23	1	2				1
BANF1	26,97	1	4				1
SNRNP70	7,78	2	3				1
HNRNPA1	25,81	7	20				1
ASPH	2,37	1	3				1
TPM4	8,06	1	2				1
RPS21	12,05	1	2				1
HSPA8	37,77	20	69	19,04	10	20	1
KCTD3	18,65	12	41				1
POLDIP3	6,41	2	4				1
CCT5	11,09	2	4				1
HIST2H3A	47,79	5	23	13,24	2	5	1
SAR1A	17,17	3	5				1
SEPT9	21,33	7	13	2,56	1	2	1
THOC5	44,22	26	114				1
RPL35A	9,09	1	3				1
HNRNPUL1	8,76	5	7				1
PPA1	7,61	1	3				1
ZBTB45	10,37	4	18				1
EPRS	4,30	4	8				1
WIZ	3,69	3	4				1
MYH9	14,69	19	50	6,02	7	15	1
NPM1	50,00	9	36	21,77	3	9	1

Supplementary table 5. Continuation.

GENE	THOC5 IP			Rabbit IP			SP
	Coverage	Peptides	Spectra	Coverage	Peptides	Spectra	
RBM8A	14,94	1	3				1
CHTOP	16,94	3	6	5,24	1	1	1
RPL6	29,17	8	16	11,46	3	3	1
SRSF1	17,34	3	6				1
NCOA1	4,65	4	7				1
KARS	2,68	1	2				1
H2AFY	7,80	2	5				1
KRT6A	45,39	24	103	1,60	1	1	1
KRT14	48,09	23	80	3,81	2	3	1
CAPZA1	11,19	2	5				1
MTHFD1	2,89	2	3				1
RPL27	22,06	3	6				1
RPS24	15,04	3	8				1
KRT1	48,45	35	201	21,89	10	22	1
EIF4A3	21,90	7	17	3,89	1	3	1
EIF2S1	6,98	2	4				1
SNRPD2	9,32	2	3				1
TUBB	60,14	20	112	30,63	10	37	1
RAB11A	15,74	3	4				1
MATR3	5,08	2	4				1
KRT77	5,36	3	23	3,63	2	4	1
UBA1	6,71	4	6				1
THOC2	26,99	38	153				1
PDIA3	11,49	5	8				1
CALR	15,83	3	7				1
SUPT16H	2,20	2	3				1
HDAC1	4,98	2	3				1
ACTN2	3,24	3	4				1
PPP1CB	8,87	2	4				1
TRA2B	11,46	3	4				1
SEPT7	6,41	2	3				1
SRGAP1	23,96	19	49				1
LRRC59	22,15	5	10				1
TCP1	13,85	4	9				1
TAF15	2,87	2	3				1
LSM14B	7,79	2	6				1
NACA2	6,98	1	3				1
PDLIM1	4,86	1	2				1
PPP1CA	5,45	1	2				1
CSE1L	3,71	3	7				1
SLC25A5	16,44	4	7				1
RPS15	36,55	3	10				1

Supplementary table 5. Continuation.

GENE	THOC5 IP			Rabbit IP			SP
	Coverage	Peptides	Spectra	Coverage	Peptides	Spectra	
ATP5A1	13,74	6	12				1
RPL15	14,71	3	6				1
HNRNPL	8,66	2	6				1
KLF4	14,42	4	7				1
DARS	10,18	3	6				1
YWHAZ	29,39	6	19	12,65	3	6	1
SRP9	12,79	1	2				1
RALY	15,69	3	5				1
TRIM28	13,65	5	11				1
RPN1	2,47	1	2				1
SET	9,31	2	4				1
ISOC2	23,90	2	5				1
HNRNPA2B1	42,21	12	44	7,08	2	3	1
NCOA5	13,30	3	9				1
PFN2	10,00	1	2				1
CPOX	10,13	3	9				1
HMGA1	23,36	1	11				1
KRT17	33,80	18	45	2,08	1	1	1
SAFB	3,61	2	3				1
GOLGA3	1,87	2	4				1
RAI1	9,23	8	18				1
RBM3	35,67	3	13				1
CAPZA2	11,19	2	3				1
RBBP4	9,65	2	3				1
BCLAF1	5,65	3	8				1
SRP14	19,12	2	5				1
ITGB1	1,25	1	2				1
TPD52	30,36	2	3				1
CBX3	7,65	1	3				1
PLP2	8,55	1	2				1
SFPQ	37,20	24	92	2,12	1	2	1
SPTAN1	0,77	1	2				1
KRT16	58,56	31	150	3,81	2	3	1
RPL17	21,20	4	8	4,89	1	1	1
RTN4	6,71	3	9				1
GSTP1	27,14	3	5				1
PLEC	25,58	88	175	11,14	34	53	1
EIF4H	14,92	2	3				1
HNRNPH1	13,36	4	11	3,56	1	1	1
EFTUD2	7,10	4	6				1
SNRPE	17,39	1	2				1
STIP1	6,45	2	4				1

Supplementary table 5. Continuation.

GENE	THOC5 IP			Rabbit IP			SP
	Coverage	Peptides	Spectra	Coverage	Peptides	Spectra	
ALYREF	47,86	7	30				1
RAB1B	32,34	5	14	8,46	1	1	1
ANXA1	15,61	3	5				1
RPS3	46,09	9	26	12,76	3	5	1
PTMA	12,61	1	2				1
SRSF2	18,10	2	3				1
SRP72	2,53	1	2				1
HYLS1	12,71	2	3				1
SRSF9	8,14	2	2				1
ALDH1A3	15,04	4	8				1
QARS	2,32	1	2				1
PAICS	12,24	4	9	2,59	1	2	1
HSPB1	44,39	5	10	7,80	1	2	1
RPL26	6,21	1	2				1
NUMA1	7,19	9	16				1
SND1	13,30	8	16	2,31	1	1	1
BCAP31	5,69	1	3				1
AHNAK	13,67	20	42				1
CAPRIN1	5,92	1	2				1
RBMX	27,62	11	29	7,67	2	4	1
HCFC1	5,70	7	8				1
FARSA	2,17	1	2				1
PNN	6,14	3	7				1
RPSA	27,46	5	12				1
KRT5	25,25	15	47	1,53	1	1	1
MRPL12	23,23	2	2				1
RPL18	29,26	6	15	12,23	2	4	1
XRCC5	5,60	2	4				1
HSPD1	34,55	13	45				1
PDCD6IP	3,34	2	3				1
HNRNPDL	10,24	2	2				1
THRAP3	9,74	6	20				1
CEP170	32,77	35	102				1
RUVBL2	11,88	4	5				1
CCT3	8,99	2	3				1
TOP1	4,18	2	5				1
TMSB10	68,18	2	6				1
KRT10	50,86	31	152	8,39	4	8	1
RPL23	40,71	6	22	12,86	1	3	1
RAB1A	26,83	4	8				1
HNRNPUL2	1,87	1	2				1
RAN	28,24	6	15	9,72	2	4	1

Supplementary table 5. Continuation.

GENE	THOC5 IP			Rabbit IP			SP
	Coverage	Peptides	Spectra	Coverage	Peptides	Spectra	
H1F0	7,22	1	2				1
HNRNPA3	23,28	8	32				1
KRT8	7,87	4	10	1,86	1	1	1
KRT18	35,12	9	16	2,09	1	1	1
Q8TAB7	22,94	1	2				1
THOC1	60,27	30	159				1
HSPH1	2,10	2	2				1
RBM25	3,91	2	8	2,14	1	1	1
RAB14	19,07	2	5				1
RPL37A	19,57	1	2				1
RPS7	54,64	9	41	25,26	3	4	1
RPS15A	16,92	2	4				1
VAMP3	24,00	1	2				1
THOC3	30,48	8	32				1
TUBB4B	55,06	18	91	21,12	8	30	1
ADIRF	71,05	2	6				1
ACTN4	10,21	7	11	3,51	3	3	1
CCT8	5,66	2	2				1
HSPA4	3,21	1	3				1
RAB7A	5,31	1	2				1
TMA7	15,63	1	2				1
SDC1	5,48	1	2				1
RPL7A	30,08	8	17	15,04	3	4	1
PABPC1	6,29	3	4				1
PPP1R12A	7,09	5	7				1
PKM	46,14	19	47	11,68	5	10	1
KRT7	36,25	13	31	16,42	6	7	1
HELQ	10,26	6	9				1
TMPO	6,39	2	2				1
H3F3A;H3F3B	47,79	5	22	13,24	2	5	1
RPL10A	16,13	4	8				1
CCT2	10,65	3	4				1
TFRC	3,95	2	3				1
NCL	30,00	23	110	12,96	8	19	1
IPO5	2,28	1	3				1
SEPT2	10,53	2	3				1
RBM14-RBM4	14,35	7	14				1
EIF2S3	7,84	3	4				1
NUDC	3,32	1	2				1
RUVBL1	12,28	4	8				1
KRT2	41,16	18	76	3,29	2	4	1

Supplementary table 5. Continuation.

GENE	THOC5 IP			Rabbit IP			SP
	Coverage	Peptides	Spectra	Coverage	Peptides	Spectra	
PSMC6	3,86	1	2				1
PXN	5,58	2	4				1
RPS19	37,24	7	17	20,00	3	4	1
PUF60	2,86	1	2				1
TMX1	8,21	2	3				1
PDIA6	3,18	1	2				1
TARDBP	7,25	2	3				1
SHKBP1	25,88	12	50				1
HSPA1A	14,51	7	17	6,24	3	5	1
BIN3	5,14	1	2				1
RNPS1	10,16	2	5				1
BCAS2	12,44	1	3				1
RPS20	25,21	4	15	22,69	2	3	1
SRSF7	19,75	4	8				1
NONO	42,68	19	81	4,88	1	1	1
NES	1,17	2	2				1
ILF3	10,40	6	9				1
ILF2	5,13	1	2				1
LMO7	2,44	3	4				1
RAB11FIP2	36,13	11	26				1
PTBP1	11,49	3	5				1
KHDRBS1	10,16	4	6				1
TPD52L2	14,56	1	3				1
HNRNPR	13,43	6	9				1
XRCC6	5,09	2	4				1
PARP1	4,83	4	7				1
SRRM2	5,70	10	20	0,51	1	1	1
MAP4	41,15	37	128	6,51	5	10	1
HNRNPU	24,73	13	51	6,55	2	6	1
ATP5B	20,98	7	13				1
C14orf166	12,30	2	3				1
SRSF5	3,31	1	2				1
SEPT11	7,69	2	4				1
THOC7	55,88	11	36				1
PRPF40A	7,21	5	8				1
SNRPC	13,21	1	3				1
TUBB4A	45,50	14	48	11,49	4	10	1
IGF2BP2	6,51	3	3				1
SF3B2	9,61	4	7				1
RTCB	11,29	4	5				1
MISP	6,33	3	3				1
THOC6	56,60	15	57				1

Supplementary table 5. Continuation.

GENE	THOC5 IP			Rabbit IP			SP
	Coverage	Peptides	Spectra	Coverage	Peptides	Spectra	
RPL4	22,72	6	17	7,73	2	3	1
KRT19	36,75	14	27	14,25	5	6	1
RPL5	24,58	6	11	4,38	1	1	1
CCT7	2,21	1	2				1
YWHAE	30,20	7	16	3,92	1	3	1
PSPC1	20,84	7	19				1
KPNB1	2,74	2	3				1
APOBEC3C	11,58	2	3				1
PRPF8	2,23	2	3				1
CALM1	30,87	4	17	20,13	1	2	1
S100A10	52,58	4	11				1
HSPA5	15,75	8	16	3,52	2	4	1
SRSF3	23,17	3	10				1
LMNA	6,02	3	5	2,56	1	1	0.99
RPS14	33,77	6	21	31,79	4	7	0.99
MYL6	29,14	3	8	8,61	1	2	0.99
RPS25	15,20	2	7	7,20	1	2	0.98
RPL22	51,56	4	15	31,25	3	5	0.98
EIF4A1	31,77	7	22	13,30	4	8	0.97
RPS16	42,47	7	17	24,66	3	6	0.97
RPL38	32,86	3	12	32,86	2	4	0.97
RPL11	22,47	4	9	12,92	2	3	0.96
RPL14	17,21	3	4	6,05	1	1	0.96
RPL7	34,27	9	19	16,53	3	7	0.95
RPS6	16,06	4	11	17,27	3	4	0.92
RPL23A	16,03	3	6	8,33	1	2	0.92
PGAM1	17,32	3	6	5,51	1	2	0.92
RPS9	29,90	7	11	13,40	3	4	0.92
RPL12	24,24	3	6	9,70	1	2	0.92
YWHAQ	24,49	5	11	9,80	2	4	0.92
CLIC1	23,65	3	5	4,98	1	2	0.78
YBX1	31,17	4	15	20,37	3	6	0.74

Chapter 5

A proteomic approach to the function of HMGB1 in the response of PC-3 and SKOV-3 cells to cisplatin

INTRODUCTION

Cisplatin is used in chemotherapy of prostate, ovary and other cancer types. In response to cisplatin, several cellular processes including drug uptake, activation of the DNA damage response and DNA repair, cell-cycle checkpoints, and cell death are induced. The cytotoxic effect of cisplatin has been attributed to its binding to DNA, causing structural and regulatory changes, which induce cellular death (Wang and Lippard, 2005). Cancer cells usually develop mechanisms for evading chemotherapy-induced apoptosis and other cell death pathways (Marquez and Xu, 2012) and unfortunately the efficiency of cisplatin treatment is frequently hampered by acquired resistance. The high mobility group box 1 protein (HMGB1) is a paradoxical and intriguing protein in cancer progression and therapy, which is also involved in the cellular responses to cisplatin (Kang *et al.*, 2013). HMGB1 is able to bind to cisplatin-DNA adducts with high affinity (Jamieson and Lippard, 1999).

Resistance to cisplatin depends on different mechanisms, one of them affecting DNA repair enzymes, which are able to remove lesions caused by cisplatin on DNA (Wang and Lippard, 2005). The mechanism of DNA repair is however inhibited by HMGB proteins, which contribute to cytotoxicity both *in vitro* (Huang *et al.*, 1994; Malina *et al.*, 2002; Ugrinova *et al.*, 2009) and *in vivo* assays (Yusein-Myashkova *et al.*, 2013).

HMGB1 expression is enhanced by cisplatin, increasing its levels in HeLa cells resistant to cisplatin, compared to non-resistant cells (Xia *et al.*, 2017). In SKOV-3 cells treated with cisplatin, HMGB1 is highly expressed in cytoplasm and nucleus (Zhou *et al.*, 2016). p53 down-regulates the activity

of the HMGB1 gene promoter, whereas p73α up-regulates the activity of this promoter. CTF2, a splicing variant of nuclear factor I (NF-I) enhances the DNA-binding activity of p53 and inhibits the DNA-binding activity of p73α. The functional interplay between CTF2/p53/p73 and HMGB1 expression is a factor controlling cell proliferation, apoptosis, DNA repair and cisplatin resistance (Uramoto *et al.*, 2003).

HMGB1 translocation from nucleus to cytoplasm also contributes to cisplatin resistance. It has been reported that inhibition of HMGB1 translocation by ethyl pyruvate treatment as well as interference of HMGB1 expression reduce cell viability and reverse cisplatin resistance in HeLa cells (Xia *et al.*, 2017).

Avoiding the mechanisms of cell death is crucial for the resistance to cisplatin. The balance between apoptosis (considered as programmed cell death) and autophagy (considered as a pathway for cell survival) determines cancer progression and response to therapy. The coordinated regulation of apoptosis and autophagy involves protein-protein interactions, as seen for the complex formed by the autophagy protein, Beclin 1, and the anti-apoptotic protein Bcl-2, which leads to inhibition of autophagy-associated cell death and stimulation of apoptosis (Marquez and Xu, 2012). Curiously, HMGB1 shares considerable sequence homology with Beclin 1, and therefore competes with Bcl-2 for the interaction with Beclin 1, directing Beclin 1 to autophagosomes and functions as an pro-autophagy effector by regulation of autophagosome formation (Kang *et al.*, 2010). In the cytoplasm, HMGB1 has a surveillance function on mitochondrial quality control (Tang *et al.*, 2011). The nuclear form of HMGB1 controls the expression of genes critical for dynamic intracellular

trafficking during autophagy (Kang *et al.*, 2011). The extracellular form of HMGB1, released with sustained autophagy, late apoptosis and necrosis, has different effects in its reduced or oxidized form over other cells. The reduced form induces Beclin 1-dependent autophagy and promotes tumor cell resistance to chemotherapeutic agents or ionizing radiation. In contrast, oxidized HMGB1 increases the cytotoxicity of these agents and induces apoptosis via the mitochondrial pathway (Tang *et al.*, 2010). HMGB1-regulated autophagy is a significant contributor in drug resistances (Pan *et al.*, 2014) including the resistance of neuroblastoma cells to cisplatin .

In SKOV-3, A2780 and OVCAR3 ovarian cancer cells, suppression of autophagy increases the sensitivity to cisplatin (Zhang *et al.*, 2012). Oppositely, active autophagy was involved in NAC1-HMGB1-mediated resistance to cisplatin (Zhang *et al.*, 2012).

In the present work we have used methods of immunoprecipitation with an HMGB1-antibody for Mass spectrometry (MS) identification of proteins that interact specifically with HMGB1 in prostate and ovary cancer cells treated with cisplatin. Results are discussed in relation to mechanisms of cisplatin resistance.

MATERIALS AND METHODS

Cell culture and cisplatin treatment

PC-3 and SKOV-3 cell lines were grown in RPMI-1640 (Thermo Fisher Scientific, Inc.) and McCoy's 5a Modified Medium (Thermo Fisher Scientific, Inc.) supplemented with 10% heat-inactivated fetal bovine

serum (Thermo Fisher Scientific, Inc.) and 1% penicillin-streptomycin (Thermo Fisher Scientific, Inc.) respectively. For cisplatin treatment the adequate volume of cisplatin diluted in 0,9 % NaCl was added to the cell culture media to a final concentration of 25 µM. Treatment was carried out for 24 hours after which cells were pelleted down and frozen.

Large-scale immunoprecipitation, mass spectrometry and data analysis

Lysates from PC-3, SKOV-3 and PC-3 cisplatin treated cells were obtained as described in chapter 4. HMGB1 Immunoprecipitation assays, mass spectrometry and data analysis were carried out as explained in chapter 4 as well.

RESULTS AND DISCUSSION

We immunoprecipitated HMGB1 and identified its binding proteins (interactants) by MS, starting from cell extracts of PC-3 cultures grown in presence or absence of cisplatin, as explained in materials and methods. After identifying proteins that only interact with HMGB1 in treated cells, we made the intersection of these results with those obtained in a second round of immunoprecipitations, using cisplatin-treated SKOV3 cells as starting material. The limited number of proteins, which are able to interact with HMGB1 in both prostate and ovary cancer cell lines treated with the drug is summarized in Table 1. With this strategy we tried to identify proteins that could be related to cisplatin response, and which were not specific of cell-line, but could be part of a general mechanism induced by cisplatin and mediated by interaction with HMGB1.

Two proteins from Table 1 had been previously related to the cellular response to cisplatin. The MSN gene, encoding for moesin, was found to be a cisplatin sensitive gene in lung cancer cell lines although its connection with HMGB1 was unknown (Li *et al.*, 2008). Importin subunit alpha-1, encoded by the *KPNA2* gene, is an adaptor for transporting several proteins to the nucleus. *KPNA2* suppression with siRNA enhances cisplatin-induced apoptosis and reduces proliferation in gastric cancer cells (Altan *et al.*, 2013). Karypherin-alpha1 binds to HMGB1 and allows its nuclear import in immune cells (Youn and Shin, 2006). PAICS, encoding an enzyme required for *de novo* purine biosynthesis, is overexpressed in tumor cells and it is capable of suppressing apoptosis in human cells (Eissmann *et al.*, 2013), although to our knowledge it has not been previously associated to cisplatin resistance or HMGB1 functions. As shown in Figure 1 the indirect, but common, STRING partner to HMGB1 and Moesin, Importin subunit alpha-1, PAICS, 14-3-3ζ and 14-3-3γ is Nuclear factor-kappa B1 (NF-κβ1), a pleiotropic transcription factor and key contributor to tumorigenesis in many types of cancer including prostate and ovary (Fu *et al.*, 2017).

Table 1. HMGB1 interactors, cisplatin-specific

ID	GENE	Protein	Function
P63104	YWHAZ	14-3-3Zeta	Adapter protein implicated in the regulation of a large spectrum of both general and specialized signaling pathways. Binds to a large number of partners, usually by recognition of a phosphoserine or phosphothreonine motif. Binding generally results in the modulation of the activity of the binding partner.
P52292	KPNA2	Importin subunit alfa-1	Functions in nuclear protein import as an adapter protein for nuclear receptor KPNB1. Binds specifically and directly to substrates containing either a simple or bipartite NLS motif. Docking of the importin/substrate complex to the nuclear pore complex (NPC) is mediated by KPNB1 through binding to nucleoporin FxFG repeats and the complex is subsequently translocated through the pore by an energy requiring, Ran-dependent mechanism. At the nucleoplasmic side of the NPC, Ran binds to importin-beta and the three components separate and importin-alpha and -beta are re-exported from the nucleus to the cytoplasm where GTP hydrolysis releases Ran from importin. The directionality of nuclear import is thought to be conferred by an asymmetric distribution of the GTP- and GDP-bound forms of Ran between the cytoplasm and nucleus.
P27348	YWHAQ	14-3-3Gamma	Adapter protein implicated in the regulation of a large spectrum of both general and specialized signaling pathways. Binds to a large number of partners, usually by recognition of a phosphoserine or phosphothreonine motif. Binding generally results in the modulation of the activity of the binding partner. Negatively regulates the kinase activity of PDPK1.
P26038	MSN	Moesin	Probably involved in connections of major cytoskeletal structures to the plasma membrane. May inhibit herpes simplex virus 1 infection at an early stage. Plays a role in regulating the proliferation, migration, and adhesion of human lymphoid cells and participates in immunologic synapse formation.
P22234	PAICS	Phosphoribosyl aminoimidazole carboxylase	IMP biosynthesis via de novo pathway. This protein is involved in step 1 of the subpathway that synthesizes 5-amino-1-(5-phospho-D-ribosyl)imidazole-4-carboxamide from 5-amino-1-(5-phospho-D-ribosyl)imidazole-4-carboxylate.

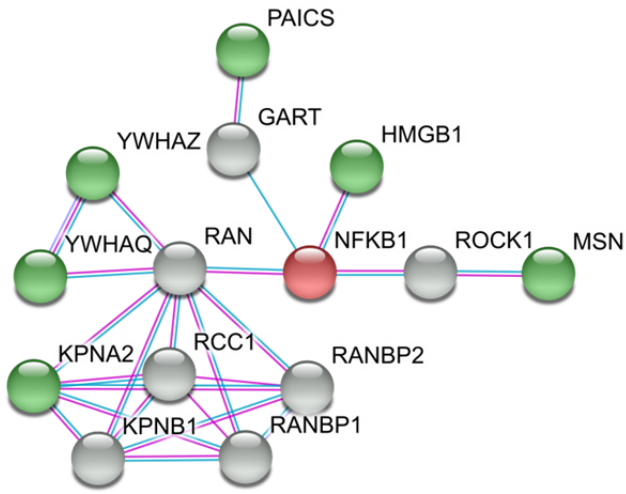

Figure 1. String interaction network of HMGB1, KPNA2, YWHAZ, YWHAQ, MSN and PAICS connected by NFκB1. HMGB1 and KPNA2 interaction was described by Youn and Shin (Youn and Shin, 2006) in immune cells however, this interaction is not recorded in STRING.

The most interesting finding was that two proteins in Table 1 belong to the 14-3-3 family. The 14-3-3 family of proteins, has been implicated in the initiation and progression of cancers including prostate and gynecologic cases (Nishimura *et al.*, 2013; Zhang *et al.*, 2015; Murata *et al.*, 2012). The 14-3-3 proteins were the first phosphoserine/phosphothreonine-binding proteins to be discovered, and interact with transcription factors, biosynthetic enzymes, cytoskeletal proteins, signaling molecules, apoptosis factors, and tumor suppressors. The 14-3-3 family members are scaffold proteins that, by phosphor-dependent protein-protein interactions, affect the cellular localization and availability of their partners. They coordinate progression of cells through the cell cycle, regulate cellular response to DNA damage, and influence life-death fate following internal injury or external cytokine-mediated signals (Gardino and Yaffe, 2011). They control apoptosis since the pro-

apoptotic Bad protein remains sequestered by 14-3-3 scaffold proteins after phosphorylation by Akt1. Bad dephosphorylation, promoted by calcineurin, releases the interaction and allows Bad interaction with mitochondria, activating apoptosis (Wang *et al.*, 1999). Besides, 14-3-3 proteins are positive regulators of the tumor suppressor p53 and small-molecule stabilization of the protein-protein interaction between 14-3-3 proteins and p53 has potential use in therapy (Doveston *et al.*, 2017).

There are seven known 14-3-3 isoforms in human with high similarity (Babula and Liu, 2015), but only two have been detected in our analysis, and they are among those less studied so far. 14-3-3ζ, encoded by YWHAZ, an androgen responsive gene, activates androgen receptor transcriptional activity, cell proliferation and survival in prostate cancer (Murata *et al.*, 2012). Indeed, 14-3-3ζ regulates multiple signaling pathways involved in cancer development, progression and therapeutic resistance and has been proposed as a novel target for cancer therapy (Matta *et al.*, 2012; Yang *et al.*, 2012). 14-3-3γ, encoded by YWHAG, has not been previously related to ovary or prostate cancers, but it has been recently shown that it is a direct target of miR-509-5p, and YWHAG knockdown inhibits cell proliferation and motility of non-small cell lung cancer (Wang *et al.*, 2017).

Looking in BIOGRID and STRING for proteins that could be common partners of HMGB1 and 14-3-3ζ or 14-3-3γ isoforms, and which could be involved in cell dead-survival decisions we found p53 (Figure 2).

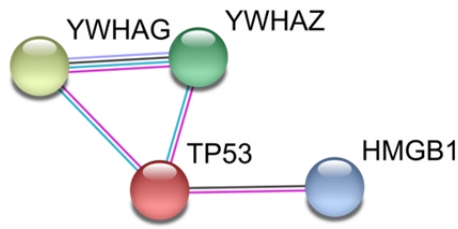

Figure 2. Common interacting protein for HMGB1, YWHAG and YWHAZ already described.

The p53 tumor-suppressor protein is a transcription factor that recognizes specific sequences of DNA and produces cell cycle arrest or apoptosis in response to genotoxic stress (Waterman *et al.*, 1998). In the nucleus, HMGB1, through the HMGB1-boxA, interacts with p53 and this interaction enhances HMGB1-binding to cisplatin-modified DNA and DNA repair (Jayaraman *et al.*, 1998; Imamura *et al.*, 2001). The structure of the HMGB1-boxA/p53(1-93) complex has been solved by nuclear magnetic resonance spectroscopy (Rowell *et al.*, 2012). The complex formed between HMGB1 and p53 also regulates the balance between tumor cell death and survival. In the cytoplasm p53 is a negative regulator of the HMGB1/Beclin 1 complex. Therefore, when p53 expression is diminished, HMGB1 promotes autophagy and tumor cell survival (Livesey *et al.*, 2012). When cells are irradiated, dephosphorylation of p53 at Ser376 is produced and this allows binding of p53 to 14-3-3 proteins, also increasing p53 affinity for DNA (Waterman *et al.*, 1998). The dimerization of 14-3-3ζ is necessary to get functional interaction with p53, but dimerization of 14-3-3ζ is impaired by phosphorylation of its Ser58 by Protein Kinase A (Gu *et al.*, 2006).

In a wide-genome search of gene sets associated with platinum resistance in ovarian cancer, p53 signaling and transforming growth factor beta (TGF-β) signaling were identified (Helleman, Jansen, *et al.*, 2010; Helleman, Smid, *et al.*, 2010). TGF-β superfamily regulates essential reproductive functions and deregulation of TGF-β signaling results in cellular and molecular deficiencies in the ovary, prostate and other organs, leading to reproductive diseases and cancer development (Stoika *et al.*, 2003; Li, 2015). In a murine model of leukemia, L1210 cells resistant to the cytotoxic action of cisplatin were also refractory to TGF-β1-dependent growth inhibition and apoptosis (Stoika *et al.*, 2003). The putative interplay between HMGB1, p53, 14-3-3 proteins and TGF-β in determining autophagy/apoptosis decisions and cisplatin responsiveness is interesting, but of great complexity because of multiple interconnections among different signaling pathways. Smad proteins are canonical TGF-βsignaling components, and 14-3-3ζ drives changes of Smad partners from p53 to Gli2, a Hedgehog pathway molecule; this change turns the function of TGF-β from a tumor suppressor, in premalignant cells, to a metastasis promoter in cancer cells (Xu *et al.*, 2015).

As suggested by the results of the proteomic analysis, cisplatin treatment of PC-3 and SKOV-3 cells, by inducing specific binding of HMGB1 to 14-3-3ζ and 14-3-3γ, might alter other specific interactions of 14-3-3ζ and 14-3-3γ with p53 and other components of TGF-β signaling pathways. We have analyzed with STRING the network of first-shell interactions of HMGB1, 14-3-3ζ, 14-3-3γ and p53 (Figure 3).

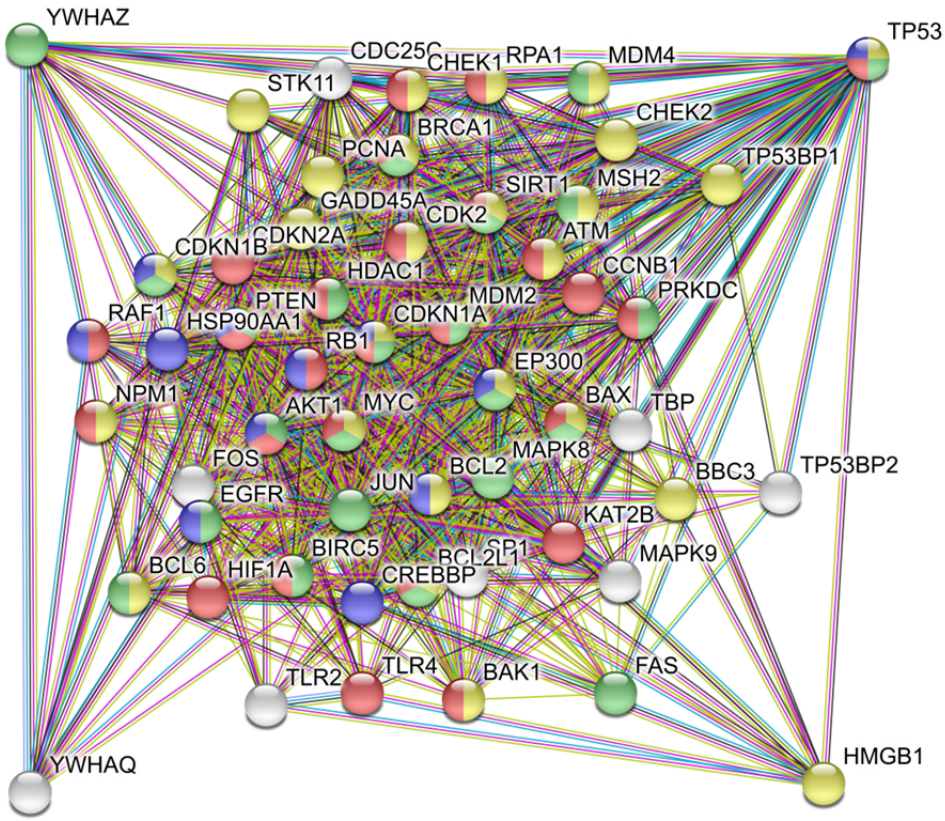

Figure 3. STRING network of first-shell interactions of HMGB1, 14-3-3ζ, 14-3-3 ζ and p53. A GO enrichment analysis was carried out using STRING, blue denotes proteins related to prostate cancer; red, regulation of cell proliferation proteins; green, proteins associated to negative regulation of apoptotic process and yellow proteins related to response to DNA damage stimulus.

GO-term enrichment analysis shows that 24% of nodes have been previously related to prostate cancer, 42% to regulation of apoptosis, 48% to cell proliferation and 50% to DNA-damage response (Figure 3). This figure clearly illustrates how the cisplatin-induced interaction between HMGB1 and 14-3-3ζ/14-3-3γ proteins may affect a complex network of broader interactions that could have implications for cell survival, although the precise mechanisms should be addressed in future

experiments. The fact that the binding of 14-3-3 proteins to their partners is generally regulated by phosphorylation of specific residues Ser and Thr, might also contribute to functional changes in the intracellular traffic of HMGB1. It has been reported that only the non-phosphorylated protein might be imported to the nucleus by Importin subunit alpha-1 that binds to HMGB1 (Youn and Shin, 2006). In support of this hypothesis, diverse anticancer agents, including cisplatin, induce HMGB1 upregulation, cytosolic HMGB1 enrichment, and the elevation of autophagic activity in human neuroblastoma cells (Wang *et al.*, 2015).

REFERENCES

Altan B, Yokobori T, Mochiki E, Ohno T, Ogata K, Ogawa A, Yanai M, Kobayashi T, Luvsandagva B, Asao T, Kuwano H. 2013. Nuclear karyopherin-alpha2 expression in primary lesions and metastatic lymph nodes was associated with poor prognosis and progression in gastric cancer. *Carcinogenesis*, **34**: 2314–2321.

Babula JJ, Liu JY. 2015. Integrate Omics Data and Molecular Dynamics Simulations toward Better Understanding of Human 14-3-3 Interactomes and Better Drugs for Cancer Therapy. *J. Genet. genomics*, **42**: 531–547.

Doveston RG, Kuusk A, Andrei S, Leysen S, Cao Q, Castaldi P, Hendricks A, Chen H, Boyd H, Ottmann C. 2017. Small-Molecule Stabilization of the p53 - 14-3-3 Protein-Protein Interaction. *FEBS Lett.*, **591**: 2449–2457.

Eissmann M, Schwamb B, Melzer IM, Moser J, Siele D, Kohl U, Rieker RJ, Wachter DL, Agaimy A, Herpel E, Baumgarten P, Mittelbronn M, Rakel S, Kogel D, Bohm S, Gutschner T, Diederichs S, Zornig M. 2013. A functional yeast survival screen of tumor-derived cDNA libraries designed to identify anti-apoptotic mammalian oncogenes. *PLoS One*, **8**: e64873.

Fu W, Zhuo ZJ, Chen YC, Zhu J, Zhao Z, Jia W, Hu JH, Fu K, Zhu SB, He J, Liu GC. 2017. NFKB1 -94insertion/deletion ATTG polymorphism and cancer risk: Evidence from 50 case-control studies. *Oncotarget*, **8**: 9806–9822.

Gardino AK, Yaffe MB. 2011. 14-3-3 Proteins as Signaling Integration Points for Cell Cycle Control and Apoptosis. *Semin. Cell Dev. Biol.*, **22**: 688–

695.

Gu YM, Jin YH, Choi JK, Baek KH, Yeo CY, Lee KY. 2006. Protein kinase A phosphorylates and regulates dimerization of 14-3-3 epsilon. *FEBS Lett.*, **580**: 305–310.

Helleman J, Jansen MP, Burger C, van der Burg ME, Berns EM. 2010. Integrated genomics of chemotherapy resistant ovarian cancer: a role for extracellular matrix, TGFbeta and regulating microRNAs. *Int. J. Biochem. Cell Biol.*, **42**: 25–30.

Helleman J, Smid M, Jansen MP, van der Burg ME, Berns EM. 2010. Pathway analysis of gene lists associated with platinum-based chemotherapy resistance in ovarian cancer: the big picture. *Gynecol. Oncol.*, **117**: 170–176.

Huang JC, Zamble DB, Reardon JT, Lippard SJ, Sancar A. 1994. HMG-domain proteins specifically inhibit the repair of the major DNA adduct of the anticancer drug cisplatin by human excision nuclease. *Proc. Natl. Acad. Sci. U. S. A.*, **91**: 10394–10398.

Imamura T, Izumi H, Nagatani G, Ise T, Nomoto M, Iwamoto Y, Kohno K. 2001. Interaction with p53 enhances binding of cisplatin-modified DNA by high mobility group 1 protein. *J. Biol. Chem.*, **276**: 7534–7540.

Jamieson ER, Lippard SJ. 1999. Structure, Recognition, and Processing of Cisplatin-DNA Adducts. *Chem. Rev.*, **99**: 2467–2498.

Jayaraman L, Moorthy NC, Murthy KG, Manley JL, Bustin M, Prives C. 1998. High mobility group protein-1 (HMG-1) is a unique activator of p53. *Genes Dev.*, **12**: 462–472.

Kang R, Livesey KM, Zeh HJ, Lotze MT, Tang D. 2011. Metabolic regulation by HMGB1-mediated autophagy and mitophagy. *Autophagy*, **7**: 1256–1258.

Kang R, Livesey KM, Zeh HJ, Loze MT, Tang D. 2010. HMGB1: a novel Beclin 1-binding protein active in autophagy. *Autophagy*, **6**: 1209–1211.

Kang R, Zhang Q, Zeh 3rd HJ, Lotze MT, Tang D. 2013. HMGB1 in cancer: good, bad, or both? *Clin. Cancer Res.*, **19**: 4046–4057.

Li CH, Cai L, Chen XS, Meng QW, Sui GJ. 2008. DDP-sensitivity-related genes in 10 lung cancer cell lines. *Zhonghua Zhong Liu Za Zhi*, **30**: 418–421.

Li Q. 2015. Inhibitory SMADs: potential regulators of ovarian function. *Biol. Reprod.*, **92**: 50.

Livesey KM, Kang R, Vernon P, Buchser W, Loughran P, Watkins SC, Zhang L, Manfredi JJ, Zeh 3rd HJ, Li L, Lotze MT, Tang D. 2012. p53/HMGB1 complexes regulate autophagy and apoptosis. *Cancer Res.*, **72**: 1996–2005.

Malina J, Kasparkova J, Natile G, Brabec V. 2002. Recognition of major DNA adducts of enantiomeric cisplatin analogs by HMG box proteins and nucleotide excision repair of these adducts. *Chem. Biol.*, **9**: 629–638.

Marquez RT, Xu L. 2012. Bcl-2:Beclin 1 complex: multiple, mechanisms regulating autophagy/apoptosis toggle switch. *Am. J. Cancer Res.*, **2**: 214–221.

Matta A, Siu KW, Ralhan R. 2012. 14-3-3 Zeta as Novel Molecular Target for Cancer Therapy. *Expert Opin. Ther. Targets*, **16**: 515–523.

Murata T, Takayama K, Urano T, Fujimura T, Ashikari D, Obinata D, Horie-Inoue K, Takahashi S, Ouchi Y, Homma Y, Inoue S. 2012. 14-3-3zeta, a Novel Androgen-Responsive Gene, is Upregulated in Prostate Cancer and Promotes Prostate Cancer Cell Proliferation and Survival. *Clin. Cancer Res.*, **18**: 5617–5627.

Nishimura Y, Komatsu S, Ichikawa D, Nagata H, Hirajima S, Takeshita H, Kawaguchi T, Arita T, Konishi H, Kashimoto K, Shiozaki A, Fujiwara H, Okamoto K, Tsuda H, Otsuji E. 2013. Overexpression of YWHAZ relates to tumor cell proliferation and malignant outcome of gastric carcinoma. *Br. J. Cancer*, **108**: 1324–1331.

Pan B, Chen D, Huang J, Wang R, Feng B, Song H, Chen L. 2014. HMGB1-mediated autophagy promotes docetaxel resistance in human lung adenocarcinoma. *Mol. Cancer*, **13**: 165.

Rowell JP, Simpson KL, Stott K, Watson M, Thomas JO. 2012. HMGB1-facilitated p53 DNA binding occurs via HMG-Box/p53 transactivation domain interaction, regulated by the acidic tail. *Structure*, **20**: 2014–2024.

Stoika R, Yakymovych M, Souchelnytskyi S, Yakymovych I. 2003. Potential role of transforming growth factor beta1 in drug resistance of tumor cells. *Acta Biochim. Pol.*, **50**: 497–508.

Tang D, Kang R, Livesey KM, Kroemer G, Billiar TR, Van Houten B, Zeh 3rd HJ, Lotze MT. 2011. High-mobility group box 1 is essential for

mitochondrial quality control. *Cell Metab.*, **13**: 701–711.

Tang D, Loze MT, Zeh HJ, Kang R. 2010. The redox protein HMGB1 regulates cell death and survival in cancer treatment. *Autophagy*, **6**: 1181–1183.

Ugrinova I, Zlateva S, Pashev IG, Pasheva EA. 2009. Native HMGB1 protein inhibits repair of cisplatin-damaged nucleosomes in vitro. *Int. J. Biochem. Cell Biol.*, **41**: 1556–1562.

Uramoto H, Izumi H, Nagatani G, Ohmori H, Nagasue N, Ise T, Yoshida T, Yasumoto K, Kohno K. 2003. Physical interaction of tumour suppressor p53/p73 with CCAAT-binding transcription factor 2 (CTF2) and differential regulation of human high-mobility group 1 (HMG1) gene expression. *Biochem. J.*, **371**: 301–310.

Wang D, Lippard SJ. 2005. Cellular processing of platinum anticancer drugs. *Nat. Rev. Discov.*, **4**: 307–320.

Wang HG, Pathan N, Ethell IM, Krajewski S, Yamaguchi Y, Shibasaki F, McKeon F, Bobo T, Franke TF, Reed JC. 1999. Ca2+-induced apoptosis through calcineurin dephosphorylation of BAD. *Science*, **284**: 339–343.

Wang L, Zhang H, Sun M, Yin Z, Qian J. 2015. High mobility group box 1-mediated autophagy promotes neuroblastoma cell chemoresistance. *Oncol. Rep.*, **34**: 2969–2976.

Wang P, Deng Y, Fu X. 2017. MiR-509-5p suppresses the proliferation, migration, and invasion of non-small cell lung cancer by targeting YWHAG. *Biochem. Biophys. Res. Commun.*, **482**: 935–941.

Waterman MJ, Stavridi ES, Waterman JL, Halazonetis TD. 1998. ATM-dependent activation of p53 involves dephosphorylation and association with 14-3-3 proteins. *Nat. Genet.*, **19**: 175–178.

Xia J, Yu X, Song X, Li G, Mao X, Zhang Y. 2017. Inhibiting the cytoplasmic location of HMGB1 reverses cisplatin resistance in human cervical cancer cells. *Mol. Med. Rep.*, **15**: 488–494.

Xu J, Acharya S, Sahin O, Zhang Q, Saito Y, Yao J, Wang H, Li P, Zhang L, Lowery FJ, Kuo WL, Xiao Y, Ensor J, Sahin AA, Zhang XH, Hung MC, Zhang JD, Yu D. 2015. 14-3-3zeta turns TGF-beta's function from tumor suppressor to metastasis promoter in breast cancer by contextual changes of Smad partners from p53 to Gli2. *Cancer Cell*, **27**: 177–192.

Yang X, Cao W, Zhang L, Zhang W, Zhang X, Lin H. 2012. Targeting 14-3-

3zeta in cancer therapy. *Cancer Gene Ther.*, **19**: 153–159.

Youn JH, Shin J-S. 2006. Nucleocytoplasmic Shuttling of HMGB1 Is Regulated by Phosphorylation That Redirects It toward Secretion. *J. Immunol.*, **177**: 7889–7897.

Yusein-Myashkova S, Ugrinova I, Pasheva E. 2013. Non-histone protein HMGB1 inhibits the repair of cisplatin damaged DNA in NIH-3T3 murine fibroblasts. *BMB Rep.*, **49**: 99–104.

Zhang W, Shen Q, Chen M, Wang Y, Zhou Q, Tao X, Zhu X. 2015. The role of 14-3-3 proteins in gynecological tumors. *Front. Biosci. (Landmark Ed.*, **20**: 934–945.

Zhang Y, Cheng Y, Ren X, Zhang L, Yap KL, Wu H, Patel R, Liu D, Qin ZH, Shih IM, Yang JM. 2012. NAC1 modulates sensitivity of ovarian cancer cells to cisplatin by altering the HMGB1-mediated autophagic response. *Oncogene*, **31**: 1055–1064.

Zhou LY, Shi LY, Xiao Y. 2016. Changes of HMGB1 expression on angiogenesis of ovarian cancer and its mechanism. *J. Biol. Regul. Homeost. Agents*, **30**: 233–238.

Concluding Remarks

Interactions of Ixr1 with other yeast proteins and interactions of HMGB1 and HMGB2 with proteins in epithelial human cells have been analyzed in this work by proteomic approaches based on Yeast-Two-Hybrid (Y2H) and Co-purification/Mass Spectrometry (CoIP-MS).

The study of Ixr1 interactions in yeast allows to conclude:

1. The NH_2 terminus of Ixr1 is necessary for transcriptional activation.

2. Ixr1 interacts with Ssn8 (Srb11) that forms part of the Cdk8 subcomplex, involved majorly in transcriptional repression, and with Tdh3, involved in transcriptional silencing.

3. Ixr1 purified from aerobic or hypoxic conditions presents different post-translational modifications. The amino acids S6 and S83 are phosphorylated in aerobic conditions, while T45 and S559 are phosphorylated in hypoxia.

The study of HMGB1 and HMGB2 interactions allows to conclude:

4. New interactions of HMGB1 and HMGB2 have been found in different epithelial cells from ovary and prostate. High confidence interactors based on repeated identification in different cell types or by two experimental approaches include: the ribosomal proteins RPS12 and RSP20, cytokeratin 7 (KRT7), cell division cycle and apoptosis regulator 1 (CCAR1), histone 3.3 (H3F3A) and the zinc finger factor 428 (ZNF428).

5. Previously unreported HMGB1 and HMGB2 binding proteins have been found in ovarian and prostate cancer cells using the Y2H approach. Only two common interacting partners for HMGB1 and HMGB2 were found, E3 ubiquitin-protein ligase UHRF2 (UHRF2) and ZNF428, which reflects the

specificity of these proteins and their interactions to contribute to cellular functions.

6. Focusing on HMGB1, the cytoplasmic interaction of this protein with the cytoskeleton protein, cytokeratin 7 (KRT7) was validated by co-localization and immunoprecipitation studies. This interaction was found both in cancerous and non-cancerous cells. The genes *HMGB1* and *KRT7* are both over-expressed in ovary-epithelial cancerous cells, while having opposite regulation in prostate-epithelial cancerous cells; *HMGB1* is up-regulated and *KRT7* down-regulated. Co-localization studies also suggest the interaction between HMGB1 and the transcription factor HOXA10 in the nucleus. However, this interaction could not be verified by co-immunoprecipitation. *HOXA10* is up-regulated both in prostate and ovary cancerous cells from epithelial origin.

7. The interactomes of HMGB1, obtained in ovarian and prostate cancerous cells using the CoIP/MS approach, share common proteins. They are involved in the THO complex (a subcomplex of the TREX complex), mRNA transcription, spliceosome, mRNA processing and export, cytoskeleton reorganization; and also proteins from the NuRD complex, a chromatin remodeling complex associated to oncogenesis and cancer progression. Direct interaction between HMGB1 and the histone binding protein RBBP7, a component of the NuRD complex, was validated using Y2H assays.

8. Cell fractionation, followed by CoIP/MS has allowed to distinguish between HMGB1 interactions produced in nucleus and cytoplasm.

9. The obtained results have also revealed a non-previously detected interaction between septins, which are cytoskeleton GTP binding proteins,

and THOC proteins that are part of the “transcription/export” complex (TREX complex). These interactions have been validated in cancer prostate cells by small scale immunoprecipitations and western blot, as well as by a second CoIP/MS analysis with an antibody directed to THOC5.

10. Rab11 is a common interactor of HMGB1, THOC5 and THOC2 in cancer prostate cells.

11. HMGB1 interactants identified in ovary and prostate cancer cells after cisplatin treatment are moesin (MSN), importin-alfa1 (KPNA2), phosphoribosyl amino-imidazole carboxylase (PAICS), 14-3-3Zeta (YWHAZ) and 14-3-3Gamma (YWHAG).

Appendix

Resumen

Introducción

La proteína de *Saccharomyces cerevisiae* Ixr1, y las proteínas humanas HMGB1 y HMGB2 se engloban dentro de la superfamilia HMG, concretamente en la familia HMGB. Las proteínas de dicha familia se caracterizan por la presencia del dominio "HMG-box" (Bustin, 2001). Estas tres proteínas son estructuralmente similares por la presencia de dos dominios "HMG-box" dispuestos en tándem, y presentando cada uno una estructura en forma de L formada por plegamientos en hélice alfa.

Ixr1 es un factor de transcripción en levaduras que juega un papel clave en condiciones de hipoxia y de estrés oxidativo, cumpliendo también una función relevante en la reparación de ADN (Castro-Prego *et al.*, 2010; Vizoso-Vázquez *et al.*, 2017).

HMGB1 y HMGB2 al igual que Ixr1 están implicados en procesos de regulación de la transcripción y reparación de ADN (Liu *et al.*, 2010). Así mismo, HMGB1 juega un papel relevante en procesos de autofagia/apoptosis (Kang *et al.*, 2010) y en procesos inflamatorios, pues es secretada al medio extracelular donde se puede unir a diferentes receptores como "Receptor for advanced glycation end products" (RAGE) y "toll-like receptors" (TLRs),, activando diferentes cascadas pro-inflamatorias (Park *et al.*, 2004; Magna and Pisetsky, 2014). HMGB1 y HMGB2 están implicadas en el desarrollo de enfermedades neurodegenerativas, autoinmunes y cáncer, entre otras. Así, se ha visto que la expresión de ambas proteínas se incrementa en diferentes tipos de cáncer, entre los que se encuentran aquellos donde el estrés oxidativo juega un papel clave para su desarrollo (Barreiro-Alonso *et al.*, 2016). Debido a las funciones asociadas

a HMGB1, esta proteína está implicada en los principales procesos de carcinogénesis como la migración, angiogénesis o la transición epitelio-mesénquima entre otros (Zhu *et al.*, 2015; Chandrasekaran *et al.*, 2016; Zhou *et al.*, 2016).

Otra característica común entre la proteína de levaduras Ixr1 y las proteínas humanas HMGB1 y HMGB2 es su capacidad de unión a los aductos de DNA-cisplatino. Este fármaco se emplea en tratamientos de quimioterapia de diferentes tipos de cáncer como el de próstata y el de ovario (Zamble *et al.*, 1996), pero su efectividad se ve afectada debido al desarrollo de mecanismos de resistencia por parte de las células.

Para mejorar el conocimiento sobre las funciones celulares de las proteínas es importante la identificación de las interacciones que se producen entre ellas y condicionan su función. Por ello el principal objetivo de este trabajo ha sido esclarecer el interactoma de Ixr1, HMGB1 y HMGB2. En el caso de las dos últimas, dada su implicación en procesos tumorales, se ha centrado el estudio de estas interacciones en células de ovario y próstata epiteliales cancerosas o no cancerosas. En el caso de HMGB1 se ha ampliado este estudio a células tratadas con cisplatino, dada la posible relación de esta proteína con el desarrollo de resistencia a dicho fármaco.

Objetivos

El principal objetivo de esta tesis doctoral es el análisis de las interacciones de Ixr1, HMGB1 y HMGB2 con otras proteínas utilizando diferentes metodologías. La caracterización de estas interacciones es de gran ayuda para entender el papel de las proteínas HMGB en los mecanismos celulares

de respuesta a hipoxia y daño al ADN. Este conocimiento puede ser utilizado en el futuro para el desarrollo de estrategias de diagnóstico y tratamiento, así como en el control de mecanismos de resistencia a fármacos derivados del platino y empleados en la quimioterapia del cáncer.

Los objetivos específicos de este trabajo son:

1. Encontrar proteínas que interaccionan con Ixr1 implicadas en la regulación transcripcional de *Saccharomyces cerevisiae*.

2. Descubrir nuevas proteínas que interaccionen con HMGB1 y HMGB2 en células epiteliales humanas de ovario y próstata.

3. Analizar el interactoma de HMGB1 y HMGB2 en células cancerosas humanas de origen epitelial de ovario y próstata, usando el sistema de Doble Híbrido (DH) en levaduras.

4. Analizar el interactoma en núcleo y citoplasma de HMGB1 en células cancerosas de origen epitelial de ovario y próstata, empleando la estrategia de Inmunoprecipitatión/Espectrometría de masas.

5. Descubrir proteínas específicas que se unen a HMGB1 tras el tratamiento con cisplatino en células cancerosas de origen epitelial de ovario y próstata.

Capítulo 1. La proteína HMGB, Ixr1, interacciona con otras proteínas implicadas en la regulación transcripcional

Ixr1 es un regulador transcripcional cuyos mecanismos específicos de activación aún están en estudio. Dado que Ixr1 juega un papel clave en la regulación de la respuesta a hipoxia, en este estudio se ha analizado la

interacción de Ixr1 con tres factores que previamente se habían identificado como proteínas clave en la respuesta hipóxica de levaduras. Las proteínas estudiadas fueron Cyc8 (alias Ssn6) y Tup1, proteínas que conforman el complejo co-represor de genes hipóxicos activo durante el crecimiento en aerobiosis, y la ciclina Ssn8 (alias Srb11) que junto con la quinasa Ssn3 (Srb10) y Med12 y 13 conforman el módulo de cuatro subunidades Cdk8, el cual puede asociarse con el complejo Mediador. Ensayos de DH pusieron de manifiesto la interacción física de Ixr1 con Ssn8, mientras que el resultado fue negativo para Cyc8 y Tup1. La conexión de Ixr1, vía el módulo Cdk8 Quinasa, con la maquinaria basal de transcripción a través del Mediador es interesante, ya que el complejo Mediador es considerado como un sensor de múltiples cambios ambientales y celulares que afectan a la transcripción (Poss *et al.*, 2013). En conjunto estos resultados ponen de manifiesto que la función represora de Ixr1 no depende de la interacción directa con el co-represor Ccy8-Tup1. La interacción detectada con Ssn8, podría afectar a la función co-activadora del Mediador, o reclutar indirectamente al complejo co-represor Cyc8-Tup1.

Para estudiar la función activadora de Ixr1 sobre la transcripción se llevó a cabo la fusión entre Ixr1 y el dominio de unión a ADN de Gal4. Se observó que esta unión permitía la expresión de genes regulados bajo control de Gal4 sin necesidad del dominio de activación de Gal4, confirmado la capacidad de Ixr1 de activar la transcripción por reclutamiento de Ixr1 a un promotor heterólogo. El experimento anterior se llevó a cabo con la proteína nativa junto con tres construcciones diferentes de Ixr1, una con una deleción en el extremo N'-terminal (43 aa), otra con la deleción del extremo C'-terminal (28 aa) y una última con ambas. Así se puso de

manifiesto que los primeros 43 aminoácidos forman parte del dominio de activación, ya que su eliminación conlleva la pérdida de dicha actividad.

Para ampliar el conocimiento sobre el interactoma de Ixr1 también se realizaron ensayos de purificación de Ixr1. El primer método permitía una alta expresión de Ixr1 etiquetado con el péptido FLAG en normoxia, realizando la purificación de la proteína por afinidad empleando el anticuerpo anti-FLAG. Esta purificación acoplada a espectrometría de masas permitió identificar 65 proteínas capaces de interaccionar con Ixr1. Dado que el ensayo anterior implicaba una sobreexpresión de Ixr1, se llevó a cabo un segundo ensayo en el que su expresión estaba controlada por su propio promotor. En este caso de identificaron 38 proteínas. La intersección entre los resultados de las dos purificaciones identifica 14 proteínas, 7 relacionadas con el metabolismo de la glucosa (Pgk1, Eno2, Tdh3, Eno1, Tdh1, Pdc1, Adh1), 2 relacionadas con estrés (Ssa1, Hsc82), 2 proteínas ribosomales (Rpp0, Rpl5), 1 factor de elongación transcripcional (Tef1), actina (Act1), y una proteína relacionada con el ciclo celular (Cdc9). Los resultados de estos experimentos ponen de manifiesto que Ixr1 no sólo está implicado con funciones asociadas a DNA, sino que también interacciona con proteínas vinculadas al ribosoma, al citoplasma y a la membrana plasmática.

Dado que se han descrito diferentes estados de fosforilación de Ixr1, se analizó la fosforilación diferencial de dicha proteína en condiciones de aerobiosis e hipoxia. Los resultados del análisis por espectrometría de masas muestran la fosforilación de la S6 y S83 en condiciones aeróbicas, mientras que en hipoxia son la T45 y la S559 las que presentan fosforilaciones. La interacción de Ixr1 con otras proteínas relacionadas con

la activación o represión transcripcional podría estar condicionada por el estado de fosforilación de Ixr1.

Capítulo 2. Caracterización del interactoma de HMGB1 y HMGB2 en células epiteliales de próstata y ovario y su relación con cáncer

En este capítulo se ha llevado a cabo un estudio de las interacciones proteicas de HMGB1 y HMGB2 en células epiteliales de próstata y de ovario. Dado que los carcinomas son los tipos más comunes de cáncer, y durante el desarrollo de los mismos las células epiteliales sufren una serie de cambios importantes, la identificación de interacciones proteína-proteína de HMGB1 y HMGB2 en células epiteliales de ovario y próstata podría ayudar a entender el origen y desarrollo de adenocarcinomas de estos dos órganos.

Para este fin se realizaron ensayos de inmunoprecipitación a gran escala de HMGB1 acoplados a espectrometría de masas en la línea celular PNT2 (células epiteliales de próstata benignas). Se realizaron también ensayos de DH en los que se emplearon librerías de ADNc construidas a partir de ARN de cultivos primarios de HOSEpiC (células epiteliales de ovario no tumoral) y HPEpiC (células epiteliales de próstata no tumorales), así como ARN de tejido de ovario sano. En el caso del DH el estudio se amplió a HMGB2.

Los ensayos de inmunoprecipitación de HMGB1 en células epiteliales de próstata permitieron identificar 159 proteínas, entre las que se encuentran como era de esperar la propia HMGB1 y 6 proteínas cuya interacción con HMGB1 ya había sido descrita. Las proteínas de interacción con HMGB1 identificadas en estos ensayos se pueden englobar en 4 grupos principales: Proteínas de unión a ADN, proteínas relacionadas con la maduración del

ARN, proteínas ribosomales, y proteínas implicadas en la traducción mitocondrial. Así mismo, también se encontraron proteínas relacionadas con otras funciones como TJP1 y TJP2, las cuales participan en las uniones estrechas entre las células.

Los ensayos de DH empleando las librerías de próstata y ovario pusieron de manifiesto 16 proteínas que interaccionan físicamente con HMGB1 y que no se habían asociado con HMGB1 con anterioridad. Estas proteínas pueden ser clasificadas en: componentes del citoesqueleto; proteínas de señalización en respuesta a factores de crecimiento, componentes de la membrana celular y de la matriz extracelular, reguladores de la invasión celular y migración en células tumorales, y proteínas relacionadas con apoptosis. Todas las proteínas identificadas están relacionadas con el desarrollo de tumores o con diferentes procesos oncogénicos.

En el caso de HMGB2 se identificaron 16 proteínas que interaccionan con dicha proteína en células epiteliales de próstata y de ovario. Al igual que las proteínas identificadas para HMGB1, ninguna había sido descrita con anterioridad como de unión a HMGB2, y para todas ellas se ha encontrado relación con procesos tumorales. Entre las proteínas identificadas se encuentran proteínas relacionadas con apoptosis, con proliferación celular y con movilidad celular.

Se identificaron 5 proteínas en el ensayo realizado con la librería de tejido de ovario sano empleando como presa HMGB1. Al igual que ocurrió en los casos anteriores, todas ellas están relacionadas con procesos tumorales.

De las proteínas de interacción con HMGB1, 2 fueron identificadas en dos tipos de células epiteliales diferentes (CCAR1 y KRT7) mientras que para

HMGB2 sólo una interacción se encontró en dos tipos celulares distintos (ZNF428). Comparando los resultados obtenidos para HMGB1 y HMGB2 sólo se han encontrados 4 proteínas comunes a las proteínas de estudio, ZNF428, EIF1, C1QBP y Nelin (NEXN). Dada la alta similitud de secuencia entre HMGB1 y HMGB2 llama la atención el bajo número de interacciones comunes, que podría estar indicando la alta especificidad de las interacciones encontradas.

Estos resultados ponen de manifiesto la compleja regulación que puede ejercer HMGB1 en la regulación de la expresión génica, y que abarca desde la interacción con el molde de DNA, maduración y exporte del ARN hasta la propia síntesis de proteínas. Así mismo, estos resultados muestran que tanto HMGB1 como HMGB2 además de interaccionar con proteínas nucleares, también interaccionan con proteínas que forman parte del citoesqueleto, adhesiones célula-célula, y que muchas de estas proteínas están implicadas en procesos tumorales como la migración e invasión y la supervivencia celular.

Capítulo 3. Nuevas proteínas de interacción de HMGB1 y HMGB2 en células tumorales de próstata y ovario

Dado que las proteínas HMGB son necesarias en células sanas, pero se ha comprobado que también están directamente implicadas en el desarrollo del cáncer, es de esperar que su cambio de funcionalidad sea debido a cambios en determinadas interacciones con otras proteínas. Mientras que en capítulo anterior se llevó a cabo la búsqueda de proteínas de unión de HMGB1 y HGMGB2 en células epiteliales de próstata y ovario sanas, en este capítulo se ha empleado el sistema de DH para la búsqueda de nuevas

interacciones de HMGB1 y HMGB2 en células de las líneas celulares tumorales de próstata y ovario, PC-3 y SKOV-3, derivadas de células epiteliales. Los resultados de estos estudios pueden poner de manifiesto interacciones implicadas en procesos de malignización.

Los ensayos de DH muestran un nuevo grupo de interacciones de HMGB1 y HMGB2 no descritas con anterioridad. Se identificaron 4 proteínas de unión a HMGB1 y un ARN no codificante en células de ovario tumorales; 10 en células de próstata tumoral. Dos proteínas se identificaron en los dos tipos celulares. En el caso de HMGB2 se encontraron 7 interacciones en células de ovario tumoral y 6 en células de próstata tumoral; 2 de ellas comunes en los dos tipos celulares.

Al igual que en el caso de las proteínas de interacción para HMGB1 y HMGB2 encontradas en células epiteliales sanas de próstata y ovario, las proteínas identificadas en estos ensayos están asociadas con diversas funciones, desde funciones nucleares como splicing y transcripción hasta funciones citoplasmáticas relacionadas con el proteasoma o el citoesqueleto. Al igual que lo expuesto en el capítulo anterior, las proteínas identificadas en estos ensayos pueden relacionarse con procesos tumorales y muchas se desregulan en diferentes tipos de cáncer.

Entre las proteínas de interacción con HMGB1 encontradas, se incluye la citoqueratina 7 (KRT7), la cual también se había identificado en ensayos con librerías de células sanas de próstata. Debido a la implicación de dicha proteína en procesos tumorales (Ichimi *et al.*, 2009; Ibragimova *et al.*, 2010) se profundizó en el estudio de interacción HMGB1-KRT7. Ensayos de inmunoprecipitación a pequeña escala junto con estudios de co-localización

realizados en la línea PC-3 validan esta interacción. Así mismo, el ensayo de co-localización pone de manifiesto que dicha interacción tiene lugar en el citoplasma.

En los ensayos de DH de HMGB1 empleando la librería de próstata tumoral se encontró la interacción de dicha proteína con HOXA10. Esta interacción no había sido descrita con anterioridad, sin embargo la interacción de HMGB1 con otras proteínas homeobox (HOX) si se había observado previamente (Zappavigna *et al.*, 1996). Esta interacción no se puedo probar por inmunoprecipitación y un estudio de la secuencia del clon del gen *HOXA10* obtenido en el DH puso de manifiesto que la secuencia clonada no se encontraba dentro de la región codificante de dicho gen. Sin embargo, ensayos de co-localización de las proteínas HMGB1 y HOXA10 en células PC-3 sugieren la interacción de estas dos proteínas en determinadas zonas nucleares en células de próstata tumorales; un dato que necesitará futura comprobación experimental.

Por último, también se estudió la expresión de los genes *HMGB1*, *KRT7* y *HOXA10* en células tumorales PC-3 y SKOV-3 y en células sanas, HPEpiC y HOSEpiC. Los resultados de qRT-PCR muestran un aumento en la expresión de *HMGB1* y *HOXA10* en las líneas celulares de ovario y próstata. *KRT7* se sobre-expresa en células de ovario tumorales mientras que su expresión disminuye en células tumorales de próstata.

Capítulo 4. Interacciones nucleares y citoplasmáticas de HMGB1 en células tumorales de próstata y ovario mediante Inmunoprecipitación/Espectrometría de masas

Los estudios de proteómica en los que se combinan purificaciones con espectrometría de masas son de gran ayuda para los estudios del interactoma de proteínas, ya que permiten la identificación precisa de un gran número de proteínas. En este capítulo se ha ampliado el estudio del interactoma de HMGB1 en células tumorales de próstata y ovario de origen epitelial, realizando purificaciones/inmunoprecipitaciones a gran escala acopladas a MS. Así mismo, también se han llevado a cabo ensayos de fraccionamiento celular para determinar la localización celular de las interacciones encontradas.

Los resultados de las purificaciones a gran escala de HMGB1 en las líneas celulares SKOV-3 y PC-3 muestran una fuerte asociación de HMGB1 con procesos metabólicos de RNA, así se identificaron un gran número de proteínas que están implicadas en procesos como *splicing* o el exporte de ARNm del núcleo, entre las que se encuentran proteínas del complejo THO como THOC5 y THOC2. Así mismo entre las proteínas encontradas hay un alto número de proteínas ribosomales, tanto en el núcleo como en el citoplasma. Entre las proteínas relacionadas con el ribosoma también se identificaron proteínas nucleolares implicadas en la biogénesis de ribosomas, lo cual revela la posible implicación de HMGB1 en la transcripción de genes ribosomales así como en distintos procesos post-transcripcionales previos al ensamblaje del ribosoma.

Este estudio ha puesto también de manifiesto la interacción de HMGB1 con distintas proteínas del citoesqueleto como las septinas, proteínas de organización de microtúbulos, proteínas relacionadas con la polimerización de la actina y queratinas. Esto refuerza la implicación de HMGB1 en procesos de división celular, movilidad y diferenciación, los cuales se encuentran alterados en cáncer.

Entre las interacciones nucleares de HMGB1 identificadas en los ensayos de inmunoprecipitación se encuentra la interacción con proteínas del complejo NuRD (RBBP4, RBBP7, HDAC1, HDAC2 y MTA2). Dada la implicación de este complejo en procesos pro-tumorales como el silenciamiento de genes supresores de tumores (Cai *et al.*, 2014), se validó la interacción de HMBGB1 con la proteína RBBP7 mediante la técnica de DH.

En este capítulo también se pone de manifiesto la interacción mutua entre las proteínas del complejo THO, las septinas y la GTPasa Rab11, interacciones que no habían sido descritas con anterioridad.

Capítulo 5. Estudio proteómico del papel de HMGB1 en la respuesta a cisplatino en células PC-3 y SKOV-3

El cisplatino es un compuesto utilizado en quimioterapia en el tratamiento de cáncer de próstata y ovario, entre otros. Desgraciadamente, la eficacia de este fármaco se ve mermada por el desarrollo de resistencia al mismo en los pacientes. Estudios previos han puesto de manifiesto la relación de HMGB1 con la respuesta a cisplatino (Kang *et al.*, 2013).

En este estudio se han llevado a cabo tratamientos de cisplatino a las líneas tumorales PC-3 y SKOV-3. Empleando ensayos de inmunoprecipitación de

HMGB1 a gran escala junto con espectrometría de masas, se han identificado proteínas de interacción con HMGB1 específicas de células de próstata y ovario tratadas con dicho compuesto. Se identificaron 5 proteínas específicas: Moesin (MSM), Importin subunit alpha-1 (KPNA2), Phosphoribosyl aminoimidazole carboxylase (PAICS), 14-3-3Zeta (YWHAZ) y 14-3-3Gamma (YWHAQ).

La interacción de HMGB1 y KPNA2 ya había sido descrita por Youn y Shin (Youn and Shin, 2006), cuyo trabajo indica que KPNA2 está implicada en el importe de HMGB1 al núcleo cuando esta última no está fosforilada. No se ha descrito interacción previa de HMGB1 con las otras cuatro proteínas, sin embargo estas 5 proteínas interaccionan directa o indirectamente con el Nuclear factor-kappa B1 (NF-κβ1), proteína estrechamente relacionada con procesos tumorales (Fu *et al.*, 2017). No obstante, sí se ha descrito el papel de MSM en la sensibilidad a cisplatino en líneas celulares (Li *et al.*, 2008). Aunque las tres proteínas restantes no se han relacionado previamente con resistencia a cisplatino, diversos resultados las relacionan con procesos tumorales. Así, diversos estudios han puesto de manifiesto que proteínas de la familia 14-3-3, entre las que se encuentran 14-3-3Zeta y 14-3-3Gamma están implicadas en el inicio y la progresión de diferentes tipos de cáncer, entre los que se incluyen el cáncer de próstata y cáncer de origen ginecológico (Nishimura *et al.*, 2013; Zhang *et al.*, 2015; Murata *et al.*, 2012). Por otro lado, también se ha observado sobrexpresión de PAICS en células tumorales asociándose con procesos pro-tumorales (Eissmann *et al.*, 2013).

Conclusiones

En este estudio se han analizado las interacciones de Ixr1 con otras proteínas de levadura y las interacciones proteicas de HMGB1 y HMGB2 en células epiteliales humanas mediante el ensayo del DH y Purificación/Espectrometría de masas.

El estudio de las interacciones de Ixr1 en levaduras ha permitido concluir lo siguiente:

1. El extremo NH_2 de Ixr1 es necesario para la activación transcripcional.

2. Ixr1 interacciona con Ssn8 (Srb11), el cual forma parte del subcomplejo Cdk8 que está implicado principalmente en la represión transcipcional, y con Tdh3 relacionada con el silenciamiento transcripcional.

3. Ixr1 purificado en condiciones de aerobiosis o hipoxia presenta modificaciones postraduccionales diferenciales. S6 y S83 están fosforiladas en condiciones de aerobiosis mientras que T45 y S559 se encuentran fosforiladas en hipoxia.

El estudio de las interacciones de HMGB1 y HMGB2 permite concluir:

4. Se han encontrado nuevas interacciones de HMGB1 y HMGB2 en células epiteliales de ovario y próstata. Las proteínas identificadas reiteradamente en diferentes tipos celulares, o mediante aproximaciones experimentales diferentes, incluyen: las proteinas ribosomales RPS12 y RPS20, citoqueratina 7 (KRT7), cell division cycle and apoptosis regulator 1 (CCAR1), Histone 3.3 (H3F3A) y el zinc finger factor 428 (ZNF428).

5. Se han encontrado proteínas que interaccionan con HMGB1 y HMGB2 en células de cáncer de ovario y próstata utilizando el sistema de doble hibrido que no habían sido descritas con anterioridad. Solamente se han encontrado dos proteínas que interaccionen tanto con HMGB1 como con HMGB2, E3 ubiquitin-protein ligase UHRF2 (UHRF2) y ZNF428, lo cual refleja la especificidad de estas proteínas y de sus interacciones para contribuir a sus funciones celulares.

6. Con respecto a HMGB1, se ha validado mediante estudios de inmunoprecipitación y co-localización la interacción citoplasmática de esta proteína con la proteína del citoesqueleto, cytoqueratin 7 (KRT7). Esta interacción se encontró tanto en células cancerosas como en no cancerosas. Los genes *HMGB1* y *KRT7* se sobre-expresan en células de ovario epiteliales cancerosas mientras que presentar una regulación opuesta en células de próstata epiteliales cancerosas, *HMGB1* se sobre-expresa, mientras que los niveles de expresión de *KRT7* disminuyen. Estudios de co-localización también sugieren la interacción entre HMGB1 y el factor de transcripción HOXA10 en el compartimento nuclear aunque esta interacción no pudo ser validada por inmunoprecipitación. Además *HOXA10* se sobre-expresa en células de próstata y ovario cancerosas de origen epitelial.

7. Los interactomas de HMGB1 obtenidos en células de ovario y próstata cancerosas empleando técnicas de CoIP/Espectrometría de masas comparten proteínas implicadas en el complejo THO, en la transcripción de ARNm, procesamiento y exporte, proteínas del espliceosoma, en la reorganización del citoesqueleto y proteínas pertenecientes al complejo NuRD, un complejo remodelador de la cromatina que se asocia con la progresión del cáncer y la oncogénesis. La interacción directa entre HMGB1

y la proteína de unión a histonas RBBP7, un componente del complejo NuRD, fue validada empleando ensayos de DH.

8. El fraccionamiento celular seguido de CoIP/Espectrometría de masas ha permitido distinguir entre interacciones de HMGB1 que ocurren en el núcleo o en el citoplasma.

9. Los resultados obtenidos han revelado interacciones no descritas previamente entre las Septinas, las cuales son proteínas del citoesqueleto que unen GTP, y las proteínas del complejo THO que es parte del complejo de "transcripción/exporte" (complejo TREX). Estas interacciones han sido validadas en células cancerosas de próstata por inmunoprecipitaciones a pequeña escala y western blot, así como por un segundo ensayo de CoIP/Espectrometría de masas empleando un anticuerpo dirigido contra THOC5.

10. Rab11 interacciona con HMGB1, THOC5 y THOC2 en células de cáncer de próstata.

11. Las proteínas que interactúan con HMGB1 identificadas en células de ovario y próstata tumorales tras un tratamiento con cisplatino son Moesin (MSN), Importin subunit alfa-1 (KPNA2), Phosphoribosyl amino-imidazole carboxylase (PAICS), 14-3-3Zeta (YWHAZ) y 14-3-3Gamma (YWHAQ).

Referencias

Barreiro-Alonso A, Lamas-Maceiras M, Rodríguez-Belmonte E, Vizoso-Vázquez Á, Quindós M, Cerdán ME. 2016. High Mobility Group B Proteins, Their Partners, and Other Redox Sensors in Ovarian and Prostate Cancer. *Oxid. Med. Cell. Longev.*, **2016**: 5845061.

Bustin M. 2001. Revised nomenclature for high mobility group (HMG)

chromosomal proteins. *Trends Biochem. Sci.*, **26**: 152–153.

Cai Y, Geutjes E-J, Lint K de, Roepman P, Bruurs L, Yu L-R, Wang W, Blijswijk J van, Mohammad H, Rink I de, Bernards R, Baylin S. 2014. The NuRD complex cooperates with DNMTs to maintain silencing of key colorectal tumor suppressor genes. *Oncogene*, **33**: 2157–2168.

Castro-Prego R, Lamas-Maceiras M, Soengas P, Fernandez-Leiro R, Carneiro I, Becerra M, Gonzalez-Siso MI, Cerdan ME. 2010. Ixr1p regulates oxygen-dependent HEM13 transcription. *FEMS Yeast Res.*, **10**: 309–321.

Chandrasekaran KS, Sathyanarayanan A, Karunagaran D. 2016. Downregulation of HMGB1 by miR-34a is sufficient to suppress proliferation, migration and invasion of human cervical and colorectal cancer cells. *Tumor Biol.*, **37**: 13155–13166.

Eissmann M, Schwamb B, Melzer IM, Moser J, Siele D, Kohl U, Rieker RJ, Wachter DL, Agaimy A, Herpel E, Baumgarten P, Mittelbronn M, Rakel S, Kogel D, Bohm S, Gutschner T, Diederichs S, Zornig M. 2013. A functional yeast survival screen of tumor-derived cDNA libraries designed to identify anti-apoptotic mammalian oncogenes. *PLoS One*, **8**: e64873.

Fu W, Zhuo ZJ, Chen YC, Zhu J, Zhao Z, Jia W, Hu JH, Fu K, Zhu SB, He J, Liu GC. 2017. NFKB1 -94insertion/deletion ATTG polymorphism and cancer risk: Evidence from 50 case-control studies. *Oncotarget*, **8**: 9806–9822.

Ibragimova I, Ibanez de Caceres I, Hoffman AM, Potapova A, Dulaimi E, Al-Saleem T, Hudes GR, Ochs MF, Cairns P. 2010. Global reactivation of epigenetically silenced genes in prostate cancer. *Cancer Prev. Res. (Phila).*, **3**: 1084–1092.

Ichimi T, Enokida H, Okuno Y, Kunimoto R, Chiyomaru T, Kawamoto K, Kawahara K, Toki K, Kawakami K, Nishiyama K, Tsujimoto G, Nakagawa M, Seki N. 2009. Identification of novel microRNA targets based on microRNA signatures in bladder cancer. *Int. J. Cancer*, **125**: 345–352.

Kang R, Livesey KM, Zeh HJ, Loze MT, Tang D. 2010. HMGB1: a novel Beclin 1-binding protein active in autophagy. *Autophagy*, **6**: 1209–1211.

Kang R, Zhang Q, Zeh 3rd HJ, Lotze MT, Tang D. 2013. HMGB1 in cancer: good, bad, or both? *Clin. Cancer Res.*, **19**: 4046–4057.

Li CH, Cai L, Chen XS, Meng QW, Sui GJ. 2008. DDP-sensitivity-related genes in 10 lung cancer cell lines. *Zhonghua Zhong Liu Za Zhi*, **30**: 418–421.

Liu Y, Prasad R, Wilson SH. 2010. HMGB1: roles in base excision repair and

related function. *Biochim. Biophys. Acta*, **1799**: 119–130.

Magna M, Pisetsky D. 2014. The Role of HMGB1 in the Pathogenesis of Inflammatory and Autoimmune Diseases. *Mol. Med.*, **20**: 138–146.

Murata T, Takayama K, Urano T, Fujimura T, Ashikari D, Obinata D, Horie-Inoue K, Takahashi S, Ouchi Y, Homma Y, Inoue S. 2012. 14-3-3zeta, a Novel Androgen-Responsive Gene, is Upregulated in Prostate Cancer and Promotes Prostate Cancer Cell Proliferation and Survival. *Clin. Cancer Res.*, **18**: 5617–5627.

Nishimura Y, Komatsu S, Ichikawa D, Nagata H, Hirajima S, Takeshita H, Kawaguchi T, Arita T, Konishi H, Kashimoto K, Shiozaki A, Fujiwara H, Okamoto K, Tsuda H, Otsuji E. 2013. Overexpression of YWHAZ relates to tumor cell proliferation and malignant outcome of gastric carcinoma. *Br. J. Cancer*, **108**: 1324–1331.

Park JS, Svetkauskaite D, He Q, Kim J-Y, Strassheim D, Ishizaka A, Abraham E. 2004. Involvement of Toll-like Receptors 2 and 4 in Cellular Activation by High Mobility Group Box 1 Protein. *J. Biol. Chem.*, **279**: 7370–7377.

Poss ZC, Ebmeier CC, Taatjes DJ. 2013. The Mediator complex and transcription regulation. *Crit. Rev. Biochem. Mol. Biol.*, **48**: 575–608.

Vizoso-Vázquez A, Lamas-Maceiras M, Fernandez-Leiro R, Rico-Diaz A, Becerra M, Cerdan ME. 2017. Dual function of Ixr1 in transcriptional regulation and recognition of cisplatin-DNA adducts is caused by differential binding through its two HMG-boxes. *Biochim. Biophys. Acta*, **1860**: 256–269.

Youn JH, Shin J-S. 2006. Nucleocytoplasmic Shuttling of HMGB1 Is Regulated by Phosphorylation That Redirects It toward Secretion. *J. Immunol.*, **177**: 7889–7897.

Zamble DB, Mu D, Reardon JT, Sancar A, Lippard SJ. 1996. Repair of cisplatin-DNA adducts by the mammalian excision nuclease. *Biochemistry*, **35**: 10004–10013.

Zappavigna V, Falciola L, Helmer-Citterich M, Mavilio F, Bianchi ME. 1996. HMG1 interacts with HOX proteins and enhances their DNA binding and transcriptional activation. *Embo Jour*, **15**: 4981–4991.

Zhang W, Shen Q, Chen M, Wang Y, Zhou Q, Tao X, Zhu X. 2015. The role of 14-3-3 proteins in gynecological tumors. *Front. Biosci. (Landmark Ed.*, **20**: 934–945.

Zhou LY, Shi LY, Xiao Y. 2016. Changes of HMGB1 expression on

angiogenesis of ovarian cancer and its mechanism. *J. Biol. Regul. Homeost. Agents*, **30**: 233–238.

Zhu L, Li X, Chen Y, Fang J, Ge Z. 2015. High-mobility group Box 1: A novel inducer of the epithelial-mesenchymal transition in colorectal carcinoma. *Cancer Lett.*, **357**: 527–534.